The Biology of the Ovine Functional Spinal Unit: Facet Cartilage and Intervertebral Disc

Caroline Shanni Gough

BSc (Hons), MRes

Submitted in accordance with the requirements for the degree of

Doctor of Philosophy

University of Leeds

Faculty of Biological Sciences

September 2013

The candidate confirms that the work submitted is her own and that appropriate credit has been given where reference has been made to the work of others.

This copy has been supplied on the understanding that it is copyright material and that no quotation from the thesis may be published without proper acknowledgement.

© 2013 The University of Leeds and Caroline Shanni Gough

The right of Caroline Shanni Gough to be identified as Author of this work has been asserted by her in accordance with the Copyright, Designs and Patents Act 1988.

Acknowledgements

My first thanks goes to my supervisor Eileen Ingham for giving me the opportunity to carry out this research, believing in my abilities and her support and guidance over the past four years. I cannot express how grateful I am to you for being so approachable, always making time for me, reading my work and your enthusiasm. I also want to thank my other supervisors Joanne Tipper, Ruth Wilcox and Richard Hall for all their constant support and advice.

The members of the iMBE have also been very supportive and I am grateful for all their help and guidance throughout the project. In particular I would like to thank Nagitha Wijayathunga for introducing me to the labs in biology and mechanical engineering and helping me understand the engineering aspects of the work. I cannot thank you enough for being so approachable and supportive throughout my research and always being there when I needed help. I especially appreciate your hard efforts to get all those sheep spines for me! Special thanks also goes to Iraklis Papageorgiou for being my lab buddy in the early stages of my research. Your support and friendliness helped me settle in the lab and allowed me to learn techniques and begin generating data quickly. It would've been much harder without you. I also must thank Liz Mitchell for giving me inspiration for some of my work and for always being there to teach me new techniques and give advice. Your enthusiasm and guidance was so valuable. I also thank Liz, Louise France and Philippa Garner for doing the grading in this work for me which I know took so long and required a lot of effort. Thanks to Sami Tarsuslugil who provided much support with analysing µCT data and was always there to answer my questions. I also would like to thank Abdellatif Abdelgaied for his support and guidance with the indentation work.

I have been so fortunate to have made such great friends whilst undertaking this research. Carly Taylor, Hazel Fermor and Nic Gowland have made this whole process so much easier and enjoyable. Our time together during and outside of work has provided me with stress relief and endless lols and memories. It was comforting to know I could talk to you about anything and would always get great advice and support.

I would like to give special thanks to my fiancé and best friend, Paul. You have been my rock throughout all my time at University and I don’t want to think about much how tougher it all would’ve been without you. I may not show it, but I am so thankful for everything. Finally, none of this would have been possible without my parents. I don’t know how I can thank you enough. You have supported me in every possible way throughout everything and your dedication and efforts have allowed me to do what I have always dreamt of. I will never forget all the obstacles and how you never gave up on me. You really have made all things possible.

Summary

Back pain will affect up to 84 % of people at some point in their lives. It is a major public health problem in Western society leading to disability and economic loss through work absence, physician visits and hospitalisation. A major cause of back pain is the natural degeneration of the intervertebral discs (IVDs) and osteoarthritis of the facet joints which increase with age. Spinal fusion is a common treatment that has been used for decades. The procedure involves the fusion of two vertebrae restricting motion in the functional spinal unit (FSU). Currently, tissue engineering methods are being researched to develop facet cartilage and IVD repair and replacement therapies for early intervention in the disease process with the aim of restoring tissue function and motion. There is a need for pre-clinical simulations to test these novel early intervention therapies.

The aim of this study was to characterise facet cartilage and IVD tissue in an ovine model in order to develop models of the healthy and degenerated ovine FSU which could be used in pre-clinical simulations of future therapies.

Ovine spines from animals of different ages were dissected and IVDs and facets from cervical, thoracic and lumbar regions were studied using photography, µCT and histology. The results showed that degeneration in the FSU began at 5-6 years of age. Since tissue from one year old sheep was skeletally immature, tissue from 3-4 year olds was accepted as healthy and used for further characterisation in order for comparisons to be made between ovine and human tissue.

IVDs and facet cartilage from cervical, thoracic and lumbar regions of the spines of 3-4 year old sheep were characterised using photography, histology, (haematoxylin and eosin, alcian blue, Sirius red and Miller's elastin stains), immunohistochemistry, assay for glycosaminoglycan (GAG) content and indentation testing to determine the biomechanical properties. The cells were isolated from FSU`s tissues, cultured and phenotyped using immunofluorescence. Facet cartilage was rich in GAGs throughout the tissue

structure with normal articular cartilage collagen distribution. The percentage of GAGs in dry weight facet cartilage was 8.47 %. Elastin was also found within the lamellae layers of the annulus fibrosus (AF) and cartilage end plate (CEP). Immunohistochemistry showed high expression of collagen II, chondroitin sulphate, collagen VI, collagen III and fibronectin in both facet cartilage and IVD tissue with varying distributions and intensities. The isolated FSU cells showed high expression of collagen types II, III and VI, fibronectin, CD44, SOX-9 and chondroitin-6-sulphate.

Facet cartilage showed very similar characteristics to other articular cartilages in terms of the key macromolecules present. Facet cartilage in the cervical region appeared thicker and contained more GAGs in comparison to the thoracic and lumbar regions. This may be due to the greater range of motion experienced in the cervical region and the need for extra support. A relationship between the presence of collagen types III and VI and elastin was also observed in facet cartilage. This may be due to the similar role of these proteins in providing anchorage of the chondrocyte to the ECM in facet cartilage.

In order to mimic degenerated human facets, ovine facets were treated with chondroitinase ABC in order to remove GAGs from the cartilage. Eight cervical facets were treated with 0.05 $U.ml^{-1}$ (w/v) chondroitinase ABC solution and analysed using photography, indentation, GAG assay, histology and immunohistochemistry to determine their effect.

The chondroitinase ABC method was shown to remove GAGs from facet cartilage, as seen in degenerated cartilage. This approach can be used to treat ovine FSU's to create degenerate models for *in vitro* pre-clinical simulations for testing future therapies such as those developed through tissue engineering.

Table of Contents

Acknowledgements i

Summary iii

Contents v

List of Figures xiv

List of Tables xxiv

Abbreviations xxvi

Chapter 1: Introduction **1**

1.1. Introduction 2

1.1.1. The Anatomy of the Human Spine 2

1.1.2. The FSU 4

1.2. The Composition of the FSU 5

1.2.1. Structural Components of FSU Tissues 5

1.2.1.1. Collagen 5

1.2.1.2. Proteoglycans 8

1.2.1.3. Elastin 11

1.2.2. The IVD 12

1.2.2.1. The NP 13

1.2.2.2. The AF 15

1.2.3. The CEP 16

1.2.4. The Facet Joints 17

1.2.4.1. Articular Cartilage 18

1.2.4.2. The Joint Capsule 22
1.2.4.3. Synovial Fluid 22
1.3. The Biomechanics of the FSU 23
1.3.1. Load bearing characteristics of the FSU 23
1.3.1.1. Compressive load and the IVD 24
1.3.1.2. Load Transmission and Motion in the Facet Joints 24
1.3.2. Cartilage Biomechanics 25
1.3.3. Cartilage Lubrication 26
1.4. Spinal Degenerative Disease 27
1.4.1. Degeneration of the Human IVD 27
1.4.2. Facet Joint Osteoarthritis: Spondylarthrosis 30
1.4.3. Degeneration of the FSU with age 32
1.5. Current Therapies for the Degenerated FSU 33
1.5.1. Analgesics 34
1.5.2. Physical and Rehabilitation Medicine 35
1.5.3. Spinal Fusion 35
1.5.4. Total Disc Replacement 35
1.5.5. Facet Joint Therapies 37
1.6. Novel Approaches for the Treatment of the FSU 38
1.6.1. Hydrogels for NP Replacement 41
1.6.2. Tissue Engineering of the AF 43
1.6.3. Tissue Engineering of the Whole IVD 44
1.6.4. Tissue Engineering of Facet Cartilage 44
1.7. The Need for Pre-Clinical Models 45

1.8. Conclusions 47

1.8.1. Aims and Objectives 48

Chapter 2: Materials and Methods **50**

2.1. General Materials 51

2.1.1. Chemicals and reagents 51

2.1.2. Solutions 51

2.1.3. Antibodies 54

2.1.4. Equipment, consumables, plastic and glass ware 55

2.2. General Methods 55

2.2.1. Washing and disinfection of equipment 55

2.2.2. Sterilisation 56

2.2.3. pH measurements 56

2.2.4. Microscopy 56

2.2.5. Ovine tissue dissection 56

2.2.5.1. Procurement of tissue 56

2.2.5.2. Dissection for tissue characterisation 57

2.2.5.3. Dissection for cell isolation 59

2.2.6. Photography 61

2.2.7. Histology 62

2.2.7.1. Tissue fixation and decalcification 62

2.2.7.2. Tissue processing 62

2.2.7.3. Paraffin wax embedding 63

2.2.7.4. Sectioning paraffin wax blocks 63

2.2.7.5. Haematoxylin and Eosin Staining 64

2.2.7.6. Alcian blue Staining 64

2.2.7.7. Sirius red/Miller's Elastin Staining 65

2.2.7.8. Grading systems for degeneration 65

2.2.8. Cell culture 69

2.2.8.1. Cell isolation 69

2.2.8.2. Passage and maintenance 69

2.2.8.3. Cell count and viability 69

2.2.8.4. Cryopreservation 70

2.2.8.5. Cell revival from frozen 70

2.2.9. Indirect immunofluorescent labelling of cell markers 71

2.2.9.1. Indirect immunofluorescence 71

2.2.9.2. Antibody dilution titrations 72

2.2.10. Immunohistochemical analysis of tissue sections 73

2.2.10.1. DAKO EnVision method 73

2.2.10.2. Streptavidin-Biotin method 73

2.2.11. Assay for sulphated GAGs 74

2.2.12. µCT analysis of FSUs 75

2.2.13. Indentation testing 76

2.2.13.1. Pin extraction 77

2.2.13.2. Indentation test to determine the deformation properties 77

2.2.13.3. Needle indentation for determination of cartilage thickness 78

2.2.14. Degeneration model of ovine facet cartilage using

chondroitinase ABC 78
2.2.15. Statistical Analysis 79
2.3. Validation of Methodologies 81
2.3.1. Determination of the working dilutions of primary and secondary antibodies using indirect immunofluorescence 81
2.3.2. Determination of the effect of passage number on expression of markers by FSU cells 83
2.3.3. Validation of methods for the immunohistochemical staining of tissue sections 87
2.3.4. Validation of papain digestion method and diluent for use in the GAG assay 95
Chapter 3: Anatomical Study of Ovine FSUs **98**
3.1. Introduction 99
3.2. Aims and Objectives 101
3.3. Experimental Approach 102
3.4. Results 104
3.4.1. Morphological analysis of FSUs using photography 104
3.4.2. Grading of H&E stained sections of transverse IVDs for degeneration 107
3.4.3. Grading of H&E stained sections of sagittal IVDs for degeneration 113
3.4.4. Morphological grading of facets using photography 120
3.4.5. Grading of H&E stained sections of facets for degeneration 127
3.4.6. Analysis of the bone in ovine FSUs 134

3.4.6.1. Bone volume/total volume of ovine FSUs 134

3.4.6.2. Hydroxyapatite concentration of ovine FSUs 137

3.4.7. IVD height and facet spacing measurements of ovine FSUs 139

3.4.7.1. IVD height 140

3.4.7.2. Facet joint spacing measurements 144

3.5. Discussion and conclusions 150

Chapter 4: Biological Characterisation of the Ovine FSU and Biomechanical Evaluation of the Facet Joint Cartilage **155**

4.1. Introduction 156

4.2. Aims and Objectives 160

4.3. Experimental Approach 161

4.4. Results 164

4.4.1. Growth characteristics of isolated cells 164

4.4.2. Phenotype of FSU cells 165

4.4.2.1. Collagen type I 167

4.4.2.2. Collagen type II 168

4.4.2.3. Collagen type III 169

4.4.2.4. Collagen type V 171

4.4.2.5. Collagen type VI 171

4.4.2.6. Collagen type X 172

4.4.2.7. Chondroitin-6-sulphate 173

4.4.2.8. CD44 174

4.4.2.9. Fibronectin 175

4.4.2.10. SOX-9 177
4.4.3. Characterisation of the IVD and facet cartilage using H&E stained histological sections of ovine FSU tissue 178
4.4.4. Characterisation of the IVD and facet cartilage using Alcian blue stained histological sections of ovine FSU tissue 183
4.4.5. Characterisation of the IVD and facet cartilage using Sirius red stained histological sections of ovine FSU tissue 187
4.4.6. Characterisation of the IVD and facet cartilage using Miller's elastin stained histological sections of ovine FSU tissue 192
4.4.7. Localisation of specific markers within the ovine IVD and facet cartilage 196
4.4.7.1. Collagen type I 196
4.4.7.2. Collagen type II 198
4.4.7.3. Collagen type III 199
4.4.7.4. Collagen type VI 201
4.4.7.5. Chondroitin Sulphate 203
4.4.7.6. Fibronectin 205
4.4.7.7. Osteocalcin 207
4.4.8. Deformation characteristics of facet cartilage 209
4.4.9. Quantification of GAG content in facet cartilage 212
4.5. Discussion and conclusions 215
***Chapter 5: A Degeneration Model of Ovine Facet Cartilage* 223**
5.1. Introduction 224
5.2. Aims and objectives 225

5.3. Experimental approach 226

5.4. Methods 227

5.4.1. Determination of the method of chondroitinase ABC treatment 227

5.4.2. Treatment of ovine cervical facet cartilage with chondroitinase ABC 228

5.5. Results 230

5.5.1. Determination of the method of chondroitinase ABC Treatment of facet cartilage 230

5.5.2. Morphology of chondroitinase ABC treated ovine facet cartilage 231

5.5.3. Quantification of GAG content in chondroitinase ABC treated ovine facet cartilage 234

5.5.4. Indentation testing of chondroitinase ABC treated ovine facet cartilage 235

5.5.5. Histological characterisation of chondroitinase ABC treated ovine facet cartilage 237

5.5.6. Characterisation of chondroitinase ABC treated ovine facet cartilage sections stained with Alcian blue 240

5.5.7. Characterisation of chondroitinase ABC treated ovine facet cartilage sections stained with Sirius red 242

5.5.8. Characterisation of chondroitinase ABC treated ovine facet cartilage sections stained with Miller's elastin 244

5.5.9. Localisation of specific markers in sections of chondroitinase

Treated ovine facet cartilage 246

5.5.9.1. Chondroitin sulphate 246

5.5.9.2. Collagen type II 249

5.6. Discussion and conclusions 252

Chapter 6: General Discussion **257**

6.1. Conclusions 270

Chapter 7: References **271**

Appendix I: Distributers of Materials and Chemicals **307**

Appendix II: Distributers of Equipment, Consumables, Plastic and Glassware **310**

Appendix III: Presentation and Publications **313**

List of Figures

Figure Number	Title	Page Number
1.1	The vertebral column showing how it is split into different regions.	2
1.2	A typical vertebra in the spine.	3
1.3	The structure of human cervical, thoracic and lumbar vertebrae.	4
1.4	A human functional spinal unit.	5
1.5	The biosynthesis and assembly of collagen.	7
1.6	The structure of a proteoglycan.	9
1.7	The structure of an aggrecan monomer and an aggrecan macromolecule	10
1.8	The structure of elastin before and after elongation.	12
1.9	An ovine lumbar IVD attached to its vertebra.	13
1.10	The structure of a typical AF.	15
1.11	Facet joints along two FSUs.	18
1.12	The organisation of collagen fibres into four zones in general articular cartilage.	21
1.13	The distribution of load along a FSU as a percentage during standing.	24
1.14	A biomechanical profile of the human, calf, sheep, pig and kangaroo.	46
1.15	Four studies at Leeds, including the study described in this thesis, running parallel to each other.	49
2.1	An ovine three year old Suffolk spine.	57
2.2	Cervical, thoracic and lumbar regions of a three year old ovine Suffolk Mule spine.	58
2.3	An ovine FSU cut sagittally in half using a bone saw.	59
2.4	A section of an ovine lumbar spine through the IVD.	61
2.5	A haemocytometer grid.	70
2.6	A µCT image of a pair of ovine thoracic facets joints.	76

2.7	The indentation test rig used to determine the indentation properties of facet cartilage.	77
2.8	Collagen II antibody titrations.	82
2.9	Facet cartilage cells in monolayer culture.	84
2.10	CEP cells stained with three different primary antibodies using in direct immunofluorescence using method A.	86
2.11	AF cells immunostained with three different primary antibodies using in direct immunofluorescence Method B.	87
2.12	The validation of immunohistochemical staining using antibodies to collagen II on ovine femoral head cartilage.	88
2.13	The validation of immunohistochemical staining using antibodies to chondroitin-6-sulphate on ovine femoral head cartilage.	89
2.14	The validation of immunohistochemical staining using antibodies to collagen I on ovine spinous ligament.	90
2.15	The validation of immunohistochemical staining using antibodies to collagen III on ovine spinous ligament.	91
2.16	The validation of immunohistochemical staining using antibodies to collagen VI on ovine femoral head cartilage.	92
2.17	The validation of immunohistochemical staining using antibodies to collagen X. on ovine femoral head cartilage.	93
2.18	The validation of immunohistochemical staining using antibodies to desmin on ovine spinous muscle.	93
2.19	The validation of immunohistochemical staining using antibodies to fibronectin on ovine spinous ligament.	94
2.20	The validation optimisation of immunohistochemical staining antibodies to osteocalcin on ovine femoral head bone.	95
2.21	Standard curves for chondroitin sulphate B against absorbance at 525 nm.	96

3.1	Four different breeds of sheep used in the study.	100
3.2	Images of FSUs from a three year old Texel sheep.	104
3.3	Images of lumbar L3/L4 FSUs from 1, 3-4, 5-6 and 8-10 year old sheep.	106
3.4	The distribution of grading scores for H&E stained sections of ovine cervical (C4/C5) transverse IVDs in four age groups and three breeds of 3-4 year old sheep.	108
3.5	The distribution of degeneration grading scores for H&E stained sections of ovine thoracic (T8/T9) transverse IVDs in four age groups and three 3-4 year old breeds of sheep	110
3.6	The distribution of degeneration grading scores for H&E stained sections of ovine lumbar (L3/L4) transverse IVDs in all four age groups and three 3-4 year old breeds of sheep.	112
3.7	The distribution of degeneration grading scores for H&E stained ovine cervical (C6/C7) sagittal IVD sections in four age groups and three 3-4 year old breeds of sheep.	114
3.8	The distribution of degeneration grading scores for H&E stained ovine thoracic (T11/T12) sagittal IVD sections in four age groups and three 3-4 year old breeds of sheep.	116
3.9	The distribution of degeneration grading scores for H&E stained ovine lumbar (L1/L2) sagittal IVD sections in four age groups and three 3-4 year old breeds of sheep.	118
3.10	H&E stained CEP of lumbar sagittal IVD sections in four different age groups.	119
3.11	Images of ovine cervical (C6/C7), thoracic (T11/T12) and (L1/L2) lumbar left superior (S) and inferior (I) facets from one, three to four, five to six and eight to 10 year old sheep.	120
3.12	The distribution of grading scores for the macroscopic left ovine cervical (C6/C7) facets in four age groups and three 3-4 year old breeds of sheep.	122
3.13	The distribution of grading scores for the macroscopic	124

	left ovine thoracic (T11/T12) facets in all four age groups and three 3-4 year old breeds of sheep.	
3.14	The distribution of grading scores for the macroscopic left ovine lumbar (L1/L2) facets in all four age groups and three 3-4 year old breeds of sheep.	126
3.15	The distribution of degeneration grading scores for H&E stained ovine cervical (C6/C7) left inferior facet cartilage sections in four age groups and three 3-4 year old breeds of sheep.	128
3.16	The distribution of degeneration grading scores for H&E stained ovine thoracic (T11/T12) left inferior facet cartilage sections in four age groups and three 3-4 year old breeds of sheep	130
3.17	The distribution of degeneration grading scores for H&E stained ovine lumbar (L1/L2) left inferior facet cartilage sections in four age groups and three 3-4 year old breeds of sheep.	132
3.18	H&E stained sections of ovine cervical (C6/C7) facet cartilage from four different age groups.	133
3.19	The mean BV/TV of ovine cervical (C6/C7) FSUs from four age groups and three 3-4 year old breeds of sheep.	134
3.20	The mean BV/TV of ovine thoracic (T11/T12) FSUs from four age groups and three 3-4 year old breeds of sheep.	135
3.21	The mean BV/TV of ovine lumbar (L1/L2) FSUs from four age groups and three 3-4 year old breeds of sheep.	136
3.22	The mean HA concentration in ovine cervical (C6/C7) FSUs from four age groups and three 3-4 year old breeds of sheep.	137
3.23	The mean HA concentration in ovine thoracic (T11/T12) FSUs from four age groups and three 3-4 year old breeds of sheep.	138
3.24	The mean HA concentration in ovine lumbar (L1/L2) FSUs from four age groups and three 3-4 year old breeds of sheep.	139

3.25	The IVD height in ovine cervical (C6/C7) FSUs from four age groups and three 3-4 year old breeds of sheep.	141
3.26	The mean IVD height in ovine thoracic (T11/T12) FSUs from four age groups and three 3-4 year old breeds of sheep.	142
3.27	The mean IVD height in ovine lumbar (L1/L2) FSUs from four age groups and three 3-4 year old breeds of sheep.	143
3.28	The mean facet joint spacing in ovine cervical (C6/C7) FSUs from four age groups and three 3-4 year old breeds of sheep.	144
3.29	The mean facet joint spacing in ovine thoracic (T11/T12) FSUs from four age groups and three 3-4 year old breeds of sheep.	145
3.30	The mean facet joint spacing in ovine lumbar (L1/L2) FSUs from four age groups and three 3-4 year old breeds of sheep.	146
4.1	A human chondrocyte making multiple interactions with different macromolecules.	158
4.2	The allocation of tissue for each analysis.	163
4.3	Light microscope images of FSU cells growing 12 days after isolation and before passage.	164
4.4	Ovine thoracic (T5-T7) facet cartilage (A) and outer AF (B) cells stained with mouse anti-sheep collagen type I monoclonal antibody (i) and mouse IgG1 isotype control (ii) together with rabbit anti-mouse FITC-conjugated secondary antibodies.	168
4.5	Ovine cervical (C2/C3) facet cartilage (A) and inner AF (B) cells stained with mouse anti-sheep collagen type II monoclonal antibody (i) and mouse IgG1 isotype control (ii) together with rabbit anti-mouse FITC-conjugated secondary antibodies.	169
4.6	Ovine cervical (C2/C3) inner AF (A) and outer AF (B) cells stained with rabbit anti-sheep collagen type III	170

	rabbit polyclonal antibody (i) and rabbit IgG isotype control (ii) together with Goat anti-rabbit FITC-conjugated secondary antibodies.	
4.7	Ovine cervical (C2/C3) outer AF (A) and lumbar (L5/6) outer AF (B) cells stained with mouse anti-sheep collagen type V monoclonal antibody (i) and mouse IgG2a isotype control (ii) together with Goat anti-mouse FITC-conjugated secondary antibodies.	171
4.8	Ovine lumbar (L5/L6) outer AF (A) and thoracic (T5-T7) inner AF (B) cells stained with rabbit anti-sheep collagen type VI polyclonal antibody (i) and rabbit IgG isotype control (ii) together with Goat anti-rabbit FITC-conjugated secondary antibodies.	172
4.9	Ovine cervical (C2/C3) outer AF (A) and thoracic (T5-T7) facet (B) cells stained with mouse anti-sheep collagen type X monoclonal antibody (i) and mouse IgM isotype control (ii) together with Goat anti-mouse FITC-conjugated secondary antibodies.	173
4.10	Ovine thoracic (T5-T7) facet cartilage (A) and lumbar (L5/L6) inner AF (B) cells stained with mouse anti-sheep chondroitin-6-sulphate monoclonal antibody (i) and mouse IgG1 isotype control (ii) together with goat anti-mouse FITC-conjugated secondary antibodies.	174
4.11	Ovine cervical (C2/C3) inner AF (A) and lumbar (L5/L6) facet cartilage (B) cells stained with rat anti-sheep CD44 monoclonal antibody (i) and rat IgG1 isotype control (ii) together with rabbit anti-rat FITC-conjugated secondary antibodies.	175
4.12	Ovine lumbar (L5/L6) facet (A) and cervical (C2/C3) NP cartilage (B) cells stained with mouse anti-sheep fibronectin monoclonal antibody (i) and mouse IgG1 isotype control (ii) together with goat anti-mouse FITC-conjugated secondary antibodies.	176
4.13	Ovine cervical (C2/C3) outer AF (A) and lumbar (L5/L6)	177

	facet cartilage (B) cells stained with rabbit anti-sheep SOX-9 polyclonal antibody (i) and rabbit IgG isotype control (ii) together with goat anti-rabbit FITC-conjugated secondary antibodies.	
4.14	H&E stained facet cartilage and IVD sagittal sections from C6/C7.	179
4.15	H&E stained facet cartilage and IVD sagittal sections from T11/T12.	181
4.16	H&E stained facet cartilage IVD sagittal sections from L1/L2.	183
4.17	Alcian blue stained facet cartilage and IVD sagittal sections from C6/C7.	184
4.18	Alcian blue stained facet cartilage and IVD sagittal sections from T11/T12.	186
4.19	Alcian blue stained facet cartilage and IVD sagittal sections from L1/L2.	187
4.20	Sirius Red stained facet cartilage and IVD sagittal sections from C6/C7.	189
4.21	Sirius Red stained facet cartilage and IVD sagittal sections from T11/T12.	190
4.22	Sirius red staining of facet cartilage and IVD sagittal sections from L1/L2.	191
4.23	Miller’s elastin stained facet cartilage and IVD sagittal sections from C6/C7.	193
4.24	Miller’s elastin stained facet cartilage and IVD sagittal sections from T11/T12.	194
4.25	Miller’s elastin stained facet cartilage and IVD sagittal sections from L1/L2.	195
4.26	Ovine cervical (5.C6/C7) facet cartilage stained with mouse anti-sheep collagen type I monoclonal antibody (A) and mouse IgG1 isotype control (B).	196
4.27	Ovine lumbar (6.L1/L2) AF (A), thoracic (6.T11/T12) CEP (B) and lumbar (7.L1/L2) NP (C) sections stained with mouse anti-sheep collagen type I monoclonal	197

	antibody (i) and mouse IgG1 isotype control (ii).	
4.28	Ovine cervical (6.C6/C7) facet cartilage sections stained with mouse anti-sheep collagen type II monoclonal antibody (A) and mouse IgG1 isotype control (B).	198
4.29	Ovine cervical (6.C6/C7) AF (A), lumbar (7.L1/L2) CEP (B) and thoracic (5.T11/T12) NP (C) sections stained with mouse anti-sheep collagen type II monoclonal antibody (i) and mouse IgG1 isotype control (ii).	199
4.30	Ovine cervical (6.C6/C7) facet cartilage sections stained with rabbit anti-sheep collagen type III polyclonal antibody (A) and rabbit IgG isotype control (B).	200
4.31	Ovine lumbar (6.L1/L2) AF (A), thoracic (7.T11/T12) CEP (B) and lumbar (6.L1/L2) NP (C) sections stained with rabbit anti-sheep collagen type III polyclonal antibody (i) and rabbit IgG isotype control (ii).	201
4.32	Ovine cervical (6.C6/C7) facet cartilage sections stained with rabbit anti-sheep collagen type VI polyclonal antibody (A) and rabbit IgG isotype control (B).	202
4.33	Ovine thoracic (5.T11/T12) AF (A), lumbar (7.L1/L2) CEP (B) and cervical (6.C6/C7) NP (C) sections stained with rabbit anti-sheep collagen type VI polyclonal antibody (i) and rabbit IgG isotype control (ii).	203
4.34	Ovine cervical (7.C6/C7) facet cartilage sections stained with rabbit anti-sheep chondroitin sulphate polyclonal antibody (A) and rabbit IgG isotype control (B).	204
4.35	Ovine cervical (7.C6/C7) AF (A), cervical (5.C6/C7) CEP (B) and cervical (5.C6/C7) NP (C) sections stained with rabbit anti-sheep chondroitin sulphate polyclonal antibody (i) and rabbit IgG isotype control (ii).	205
4.36	Ovine cervical (7.C6/C7) facet cartilage sections stained with mouse anti-sheep fibronectin monoclonal antibody (A) and rabbit IgG1 isotype control (B).	206
4.37	Ovine lumbar (5.L1/L2) AF (A), cervical (5.C6/C7) CEP (B) and lumbar (7.L1/L2) NP (C) sections stained with	207

	mouse anti-sheep fibronectin monoclonal antibody (i) and mouse IgG1 isotype control (ii).	
4.38	Ovine thoracic (5.T11/T12) facet cartilage sections stained with mouse anti-sheep osteocalcin monoclonal antibody (A) and mouse IgG2a isotype control (B).	208
4.39	Ovine thoracic (5.T11/T12) AF (A), lumbar (5.L1/L2) CEP (B) and lumbar (7.L1/L2) NP (C) stained with mouse anti-sheep osteocalcin monoclonal antibody (i) and mouse IgG2a isotype control (ii).	209
4.40	The thickness of the cartilage on all four C6/C7 ovine facets.	210
4.41	Strain curves for four C6/C7 ovine facets.	211
4.42	Strain curve of the mean for all four C6/C7 ovine facets.	212
4.43	GAG concentration (mg/ml dry weight) in ovine thoracic facets across four age groups.	213
4.44	GAG concentration (mg/ml dry weight) in ovine thoracic facets across four age groups.	214
5.1	The GAG concentration (as a percentage of dry weight) in facets treated with various concentrations of chondroitinase ABC.	230
5.2	C4/C5 facets before and after chondroitinase ABC treatment.	232
5.3	C5/C6 facets before and after chondroitinase ABC treatment.	233
5.4	The percentage of GAGs in facet cartilage after chondroitinase ABC treatment including negative controls.	234
5.5	The thickness of the cartilage on all eight C4/C5 and C5/C6 ovine facets.	235
5.6	The indentation data for ovine C4/C5 and C5/C6 facet cartilage with and without treatment with chondroitinase ABC.	236
5.7	The indentation data for ovine C4/C5 and C5/C6 chondroitinase ABC treated facet cartilage including	237

	negative controls.	
5.8	C4/C5 and C5/C6 facet sections stained with H&E after chondroitinase ABC treatment including negative controls.	239
5.9	C4/C5 and C5/C6 facet sections stained with Alcian blue after chondroitinase ABC treatment including negative controls.	241
5.10	C4/C5 and C5/C6 facet sections stained with Sirius Red after chondroitinase ABC treatment including negative controls.	243
5.11	C4/C5 and C5/C6 facet sections stained with Miller's Elastin after chondroitinase ABC treatment including negative controls.	245
5.12	C4/C5 facet sections immunohistochemically stained with antibodies to chondroitin sulphate including negative controls.	247
5.13	C5/C6 facet sections immunohistochemically stained with antibodies to chondroitin sulphate.	248
5.14	C4/C5 facet sections immunohistochemically stained with antibodies for collagen type II including negative controls.	250
5.15	C5/C6 facet sections immunohistochemically stained with antibodies for collagen type II.	251

List of Tables

Table Number	Title	Page Number
2.1	Primary antibodies used throughout the study.	54
2.2	Secondary antibodies used throughout the study.	55
2.3	Isotype control antibodies used throughout the study.	55
2.4	Grading system used to grade facet cartilage degeneration from digital images based on the surface of the cartilage.	62
2.5	Tissue processor programme 8 and 9.	63
2.6	The histological grading system used for grading degeneration in transverse IVD sections.	66
2.7	The histological grading system used to grade degeneration in sagittal IVD sections.	67
2.8	The grading system used to grade degeneration in histological sections of the facets.	68
2.9	The interpretation of kappa scores.	79
2.10	The significance of r values generated from the Spearman's rank correlation and Pearson's moment correlation.	80
2.11	Summary of all working primary and secondary antibody dilutions.	83
2.12	The phenotype of all ovine FSU cell types.	85
3.1	A summary of the data for the cervical FSUs.	147
3.2	A summary of the data for the thoracic FSUs.	148
3.3	A summary of the data for the lumbar FSUs.	149
4.1	Expression of collagens and levels of collagen expression in FSU cell types at passage two.	166
4.2	The expression of non-collagenous markers and the level of expression in FSU cell types at passage two.	167
5.1	Thoracic facets incubated with a range of chondroitinase ABC concentrations and incubation	227

	times.	

Abbreviations

AF: Annulus fibrosus

AFM: Atomic force microscopy

ANOVA: Analysis of variance

ASD: Adjacent segment disease

BMD: Bone mineral density

BV: Bone volume

CEP: Cartilage end plate

COMP: Cartilage oligomeric matrix protein

DAB: 3,3-diaminobenzidine

DAPI: 4,6-diamidino-2-phenyllindole

DMB: 1,9-dimethylene blue

DMEM: Dulbecco's Modified Eagle Medium

DMSO: Dimethyl sulfoxide

DNA: Deoxyribonucleic acid

DPPC: Dipalmitoyl phosphotidylcholine

ECM: Extracellular matrix

EDTA: Ethylenediaminetetraacetic acid

ER: Endoplasmic reticulum

FBS: Fetal bovine serum

FCD: Fixed charge density

FE: Finite element

FITC: Fluorescein isothiocyanate

FSU: Functional spinal unit

GAGs: Glycosaminoglycans

H&E: Haematoxylin and Eosin

HA: Hydroxyapetite

HABR: Hyaluronic acid binding region

IVD: Intervertebral disc

LOX: Lysyl oxidase

LVDT: Linear variable differential transformer

MMP: Matrix metalloproteinase

MRI: Magnetic resonance imaging

MSC: Mesenchymal stem cell

mTGases: Microbial transglutaminases

NP: Nucleus pulposus

PBS: Phosphate buffered saline

PLLA: poly(L-lactic acid)

PRELP: Proline arginine-rich end leucine-rich repeat protein

SEM: Scanning electron microscopy

SLRPs: Small leucine-rich proteoglycans

TBS: Tris buffered saline

TDR: Total disc replacement

TEM: Transmission electron microscopy

TIMP: Tissue inhibitors of metalloproteinases

TV: Total volume

UHMWPE: Ultra-high molecular weight polyethylene

UV: Ultraviolet

μCT: Micro computed-tomography

Chapter 1:

Introduction

Chapter 1: Introduction

1.1. Introduction

The spine is an important musculoskeletal structure, both in humans and other vertebrate animals. Whilst providing the organism with stability and support, the spine also gives rise to mobility such as flexion allowed by the presence of associated muscles, ligaments and tendons. The spine allows the weight of an organism to be distributed evenly and adapt to change. The essential spinal nerves are protected within the vertebral column and the vertebral bones produce bone marrow providing the structures with necessary blood cells. In addition, the spine, through the vertebrate muscles, is able to absorb impact forces, providing protection.

1.1.1 The Anatomy of the Human Spine

The vertebral column is composed of five regions. These are the cervical, thoracic, lumbar, sacrum and coccyx regions. Together, the human spine contains 24 vertebrae accompanied by intervertebral discs between each pair linked together by ligaments and facet joints. In addition, the sacrum and coccyx add an extra five and four fused vertebrae, respectively (Maurice, 1981; Grieve, 1991; Boszczyk *et al.*, 2001B). This is shown in Figure 1.1.

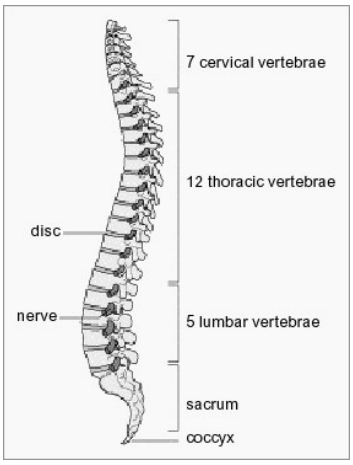


Figure 1.1: The vertebral column showing how it is split into different regions. The spine consists of four regions, the cervical, thoracic, lumbar and the sacrum and coccyx region. (Derived from http://www.eurospine.org/p31000298.html)

For all of the vertebrae along the spinal column, a vertebral body, which sits between two intervertebral discs (IVDs), is attached to a laminal arch composed of two laminae, via two pedicles. In the centre of the vertebra is a small cleft, the spinal canal. This allows the spinal cord to pass through the column whilst ensuring maximum protection. On each side of the laminal arch is a pair of articular processes, superior and inferior. Behind the laminal arch is the spinous process. For each vertebral section, this has a characteristic shape (Maurice, 1981; Boszczyk *et al.*, 2001B). A diagram of a typical vertebra is shown in Figure 1.2.

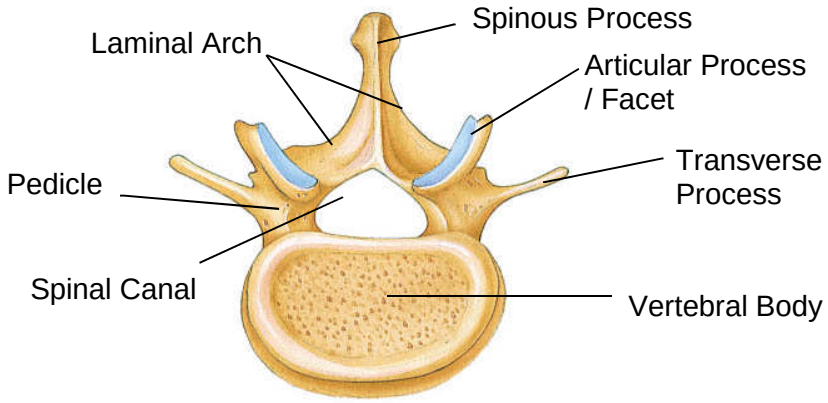


Figure 1.2: A typical vertebra in the spine. Each vertebra contains a vertebral body, laminal arch, pedicles, spinal canal, articular processes/facets and spinous process. (Derived from http://waukesha.uwc.edu.lib.reserves/pdf/zillgitt/zoo170/diagrams2/axial%20skeleton/F06.16%20Typical%20Vertebrae.jpg)

The cervical vertebrae (C1-C7) are located at the top of the vertebral column starting at the base of the cranium. The first and second cervical vertebrae, C1 (atlas) and C2 (axis) respectively, fit together via the odontoid process (dens) which allows C1 to rotate (Bland and Boushey, 1990). The thoracic vertebrae (T1-T12) are located in between the cervical and lumbar vertebrae (Maurice, 1981; Grieve, 1991). The upper section of the thoracic spine is capable of less motion in comparison to the lower section and contains a narrower spinal canal which is generally small and circular in both sections. The superior facets lay at upright angles (Crock and Yoshizawa, 1977; Bohlman *et al.*, 1985). The lumbar vertebrae (L1-L5) are very often associated with back pain as this is the part of the vertebral column which supports the majority of body weight, stresses and

strains (Boszczyk *et al.*, 2001B). Lumbar vertebrae are the largest and bulkiest vertebrae containing a large intervertebral spinal canal. The sacrum and coccyx make up the terminal end of the vertebral column located at the pelvic region. The sacrum is composed of five sacral vertebrae (S1-S5) fused together whilst the coccyx has three to four coccygeal vertebrae also fused together. (Maurice, 1981; Grieve, 1991; Fogel *et al.*, 2004). All the vertebrae described are shown in Figure 1.3.

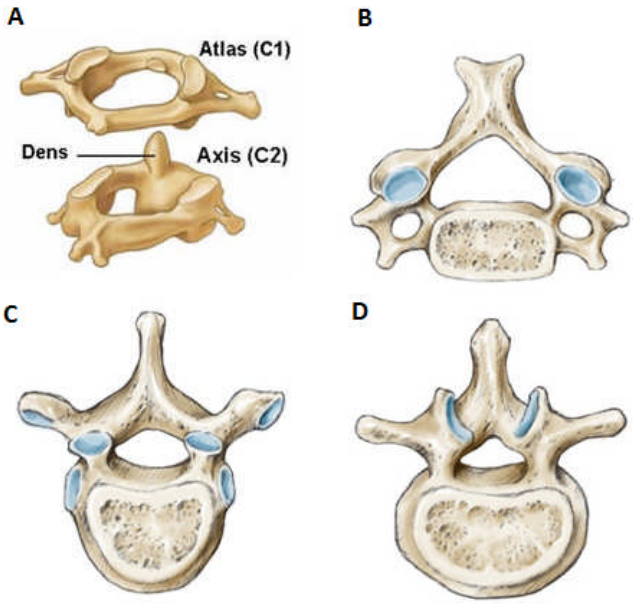


Figure 1.3: The structure of human cervical, thoracic and lumbar vertebrae. A: The atlas (C1) and axis (C2). The two structures fit together via the odontoid process (dens) allowing the head to rotate. B: A typical cervical vertebra. The cervical vertebrae consist of a spinous process, spinal canal and vertebral body and a pair of facets, superior articular processes, pedicles, transverse processes, foramen and lamina. C: A typical thoracic vertebra. The thoracic vertebrae consist of a spinous process, vertebral body and spinal canal and a pair of superior articular processes, transverse processes, pedicles, facets and lamina. D: A typical lumbar vertebra. The lumbar vertebrae consist of a spinous process, vertebral body and spinal canal and a pair of transverse processes, pedicles, articular processes and lamina.
(http://nobacksurgeryinfo.com/backanatomy.php;
http://www.zimmerspine.eu/z/ctl.op/global/action/1/id/9024/template/PC)

1.1.2 The Functional Spinal Unit

The functional spinal unit (FSU) is the smallest unit of the spine responsible for physiological movement and exhibits kinetic features which represent that of the

whole spine. Within the FSU are four major components. These include two adjacent vertebrae and an IVD in between, separated by cartilage end plates (CEPs), which are connected by ligamentous tissue and two facet joints on either side. Spinal muscles and other related tissue surround the FSU (Morishita *et al.*, 2008). Although the biology of the FSU has not been extensively characterised, the biomechanical characteristics have been widely researched. A typical FSU is shown in Figure 1.4.

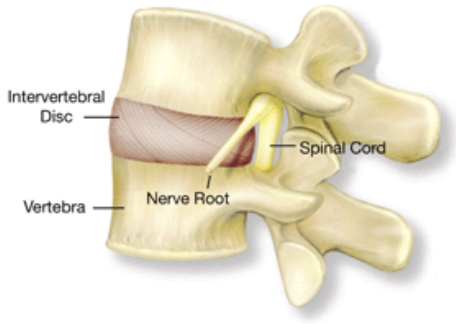


Figure 1.4: A human FSU. The FSU typically consists of vertebrae, CEPs, an IVD and a pair of facet joints. FSU: Functional spinal unit. (http://www.delawarebackpain.com/patient%20information/anatomy.htm)

1.2. The Composition of the FSU

The most important components of the FSU which allow its function are the IVD, the CEPs and the facet joints. Each part is composed of different tissues which act together to give rise to physiological movement and function.

1.2.1 Structural Components of FSU Tissues

The tissues which make up the FSU are comprised of cells and an extracellular matrix (ECM). The ECM is comprised of collagens, non-collagenous proteins and proteoglycans plus other minor glycoproteins. These molecules are directly related to the function of the specific tissue and thus an understanding of their structure and function is necessary.

1.2.1.1. Collagen

Collagen is found in great abundance throughout connective tissue in the human body. It is highly organised within articular cartilage, the CEP and the IVD providing a fibrous ultrastructure that is essential for its function in joints

such as the facet joint and the IVD (Von der Mark, 1999; Nordin and Frankel, 2001). The basic biological unit of collagen is tropocollagen. Tropocollagen consists of three polypeptide chains arranged in a left handed triple helix held together by hydrogen bonds (Nordin and Frankel, 2001). Each procollagen chain is composed of repeating units of the $(Gly\text{-}X\text{-}Y)_n$ where X and Y are usually proline and hydroxyproline respectively. The synthesis and biosynthesis of collagen is a complex multistep process.

Collagen propeptides are stabilised by intrachain disulphide bonds and an N-linked carbohydrate group is added. Three α-chains form a triple helix which involves the alignment of the C- terminal domains to give a procollagen molecule (Gelse *et al.*, 2003). Modifications are carried out by procollagen Zn^{2+} dependant metalloproteinases which cleave N- and C-terminal propeptides to form tropocollagen. Tropocollagen undergoes extensive cross-linking and self-assembly (Kyle *et al.*, 2009). The tropocollagen chains arrange themselves around a central axis ensuring that glycine residues are positioned inside the helix and bulkier residues are outside forming a close packed structure. Tropocollagen molecules, typically 1.4 nm in diameter and 300 nm long, polymerise to form collagen fibrils, typically 25-40 nm in diameter in human articular cartilage. Covalent cross links are formed between tropocollagen molecules which contribute to their high tensile strength and the physical and mechanical properties of collagen fibrils. Hydrophobic and electrostatic interactions also contribute to the stability between collagen monomers (Gelse *et al.*, 2003). Furthermore, collagen fibrils aggregate together to form a collagen fibre (Nordin and Frankel, 2001; Kyle *et al.*, 2009). Different collagen types assemble themselves in different orientations. Collagen biosynthesis and assembly is illustrated in Figure 1.5.

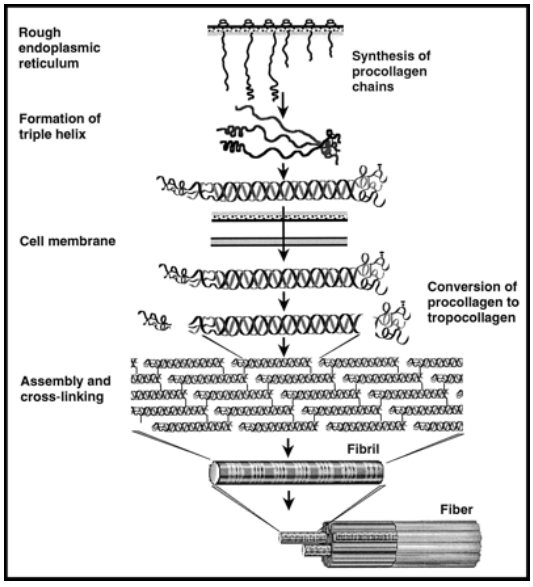


Figure 1.5: The biosynthesis and assembly of collagen. Procollagen is synthesised within the cell and secreted by exocytosis. Procollagen is converted to tropocollagen before the collagen fibrils and fibres are assembled. (Derived from Culav *et al.*, 1999)

There are three main types of collagen commonly found in cartilage; collagen types II, IX and XI (Wotton *et al.*, 1988; Bruehlmann *et al.*, 2002). Each collagen type forms a particular arrangement in relation to other collagen fibres (Wu *et al.*, 1992). Collagen type II is the major collagen component consisting of a single triple helical domain and has a length of approximately three hundred nm. It forms a network of fibrils in which proteoglycans, which contribute to cartilage hydration (Section 1.2.1.2), are contained (Mayne, 1989). Collagen type IX consists of three triple helical domains interlinked by flexible regions and a globular domain with a length of one hundred and ninety nm. Finally, collagen type XI contains a triple helix three hundred nm in length with an amino terminal non-collagenous domain. Various other types of collagen exist within cartilage including types III, VI and X. (Mayne, 1989; Wotton and Duance, 1994; Pullig *et al.*, 1999). The main types of collagen found in the IVD are collagens type I and II. Type I is found largely in the outer annulus fibrosus (AF) whilst type II is located largely in the inner AF and nucleus pulposus (NP) (Eyre and Muir, 1977). Previous studies have also reported the presence of collagen types III, V, VI, IX, and XI in the AF and types VI, IX and XI in the NP (Eyre, 1988; Roberts *et al.*, 1991A; Roberts *et al.*, 1991B; Boos *et al.*, 1997). Whilst each collagen type has its unique function, the main overall function of collagen is to

provide mechanical support whilst resisting compressive forces and structural stabilisation (Mendler *et al.*, 1989).

1.2.1.2. Proteoglycans

Proteoglycans are macromolecules comprising glycosaminoglycan (GAG) chains, surrounding a protein core and are produced by most eukaryotic cells. A wide variety of proteoglycans exist which may have different functions. For example, some proteoglycans provide cell surface receptors whilst others provide physical support (Hardingham and Fosang, 1992).

Proteoglycans consist of a large protein core to which many highly charged, large and extended GAGs including chondroitin sulphate and keratan sulphate chains, are attached. The GAG chains consist of repeating disaccharides and the size and ratio of these chains may change with age and/or disease. Chondroitin sulphate contains 40-50 disaccharide units of glucuronic acid and 4/6-sulphated N-acetyl galactosamine (Chandran and Horkay, 2012). Earlier research showed that chondroitin sulphate links to the protein core through serine residues (Muir and Jacobs, 1967). Further work showed the presence of a covalent glycosidic linkage between xylose and the hydroxyl group of serine in the chondroitin sulphate-protein complex (Lindahl and Roden, 1966; Bushell *et al.*, 1977). Keratan sulphate consists of between 20-25 repeating disaccharides of sulphated N-acetyl-glucosamine and galactose. The molecule is linked to the protein core of a proteoglycan via serine and threonine residues via an N-acetyl-galactosamine residue (Bray *et al.*, 1967). A large majority of the keratan sulphate chains lie next to a hexapeptide repeat domain with a higher number of proline residues in the core protein (Heinegard, 2009). The structure of a proteoglycan is illustrated in Figure 1.6.

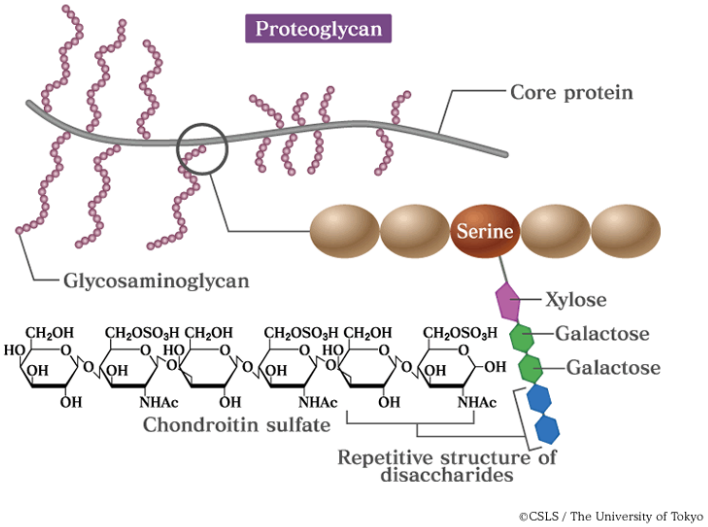


Figure 1.6: The structure of a proteoglycan. Repetitive disaccharides are attached to a galactose-galactose-xylose carbohydrate chain which makes up the GAG. At physiological pH 7.4, the CH_2OSO_3H and CH_2OH groups lose their hydrogen atom to form negatively charged groups. The GAG chondroitin sulphate makes a connection with a serine residue on the core protein via a glycosidic bond. A proteoglycan is made up of many GAGs that are covalently attached to a core protein. GAG: Glycosaminoglycan. (Derived from http://csls-text.c.u-tokyo.ac.jp/active/11_02.html)

The GAGs are responsible for the physical properties of the proteoglycan. Proteoglycans generally act to hydrate the ECM in which they are present. This is possible due to the negatively charged GAGs which attract counter ions leading to an osmotic pressure which therefore attracts water from the surroundings. Proteoglycans are also capable of interacting with other components and aid the molecular organisation of ECMs (Hardingham and Fosang, 1992). Aggrecan is a large negatively charged aggregating proteoglycan macromolecule present in cartilage. It has a bottle brush structure which becomes enmeshed within the collagen fibres in articular cartilage (Chandran and Horkay, 2012). Aggrecan attaches to a linear hyaluronan molecule via a hyaluronic acid binding region (HABR). Hyaluronic acid is a GAG comprised of the disaccharides D-glucuronic acid and D-N-acetylglucosamine (Bushell *et al.*, 1977; Chandran and Horkay, 2012). This interaction is stabilised by a link protein. This stabilisation effect is vital for the function of healthy tissues such as articular cartilage preventing the breakdown of proteoglycans and ensuring they remain within the tissue. Three highly conserved globular

regions are present within the aggrecan core protein. The first, G_1, is the HABR which is located at the N terminus containing a small amount of keratan sulphate and few N-linked oligosaccharides. The second globular region is G_2 which is found between the HABR (G_1) and the keratan sulphate rich region. Lastly, G_3 is the core protein C-terminus (Nordin and Frankel, 2001). GAG chains are located between the G_2 and G_3 domains. Chondroitin sulphate makes up the majority of GAGs in the aggrecan monomer with up to 100 chains, whilst up to 30 keratan sulphate chains are found. In addition, between eight and 10 short N- and O-linked oligosaccharides are distributed amongst the GAGs chain (Chandran and Horkay, 2012). The structure of aggrecan as a monomer and macromolecule is shown in Figure 1.7.

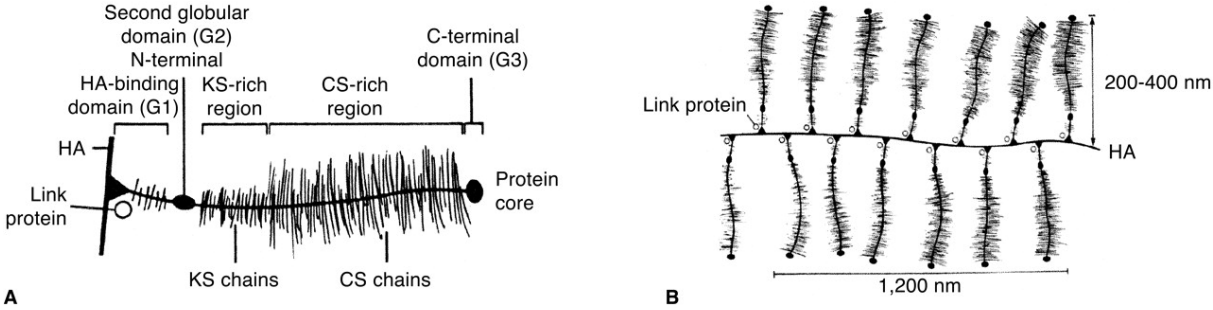


Figure 1.7: The structure of an aggrecan monomer and an aggrecan macromolecule. A: An aggrecan monomer which has a bottlebrush-like architecture consisting of three globular domains. B: The aggrecan macromolecule consists of many aggrecan monomers attached to a linear hyaluronic acid molecule via the G_1 domain. (Derived from Mankin *et al.*, 2000)

The primary function of aggrecan is to distribute loads within joints and resist compressive loads (Hardingham and Fosang, 1992). This is achieved by the macromolecules extremely high fixed charge density which creates a high osmotic environment therefore allowing water to be retained within tissue. Keratan sulphate and dermatan sulphate have also been shown to contribute to the function of aggrecan by binding with high affinity to collagen within the ECM of cartilage (Rosenberg, 1992; Hedlund *et al.*, 1999). The bottlebrush-like structure of aggrecan also allows it to behave as a space-filling molecule and to exert large frictional drag which in turns gives rise to decreased hydraulic permeability and damping properties (Chandran and Horkay, 2012).

Other minor proteoglycans present in the ECM of tissues such as cartilage and the IVD are small leucine-rich proteoglycans (SLRPs). SLRPs can be divided into three classes. Class I includes decorin and biglycan. Decorin carries one chondroitin or dematan sulphate side chain and interacts with collagen fibrils through one triple helix. Biglycan carries two chondroitin or dematan sulphate chains and is a positive regulator of bone formation and mass. The class II SLRPs include fibromodulin, lumican and proline arginine-rich end leucine-rich repeat protein (PRELP). Fibromodulin carries up to four keratin sulphate side chains and regulates the diameter of collagen fibrils, lumican is a major keratan sulphate proteoglycan found largely in cartilage and PRELP is a cartilage matrix protein involved in matrix organisation. Lastly, epiphycan is a class III SLRP containing dermatan sulphate and is present in epiphyseal cartilage (Knudson and Knudson, 2001).

1.2.1.3. Elastin

Elastin is an ECM protein and the major component of elastic fibres. The major function of elastin is to provide elasticity and resilience in tissue where elastic recoil is essential for maintaining tissue structure (Kyle *et al.*, 2009). Elastin is a highly insoluble cross-linked polymer of the monomeric protein tropoelastin. Tropoelastin is composed of two major domains. These include a hydrophobic domain and a cross linking domain. The hydrophobic domain is composed largely of glycine, valine and proline residues whilst the cross linking domain is rich in lysine and alanine. The alanine residues are important for providing gaps allowing the lysine residues to be fully exposed. This is vital for cross linking. The tropoelastin monomers become extensively cross linked in the ECM via the lysine residues and form large complex arrays (Figure 1.11). Cross linking is catalysed by various members of the lysyl oxidase (LOX) gene family. Most of the 40 lysine residues are covalently cross linked by LOX. The mechanism by which tropoelastin assembles into elastin is not very well understood. The cross linking of tropoelastin is essential for the stabilisation of elastin. This protects the protein from breaking down with age (Wagenseil and Mecham, 2007; Kyle *et al.*, 2009). Elastin in both forms is shown in Figure 1.8.

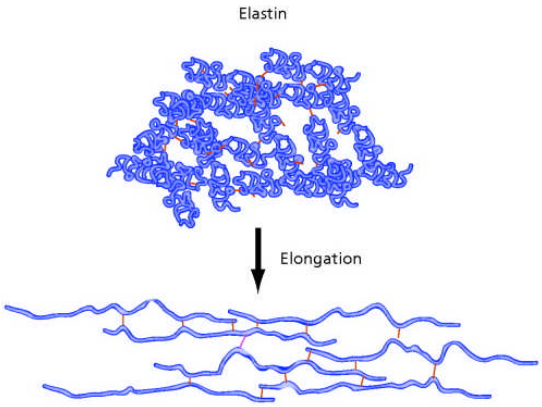


Figure 1.8: The structure of elastin before and after elongation. The ECM protein is composed of tropoelastin monomers which are cross linked via lysine residues. When tissue is stretched, the monomers become elongated. ECM: Extracellular matrix. (Derived from http://www.sigmaaldrich.com/life-science/biochemicals/biochemical-products.html?TablePage=21735546)

Elastin interacts with microfibrils of fibrillin, the second major component of elastic fibres. Fibrillins are cysteine-rich glycoproteins of which there are three types (Sakai *et al.*, 1991). These components are thought to provide a scaffold to which elastin can undergo molecular alignment and cross linking (Wagenseil and Mecham, 2007).

1.2.2 The IVD

The IVD is the largest avascular structure in the body and one of the most important structures in the spine. The IVD is attached to fibrocartilage which is blended in with the CEPs. The structure and composition of the IVD adapts to changes which occur through ageing. The main function of the IVD is to provide mechanical movement through six degrees of freedom including three translations and rotations. In addition, the IVDs support body weight and muscle loads and link adjacent vertebrae. The IVD is divided into two sections, the NP and the AF, as shown in Figure 1.9 (Keyes and Compere, 1932).

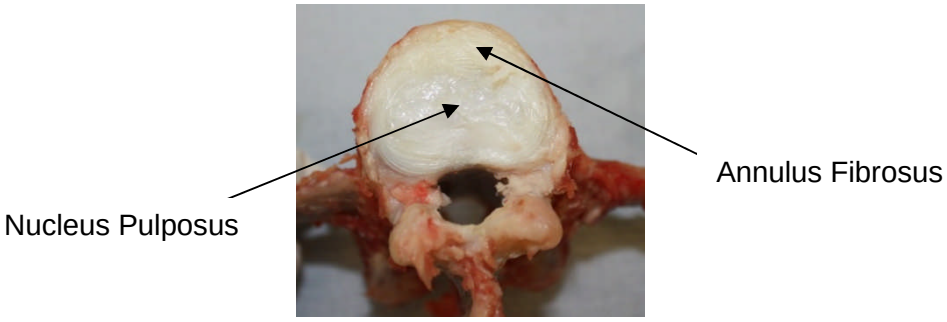


Figure 1.9: An ovine lumbar IVD attached to its vertebra. The IVD is divided into two main sections, the NP and AF. IVD: Intervertebral disc, AF: Annulus fibrosus, NP: Nucleus pulposus.

The AF is a tough collagenous structure arranged in lamellae layers comprised largely of collagen types I and II. The AF surrounds the NP which is a soft hydrophilic tissue in the centre of the IVD, consisting largely of water and GAGs. The composition of the ECM of both the AF and NP is important for their mechanical function (Urban *et al.*, 2000; Roberts *et al.*, 2006).

1.2.2.1. The NP

The NP is located in the centre of the IVD and consists of collagen fibers distributed randomly in a highly hydrated extrafibrillar matrix. The main components of the tissue are water (70-80 % of total weight), fibrillar collagens (20 % dry weight) and proteoglycans (30-50 % dry weight). Non-collagenous proteins are thought to make up the remainder of the dry weight (Eyre, 1979).

In the NP, type II collagen is the most abundant type. In addition, type IX, VI and III collagen have also been identified and these collagens interact with type II collagen fibrils forming an ECM network that surrounds the cells within the NP (Eyre, 1979; Beard *et al.*, 1980; Gan *et al.*, 2003A; Gan *et al.*, 2003B; Roughley, 2004). The major proteoglycans are aggrecan and versican, alongside small proteoglycans including decorin, biglycan, lumican and fibromodulin (Roberts *et al.*, 1994; Urban *et al.*, 2000). Melrose and Ghosh (1988) also identified elastin and fibronectin in the NP but did not characterise the distribution of these proteins in detail.

The concentration of GAGs within the NP is important for its function. GAGs form negatively charged groups, COO^- and SO_4^-, at physiological pH due to

ionisation. This attracts extracellular cations such as Na^+ within the NP achieving neutralisation. As a result, the ionic concentration within the NP is greater than that of the surrounding tissues. An osmotic pressure is thus created due to the attraction of water to the NP. This leads to high water content and a swelling pressure which acts on the AF and CEPs. During muscular activity, when pressure upon the IVDs increases the water content is at its highest (Urban *et al.*, 2000). This observed pressure allows hydration to be maintained and gives rise to the hydrodynamic and viscoelastic properties of the NP (Melrose *et al.*, 2001). Elastin has also been reported to be present within the bovine NP (Yu *et al.*, 2002). In this study, orcein immunostaining was used to visualise elastic fibres and their orientations were described. The elastic fibres appeared to run horizontally from the AF straight across the NP. In the sagittal plane, the fibres were shorter and radiated into the inner AF. In the central region of the NP, elastic fibres were aligned parallel to each other whilst near the end plate region the fibres were still parallel but vertically positioned towards the endplate (Yu *et al.,* 2002). As the main function of elastin is to allow tissues to return to their original orientation, elastic recoil after flexion, torsion and extension, it is an essential macromolecule and it would be of interest to investigate elastin distribution in the human NP. Elastin has been reported to make up 1.7 % of the dry weight of both the AF and NP in human IVDs (Mikawa *et al.*, 1986). Although this is a low percentage, the distribution of the elastin fibres is undoubtedly vital to the mechanical function.

The NP has a low cell density in comparison to other tissues. The NP is the remnant of the embryonic notochord. In humans, most notochordal cells, from early embryonic development, disappear within the first few years of life although some remain (O'Halloran and Pandit, 2007). It is unknown whether the lost cells are replaced by migrating cells from the AF or whether they differentiate into chondrocytes. It is known, however, that the cells of the NP are chondrocyte-like and are essential for maintaining appropriate levels of macromolecules through their synthesis and breakdown which contribute to the physiological and biomechanical functions of the NP (Gruber and Hanley, 2003). The chondrocytes of the NP are round in appearance and exhibit cytoplasm filled cellular processes. These cytoplasmic processes link adjacent

cells together forming cell clusters. With age, the processes become thinner leading to large extracellular spaces. However, there have been reports suggesting that cell cluster formation is associated with IVD degeneration which may be due to a matrix repair response (Johnson *et al.*, 2001). The NP has a low partial pressure of oxygen (pO_2) and an acidic pH in comparison to the AF (Holm *et al.*, 1981). This is likely to have great impact on the cells and molecular synthesis.

1.2.2.2. The AF

The AF surrounds the NP and makes up the remaining part of the IVD. In contrast to the soft NP, it is composed of tough collagen fibres arranged in lamellae in a proteoglycan matrix attached to the adjacent vertebra or the CEPs depending on location. These lamellar layers have a low percentage of water and aggrecan and a high percentage of collagen (Urban *et al.*, 2000; Roberts *et al.*, 2006). The layers are interwoven with each other and incomplete around the structure as shown in Figure 1.10.

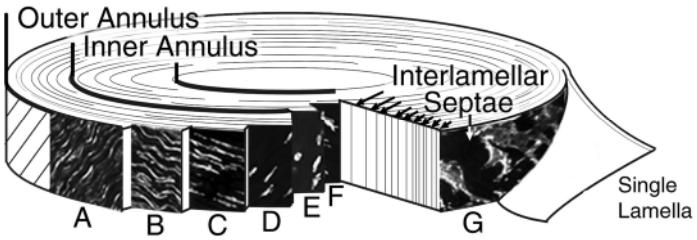


Figure 1.10: The structure of a typical AF. The AF is split into three distinct regions: the outer AF, the inner AF and the interlamellar septae. AF: Annulus fibrosus (Bruehlmann, 2002).

The AF is rich in both collagen types I and II in both human and animal tissues. The outer annular region is high in collagen type I, which accounts for approximately 70 percent of the dry weight. The inner region is nearly pure type II collagen (Eyre and Muir, 1977; Schollmeier *et al.*, 2000). In addition, the proteoglycan content has been reported to increase towards the inner annular region, increasing the hydration, whilst the collagen content decreases (Roberts *et al.*, 1994). This is mostly in the form of aggrecan, aggregated with hyaluronic acid. This is a major factor involved in resisting compressive forces generated in the FSU (Chelberg *et al.*, 1995).

As in the NP, elastin has an important role in the AF. Elastin has previously been located in bovine IVDs within the AF (Yu *et al.*, 2002). The elastic fibres were found to run parallel to the collagen fibres in the outer AF and were radially distributed in the inner AF forming a criss-cross pattern. Elastic fibres were particularly abundant in between lamellar layers of the AF, more so in the outer AF (Bruehlmann *et al.*, 2002). These features are believed to contribute to the realignment of the AF after loading and deformation which is essential since collagen fibres do not have great extensibility. Similar features exist in the human AF where there is an abundant and highly organised elastic fibre network (Yu *et al.*, 2005).

The organisation of cells has been reported to vary across the bovine AF and has been divided into two sections based on cell morphology, the inner and outer regions (Bruehlmann *et al.*, 2002; Horner *et al.*, 2002). The cells produce collagens and the ECM and like the NP, are present at very low density in comparison to other tissues. The outer layer of the bovine AF is composed mainly of fusiform shaped cells which have long, thin processes. The inner bovine AF contains spherical connective tissue cells which have only one or two short processes. Between the bovine lamellar layers is a connective tissue cell population of another type, the interlamellar cells. In this region the cells are flat and disc-shaped. Their cellular processes are typically broad and flat with many branching sites extended in various directions (Bruehlmann *et al.*, 2002).

1.2.3. The CEP

The CEPs separate the IVDs from the bone on the vertebral body. They have very important tensile and compressive biomechanical properties which support the IVDs when they function as well as providing stability and decreasing friction. The CEP makes direct connections with the IVD through the inner lamellae of the AF (Hukins, 1988). An important function of the CEPs is to provide a barrier allowing diffusion of essential nutrients to occur from the vertebral body to the IVD (Moore, 2000). Vascular terminations at the end plate have been studied by Crock & Goldwasser (1984) in greyhounds and they concluded through radiological and histological techniques that the central region is essential for the metabolic processes of the IVD. The rims of the end

plate into which the annular fibres are rooted do not allow any solute transfer. The central and annulus regions have been shown to be fully permeable (Holm *et al.*, 1981). However, as the CEP matures it undergoes mineralisation and resorption and is replaced by bone, limiting this function (Bernick and Caillet, 1982; Oda *et al.*, 1988; Moore, 2006).

The human CEP has been studied to some extent previously (Maroudas *et al.*, 1975; Roberts *et al.*, 1989; Roberts *et al.*, 1991B; Roberts *et al.*, 1994). It was described as a layer of hydrated proteoglycans within a network of collagen II fibrils. Proteoglycans appear to be important for regulating the transport of essential molecules through the IVD. This layer is less than 1 mm thick and thinnest towards the centre where the NP is present. The chondrocytes within the cartilage are homogeneously arranged but lack the specific structure displayed in articular cartilage (Maroudas *et al.*, 1975; Roberts *et al.*, 1989). The ECM of the CEP appears to be rich in collagen types II and X. Collagen X is important in cartilage calcification and has been found mainly in the central region of the CEP and increases in presence with age (Lammi *et al.*, 1998).

1.2.4. The Facet Joints

The facets joints are paired synovial joints found in each FSU along the length of the vertebral column (Figure 1.11). They comprise two facets, the superior and inferior articular processes, articulating together. The superior facet is a large posterior and medially facing process, whereas the inferior one is a smaller laterally facing process (Kalichman and Hunter, 2007). The main function of the facet joints is to enable motion of the vertebral column whilst resisting other forces including compression, shear and rotation (Haher *et al.*, 1994). Facet joints are part of a ‘three joint complex’ (two facet joints and an IVD) and contain articular cartilage, a joint capsule lined with synovial membrane and a joint space filled with synovial fluid. Some studies have been previously carried out to investigate the joint (Bogduk *et al.*, 1984; Taylor and McCormick, 1991; Ziv *et al.*, 1992; Yamashita *et al.*, 1996; Inami *et al.*, 2000; Boszczyk *et al.*, 2001A; Boszczyk *et al.*, 2001B; Yoganandan *et al.*, 2003; Elder *et al.*, 2009; Varlotta *et al.*, 2011A; Varlotta *et al.*, 2011B). The majority of these

studies however are focused on the facet joint as a whole, in particular the biomechanical aspects. Studies on the facet cartilage itself are lacking.

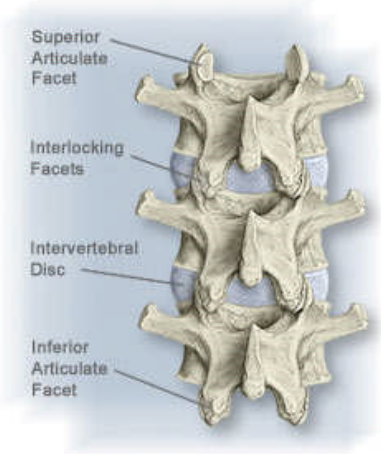


Figure 1.11: Facet joints along two FSUs. The facets joints are composed of two superior and two inferior facets which interlock together. (Derived from http://www.triangledisc.com/anatomy.php)

1.2.4.1. Articular Cartilage

Articular cartilage has a white and shiny appearance. In the facet joints, the cartilage covering the bone is thickest at the centre (Bogduk and Twomey, 1987; Buckwalter and Mankin, 1997; Temenoff and Mikos, 2000). Within articular cartilage there are different types of macromolecules, however, there is only one type of cell, the chondrocyte. The ECM comprises collagen, proteoglycans and non-collagenous proteins in tissue fluid (Buckwalter and Mankin, 1997; Temenoff and Mikos, 2001; Sandell and Aigner, 2001). Blood vessels and nerves are not present.

Chondrocytes make up a small proportion of articular cartilage; however, they are the most important component. This is due to the ability of chondrocytes to replace the ECM enabling the volume of cartilage to be maintained at the correct level whilst also maintaining the unique mechanical properties. At different zones within cartilage, chondrocytes can appear to be different in size and shape. In addition, structural features needed to sense mechanical changes within the matrix are also essential, such as cilia and other intracytoplasmic filaments. The highly metabolically active chondrocyte cells are very different and unique compared to other cell types. They are able to produce collagen, proteoglycans and non-collagenous proteins and arrange

them into a cartilaginous ECM (Buckwalter and Mankin, 1997; Temenoff and Mikos, 2000). Chondrocytes sit in a pericellular environment within chondrons or lacunae enclosed by a fibrillar pericellular capsule (Poole, 1997). The canine pericellular environment surrounding the chondrocyte has been reported to be rich in GAGs such as aggrecan with high concentrations of hyaluronan and link protein (Poole *et al.*, 1991). Fibronectin has also been shown to be present within the pericellular matrix alongside the small proteoglycan decorin which is thought to mediate collagen-proteoglycan interactions and may interact with other macromolecules within chondrons (Glant *et al.*, 1985; Scott, 1993). There is also collagen present within the pericellular matrix including type XI and II.

Water contributes up to 80 percent of the cartilage wet weight. Other components of the tissue fluid include gases, small proteins and metabolites. In order to balance the negative charge of proteoglycans, a large amount of cations are also present within the tissue fluid. Oxygen and nutrients are supplied to the articular cartilage through the exchange of tissue fluid with synovial fluid of the joint capsule. (Buckwalter and Mankin, 1997; Temenoff and Mikos, 2000).

The collagen content of the ECM of articular cartilage is composed of types II, VI, IX, X, XI, XII and XIV (Mackie *et al.*, 2011). The collagen fibres are organised into a tight meshwork which trap proteoglycan molecules. It is this structure which gives rise to mechanical properties of stiffness and strength in cartilage. Type II collagen is the most abundant making up almost ninety five percent of the collagen content in articular cartilage (Buckwalter and Mankin, 1997; Temenoff and Mikos, 2000). Various collagen types have been shown to be expressed in articular cartilage which has been shown to make up approximately two thirds of its dry weight. The importance of collagen in articular cartilage is due to its ability to form extensive cross links which gives rise to its material strength. The organisation of the collagen fibrils within articular cartilage varies in each zone. In the superficial zone, the fibrils run parallel to the surface and are thin with a small diameter. Below the superficial zone into the transitional zone the organisation of collagen is much more random with thicker fibrils. In the radial zone, the collagen fibrils bundle together

and orient themselves perpendicular to the surface (Eyre, 2002). The major collagen types in articular cartilage, including types II, IX and XI, do not appear to differ between the zones although this has been reported to change with maturation when the proportion of collagen II increases from 80 % to 90 %. The main function of collagen IX is to coat thin fibril surfaces by forming cross links. Collagen XI has a similar function and is also known to cross link with itself and collagen II and coat thin fibrils in the pericellular matrix (Eyre, 2002). Other minor collagens have been shown to exist in articular cartilage. This includes type I and III collagen which are both found in soft connective tissues such as the skin and muscle. These collagens are often associated with tissue repair and are expressed by osteoarthritic cartilage. Under these conditions, types I and III collagen co-exist together with type III making up a greater proportion than type I (Gay and Miller, 1978). Another study reported the expression of collagen III in the absence of collagen I in the superficial and transitional zones in osteoarthritic cartilage (Aigner *et al.*, 1993). However, a later study found that collagen type III is expressed in healthy articular cartilage (Wotton and Duance, 1991A). In addition to this, collagen III has been reported to co-localise with collagen II as a minor but regular component (Wu *et al.*, 1996). Collagen VI is another collagen type found in articular cartilage and is thought to make up less than 1% of the total collagen content (Eyre *et al.*, 1987). Its main function is to provide integrity to the structure of cartilage and acts as a bridging molecule by anchoring chondrocytes to the surrounding ECM (Pullig *et al.*, 1999). Studies have shown that collagen VI is located next to the cell membrane of chondrocytes in the pericellular matrix (Poole *et al.*, 1987; Poole *et al.*, 1988). Collagen X is found in the calcified zone of articular cartilage and is expressed by hypertrophic chondrocytes. It has important functions in the formation and development of the growth plate and calcified cartilage (Mayne, 1989; Eerola *et al.*, 1998).

Two classes of proteoglycans are commonly found in articular cartilage. These include large aggregating proteoglycans or aggrecan and small proteoglycans such as the leucine rich proteoglycans decorin, biglycan and fibromodulin (Mackie *et al.*, 2011). In addition, non-aggregating proteoglycans are also found. Most of the interfibrillar space in the ECM of articular cartilage is

occupied by aggrecan molecules described previously. Aggrecan enables GAGs to be fixed to the matrix whilst stabilising and organising the interaction with the collagen fibres. This anchoring function also prevents displacement of the macromolecules during deformation (Buckwalter and Mankin, 1997; Temenoff and Mikos, 2000).

Non-collagenous proteins comprise proteins with associated monosaccharides and oligosaccharides. Although wide varieties are thought to exist within articular cartilage, most are poorly understood. A common function of some of these proteins is to organise and maintain the structure of the ECM. Anchorin II and cartilage oligomeric matrix protein (COMP) have been studied to some extent and both proteins have been shown to bind to chondrocytes. This may help stabilise interactions between chondrocytes and collagen fibres in the ECM (Buckwalter and Mankin, 1997; Temenoff and Mikos, 2000).

Within typical, healthy articular cartilage, four cellular zones are found (Figure 1.12). These include the superficial, transitional, radial and calcified zones in order of depth (Broom, 1984; Buckwalter and Mankin, 1997).

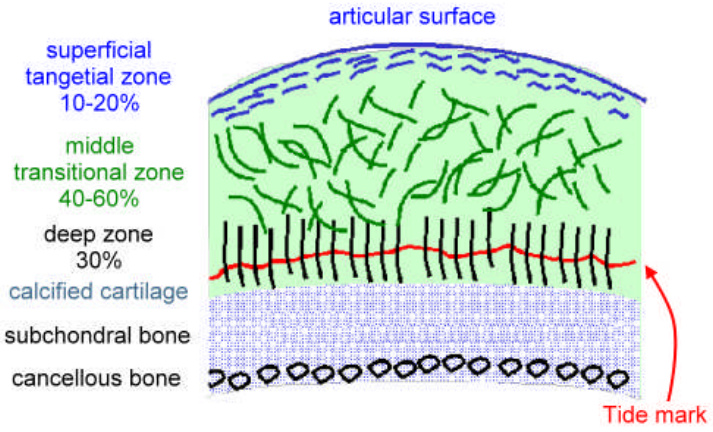


Figure 1.12: The organisation of collagen fibres into four zones in general articular cartilage. The structure consists of four major zones which lie above subchondral bone. (Derived from http://www.pt.ntu.edu.tw/hmchai/Biomechanics/BMmaterial/Cartilage.htm)

The first layer, the superficial zone, at the surface consists of collagen fibres and flat chondrocytes. The ECM within this zone contains large amounts of fibronectin and water. In addition, a higher proportion of collagen and smaller

amount of proteoglycans are seen in comparison to other zones giving this region of cartilage great tensile strength. The transitional zone contains clusters of chondrocytes in groups of three or four which are rounder in appearance. The ECM contains a larger number of collagen fibres and PG molecules and smaller amounts of water and collagen fibrils. The deep zone or radial zone also contains clusters of spherical chondrocytes; however, they are larger in groups of six to eight and stack on top of each other at right angles to the surface. The calcified zone is the deepest layer covering the subchondral bone. The chondrocytes found in this area are small and it has been suggested that there is very low metabolic activity in this region of cartilage due to the high content of calcified ECM (Bogduk and Twomey, 1987, Buckwalter and Mankin, 1997; Temenoff and Mikos, 2000).

1.2.4.2. The Joint Capsule

The main function of the joint capsule is to limit rotational forces whilst resisting backward sliding motions which result during extension (Cyron and Hutton, 1981). The macroscopic and microscopic morphology of the human facet joint capsule consists of a fibrous capsule and synovial membrane (Yamashita *et al.*, 1996). The synovium of the human joint capsule appears as a white, smooth tissue. Synovial cells produce the macromolecules present in synovial fluid which lubricates the joint. The synovium attaches to articular cartilage on one facet surface and stretches over the joint to the articular cartilage of the opposite facet (Bogduk and Twomey, 1987).

1.2.4.3. Synovial Fluid

Synovial fluid fills the space between two articular cartilage surfaces and nourishes them within the joint capsule. It is an ultrafiltrate of the blood, excluding haemoglobin and fibrinogen, and contains additives that are synthesised and excreted by the synovium. Its main function is to provide articular cartilage with lubrication and protection (Jay *et al.*, 2007; Katta *et al.*, 2008a). The main components of synovial fluid include hyaluronate and lubricin. Hyaluronate (Section 1.2.1.2.) gives the fluid viscosity whilst lubricin reduces friction during articulation. Lubricin is a mucinous glycoprotein produced by synoviocytes, the cells which line the joint capsule, and chondrocytes in the

superficial zone of articular cartilage (Section 1.2.4.1.; Jay *et al.*, 2007; Katta *et al.*, 2007). Other macromolecules are also present within synovial fluid which contributes to its lubricating properties. Small quantities of GAGs including chondroitin-4-sulphate, chondroitin-6-sulphate and keratan sulphate are present (Katta *et al.*, 2007).

1.3. The Biomechanics of the FSU

The spine supports the loads of the body whilst allowing six degrees of motion. The characteristics of these actions are defined by spinal biomechanics. Spinal biomechanics has been researched extensively and information concerning features such as spinal stability, torque resistance, intervertebral pressure and load bearing characteristics are readily available. When describing the geometry and motion of the FSU, a three axis coordinate system, involving an x, y and z axis, are used when referring to displacements such as rotation and translation. The FSU has six degrees of freedom (Smith and Fernie, 1991).

1.3.1. Load Bearing Characteristics in the FSU

If an axial load is applied to the vertebral column, axial compression on the IVD occurs. If the load is applied away from the centre of rotation, the vertebral column will bend whilst the upper vertebrae move in relation to the lower vertebrae (Smith and Fernie, 1991). The movements may be limited by the facet joints and the spinal ligaments which can also affect the extent of flexion (Smith and Fernie, 1991). The distribution of load along a healthy and degenerated FSU is shown in Figure 1.13.

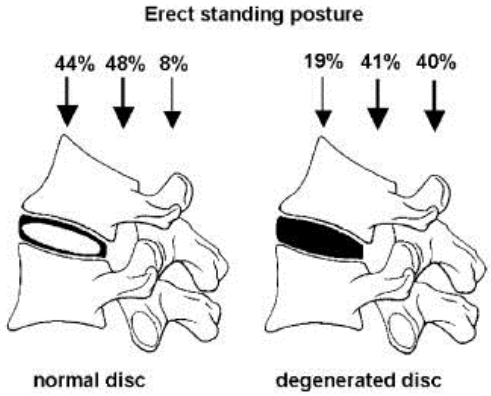


Figure 1.13: The distribution of load along a FSU as a percentage during standing. Left image: healthy disc, right image: degenerated IVD. IVD: Intervertebral disc. (from Adams and Dolan, 2005)

1.3.1.1. Compressive Load and the IVD

The AF of the IVD has layered collagenous fibres which are well suited for withstanding large compressive loads acting in various directions through the IVD. The fluid present in the NP deforms under pressure. However, due to its nature, the volume cannot be compressed. Therefore, compression forces are transmitted in all directions to allow deformation. As a result, when load is applied, the height of the NP decreases whilst the radial distance increases towards the AF. This eventually leads to equilibrium between the opposing tensions within the AF. The orientation of the fibres within the AF plays an important role in the mechanical properties of the IVD. For example, during circumferential loading, the fibres in that direction may reorient to increase their mechanical properties (Guerin and Elliot, 2006). As circumferential loading is the most common type of tensile loading, the fibres in this direction have the greatest tensile properties. Compressive forces are exerted on the CEPs above the NP. However, the deformation of the cartilage is small because it is attached to the vertebral body, therefore, the fluid in the NP does not undergo deformation in this direction. As the fluidity of the NP is determined by the proteoglycan and water content, any changes to this property will in turn alter the biomechanics of the IVD (Bogduk and Twomey, 1987).

1.3.1.2. Load Transmission and Motion in the Facet Joints

The facet joints provide the steady motion of the spine whilst preventing injury by limiting some movement. They play a major role in load transmission (Ewing

et al., 1972). As the posture of spinal column extends, the facet loads between two FSU's increases from between 22 and 25 % to 30 % of the applied load. Furthermore, the facet loads have been reported to be greater, up to 49 %, for FSU's affected by osteoarthritis. During full extension of the spinal column, the lower facet joints have been reported to support 16 % of the applied load. The facet joints resist torsion due to their bony interactions (Adams and Hutton, 1980; Adams and Hutton, 1981; Adams and Hutton, 1983; Yang and King, 1984). A study has also been carried out to determine the peak forces acting on the facet joints for different motions (Schendel *et al.*, 1993). It was found that while extension produced large forces on the facets, flexion generated none. They concluded that peak forces were found at the lateral and inferior margins of the superior facets.

1.3.2. Cartilage Biomechanics

Articular cartilage covers the facets of the FSU and exhibits low friction. The cartilage provides the facet joints with the essential biomechanical characteristics needed to maintain joint motion including wear resistance and shock absorbance (Ziv *et al.*, 1992; Lu and Mow, 2008; Varlotta *et al.*, 2011A; Latif *et al.*, 2012). The most important components of articular cartilage in relation to its function and biomechanics are the synovial fluid and cartilage ECM (Mow *et al.*, 1980; Mow and Hayes, 1997; Schmidt *et al.*, 2007A; Schmidt and Sah, 2007B). The movement of synovial fluid acts as a lubricant for the joint space in between the articulating cartilage surfaces. Articular cartilage is under constant tensile pressure which results from the balance between swelling forces and tensile strength during equilibrium. Swelling forces arise continuously within cartilage as a result of high concentrations of negatively charged proteoglycans. The macromolecules expand to occupy a large space; however, as the ECM is a collagen mesh, the molecules are prevented from reaching their full volume in solution. In addition, mobile counter ions are present within the tissue fluid which together causes the tissue to swell through the addition of water. The permeability of articular cartilage is low which indicates that the pressure generated is large. As a result of pressure, due to swelling or physical compression, fluid flows in and out of cartilage. This in turn

generates high frictional resistance which leads to the viscoelastic behaviour of articular cartilage.

1.3.3. Cartilage Lubrication

Surface friction exists between two un-lubricated surfaces rubbing against each other. The amount of friction generated is dependent on the surface area and strength of the two objects. In order to minimise surface friction, such as in synovial joints, lubrication is essential. A number of different lubrication regimes operate in cartilage to allow minimal friction under a range of different loading conditions. These many different lubrication mechanisms can be categorised under three main types occurring in synovial joints: fluid film, boundary and biphasic lubrication.

In fluid film lubrication, lubricant fills the joint space and keeps the two surfaces apart such as the superior and inferior articular process in the facet joint (Dowson *et al.*, 1969; Radin and Paul, 1972; Wright and Dowson, 1976; Schmidt *et al.*, 2007A; Schmidt and Sah, 2007B). In boundary lubrication the fluid film is negligible and the two surfaces touch; however, they are protected by boundary lubricants. In synovial joints effective boundary lubricants are thought to be hyaluronate and phospholipids. These molecules line the surface and prevent direct contact between the asperities of the surfaces (Katta *et al.*, 2008A).

Biphasic lubrication is thought to be the most important in articular cartilage. This is described as follows. The initial load is supported by the fluid phase of the cartilage tissue. As load increases it is gradually passed to the solid phase of collagen and proteoglycans as water flows out. The coefficient of friction is lower when load is carried by the fluid phase as compared to the solid phase. The biphasic lubrication mechanism operates over long periods of load bearing. During movement, the water content of the previously loaded tissue is replenished as the load is transferred to a different contact area on the surface of the cartilage. Continuous movement allows for the fluid phase to continue bearing the load at a lower coefficient of friction than if the load was borne by the solid phase (Katta *et al.*, 2008A).

1.4. Spinal Degenerative Disease

With age, spinal degenerative disease slowly develops. As a result of this natural process, each age group has a particular set of spinal characteristics. Spinal degenerative disease occurs as a result of continuous loads acting on the vertebral column which change the morphology and biochemical composition mainly of the intervertebral discs and facet joints. These spinal degenerative changes are referred to as spondylopathia deformans and can be subdivided based on the location of the degeneration. One common symptom of spinal degeneration is lower back pain which affects up to 84 % of the population at one point during their lifetime (Taylor and Twomey, 1986; Wang *et al.*, 1989; Prescher, 1998; Mosley *et al.*, 2012). There are potential risk factors associated with spine degeneration. For example, osteoarthritis is likely to increase with age. Also, an occupation involving the lifting of heavy objects and repetitive bending may increase susceptibility. Lifestyle and nutrition are also important factors (Pathria *et al.*, 1987). Currently, two imaging techniques are commonly used to diagnose spinal degenerative disease. These are computed tomography (CT) and magnetic resonance imaging (MRI). Both techniques are used to image abnormal changes such as articular cartilage thinning. However, studies comparing the effectiveness of CT and MRI have shown that MRI is less sensitive for detection of degenerative changes compared to CT imaging (Modic *et al.*, 1984; Nelemans *et al.*, 2001).

1.4.1. Degeneration of the Human IVD

The IVD allows load to be resisted by compression. In order to regulate the homeostasis of the tissue in the AF and the NP, a balance between anabolism and catabolism is constantly maintained. This is possible through regulatory molecules such as cytokines, growth factors and enzymes. However, due to degenerative pathology and age, this balance may be disrupted. This has been reported to eventually lead to the loss of essential macromolecules including proteoglycans and up-regulation of matrix-degrading enzymes (Antoniou *et al.*, 1996; Urban *et al.*, 2000; Cassinelli *et al.*, 2001; Cs-Szabo *et al.*, 2002; Urban and Roberts, 2003; Masuda *et al.*, 2004A; Masuda and An, 2004B; An *et al.*, 2006). Degeneration often results in a loss of IVD height and in turn prevents

the IVD from rehydrating after loading, increasing compressive stiffness (Kurtz and Edidin, 2006). In addition, IVD cells have been reported to cluster when becoming degenerate (Johnson *et al.*, 2001).

The enzymes reported to be responsible for the degradation of the IVD are matrix metalloproteinases (MMPs) (Goupille *et al.*, 1998; Roberts *et al.*, 2000; Freemont *et al.*, 2002; Gruber and Hanley, 2003; Le Maitre *et al.*, 2007). MMPs are secreted as inactive pro-forms which must be activated by cleavage of their N-terminal cysteine which exposes their Zn^{2+} catalytic site. There are four main subgroups of MMPs, the collagenases, stromelysins, gelatinases and membrane metalloproteinase. Each MMP within all four classes are capable of cleaving at least one component of the ECM (Goupille *et al.*, 1998).

The collagenases include MMPs 1, 8 and 13, and specifically cleave the triple helix of type I, II and III fibrillar collagens. These collagens are particularly important as they have been shown to make up over eighty per cent of the total collagen content in the IVD (Eyre, 1988). Collagen fragments may then be further cleaved by MMPs 2 and 9; the gelatinases, high levels of which have been found in degenerated IVDs (Crean *et al.*, 1997). In addition, MMP 3, also known as stromelysin, may also further degrade collagen fragments whilst also degrading proteoglycans, including aggrecan, and fibronectin. Aggrecan has been shown to be degraded by both MMPs and aggrecanase (Lark *et al.*, 1997; Roberts *et al.*, 2000).

The level of tissue inhibitors of metalloproteinases (TIMPs) plays an important role in the degeneration of the IVD. Four main types of TIMPs are known with TIMP-1 and TIMP-2 being the most studied. They bind non-covalently to MMPs and lead to inactivation (Goupille *et al.*, 1998). Some MMPs are more resistant to TIMPs than others, such as MMP-7, and studies have shown that TIMP-1 and TIMP-2 are up regulated in degenerate IVDs suggesting an attempt to restore homeostasis (Le Maitre *et al.*, 2004). Overall, however, the level of TIMPs is lower than that of MMPs leading to a deregulation of normal homeostasis (Le Maitre *et al.*, 2007).

Cytokines have also been shown to play an important role in the degenerative IVD by causing inflammation and pain (Le Maitre *et al.*, 2007). These cytokines can be divided into two groups, proinflammatory cytokines and anti-inflammatory cytokines. Proinflammatory cytokines are released during local inflammation and disappear after inflammation has passed. These include TNF-α and IL-1. Anti-inflammatory cytokines are induced by proinflammatory cytokines and have a tissue-repair function. These include IL-4 and IL-6 (Xing *et al.*, 1998; Igarashi *et al.*, 2004). IL-1 is thought to be involved in the regulation of ECM catabolism (Cawston *et al.*, 1999). Both of its isoforms, α and β, have been shown to increase the release of PGs and the production of degradative enzymes in the IVD. IL-1 has been reported to induce the production of MMPs whilst decreasing the production of TIMPs and also increase the production of pain mediators such as the eicosanoid prostaglandin E2 by human IVD cells (Martel-Pelletier *et al.*, 1994; Kang *et al.*, 1997). A report by Nemoto *et al.* showed that IL-1 increased MMP 3 production (Nemoto *et al.*, 1994). These studies suggest that the role of IL-1 in degeneration is to cause matrix degradation and pain (Freemont *et al.*, 2002).

IVD degeneration may occur as a result of poor nutrition to the CEPs and exposure to factors such as cigarette smoke and trauma (Urban *et al.*, 1977). There are several features and types of degenerative disease associated with the IVD. For example, osteophytes, also referred to as bone spurs, are small bone structures. They are believed to develop as a result of axial compression which squeezes the NP and in turn causes bulging of the AF. The annular bulging leads to the dislocation and tearing of the AF from the vertebral body rims (Osti *et al.*, 1992). Osteophytes are then formed from the elevated periosteum (Northfield, 1973). Their formation is thought to be accompanied by enlarged synovial fat pads in an attempt to cushion the surrounding area and increase their size to replace the lost tissue (Taylor and Twomey, 1986).

Chondrosis intervertebralis is a collective term used to describe two features of osteoarthritis in the spine. These are the loss of water from the NP and the decrease in height of the IVD. The IVD appears very dry and yellow/brown in appearance. The main effect of these changes is the reduction of the elasticity

of the IVD. The condition has been reported to worsen with age, with chronic overloading reported to increase the rate of development (Miller *et al.*, 1988; Prescher, 1998; Sarzi-Puttini *et al.*, 2005). Similarly, osteochondrosis intervertebralis is a condition in which the structure of the IVD changes and its height decreases. During this process it is common for the CEPs to be affected and occasionally completely destroyed. The cartilage cells may even proliferate forming ossifications. Ossifications may also be triggered by the production of blood vessels in the IVDs (Prescher, 1998).

1.4.2. Facet Joint Osteoarthritis: Spondylarthrosis

Spondylarthrosis is a collective term used to describe the degenerative changes which occur in the facet joints. Spondylarthrosis appears to affect mainly the cervical and lumbar regions of the vertebral column. This is due to the wide range of motion in the cervical region and the large load applied to the lumbar region. Similarly to IVD degeneration, its frequency increases with age (Ziv *et al.*, 1992; Prescher, 1998; Moore *et al.*, 1999; Tischer *et al.*, 2006; Kalichman and Hunter, 2007; Uhrenholt *et al.*, 2008; Gellhorn *et al.*, 2012; Simon *et al.*, 2012; Wilke *et al.*, 2012).

Recent work has suggested that cervical endplate arthrosis precedes facet arthrosis (Master *et al.*, 2012). However, several earlier studies investigated the possibility that IVD degeneration leads to facet joint degeneration (Dunlop *et al.*, 1984; Pathria *et al.*, 1987; Swanepoel *et al.*, 1995; Fujiwara *et al.*, 1999; Gries *et al.*, 2000). For example, if the IVD height within a FSU decreases, an increased load will be applied to the facet joint which will, in turn, lead to damage and cause pain. In addition, the loss in height may dislocate the articular processes of the facet joints placing the joint capsules under major stress. Changes in the IVD may also lead to cartilage erosion which decreases the joint space and allows the production of osteophytes. However, this remains debatable. There are neurons which surround and innervate the facet joint, such as the cervical facet joints, which have been shown to contain nervous tissue in the human and rat (Pathria *et al.*, 1987; Kallakuri *et al.*, 2012; Kras *et al.*, 2013). This is likely to be a major cause of pain following facet degeneration and its decreased joint space.

Osteoarthritis of the facet joints has been reported to exhibit similar features to that of other diarthrodial joints (Grenier *et al.*, 1987; Moore *et al.*, 1999). A common feature of the condition is cartilage degradation and the formation of osteophytes (Kalichman *et al.*, 2008). Fibrillation of cartilage has also been shown to occur such as vertical tears and tangential splits (Bogduk and Twomey, 1987). Studies have suggested that facet joint defects are more common on the superior facets rather than the inferior facets (Taylor and Twomey, 1986; Wang *et al.*, 1989). These points may be under considerable load and stress especially if the IVD is also undergoing degeneration (Jinkins, 2004). When the cartilage degrades, the joint capsule also becomes smaller, narrower and thin. This therefore limits the motion of the joint.

Proteoglycan degradation plays a major part in the degeneration of the ECM which leads to cartilage erosion. IL-1 is thought to be involved in cartilage catabolism by switching chondrocytes from anabolism to catabolism. TGF-β regulates cartilage anabolism therefore a net increase in IL-1 induces the breakdown of cartilage at the molecular level (Cawston *et al.*, 1999). As collagen makes up a large proportion of the structural proteins in cartilage, collagenases are also involved. The catabolism and loss of aggrecan is believed to also contribute to the development of erosion in articular cartilage. As catabolism of the macromolecule increases by proteolysis via aggrecanase, the population of hydrophilic GAGs decreases. As a result, the structure and therefore function of articular cartilage is lost (Caterson *et al.*, 2000; Sandell and Aigner, 2001).

Studies have been carried out to investigate the pathological changes in the facet joint during degeneration (Taylor and Twomey, 1986; Fletcher *et al.*, 1989; Moore *et al.*, 1999; Gries *et al.*, 2000; Kyriakos *et al.*, 2000; Boszczyk *et al.*, 2001A; Boszczyk *et al.*, 2003; Tischer *et al.*, 2006; Kalichman and Hunter, 2007; Uhrenholt *et al.*, 2008; Gellhorn *et al.*, 2012). Histological analysis carried out by Taylor and Twomey (1986) showed that degenerative changes in the lumbar facet joints occurred through aging, including severe cartilage fibrillation, gross thickening and irregularity of the calcified zone and an increase in collagen content in the superficial zone. In addition, there was a decrease in the

number of cells which appeared to have smaller nuclei and take up less haematoxylin than healthier cells and the subchondral bone plate decreased in thickness. A study conducted by Fletcher *et al.* (1989), who studied age related changes in the cervical facet joints, reported loss of articular cartilage and disorganised cortical margins. Histological analysis revealed a thin layer of articular cartilage which had a sparse matrix that was less basophilic than healthy cartilage and contained degenerated chondrocytes. There was an absence of menisci, which were present in younger, healthier specimens, and osteophytes were reported. Immunohistochemical analysis carried out on the ECM of a degenerated human posterior lumbar facet joint capsule by Boszczyk *et al.* (2003) showed that type I, III and VI collagens were found distributed throughout the joint capsule as in healthy joints. However, a large amount of collagen II was detected around the entire joint. GAGs such as keratan sulphate and chondroitin 4 and 6 sulphate were distributed widely in the degenerated joints. In particular, chondroitin-6-sulphate was found around the attachment of the joint capsule. There was an abundance of aggrecan and link protein which was detected throughout the joint. The authors reported extensive fibrocartilage proliferation around the posterior capsules, evident largely at the margins, and suggested that this feature of degeneration was due to the fact that the posterior capsule is the main ligamentous structure of the FSU which resists axial torsion (Boszczyk *et al.*, 2003).

1.4.3. Degeneration of the FSU with Age

Histological, biochemical and biomechanical differences have been reported to occur in FSUs of different ages (Bernick and Cailliet, 1982; Miller *et al.*, 1988; Moore *et al.*, 1999; Urban *et al.*, 2000; Urban *et al.*, 2003; Roberts *et al.*, 2006). For example, decreased PG content, loss of disc height and increased compressive stiffness occurs with age. These changes have been commonly identified and tracked via the use of grading systems (Weishaupt *et al.*, 1999; Gries *et al.*, 2000; Sive *et al.*, 2002; Kettler and Wilke, 2006; Tischer *et al.*, 2006; Li *et al.*, 2011; Varlotta *et al.*, 2011A; Lee *et al.*, 2012). Various grading systems exist in the literature depending on the tissue type, the type of degeneration present and the method used to analyse it. For example, histological changes can be identified through the use of stains such as

haematoxylin and eosin and alcian blue. A grading system that can be used on these tissue sections includes examining the AF, NP, CEP and subchondral bone for changes in their structure including lamellar disorganisation, cell necrosis, trabecular thickening and cartilage thinning (Gries *et al.*, 2000). Another system involves grading the degeneration features within the IVD. This includes the presence of cell clusters, fissures, haematoxyophilia and demarcation (Gries *et al.*, 2000; Sive *et al.*, 2002). Degenerative changes have also been identified through other methods such as MRI and CT imaging. Features such as facet joint space have been measured and graded on a scale from zero to three (Weishaupt *et al.*, 1999). Furthermore, photography can be a useful tool for examining the physical appearances of surfaces such as the facet cartilage and joint capsule. Facet surfaces have been graded by assessing the glossiness of the surface to reflect the amount of defects present (Tischer *et al.*, 2006; Kettler *et al.*, 2007).

1.5. Current Therapies for the Degenerated Functional Spinal Unit

Degeneration of the IVD and facet joints is a major factor contributing to lower back and neck pain (Lewinnek and Warfield, 1986). Back pain will affect up to 84 % of people at some point in their lives. It is a major public health problem in Western society leading to disability and economic loss through work absence, physician visits and hospitalisation (Maniadakis and Gray, 2000). Research into treatment strategies is currently ongoing and involves spinal fusion, total disc replacement (TDR) and tissue substitution therapies including tissue engineering. Spinal fusion is a procedure whereby two or more vertebrae are fused together by removing one or more IVDs and replacement using a bone graft or bone graft substitute. This process may or may not involve the use of materials such as plates, screws or cages. The aim of spinal fusion is to remove the source of pain, the IVD, and restrict motion of one or more FSUs (Chou, 2013). Despite the fact that spinal fusion is commonly used today, it is not the desirable method of treatment as the function of the tissues is not restored and some patients may develop additional disease in FSUs adjacent to the fusion site, due to compensatory motions. For this reason, tissue engineering has received much attention over the last decade and has great potential for the

development of effective treatments which restore tissue function and eliminate pain (Yang and Li, 2009). In addition to tissue engineering another common approach with the aim of restoring function to the FSU of vertebrae includes TDRs (van den Broek *et al.*, 2012). This section summarises the recent advancements made in approaches to therapy.

1.5.1. Analgesics

Certain groups of drugs are commonly prescribed to patients suffering from various forms of back pain in attempt to relieve their pain. These drugs improve quality of life rather than offering a permanent cure to their condition. They all have advantages and disadvantages in relation to their benefits, risks and cost (Chou *et al.*, 2007).

Non-steroidal anti-inflammatory drugs (NSAIDS), such as aspirin, are the most common class of drugs administered to patients suffering from lower back pain. Studies have investigated their effect on patient symptoms showing that they are effective for acute back pain (Koes *et al.*, 1997, van Tulder *et al.*, 2000). However, limitations associated with these drugs also need to be considered, such as the gastrointestinal and renovascular risks (Hernandez-Diaz and Rodriguez, 2000). A safer drug that can be used instead of NSAIDs is acetinophen, which is also lower in cost. The drug is weaker than a NSAID but can be used effectively in the first instance as pain relief for acute lower back pain (Towheed *et al.*, 2003; Lee *et al.*, 2004B; Wegman *et al.*, 2004).

Other drugs include opioid analgesics or tramadol which is given to patients who do not respond to either NSAIDs or acetaminophen (Furlan *et al.*, 2006; Martell *et al.*, 2007). Skeletal muscle relaxants including tizanidine, carisoprodol and dantrolene have also been reported to provide relief for lower back pain but may cause side effects relating to the central nervous system (van Tulder *et al.*, 2003). Tricyclic antidepressant drugs and herbal therapies are also commonly used today in the clinic (Staiger *et al.*, 2003; Gagnier *et al.*, 2007).

1.5.2. Physical and Rehabilitation Medicine

As the cause for most back pain in the general population is muscular, physical and rehabilitation medicine is commonly used today. This includes various treatments such as exercise therapy, massage and superficial cold and heat (Abenhaim *et al.*, 2000; Furlan *et al.*, 2002; French *et al.*, 2006). The type of treatment prescribed will depend on the individual needs of the patient and different patients will find some methods more effective than others (Deyo *et al.*, 1983; Deyo *et al.*, 1986; van Middelkoop *et al.*, 2011). Although many of these treatments have been reported to relieve back pain for some patients, the condition is rarely cured especially for non-muscular related back pain.

1.5.3. Spinal Fusion

Spinal fusion was first described in 1911 and used to treat a variety of spinal disorders. It involves the fusion of two or more vertebrae using materials such as screws and bone grafts and prevents motion in order to eliminate pain (Chou, 2013). Spinal fusion is commonly carried out today and has been reported to lead to some improvement in quality of life (Lee and Langrana, 2004B; Djurasovic *et al.*, 2011). However, several studies have shown that this procedure leads to adjacent segment disease (ASD) (Hsu *et al.*, 1988; Schlegel *et al.*, 1996; Chen *et al.*, 2001; Phillips *et al.*, 2002). ASD is an abnormality in the FSUs next to a spinal fusion. This includes IVD degeneration such as herniated NP (Park *et al.*, 2004). In addition, spinal fusion does not restore function of the diseased FSU and can lead to other complications (Deyo *et al.*, 1993). As a result, this may not be the ideal form of treatment for many patients.

1.5.4. Total Disc Replacements

Total disc replacements (TDRs) have been studied since the 50s following the success of total hip and knee replacements. They aim to restore and maintain motion within an FSU thereby preventing degeneration in adjacent FSUs and eliminating pain. TDRs that have been used clinically include the Charitè, ProDisc L, Maverick, Acroflex and Flexicore (van den Eerenbeemt *et al.*, 2010).

The Charitè TDR was the first available TDR and has a dual bearing surface enabling the centre of rotation to move as the implant articulates. Three types of

the Charite TDR exist. All types consist of two highly polished cobalt-chromium-molybdenum end plates articulating with a core composed of ultra-high molecular weight polyethylene (UHMWPE). The differences between the three types are due to changes in end plate thickness and the number of teeth anchoring them onto the vertebra (Putzier *et al.*, 2006). The clinical success of the Charitè TDR was reported in 1997 after a 51 month follow up and in 2005 after an 11.3 year follow up (Lemaire *et al.*, 1997; Lemaire *et al.*, 2005). The results from these studies showed good/excellent results reporting infrequent pain that did not require medication and continuation of activity in the same job within three months of arthroplasty. The Charitè TDR has proven to effectively restore motion and functionality within the FSU in the absence of facet joint degeneration.

Another TDR that has been used clinically is ProDisc L. This is similar to the Charitè and is composed of a UHMWPE core which articulates with two concave cobalt-chromium-molybdenum alloy endplates. Studies have claimed that the TDR is safe for use in patients and effective in restoring a normal range of motion and is statistically more effective than spinal fusion (Zigler *et al.*, 2007; van den Eerenbeemt *et al.*, 2010).

The Maverick disc is a metal on metal ball and socket TDR resembling the ProDisc L. It consists of two metal plates and articulates with a small radius core. It does not allow for pure translation and is therefore semi-constrained (Mayer, 2005). A study by Le Huec *et al.* showed an overall clinical outcome of 86 % success (Le Huec *et al.*, 2004).

There are, however, concerns regarding whether overall clinical outcome is beneficial using the Charitè, ProDisc L and Maverick TDRs as these are all ball and socket designs which lead to rigid axial motion therefore providing motion which is different to that in the natural IVD. This may lead to facet overloading, adjacent segment disease and wear. In terms of these factors TDRs are not superior to spinal fusion. This led to the development of the first deformable TDR, the Acroflex (van den Broek *et al.*, 2012). The AcroFlex TDR was composed of two titanium end plates which were bound together by a hexane-

based polyolefin rubber core. However, the material was shown to fail under mechanical loading and was abandoned (Fraser *et al.*, 2004). The Flexicore was developed and similarly to AcroFlex contains two titanium endplates and the classic ball and socket design. However, studies indicate a small overall success rate and little clinical improvement compared to spinal fusion (van den Eerenbeemt *et al.*, 2010).

Currently, non-ball and socket TDR devices are being developed to avoid issues with range of motion in order for natural IVD biomechanics to be mimicked. These include polycarbonate urethane designs such as the Physio-L. However, these still need to be studied clinically over the longer term to determine the success *in vivo* (van den Broek *et al.*, 2012).

1.5.5. Facet Joint Therapies

Common procedures to reduce the pain within the facet joints are intra-articular injections of local anaesthetics and steriods, medial branch blocks and radio frequency neurolysis. Although thought to be effective, there is no way of biologically accessing the effectiveness of these forms of treatment. Numerous studies have been carried out to evaluate the clinical outcome of intrarticular injections to reduce pain (Esses and Moro, 1993; Zdeblick, 1995). However, many of these studies were flawed due to false positive results arising from poor study design. For example, a study by Lilius *et al.* (1989) which investigated the effectiveness of lumbar steroid facet joint injections included patients with neurological deficits and did not report their diagnosis. The results from this study failed to exclude the placebo group. Another study by Barnsley *et al.* (1994) included patients who were victims of whiplash and might not have had pain originating from the cervical facet joints. A study by Carette *et al.* (1991) included results from a placebo group in the overall success rate. However, the results of a review which looked into a wide range of therapeutic facet joint interventions concluded moderate evidence for short and long term lumbar facet joint pain relief for intra-articular injections, moderate evidence of cervical and lumbar facet joint pain relief using medial branch blocks and moderate to strong evidence of cervical and lumbar facet joint pain relief using radiofrequency facet neurolysis (Boswell *et al.*, 2005).

Facet fusion systems have been described for many years. Recently, a fuse system has been developed for fusing lumbar facet joints called the TruFUSE, an allograft milled bone dowel. It was designed to be a less intrusive method of spinal fusion specifically for the facet joints. The clinical success rates have so far been promising with 95 % of patients in one study showing signs of spinal stability (Maroon *et al.*, 2013). However, this study was conducted by only one surgeon on 41 patients. Further clinical studies involving larger groups will need to be conducted to provide a more accurate assessment of this form of treatment.

1.6 Novel Approaches for the Treatment of the FSU

Tissue engineering is an approach to the problem of repair or replacement of degenerate tissues. It involves designing and manufacturing neo tissues *in vitro* with a view to restoration or replacement of a diseased or damaged tissue *in vivo*. This is a highly multidisciplinary activity involving bioengineering and biomechanics through to cellular and molecular developmental biology and morphogenesis. Three factors believed to be essential in tissue engineering are; inductive signals, responding cells and the ECM or 'scaffold'. The microenvironment of a natural ECM in particular can be replicated by the use of important macromolecules such as collagen, proteoglycans and GAGs (Reddi, 2000). Tissue engineering aims to develop tissues *in vitro* which can be used to replace tissues in patients that are degenerated or are likely to degenerate. This approach is favoured over the use of synthetic replacements due to its regenerative capacity.

The generation of new FSU tissue, including the IVD, CEP and facet cartilage, via tissue engineering is highly desirable. Methods have been investigated to generate tissue engineered articular cartilage; however these are limited to *in vitro* studies or studies in animals (Kheir *et al.*, 2011; Shahin and Doran, 2011). Tissue engineering methods have been used to produce an AF and NP *in vitro* (Rong *et al.*, 2002; Sato *et al.*, 2002; Gan *et al.*, 2003B). Many recent studies have focused on tissue engineering of the NP as this tissue is believed to be the initial site of IVD degeneration (Yang and Li, 2009). However, other authors

argue that in patients with severe IVD degeneration, without a functional AF, the NP product itself will fail to regenerate the IVD as the AF is essential for resisting pressure (Jin *et al.*, 2013).

Despite the fact that tissue engineering in the spine aims to restore tissue function and maintain movement and flexibility, there are various limitations which need to be addressed before this approach can be translated to the clinic. The first issue to consider is the source from which the cells are obtained and the cell type. There are a range of cell types that can be used including autologous or allogeneic cells of adult or embryonic origin. The cells may be obtained from the same tissue type that will be repaired or may be sourced from a different tissue. The optimal cell type has not yet been identified as there are limitations associated with each. Autologous cells isolated from the IVD may seem ideal, but problems arise due to the low cell number within the IVD and the varying cell phenotypes within the structure (Mwale *et al.*, 2004). In addition, isolation of IVD cells would involve trauma to the AF and NP, causing biochemical and biomechanical damage to these structures which may potentially lead to further degeneration. Even if cells were successfully obtained from the tissue, the issue of cell viability and metabolic activity would need to be considered, as a large proportion of IVD cells have been shown to die through apoptosis due to cell senescence (Gruber and Hanley, 1998). Autologous adult stem cells could also present limitations due to the lack of information on the characteristic molecular profile of AF and NP cells which would cause uncertainty as to whether the stem cells might be differentiated to the correct phenotype (Kandel *et al.*, 2008). Embryonic stem cells have been shown to be capable of producing IVD tissue (Ahmed *et al.*, 2007). However, the use of these cells is very controversial and there are safety and immunological issues associated with their use.

There are a wide range of biomaterials which have been studied as scaffolds for tissue engineering in the spine. Most of these biomaterials have advantages and disadvantages associated with them and there are many factors that need to be taken into consideration when deciding on the ideal scaffold. Once an ideal tissue engineered IVD is developed, whether it be a tissue engineered NP

or an IVD consisting of both an AF and NP, the method of implantation needs to be carefully considered. This is likely to have a marked effect on whether tissue engineered products will succeed in the clinic. Invasive surgery is not ideal but in many approaches would be unavoidable. For a whole tissue engineered IVD to be implanted, there would need to be some form of bony end plate to allow the implant to integrate with the vertebral body via bone ingrowth (Porto Filho *et al.*, 2005; Kandel *et al.*, 2008).

The success of tissue engineered implants may be limited by factors such as disc nutrition and mechanical loading. The CEP provides a barrier for the diffusion of nutrients from the blood vessels which surround the IVD such as capillaries which penetrate the subchondral plate. The CEP commonly becomes calcified during degeneration which limits nutrient and oxygen supply to the IVD. As the IVD cells generate ATP through glycolysis alone, this leads to low glucose supply and the accumulation of lactic acid. This in turn leads to degeneration of the IVD. Therefore, if the CEP is calcified, a tissue engineered IVD would soon degenerate irrespective of its healthy state at insertion. The mechanical properties of the IVD will ultimately depend on the organisation and composition of the macromolecules within the tissue. Therefore the mechanical properties of the natural IVD would need to be replicated to enable correct physiological responses *in vivo*. If the implant does not have the correct levels of macromolecules and is reliant on the cells producing the ECM once implanted, issues may arise due to the slow matrix production and turnover of IVD cells. It may therefore take months or years to regenerate the implant for the ECM to be similar to that of the native tissue (Kandel *et al.*, 2008).

In all cases, it is important to consider patient specificity. All forms of tissue engineering of the IVD may not be applicable to all patients. For example, a patient in the early stages of IVD degeneration may only need a cell-based treatment whereas a patient in the later stages of IVD degeneration is likely to benefit from a whole tissue engineered IVD using a scaffold.

Various biomaterials have been investigated over the last decade as support scaffolds for IVD cells, retaining them in a particular location and allowing them

to naturally produce an ECM *in vitro*. Examples of these are chitosan based hydrogels, type II collagen/aggrecan/hyaluronan, fibrin/hyaluronan, poly(L-lactic acid) (PLLA)-hyaluronan nanofibres and hyaluronic acid. Each has advantages and disadvantages with regard to future clinical use.

1.6.1. Hydrogels for NP Replacement

Various hydrogels have been developed and researched as potential NP therapies (Sun *et al.*, 2001; Park *et al.*, 2005; Boyd and Carter, 2006; Roughley *et al.*, 2006; Bader and Rochefort, 2008; Chou and Nicoll, 2008; Halloran *et al.*, 2008; Yang and Li, 2009; Park *et al.*, 2011). Hydrogels are a favourable biomaterial as they would be easy to administer to the patient in an injectable form in a relatively non-invasive way and prepared in a simple and controllable manner. Hydrogels allow the NP cells to be kept in a 3D environment, allowing cell-matrix interactions to be maintained which is essential for cell proliferation, differentiation and survival (Boyd and Carter, 2006). In addition, hydrogels facilitate diffusion of nutrients and metabolites to and from cells (Drury and Mooney, 2003).

Chitosan is a polymer of glucosamine and N-acetyl glucosamine and can be induced to form a hydrogel by two methods, self-association or covalent cross linking. Bovine NP cells were incorporated into a chitosan-based hydrogel and maintained in tissue culture (Roughley *et al.*, 2006). It was shown that the scaffold was able to retain the proteoglycans produced by the entrapped cells using either method of hydrogel induction. The authors concluded that this approach may be used for NP regeneration. The benefit of this study is that the therapy, if successfully developed, could be administered to the patient in the form an injection through the AF into the NP. This would be a relatively non-invasive procedure in comparison to IVD replacements. Polymerisation can be controlled *in situ* which would allow for easy administration. In addition, cellular entrapment of hydrogels does not depend on scaffold pore size.

Another injectable scaffold that has been developed involved the use of collagen type II, aggrecan and hyaluronan (Halloran *et al.*, 2008). In this study, bovine NP cells, previously isolated and expanded in monolayer culture, were

seeded onto the enzymatically cross-linked injectable scaffold. This scaffold consisted of all the major macromolecules found in the ECM of the NP. In order to increase the biomechanical properties of the hydrogel whilst retaining its injectable qualities, microbial transglutaminases (mTGases) were used to cross link the proteins within the scaffold. The results showed that cell viability and phenotype was maintained for over seven days *in vitro*. However, mTGase concentrations of greater than 50 $\mu g.ml^{-1}$ had a negative effect on cell viability, which in turn meant that there was a need to compromise between scaffold stability and cell viability.

A further study, also looking into developing an injectable NP replacement, was carried out by Chou and Nicoll, involving the use of photocrosslinked alginate hydrogels to encapsulate bovine NP cells (Chou and Nicoll, 2008). Alginate is a polysaccharide derived from brown algae which forms cross links in the presence of calcium. However, this means stability is dependent on calcium which may not be available *in vivo*. Therefore this study used ultraviolet (UV) light to initiate polymerisation. The results showed that the NP cells within the scaffold were capable of producing and maintaining proteoglycans which maintained osmotic pressure *in vitro*. In addition, the equilibrium Young's modulus was maintained. However, the findings showed that increasing the cross links within the scaffold compromised cell viability. In addition, greater cross linking may give rise to a stiffer gel putting the essential elastic properties of the NP at jeopardy.

In order to tackle the issues surrounding biomechanical strength and cell viability Park *et al.* investigated an injectable scaffold made from silk-fibrin and hyaluronic acid (Park *et al.*, 2011). As fibrin/hyaluronan scaffolds had previously been shown to degrade rapidly (Park *et al.*, 2005), a silk component was mixed with the fibrin/hyaluronan scaffold to improve the biomechanical strength and reduce shrinkage of the scaffold. The results showed that appropriate biomechanical and biochemical properties including uniform NP cell distribution were achieved. In addition, degradation of the scaffold was decreased whilst maintaining NP cell growth. A limitation of the study was reduced cell proliferation with increased silk content. Although a compromise must be

reached between these two factors the study achieved this and appears promising for further studies in NP regeneration.

1.6.2. Tissue Engineering of the AF

Some forms of degenerative disc disease such as disc herniation are more suitable for treatment which involves replacing parts of the AF through which the NP has escaped. For these cases, tissue engineering a patch of AF to fill the defect and integrate with the undamaged tissue is more applicable than attempting to replace the whole IVD. It would also be more cost effective and less invasive.

Various studies have been carried out in AF tissue engineering using scaffolds similar to those used in NP tissue engineering such as porous silks, alginate/chitosan, nanofibrous polyurethane, electrospun poly(ϵ-caprolactone), atelocollagen honeycomb, collagen/GAG and poly-D-L-lactide (PDLLA)/bioglass foams (Sato *et al.*, 2002; Saad and Spector, 2004; Nerurkar *et al.*, 2007; Shao and Hunter, 2007; Helen and Gough, 2008; Chang *et al.*, 2009; Yang *et al.*, 2009; Koepsell *et al.*, 2011; Bhattacharjee *et al.*, 2012; Jin *et al.*, 2013). Scaffolds used in tissue engineering of the AF can be divided into the two categories. These are single unit, which are subdivided into orientated and non-orientated with respect to the lamellae layers, and biphasic which represents both the inner and outer layers of the AF. Many of these studies have shown positive results and could be further developed to be implanted into patients. However, the studies are still in the early stages and the authors have not indicated how the constructs could be tested and used clinically.

Porous silk scaffolds have received great attention due to the nature of silk fibroin, a protein polymer made by silk worms. Silk fibroin is the strongest known natural fiber, shows resistance to failure and naturally degrades *in vivo* after two years (Chang *et al.*, 2007). A study by Chang *et al.* (2009) investigated whether porous silk scaffolds were able to support AF cell attachment and ECM accumulation. The authors found that cells successfully adhered to the scaffold and synthesised collagen and proteoglycans. However, the scaffold represented the general AF structure rather than an inner or outer AF. This may

lead to structural variations if it was implanted into a patient. In addition, the scaffold was only tested *in vitro*. There was no mention of how the construct would be implanted into the patient in the future. Other studies using the materials above have also succeeded in producing promising biological results for *in vitro* tissue engineered AF replacements but fail to identify the method by which they envisage the construct will be tested for *in vivo* use.

1.6.3. Tissue Engineering of the Whole IVD

In addition to NP and AF replacements, other studies have focused on developing a whole tissue engineered IVD using a dense scaffold for the AF together with a hydrogel component for the NP (Mizuno *et al.*, 2004; Mizuni *et al.*, 2006). Mizuno *et al.* developed a tissue engineered IVD using a synthetic nonwoven mesh of polyglycolic acid fibres and an alginate gel containing ovine IVD cells (Mizuno *et al.*, 2006). The IVD was then transplanted into mice and analysed at time points up to 16 weeks. The results revealed that shape was maintained *in vivo* and tissue/ECM formation had occurred. Certain biomechanical properties including compressive modulus and hydraulic permeability increased and decreased, respectively, with time. The authors stated that by 16 weeks, mechanical and biochemical composition was similar to that of the native tissue. However, further work needs to be carried out to ensure that identical properties are reached. Other challenges still need to be addressed including how the implant could be scaled to the size of a human IVD and delivered into the patients' spine and how it would be integrated with surrounding tissues.

Other materials used to generate both an AF and NP include using hyaluronic acid-nanofibrous and poly(caprolactone)/chitosan scaffolds (Nesti *et al.*, 2008; Wan *et al.*, 2008). Both of these studies reported acceptable biomechanical properties, ECM production and cell morphology.

1.6.4. Tissue Engineering of the Facet Cartilage

Various studies have researched ways of tissue engineering articular cartilage (Mahmoudifar and Doran, 2005; Schulz and Bader, 2007; Stapleton *et al.*, 2010; Kheir *et al.*, 2011; Shahin and Doran, 2011). Currently, facet cartilage has not

been tissue engineered. A study by Elder *et al.* (2010) attempted to create a tissue engineered replacement of the facet cartilage using a common process known as decellularisation. This procedure involves the removal of cells and immunogenic cellular proteins and nucleic acids whilst preserving the function of the ECM. Decellularisation is ideal for cartilage tissue engineering as the major functions of the tissue are due to the ECM. In addition, successful studies have been carried out on cartilage from other joint areas including the knee using this method (Kheir *et al.*, 2011). The results from the Elder study, however, failed to report an effective method for decellularisation of facet cartilage. A compromise between the complete removal of DNA content and the maintenance of biochemical and biomechanical properties was not achieved. However, the study is a starting point for research in tissue engineering of facet cartilage which is likely to grow in the future.

1.7. The Need for Pre-Clinical Models

Many studies, as described in Section 1.6, have attempted to produce substitution therapies for the spine by tissue engineering. However, what many authors fail to address is how these products will be pre-clinically tested for their effectiveness and safety. This is a vital step before they can be used in patients.

Once a potential substitution therapy is created, ideally the next step in its development towards clinical use would be testing using a pre-clinical *in vitro* model, prior to testing in living animals and then patients. One approach towards developing a pre-clinical *in vitro* model is to utilise natural joint tissue in a whole joint simulator, which reproduces the natural biomechanical motions of the spine. Ideally, the tissue engineered replacement or substitution therapy would be tested in both healthy joint tissue and joint tissue representative of the degenerated form of the tissue of interest in a simulator. The product would then be applied to the model, as it would *in vivo*, and then analysed following a period of simulation.

There are a number of factors limiting the use of human tissue for the development of *in vitro* models. These include availability of fresh tissue and

the wide variation in human tissue, including geometrical and mechanical differences with regard to age, sex, bone quality and degenerative changes (Sheng *et al.*, 2010). The sheep was chosen as the animal model for this study and was used throughout the entire study. This was due to its close resemblance to the human spine in terms of the anatomical, biomechanical, biochemical and biological properties, for example axial rotation as shown in Figure 1.14.

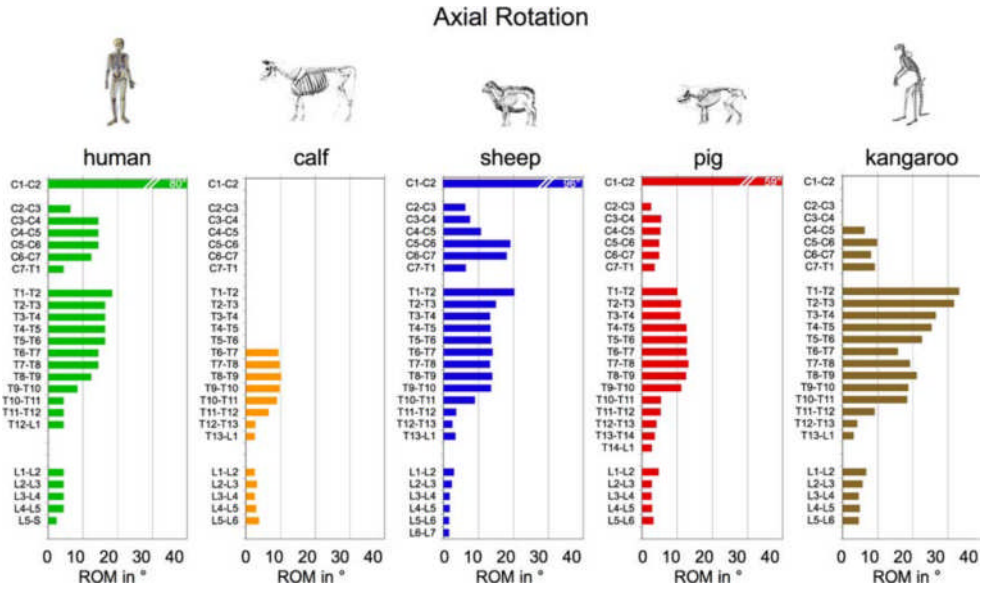


Figure 1.14: A biomechanical profile of the human, calf, sheep, pig and kangaroo. The median degree of range of motion is shown in left and right axial rotation in each FSU (White and Panjabi, 1990; Alini *et al.*, 2008).

Studies have identified various similarities between the human and ovine spine (Moore *et al.*, 1999). For example, the dimensions of the ovine spine such as vertebral body height, facet height, facet width and IVD height all show similarities, which support the use of ovine spine for research in all cervical, thoracic and lumbar regions (Wilke *et al*., 1997; Kandziora *et al*., 2001). A biological similarity is the rapid decrease of notochordal cells in the NP after birth. This has been reported to occur in humans but not in other animals such as the mouse, pig and rabbit. This may have an effect on disc degeneration since the notochordal cells and the NP cells have very different morphology and function which could interfere with studies of the IVD (Hunter *et al.*, 2003; Hunter *et al.*, 2004). Furthermore, biochemical changes with age have been identified in both the sheep and human relating to altered metabolism and

proteoglycan synthesis by IVD fibrochondrocytes in addition to IVD calcification (Bayliss *et al.*, 1988).

As the sheep is a quadruped animal there are some differences to the human spine with regards to load. A common misconception is that the lumbar region of the human spine is under greater load than that in the sheep. However, it can be argued that the ovine lumbar IVDs are more heavily loaded due to muscle contraction and tension of ligamentous tissues, which attempt to stabilize the spine horizontally, and this is thought to require greater force from these tissues than vertical alignment (Alini *et al.*, 2008). This may explain why BMD has been reported to be up to four times higher in animals such as sheep in comparison to humans (Wilke *et al.*, 1999). This needs to be taken into consideration during all studies using animals and their tissues.

Important differences between the sheep and human spines include the presence of secondary ossification centres. The primary centre is located at the central core of the vertebral body in both human and sheep. However, the secondary centre in the sheep is found above and below the physeal plates whilst in humans is present at the circumferential parts (Alini *et al.*, 2008). In addition to this, the sizes of the FSUs vary between human and sheep, with the latter being much smaller in size. In humans, the diameter and disc height of the vertebrae increases throughout the length of the column unlike in the sheep in which the diameter stays fairly constant, with disc height being larger in the cervical than the lumbar region (Wilke *et al*., 1997). The number of vertebrae in the thoracic region also differs between the species with the human spine containing 12 and the sheep having 13.

1.8. Conclusions

Much of the literature available on the FSU focuses largely on spinal biomechanics. As spinal degeneration is a common disease affecting up to 84 % of individuals at one point in their lives, effective treatment is vital. The latter part of this review summarised some treatments that have been developed so far with their respective advantages and disadvantages. TDRs help to restore

motion in the FSU but do not bring functionality back to the tissue. Tissue engineering aims to restore tissue function as well as motion but is still in its infancy. For this reason, the development of pre-clinical *in vitro* models of FSU systems is essential for pre-clinical testing of these novel therapies.

As illustrated in this review, the individual tissues of the FSU have been characterised to some extent. These include the NP, the AF and the facet joint cartilage. However, knowledge of the biology of the FSU as a whole is lacking. In particular, the characteristics of the facet joints and CEPs in natural and degenerated states. In order to begin to develop early intervention therapies for the FSU, knowledge of the biology in health and disease is essential.

1.8.1. Aims and Objectives

The aims of this study were to characterise facet cartilage, CEP, AF and NP cells and tissues from cervical, thoracic and lumbar FSUs of healthy sheep.

Objectives

- To conduct an anatomical study of ovine FSUs to determine any changes that occur in these tissues with age and whether differences occur between different breeds of sheep.
- To determine the age of sheep from which healthy and degenerate tissues can be obtained.
- To characterise the FSU tissue obtained from sheep in the healthy age group using histological, immunohistochemical and biochemical methods and to determine the phenotype of the cells isolated from the tissues using immunocytochemistry.
- To determine the biomechanical properties of healthy ovine facet cartilage using indentation methods.
- To treat ovine facet cartilage with chondroitinase ABC to mimic the biotribological properties of degenerated human facet joint cartilage.

This study was carried out in parallel with three other studies as summarised in Figure 1.15. The vision at Leeds is to develop *in vitro* ovine models of healthy

and degenerated FSUs. These will then be used to test facet cartilage/CEP/AF/NP substitution therapies.

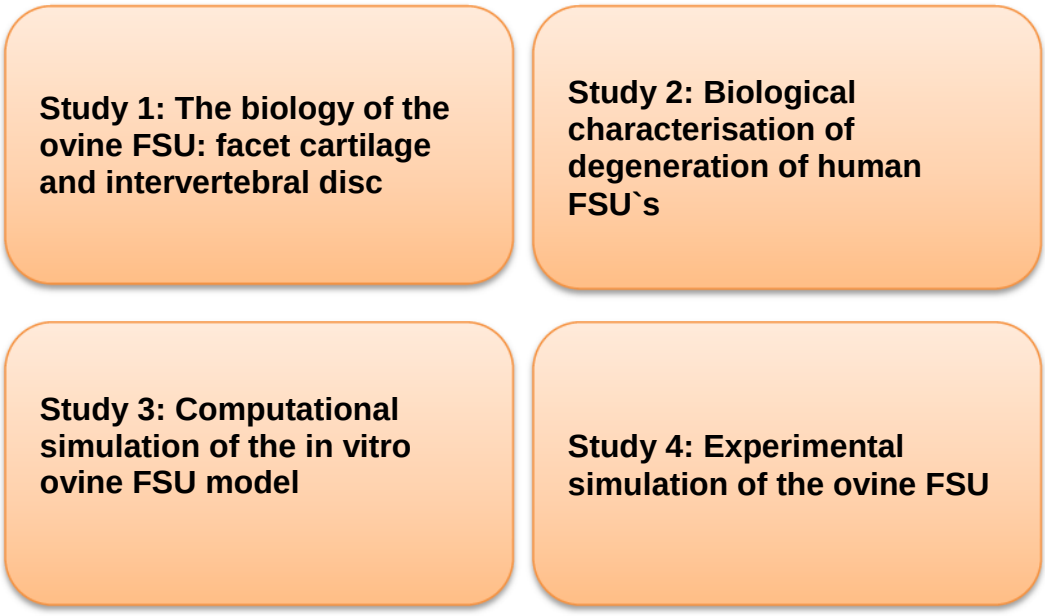


Figure 1.15: Four studies at Leeds, including the study described in this thesis, running parallel to each other. Study one is the current study involving the characterisation of the ovine FSU and the development of a degenerated ovine FSU. Study two involved the characterisation of degenerated human FSUs, whilst studies three and four focused on the experimental and computational simulation of the *in vitro* ovine FSU model. FSU: Functional spinal unit.

Chapter 2: Materials & Methods

Chapter 2: Materials and Methods

2.1. General Materials

2.1.1. Chemicals and Reagents

All chemicals and reagents used throughout the study are presented in Appendix I.

2.1.2. Solutions

Alcian Blue

Alcian blue stain was prepared by dissolving 1 g of Alcian blue in 100 ml of 3 % (v/v) acetic acid. The pH was adjusted to 2.5 by adding either 6 M HCl or 6 M NaOH drop wise. This was stored at room temperature for up to six months.

Antibiotic Solution

Antibiotic solution was prepared by dissolving 25 ml Nystatin (250 $U.ml^{-1}$), 40 µL gentamycin (20 $\mu g.ml^{-1}$), 1 ml polymixin B (200 $\mu g.ml^{-1}$), 500 µL vancomycin (50 $\mu g.ml^{-1}$), 20 mg imipenem (200 $\mu g.ml^{-1}$), 10 ml amphotericin B (25 $\mu g.ml^{-1}$) and 100 µL aprotinin (10 KIU) in 63 ml of phosphate buffered saline (PBS). The solution was divided into 12.5 ml aliquots in universals before storing at -20 ºC for up to six months.

Antibody Diluent

Antibody diluent was prepared by dissolving 600 µL 10 % (w/v) sodium azide and 300 µL 5 % (w/v) bovine serum albumin (BSA) in 59.1 ml tris buffered saline (TBS). The pH was adjusted to 7.6 by adding either 6 M HCl or 6 M NaOH drop wise and stored at 4 ºC for up to three months.

Chondroitinase ABC Solution

Chondroitinase ABC solution was prepared by dissolving 0.61 g trizma base and 0.49 g sodium acetate in 50 ml distilled water. The pH was adjusted to 8.0 by adding either 6 M HCl or 6 M NaOH drop wise before adding distilled water to a final volume of 62 ml. One ml of 5 % (w/v) bovine serum albumin (BSA)

was added. Nyastatin (25 ml, 250 $U.ml^{-1}$), 40 µL gentamycin (20 $\mu g.ml^{-1}$), 1 ml polymixin B (200 $\mu g.ml^{-1}$), 500 µL vancomycin (50 $\mu g.ml^{-1}$), 20 mg impenem (200 $\mu g.ml^{-1}$), 10 ml amphotericin B (25 $\mu g.ml^{-1}$) and 100 µL aprotonin (10 KIU) were added to the solution before 0.05 $U.ml^{-1}$ chondroitinase ABC was added. The solution was divided into 12.5 ml aliquots in universals before storing at -20 ºC for up to six months.

Dimethylene Blue Solution

1,9 Dimethylene blue (DMB) solution for the GAG assay was prepared by dissolving 16 mg of DMB into 5 ml of ethanol and 2 ml of formic acid using a magnetic stirrer. Sodium formate (2 g) was added and the volume was increased to 1000 ml using distilled water. The pH was adjusted to 3.0 by adding formic acid drop wise. The solution was stored at room temperature for up to three months.

EDTA Solution

EDTA solution 12.5 % (w/v) was prepared by dissolving 12.5 g of NaOH and 125 g of EDTA in 875 ml distilled water. The pH was adjusted to 7.0 by adding either 6 M HCl or 6 M NaOH drop wise. The solution was stored at room temperature for up to three months.

Glycosaminoglycan Assay Buffer

GAG assay buffer was prepared by combining 137 ml 0.1 M sodium di-hydrogen orthophosphate with 63 ml 0.1 M di-sodium hydrogen orthophosphate. The pH was adjusted to 6.8 using 6 M HCl or 6 M NaOH and stored at room temperature for up to three months.

Glycosaminoglycan Digestion Buffer

Glycosaminoglycan (GAG) digestion buffer was prepared by dissolving 0.79 g L-cysteine hydrochloride and 0.19 g disodium ethylenediaminetetracetic acid (EDTA) in 1000 ml PBS. The pH was adjusted to 6.0 by adding either 6 M HCl or 6 M NaOH drop wise. The solution was stored at room temperature for up to six months.

Papain Digestion Buffer

Papain digestion buffer (50 $U.ml^{-1}$) was prepared by dissolving 500 units of papain (2.8 $U.mg^{-1}$) in 10 ml of GAG digestion buffer. The solution was used immediately.

Permeabilisation Buffer

Permeabilisation buffer was prepared by dissolving 0.05 g saponin in 100 ml tris buffered saline (TBS). The solution was used immediately.

Phosphate Buffered Saline

Phosphate buffered saline (PBS) was prepared by dissolving 10 PBS tablets in 1000 ml of distilled water. The solution was stored at room temperature for up to one month.

Picro Sirius Red Stain

Picro Sirius red stain was prepared by dissolving 0.1 g Sirius red in 100 ml aqueous saturated picric acid solution. The solution was stored at room temperature for up to six months.

Poly(methyl methacrylate) Cement

Poly(methyl methacrylate) (PMMA) cement was made up by gently mixing by hand approximately 44 g of the powder form (Cold Cure) with 25 g of liquid monomer. This was carried out over a ventilated specimen table. The cement was used immediately.

Substrate Chromagen

Substrate chromogen for immunohistochemistry was prepared by adding 20 µL liquid 3,3-diaminobenzidine (DAB) chromogen to 1 ml substrate buffer. The solution was used immediately.

Tris Buffered Saline

Tris buffered saline (TBS) was prepared by mixing 25 ml 2 M tris-HCl with 50 ml 3 M NaCl and 925 ml distilled water. The pH was adjusted to 7.6 by adding 6 M

HCl or NaOH drop wise. The solution was stored at room temperature for up to one month.

Tween Buffer

Tween buffer (0.05 %) was prepared by adding 500 µL of Tween 20 to 1000 ml of TBS buffer. The pH was adjusted to 7.6 by adding 6 M HCl or 6 M NaOH drop wise. The solution was stored at room temperature for up to one month.

2.1.3. Antibodies

All antibodies used throughout the study are presented in Tables 2.1 to 2.3.

Antigen and Clone number	Host & Type	Isotype	Dilution	Antigen Retrieval	Positive control tissue	Supplier
CD44 MA1-80974	Rat monoclonal	IgG1	1:50	N/A	Ovine Cartilage	Thermo Scientific
Chondroitin-6-sulphate MK-302	Mouse Monoclonal	IgG1	1:200	Proteinase K	Ovine Cartilage	Abcam
Chondroitin sulphate CS-56	Rabbit Polyclonal	IgG	1:50	Proteinase K	Ovine Cartilage	Sigma
Collagen I 5D8-G9	Mouse monoclonal	IgG1	1:50	Proteinase K	Ovine Ligament	Chemicon (Millipore)
Collagen II COLL-II	Mouse monoclonal	IgG1	1:200	Proteinase K	Ovine Cartilage	Chemicon (Millipore)
Collagen III	Rabbit Polyclonal	IgG	1:100 (IFF) 1:50 (IHC)	Proteinase K	Ovine Ligament	Abcam
Collagen V IE2-IE4	Mouse monoclonal	IgG2a	1:50	N/A	Ovine Ligament	Chemicon (Millipore)
Collagen VI	Rabbit Polyclonal	IgG	1:200	Proteinase K	Ovine Cartilage	AbD Serotec
Collagen X COL-10	Mouse Monoclonal	IgM	1:50	Proteinase K	Ovine Cartilage	Abcam
Desmin DE-U-10	Mouse Monoclonal	IgG1	1:50	Proteinase K	Ovine Muscle	Abcam
Fibronectin IST-3	Mouse Monoclonal	IgG1	1:200	Proteinase K	Ovine Ligament	Sigma Aldrich
Osteocalcin OC4-30	Mouse monoclonal	IgG2a	1:100	Proteinase K	Ovine Bone	Abcam
SOX-9	Rabbit Polyclonal	IgG	1:50	Proteinase K	Ovine Cartilage	Chemicon (Millipore)

Table 2.1: Primary antibodies used throughout the study. IFF: Indirect Immunofluorecence, IHC: Immunohistochemistry.

Type	Conjugate	Dilution	Supplier
Goat anti-mouse	FITC (Alexa Fluor 488)	See Table 2.12	Invitrogen
Rabbit anti-rat	FITC (Alexa Fluor 488)	See Table 2.12	Invitrogen
Goat anti-rabbit	FITC (Alexa Fluor 488)	See Table 2.12	Invitrogen

Table 2.2: Secondary antibodies used throughout the study. FITC: Fluorescein isothiocyanate.

Antigen	Type	Host	Supplier
Aspergillus niger glucose oxidase	Isotype control IgG1	Mouse	DAKO Ltd
Ovalbumin-DNP	Isotype control IgG2a	Rat	DAKO Ltd
Unknown	Isotype control IgM	Mouse	DAKO Ltd
Unknown	IgG	Rabbit	Invitrogen

Table 2.3: Isotype control antibodies used throughout the study.

2.1.4. Equipment, Consumables, Plastic and Glassware

All equipment, consumables, plastic and glassware used in experiments are summarised in Appendix 1 and 2.

2.2. General Methods

2.2.1. Washing and Disinfection of Equipment

Following use, dissection instruments were washed and scrubbed under hot water and placed into Virkon for five hours. They were then transferred to a beaker containing 1 % Trigene disinfectant and left overnight. The following day, the instruments were washed with tap water and distilled water before being sprayed with ethanol and left to dry and sterilised. Glassware was washed thoroughly with tap water and placed into Trigene for approximately 24 hours. It was then rinsed with tap water and distilled water before being dried and sterilised if required.

Before using the class II safety cabinet for cell culture work, the surfaces inside were sprayed with Virkon and then 70 % (v/v) ethanol. Everything placed into the cabinet was sprayed with 70 % (v/v) ethanol including gloved hands.

2.2.2. Sterilisation

Instruments and equipment were sterilised by dry heat by placing into an oven set at 180 ºC for four hours. Alternatively, objects unsuitable for high temperature and solutions were moist heat sterilised. This involved autoclaving at 121 ºC, 15 psi for 20 minutes.

2.2.3. pH Measurements

In order to measure the pH of solutions, a Jenway 3020 electronic pH meter was used. Firstly, the meter was calibrated by placing it into three solutions at pH 4, 7 and 10, made from buffer tablets dissolved in distilled water. To adjust the pH of solutions, 6 M HCl or 6 M NaOH was added drop wise whilst the solution was being stirred.

2.2.4. Microscopy

A bright field upright Olympus BX51 microscope was used to view histological and immunohistochemical tissue sections. The microscope was set up for standard Köhler illumination. A bright field upright Olympus BX51 microscope was used to view cells labelled with fluorescent secondary antibodies. A BX51-RFA fluorescent illuminator was set up for fluorescence imaging using either fluorescein isothiocyanate (FITC) or 4,6-diamidino-2-phenyllindole (DAPI) filters. An optical Olympus CK-40-SLP microscope was used to view cells during cell culture studies set up for standard Köhler illumination. Images were captured from both microscopes using an Evolution MP Colour Digital camera that was controlled by Cell B imaging software version 7.

2.2.5. Ovine Tissue Dissection

2.2.5.1. Procurement of Tissue and Dissection

Sheep were slaughtered either on the day (cell isolation) or the day before (tissue characterisation) delivery at an abattoir (M & C Meats, Leeds) by electric

stun to the head and severance of the neck. The carcass was hung and skinned. Inspection and authorisation was carried out by a veterinary officer from the meat hygiene service. The spine was extracted via incisions made to the left and right sides of the spine and was delivered intact to the University of Leeds.

2.2.5.2. Dissection for Tissue Characterisation

The spine was placed on a working bench and excess surrounding ligamentous tissue, muscle and fat was removed from around the FSUs of interest (Figure 2.1).



Figure 2.1: An ovine three year old Suffolk spine. A: The spine after delivery. B: The spine after the removal of surrounding soft tissue.

The spine was divided up into three regions; cervical, thoracic and lumbar (Figure 2.2).



Figure 2.2: Cervical, thoracic and lumbar regions of a three year old ovine Suffolk Mule spine. All vertebrae are labelled depending on their vertebral level. L: Lumbar, T: Thoracic, C: Cervical.

In the cervical region, the FSUs C4/C5 and C6/C7 were removed by slicing through the IVDs of adjacent FSUs C3/C4 and C5/C6 with a scalpel and carefully cutting through the neighbouring facet joint capsules and the surrounding tissue. With gentle force, the neighbouring FSUs (C3/C4 and C5/C6) were separated. For the thoracic region, the ribs were removed from around the FSUs of interest by carefully slicing through the rib joint with a scalpel. A similar approach to the cervical FSUs was applied to remove FSUs T8/T9 and T11/T12. Lastly, FSUs L1/L2 and L3/L4 were removed from the lumbar region.

FSUs C4/C5, T8/T9 and L3/L4 were photographed whole. Following the method above, the FSUs were separated and photographed. The IVDs were removed

using a scalpel by carefully cutting through the CEP in order to keep the IVD as intact and complete as possible. The IVD was photographed in transverse orientation. Lastly, the facets, both superior and inferior, were removed using a hack saw. Both IVDs and facets were immediately fixed for histological analysis (Section 2.2.7.1).

FSUs C6/C7, T11/T12 and L1/L2 were immediately stored at -20 ºC until scanned using µCT (Section 2.2.12). Following scanning, all FSUs were sliced in the mid sagittal plane using a bone saw (Figure 2.3).

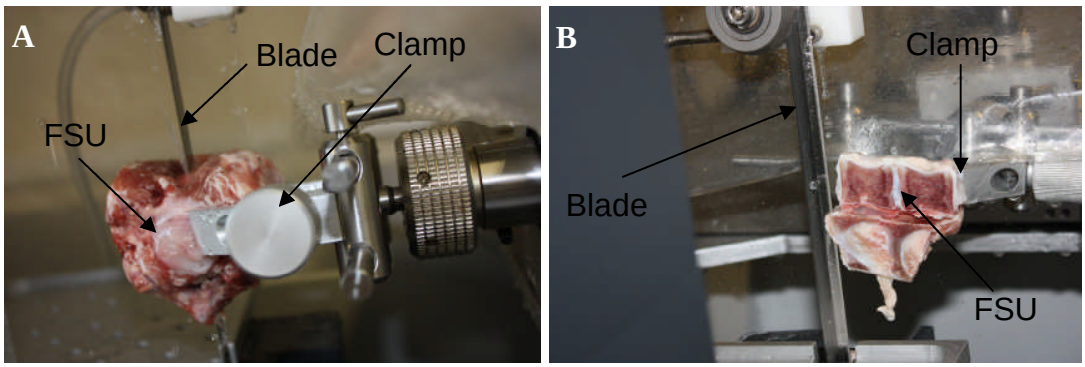


Figure 2.3: An ovine FSU cut sagittally in half using a bone saw. A: A C6/C7 FSU being cut with the blade of the bone saw. B: Half of an L1/L2 FSU after the blade of the bone saw had sliced through it.

The left half of the FSU was moved 2 mm to the left of the FSU and sliced for the second time resulting in a 2 mm sagittal slice. The facets, both inferior and superior, were removed from the remaining left half of the FSU using a hack saw before being photographed. In the same manner, the facets were cut in the mid horizontal plane to give 2 mm slices. Both IVD and facets were immediately fixed for histological analysis (Section 2.2.7.1).

2.2.5.3. Dissection for Cell Isolation

The bench space was prepared by taping yellow plastic bin liners and spraying with 70 % (v/v) ethanol twice before the spine was placed onto it. A Bunsen burner flame was lit in the centre of the dissection area to ensure sterility.

Within two hours of slaughter, the spine was placed onto the prepared bench space. All ligamentous tissue, fat and muscle around the spine were removed

using a sterile scalpel and forceps. For thoracic regions of the spine, the ribs were removed by carefully slicing through the rib joint with a sterile scalpel. The location of the IVD was found and a sterile scalpel was used to cut carefully through the IVD and the respective facets. The spine was forcefully separated in the middle of the disc revealing the AF and the NP as shown in Figure 2.4. The AF and NP tissues were removed using a sterile scalpel and forceps and placed into a sterile pot of 40 ml Dulbecco's modified Eagle medium (DMEM) culture medium containing 10 % (v/v) fetal bovine serum (FBS), 2 mM L-glutamine and 100 $U.ml^{-1}$ penicillin/streptomycin. Once the IVD had been removed, the CEP was scraped off the middle region of the IVD, where the NP had been attached, and placed into a separate pot containing DMEM culture medium. The inferior and superior facets were located and removed using bone clippers. The cartilage from these was scraped off the bone using a sterile scalpel and placed into a separate pot containing 40 ml DMEM culture medium. All pots containing tissue in DMEM were transferred to a safety cabinet before cell isolation (Section 2.2.8.1).

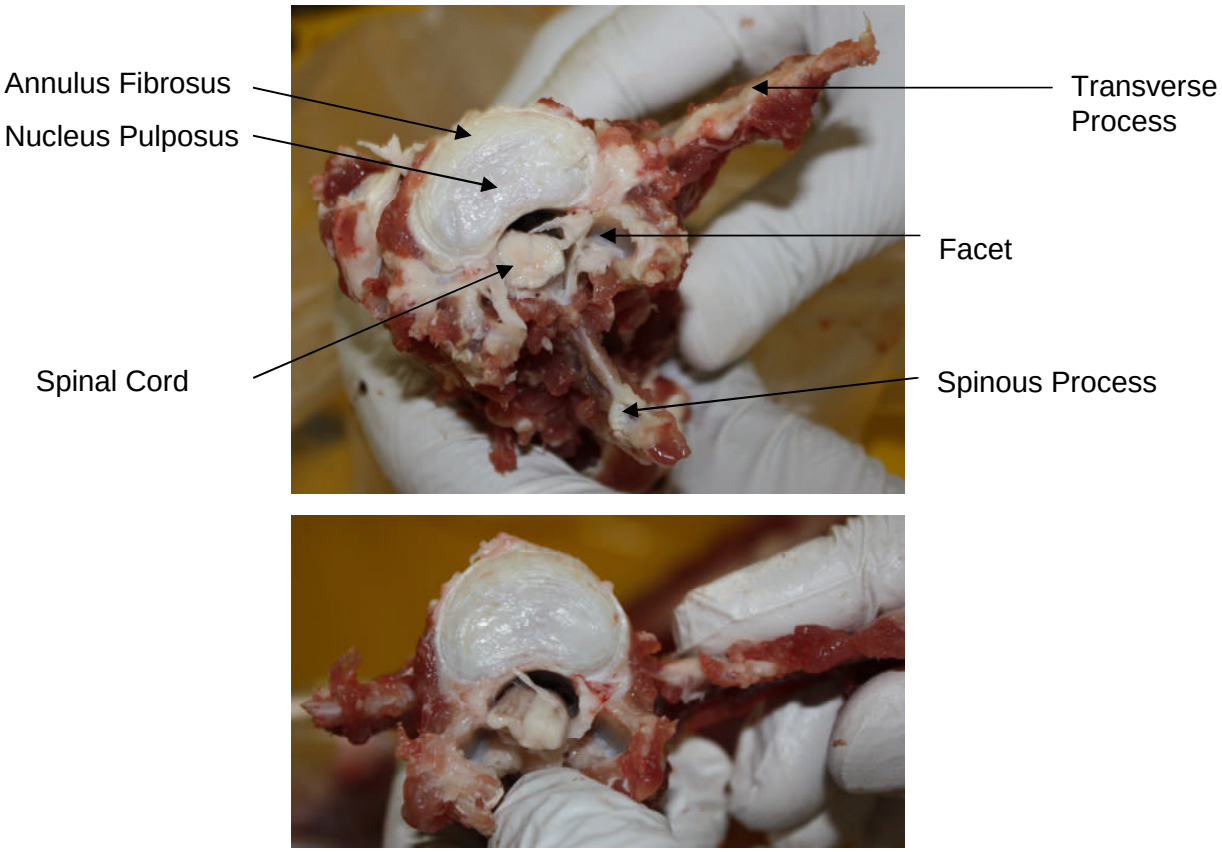


Figure 2.4: A section of an ovine lumbar spine through the IVD. The images show the different parts of the spine including the AF, NP, transverse and spinous process, facets and spinal cord. AF: Annulus fibrosus, IVD: Intervertebral disc, NP: Nucleus pulposus.

2.2.6. Photography

All photography was carried out using a Canon camera. Whole FSUs were photographed with the anterior side placed on the bench. Separated FSUs were photographed revealing the facets of the FSU of interest pointing upwards. The transverse IVDs were photographed either separated or on the vertebral body depending on thickness. IVD sagittal slices were photographed immediately. Facets were placed into PBS to wash off any material/tissue on the surface of the cartilage before being photographed.

For the anatomical study of ovine FSUs (Chapter 3), the photographs of facets from the FSUs C6/C7, T11/T12 and L1/L2 were graded for degeneration blindly by two independent graders using the grading system shown in Table 2.4.

Grade	Features
1	Overall glossy surface with occasional occurrence of small, peripherally circumscribed defects.
2	A dull, slightly uneven surface.
3	A more uneven surface with some full cartilage defects between preserved cartilage.
4	Considerable defects of the cartilage surface up to eburnation of the entire cartilage in extreme cases.

Table 2.4: Grading system used to grade facet cartilage degeneration from digital images based on the surface of the cartilage (Tischer *et al.*, 2006).

2.2.7. Histology

2.2.7.1. Tissue Fixation and Decalcification

Ovine IVD and facet slices (2 mm) were immersed in a solution of 10 % (v/v) neutral buffered formalin solution for 16-20 hours. After this, the tissue was removed from formalin and placed into a solution of PBS for 30 minutes on a plate rocker (Bibby Sterlin Ltd.) at 160 rpm. The PBS solution was replaced with fresh PBS and left on the shaker for a further 30 minutes. The PBS solution was replaced with 12 % (w/v) EDTA buffer (Section 2.1.2) for approximately two weeks (one week per 1 mm thickness of tissue). EDTA buffer was replaced after one week. The bone was cut with a scalpel to confirm that it was soft enough to be sectioned.

2.2.7.2. Tissue Processing

Sagittal IVD slices were prepared by removing the bone on either side of the IVD so that approximately 1 cm was left on each side. These samples and the facet samples were then placed into histology cassettes before the tissue was processed using an automated tissue processor (Leica Microsystems) on programme eight for IVD tissue and programme nine for facet tissue according to Table 2.5.

Pot Number	Reagent	Programme 8	Programme 9
1	10 % (v/v) NBF	2 hours	1 hour
2	70 % Alcohol	2 hours	1 hour
3	90 % Alcohol	2 hours	1 hour
4	100 % Alcohol	2 hours 20 min	2 hours 20 min
5	100 % Alcohol	2 hours 20 min	3 hours 20 min
6	100 % Alcohol	5 hours 20 min	4 hours 20 min
7	Xylene	1 hour	1 hour
8	Xylene	1 hour 30 min	1 hour 30 min
9	Xylene	3 hours	2 hours
10	Molten Wax	1 hour 30 min	1 hour 30 min
11	Molten Wax	3 hours	2 hours
12	Molten Wax	1 hour	1 hour

Table 2.5: Tissue processor programme 8 and 9. All samples were immersed in pots 1-12 for different amounts of time depending on the programme number. NBF: Neutral buffered formalin (10 %).

2.2.7.3. Paraffin Wax Embedding

Once the tissue had completed processing, the histology cassettes were removed from the tissue processor and transferred to molten wax in a wax oven. Metal wax block moulds were filled with molten wax and the tissue sample was placed in the wax in the correct orientation. The plastic cassette base was placed on top of the mould and wax was added to the top of this. The wax was left to cool and harden at room temperature. The wax block was removed from the mould leaving the cassette base attached. Excess wax was trimmed from the edges of the plastic base. The wax blocks were stored at room temperature and cooled at -20 ºC for three hours before prior to sectioning.

2.2.7.4. Sectioning of Paraffin Wax Blocks

The paraffin blocks were attached to the microtome in order to section the blocks at a thickness of 5 µm. Once the sections were cut they were transferred to a paraffin section mounting bath set at 40 ºC allowing them to float flat on the water surface. The sections were mounted onto glass slides by dipping the slide into the water allowing the section to adhere to the glass. The slides were allowed to dry on a hotplate between 56 and 60 ºC for approximately three hours.

2.2.7.5. Haematoxylin & Eosin Staining

Slides containing tissue sections were placed into a slide holder and immersed into dewax xylene (1) for 10 minutes, dewax xylene (2) for 10 minutes, 100 % ethanol (1) for three minutes, 100 % ethanol (2) for two minutes and 100 % ethanol (3) for two minutes and 70 % (v/v) ethanol for two minutes. The sections were immersed in running tap water for three minutes and immersed into haematoxylin for one minute. Sections were rinsed under tap water until the water became clear. Sections were immersed in eosin for three minutes, 70 % (v/v) ethanol for five seconds, 100 % ethanol (3) for one minute, 100 % ethanol (2) for two minutes, 100 % ethanol (1) for three minutes, clean xylene (1) for 10 minutes and clean xylene (2) for 10 minutes. Each section was mounted using DPX mountant and a coverslip was carefully placed on top. The slides were viewed by light microscopy the following day.

2.2.7.6. Alcian Blue Staining

The appropriate slides, containing tissue sections up to 48 hours old, were placed into a slide holder and immersed into dewax xylene (1) for 10 minutes, dewax xylene (2) for 10 minutes, 100 % ethanol (1) for three minutes, 100 % ethanol (2) for two minutes, 100 % ethanol (3) for one minute and 70 % (v/v) ethanol for two minutes. The slides were placed under running tap water for three minutes and immersed in alcian blue solution 1 % (w/v) for 15 minutes. Slides were placed under running tap water for one minute before being rinsed in distilled water. Slides were immersed in periodic acid for five minutes, rinsed in distilled water three times and placed into Schiffs reagent for 15 minutes. Slides were placed under running tap water for five minutes immersed into haematoxylin for 90 seconds and rinsed under running tap water until the water ran clear. Slides were immersed in 70 % (v/v) ethanol for five seconds, 100 % ethanol (3) for one minute, 100 % ethanol (2) for two minutes, 100 % ethanol (1) for three minutes, clean xylene (1) for 10 minutes, and clean xylene (2) for 10 minutes. Each section was mounted with DPX mountant and a coverslip was placed on top. The slides were left to set overnight and viewed by light microscopy the following day.

2.2.7.7. Sirius Red/Miller's Elastin Staining

Slides containing tissue sections were placed into a slide holder and immersed into xylene for 10 minutes, twice. The slides were washed sequentially in 100 % industrial methylated spirits for two minutes three times and 70 % (v/v) ethanol for two minutes. Sections were immersed under running tap water for three minutes and then into 5 % (v/v) potassium permanganate in distilled water for five minutes before rinsing using distilled water. Sections were immersed into 1 % (v/v) oxalic acid in distilled water for two minutes before rinsing in distilled water twice for one minute and four minutes. Sections were immersed in 70 % (v/v) ethanol for one minute and 95 % (v/v) ethanol for one minute before staining in Miller's stain for one hour. Sections were rinsed in 70 % (v/v) ethanol until they ran clear, immersed in 95 % (v/v) ethanol for one minute and rinsed under running tap water for two minutes. Sections were stained in haematoxylin for 10 minutes before being rinsed under running tap water for one minute and rinsing in distilled water for 30 seconds. Sections were stained using 0.1 % (w/v) picro Sirius red for one hour before rinsing in distilled water and blotting dry. Finally the sections were immersed into 70 % (v/v) ethanol for five seconds and into 100 % (v/v) industrial methylated spirits three times for five seconds, two and three minutes before immersion into clean xylene for 10 minutes, twice. All sections were mounted using DPX mountant and a glass cover slip and viewed by light microscopy the following day.

2.2.7.8. Grading of Histological Sections for Tissue Degeneration

Histology sections were graded for degeneration following staining with H&E. Transverse IVD sections were graded using the system shown in Table 2.6.

Grade	Fissures	Cell clusters	Demarcation	Haematoxophilia
0	No fissures	No cell clusters	Clear demarcation	No loss of haematoxophilia
1	Fissures present within the NP	Less than 25% of cells formed into clusters	Limited loss of demarcation	Limited loss of haematoxophilia
2	Fissures extending to junction of NP and AF	25-75% of cells formed into clusters	Substantial loss of demarcation	Substantial loss of haematoxophilia
3	Fissures extending to within AF	Over 75% of cells formed into clusters	Complete loss of demarcation	Complete loss of haematoxophilia

Table 2.6: The histological grading system used for grading degeneration in transverse IVD sections (Sive *et al.,* 2002).

Each of the four degeneration features were given a grade out of three and combined to give a total grade out of 12. Sagittal IVD sections were graded for degeneration using the system shown in Table 2.7. A grade was given for each of the four features and combined to give a total score out of 16. This number was divided by four to give the final grade. Facet sections were graded for degeneration using the grading system in Table 2.8. A grade was given for each of the four features and combined to give a total score out of 16. This number was divided by four to give the final grade.

Grade	AF	NP	CEP	Margins/ Subchondral Bone
1	Intact lamellae, narrow inter-lamellar matrix, intact AF attachment, vessels only in outer third	Homogeneity, absence of clefting	Uniform thickness, intact attachment to bone, uniform calcification <1/5 of depth, uniform cell distribution	Even thickness of BEP, lamellar bone only, distinct junction with CEP, few vascular intrusions into CEP
2	Minor lamellar splitting and disorganisation, minor widening of matrix, minor disorganisation of attachment, rim lesion without reparative reaction	Minor clefting, minor cell necrosis, minor posterior displacement of AF, minor chondron formation	Minor cartilage thinning, small transverse fissures, irregular thickening of calcified cartilage, few invading vascular channels, small chondrons	Slightly uneven BEP, schmorl's nodes, minimal remodelling of BEP, small marginal osteophytes
3	Moderate lamellar disorganisation, moderate widening of matrix, moderate fissuring of attachment, radiating fissures not involving outer third, minimal chondroid metaplasia, cystic degeneration, vessels in outer and middle third, rim lesion with minor reparative reaction	Moderate clefting, moderate cell necrosis, cystic degeneration, posterior displacement within annulus, centripetal extension of collagen, moderate chondron formation	Marked cartilage thinning, marked thickening of calcified zone, many transverse fissures, many vascular channels, many chondrons.	Moderately uneven BEP, vascularised schmorl's nodes, moderate trabecular thickening, defect in bone lamellae, minimal fibrosis tissue in marrow spaces, medium sized osteophytes
4	Extensive lamellar disorganisation, radiating tears extending into outer third, extensive chondroid metaplasia, vessels in all zones, rim lesion with marked reparative reaction	Complete loss of NP, loose body formation, marked chondron formation	Total loss of cartilage, calcification of residual cartilage, widespread fissuring	Marked uneven BEP, ossified schmorl's nodes, large osteophytes, marked trabecular thickening, marked fibrosis of marrow spaces, cartilage formation

Table 2.7: The histological grading system used to grade degeneration in sagittal IVD sections. AF: Annulus fibrosus, BEP: boney end plate, CEP: cartilage end plate, NP: Nucleus pulposus (Gries *et al.,* 2000).

Grade	Cartilage	Osteochondral Junction	Subchondral Bone	Margins
1	Smooth intact surface, orderly chondrocytes distribution, orderly collagen framework	Uniform tidemark, calcification <1/5 cartilage thickness	Uniform lamellar, subchondral bone plate, uniform vascular budding into cartilage	Smooth articular margin, normal synovium, normal capsule
2	Tangential surface flaking, minimal chondrocyte death, few chondrons	Minimal irregularity of tidemark, calcification 1/5-1/4 cartilage	Minor thickening of trabeculae, small fissures at bone-cartilage junction, occasional fibrous tissue formation	Small osteophytes, minimal capsular fibrosis
3	Fissures <1/2 total depth, loss of cartilage <1/2 depth, moderate chondrocytes death, many chondrons	Marked irregularity of tidemark, calcification ¼-1/2 cartilage	Moderate trabecular thickening, woven bone formation, moderate fibrous tissue formation	Moderate osteophytes, minimal-moderate appositional new bone, fibrocartilage formation, moderate capsular fibrosis, minimal-moderate synovial thickening
4	Deep fissures, areas of total cartilage loss, entensive chondrocyte death	Calcification >1/2 cartilage	Eburnation of exposed bone, bone sclerosis, cysts, extensive fibrosis	Extensive and large osteophytes, marked appositional new bone, marked capsular thickening, marked synovial thickening

Table 2.8: The grading system used to grade degeneration in histological sections of the facets (Gries *et al.,* 2000).

2.2.8. Cell Culture

2.2.8.1. Cell Isolation

The tissue was transferred to a class II safety cabinet and cut into 1 mm^3 pieces using a sterile scalpel. These were placed into solutions of Dulbecco's modified Eagle's medium (DMEM) containing 0.1 % (w/v) collagenase and 0.1 % (w/v) hyaluronidase and incubated on a rotator at 37 ºC (5% CO_2 (v/v) in air) overnight. The following day, the digested tissue solution was filtered by passing through a 100 µm cell sieve. The cell suspension was centrifuged at 200 g for 10 minutes at room temperature. The supernatant was discarded and the pellet was resuspended in 5 ml of supplemented DMEM culture medium and transferred into 75 cm^3 flasks.

2.2.8.2. Passage and Maintenance

Cells were cultured in standard 75 cm^3 culture flasks at 37 ºC, 5 % (v/v) CO_2 in air. The culture medium used consisted of DMEM medium supplemented with 10 % FBS (v/v), 100 $U.ml^{-1}$ penicillin, 100 $U.ml^{-1}$ streptomycin and 2 mM L-glutamine. Once cells had become confluent within their flasks, cells were passaged. This was achieved by removing the medium by suction and washing with 5 ml PBS. Once the PBS had been removed, 3 ml trypsin-EDTA 1X solution was added and the flasks placed in an incubator at 37 ºC, 5 % (v/v) CO_2 in air for five minutes. The flask was viewed under a microscope to ensure the cells had detached from the flask and 9 ml of culture medium was added. Approximately 4 ml of the cell suspension was added to two new T-75 culture flasks containing 16 ml of fresh culture medium and placed in an incubator at 37 ºC, 5 % (v/v) CO_2 in air. The culture medium was changed the following day and every two days after until the cells became confluent.

2.2.8.3. Cell Count and Viability

The cells were passaged (Section 2.2.8.2) and transferred to a sterile 60 ml pot to ensure that aggregates of cells were separated by gentle pipetting. Cell suspension (500 µL) and 500 µL of Trypan blue were mixed together in a bijoux and 20 µL of the suspension was placed onto a haemocytometer. The number of live cells, which had not taken up the dye, in 10 large squares was counted

as shown in Figure 2.5. This number was divided by 10 to obtain the number of cells in one large square and multiplied by the dilution factor of two. The number was multiplied by 10^4 to give the number of cells per ml. In order to determine the cell viability, the number of live cells and the total number of both live and dead cells in 10 squares was counted. The number of live cells was divided by the total number of cells and this was multiplied by 100.

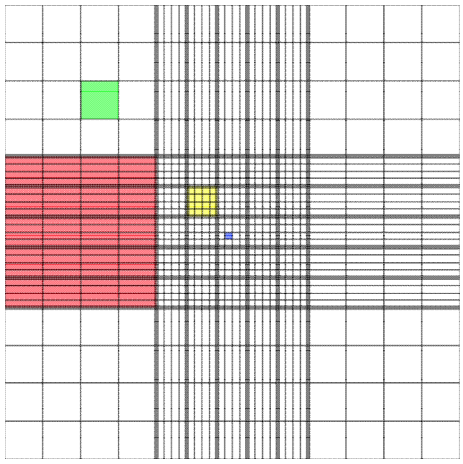


Figure 2.5: A haemocytometer grid. The image shows all the visible squares used to count cells. Two of these grids are present in a standard haemocytometer. In this study, five red squares were used to count the cells for each grid. Therefore, ten red squares were counted in total.

2.2.8.4. Cryopreservation

Cells were trypsinised by adding trypsin-EDTA solution and neutralising it with culture medium once the cells had detached from their culture flasks. The cell suspension was transferred to a centrifuge tube and centrifuged at 150 g for 10 minutes. The cells were resuspended in 10 % (v/v) dimethyl sulfoxide (DMSO) in culture medium sterilised using a 0.2 µl filter. A viable cell count was performed and the cell solution was transferred 1 ml at a time into cryovials so that each contained up to 10^6 cells. The cryovials were transferred to a Mr Frosty isopropanol cryopreservation container and then placed into a -80 ºC freezer for 24 hours before being transferred to liquid nitrogen.

2.2.8.5. Cell Revival from Frozen

A frozen vial of cells was thawed in a 37 ºC water bath for approximately two minutes. Culture medium (1 ml) was added into the cell vial and washed. The

cell suspension was transferred into a 60 ml pot containing 10 ml of warm medium. The cell suspension was transferred to a 75 cm^3 culture flask and a further 10 ml of warm medium was added to the flask. The flask was placed in an incubator at 37 ºC, 5 % (v/v) CO_2 in air.

2.2.9. Indirect Immunofluorecent Labelling of Cell Markers

2.2.9.1. Indirect Immunofluorescence

Cells were plated onto multi spot slides with each spot containing approximately 800 cells. The cells were fixed in 1:1 ice cold solution of acetone and methanol for two minutes before being left to dry in a fume hood for one hour. The slides were transferred to an air tight case before being stored at -20 ºC until required for staining.

The slides were removed from the -20 ºC freezer and thawed at room temperature for 30 minutes before being rinsed under running tap water for 10 minutes. The slides were transferred to four-well slide holders and each well was flooded with TBS and incubated for five minutes at room temperature. The TBS was decanted and replaced with permeabilisation buffer (Section 2.1.2) and incubated for five minutes. This was removed and 10 µL of the primary antibody, diluted in antibody diluent, was added to each spot on each slide and incubated for one hour at room temperature in a moist environment. Each well was flooded with Tween buffer (Section 2.1.2) and placed on a rocking table for 10 minutes at room temperature, this was repeated and then the buffer was replaced with TBS (Section 2.1.2) for 10 minutes at room temperature, twice. Secondary antibody (10 µL), diluted in antibody diluent (Section 2.1.2), was added to each spot on each slide and the slide holder was covered with aluminium foil and incubated for 30 minutes at room temperature in a moist environment. The slide wells were flooded with Tween buffer twice and TBS twice each for 10 minutes on the rocking table whilst the slide holder was covered with foil. Hoechst dye (10 µL: 1 $\mu g.ml^{-1}$), diluted in TBS, was added to each spot on each slide and incubated in the dark for 10 minutes at room temperature. The slides were finally washed with PBS three times, each for three minutes, before mounting with DABCO-glycerol 9:1 and covering with a

cover slip. The slides were kept in a box at 4 ºC overnight before being viewed by fluorescent microscopy the following day.

2.2.9.2. Antibody Dilution Titrations

Cells were plated onto multi spot slides with each spot containing approximately 800 cells. The cells were fixed in 1:1 ice cold solution of acetone and methanol for two minutes before being left to dry in a fume hood for one hour. The slides were transferred to four well slide holders and each well was flooded with distilled water and left for two minutes. The water was decanted and replaced with permeabilisation buffer (Section 2.1.2) and incubated for five minutes at room temperature. Permeabilisation buffer was removed and a thin piece of paper towel was used to dry the spaces in between the spots on the slides. Immediately after, 10 µL of the primary antibody diluted in TBS at 1:50, 1:100, 1:150 and 1:200 was added in this order to each of the four spots along three columns of spots on the multi spot slides. After one hour, each well was flooded with Tween buffer (Section 2.1.2) and placed on a rocking table for three minutes and then replaced with TBS (Section 2.1.2) for three minutes twice. A thin piece of paper towel was used to dry the spaces in between the spots on the slides and immediately before 10 µL of secondary antibody diluted in TBS at 1:100, 1:200 and 1:300 was added in that order to each of the three rows to all four spots on each row. The slide box was covered with aluminium foil and incubated for 30 minutes at room temperature. The slide wells were flooded with Tween buffer and TBS twice each for three minutes. A thin piece of paper towel was used to dry the spaces in between the spots on the slides before 10 µL of Hoechst (1 µg/ml), diluted in TBS, was added to each spot on each slide and incubated in the dark for 10 minutes at room temperature. The slides were finally washed with TBS and distilled water, each for three minutes, before mounting with DABCO-glycerol 9:1 and covering with a cover slip. The slides were kept in a box at 4^{o}C overnight before being viewed by fluorescent microscopy the following day. All antibodies were diluted in antibody diluent.

2.2.10. Immunohistochemical Analysis of Tissue Sections

2.2.10.1. DAKO EnVision Method

Paraffin wax sections of tissue on superfrost plus slides were dewaxed in two sequential washes of xylene for 20 minutes in total. The sections were washed in three sequential washes of 100 % methanol for three, two and two minutes followed by 70 % ethanol for two minutes. The sections were washed under running tap water for three minutes. Drops of ready-to-use proteinase K were placed onto all tissue sections and incubated at room temperature for 20 minutes for antigen retrieval. All slides were immersed in 3 % (v/v) hydrogen peroxide in PBS for 10 minutes before being immersed under running tap water for three minutes. A hydrophobic barrier pen was used to draw a circle around each section on each slide before rinsing in TBS for four minutes. Drops of dual endogenous enzyme block were added to each section and incubated for 10 minutes at room temperature. All slides were washed with TBS for 10 minutes on a rocking table twice. The appropriately diluted primary antibody was added to each section and incubated at room temperature for one hour. All slides were washed in 0.05 % (v/v) Tween in TBS for 10 minutes on a rocking table twice followed by washing in TBS buffer for 10 minutes on a rocking table twice. Drops of polymer-horse radish peroxidise (HRP) were added to each section and incubated for 30 minutes at room temperature in the dark. The previous wash step was repeated. The chromagen, 3,3-diaminobenzidene (DAB) was added to each section and incubated for 10 minutes at room temperature. All sections were washed in distilled water for four minutes, four times before being immersed in haematoxylin for 10 seconds and washed under running tap water. Slides were immersed in 70 % (v/v) ethanol for five seconds followed by sequential washes in 100 % methanol for one, two and three minutes. Sections were immersed in clean xylene for 20 minutes before mounting in clean DPX mountant and a glass cover slip. Slides were viewed using light microscopy the following day.

2.2.10.2. Streptavidin-Biotin Method

All slides were treated with xylene and washed sequentially in alcohol as described previously (Section 2.2.10.1). Antigen retrieval was achieved using

drops of ready-to-use proteinase K which were placed onto all tissue sections and incubated at room temperature for 20 minutes. All slides were immersed in 3 % (v/v) hydrogen peroxide in distilled water for 10 minutes at room temperature and rinsed under running tap water for five minutes. After circling each section with a hydrophobic barrier pen, the slides were washed in TBS for four minutes. Streptavidin block was added to all sections and allowed to incubate for 10 minutes before rinsing in TBS for 10 minutes, three times. This was repeated for the biotin block. The appropriately diluted primary antibody was added to each section and incubated at room temperature for one hour. After rinsing in TBS for 10 minutes, three times, the appropriately diluted secondary antibody with 10 % (v/v) serum of the tissue source was added to each section and incubated at room temperature for 30 minutes. The previous washes were repeated. Horseradish peroxidise streptavidin was added to each section and incubated at 37 ºC in a moist environment for 45 minutes. Previous wash steps were repeated. DAB substrate was added to each section and allowed to incubate for 20 minutes before the reaction was terminated by immersing under running tap water for five minutes. All slides were immersed in haematoxylin, washed in alcohol and immersed in clean xylene as previously described (see Section 2.2.10.1.) before mounting with DPX mountant and a glass cover slip. Slides were viewed using light microscopy the following day.

2.2.11. Assay for Sulphated GAGs (GAG assay)

FSUs for all assays were thawed intact overnight at 4 ºC before dissecting and cutting the appropriate tissue into approximately 1 mm^2 sized pieces. Finely cut tissue (~10 mg) was placed into pre-weighed bijous and freeze dried for four to five days until a constant dry weight was achieved. Papain (5ml; 50 $U.ml^{-1}$) in digestion solution (Section 2.1.2) was added and the mixture left to incubate in a 60 ºC water bath for 48 hours alongside digestion solution-only negative controls. Primary standard solution was made using 10 mg chondroitin sulphate B and 10 ml GAG assay buffer (Section 2.1.2). This was diluted in a 1:10 dilution of in GAG assay buffer plus 50 $U.ml^{-1}$ papain to give nine standard concentrations of 0, 3.125, 6.25, 12.5, 25, 50, 100, 150 and 200 $\mu g.ml^{-1}$. The test solution was used neat and diluted at 1:10, 1:50, 1:100 and 1:500 in 1:10 50 $U.ml^{-1}$ papain in GAG assay buffer. All standards, blanks and test solutions

(40 µL) were added to a clear, flat-bottomed 96 well plate in triplicate. DMB dye solution (250 µL; Section 2.1.2) was added to each well and placed on a plate shaker at 60 rpm for two minutes. The optical densities of each well were measured at 525 nm using a micro plate spectrophotometer. Blank values were subtracted from all standard and test values before a standard curve was plotted of chondroitin sulphate B concentration against absorbance. The unknown values were interpolated using linear regression of the standard curve before dilutions were factored and GAG concentrations were deduced.

2.2.12. µCT Analysis of FSUs

Scanco Medical µCT80 and µCT100 were used to scan the FSU specimens. The µCT80 was originally used but developed a fault half way through the study. This was then replaced with the µCT100 to scan the remaining specimens.

The FSUs C6/C7, T11/T12 and L1/L2 from each spine used in the anatomical study (Chapter 3) were scanned. Each FSU was placed into a cylinder-shaped specimen holder and was kept in place by the use of damp foam pads to prevent movement during scanning. Specimen holders of 73 mm and 88 mm were used. The specimen holder was then either attached to a metal rod (µCT80) or slotted into a position on a carousel (µCT100).

The following settings were used:

- Tube energy: 74 kVP, 114 µA
- Voxel size: 74 x 74 x 74 µm
- Integration time: 300 ms
- Resolution: Standard
- Filter: aluminium 0.5 mm (calibration 3)

All scans were analysed to determine the bone properties of the ovine vertebrae for each FSU. This involved determining the thickness (in terms of number of slices) of the vertebrae and then determining the middle slice. Once this was achieved, the length across the vertebrae (of the middle slice) was measured in order to determine the area of the circle which identified the region of interest to

analyse. The range of slices which would give a depth of 1 cm was determined and this circle was applied to each of the slices. Finally, the lower and upper threshold values of bone and bone marrow were determined in order to generate the values for total volume (TV), bone volume (BV), BV/TV, trabecular number, trabecular spacing, trabecular thickness and hydroxyapetite (HA) concentration.

In addition to bone properties, disc height was measured in three areas including the left and right sides of the IVD and in the centre.

The facet joint gap was measured at six places for each facet joint as shown in Figure 2.6. This was carried out for three slices in the scan each at equal distance along the height of the left and right facet joint. A total of 18 measurements were taken for each facet joint.

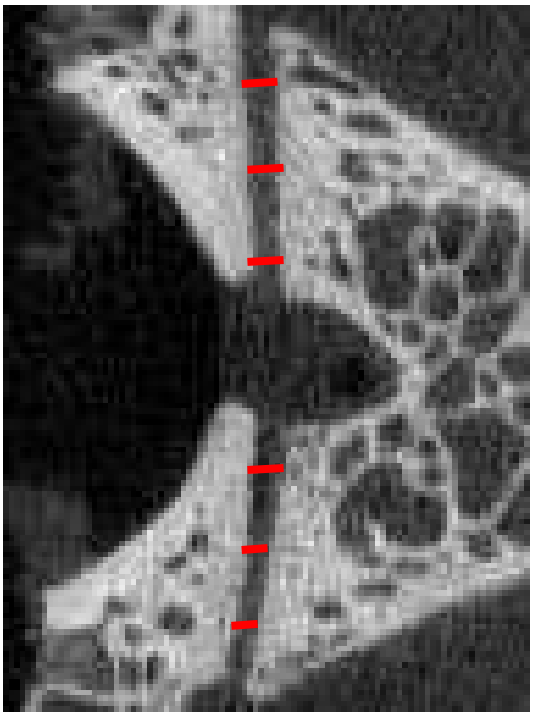


Figure 2.6: A µCT image of a pair of ovine thoracic facets joints. The red lines indicate where measurements were taken in mm.

2.2.13. Indentation Testing

In order to determine the deformation properties of facet cartilage, a method previously developed in Mechanical Engineering at Leeds was adopted (Latif *et al.*, 2012).

2.2.13.1. Pin Extraction

In order to test facet cartilage using indentation, pins of the facets were first obtained. Pins were only obtained from cervical facets since these were the only facets that had cartilage surfaces of sufficient area and flatness. Throughout the pin extraction process, PBS was used to keep the facet cartilage hydrated.

A pair of facet joints were separated and kept hydrated using a cloth soaked in PBS on the facet surface. The facets were orientated in a metal block before PMMA cement (Section 2.1.2.) was carefully added to mould them in place. The pedicles were potted in the cement leaving the facets well above the cement surface. Approximately 40 minutes later, the mould was removed from the block and placed in a secure clamp. Hand held tools were used to mark the circumference of the pin (4 mm diameter) on the cartilage surface. An electric drill was then used to cut into the bone and remove the pin. The facet pins were wrapped in paper towels soaked in PBS and stored in bijous at -20 ºC for up to one week.

2.2.13.2. Indentation Test to Determine the Deformation Properties

An indentation test rig previously used to test 4 mm facet cartilage pins was used as illustrated in Figure 2.7 (Latif *et al.*, 2012).

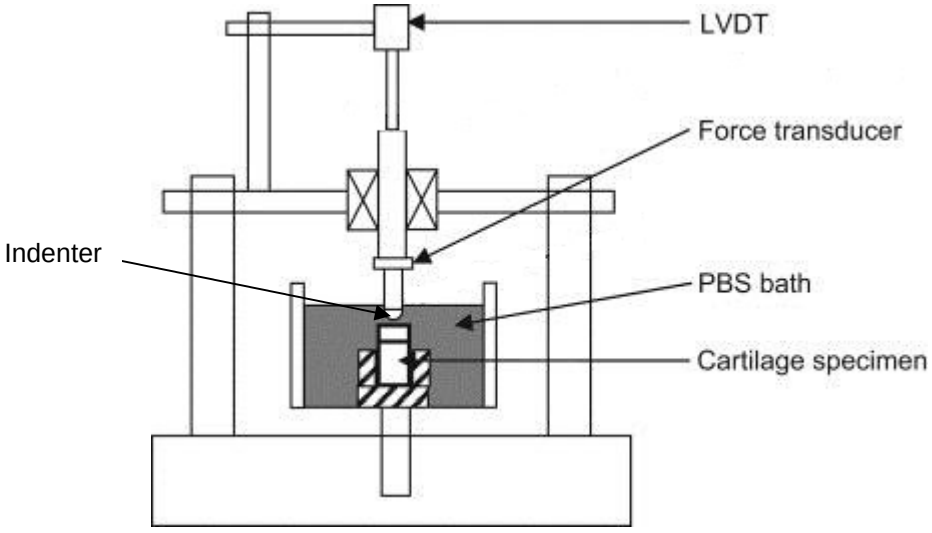


Figure 2.7: The indentation test rig used to determine the indentation properties of facet cartilage. LVDT: Linear variable differential transformer, PBS: Phosphate buffered saline (adapted from Latif *et al.*, 2012).

The facet pin was fitted in a specimen adapter and holder and tightened using an Allen key. The specimen was then placed into a fixed-based fixture and filled with PBS until the surface of the cartilage was covered.

A 2 mm flat indenter was fitted at the end of the force transducer giving a total shaft weight of 0.24 N. Upon release of the indenter, the movement of the shaft was monitored by the linear variable differential transformer (LVDT) and the force monitored by the piezoelectric force transducer as shown in Figure 2.8. Data from these were transferred through an analogue-to-digital converter and stored in a computer using the software LabVIEW 8.0 (National Instruments Corporation, Austin, Texas, USA). The test was run for approximately 60 minutes until equilibrium had been reached.

2.2.13.3. Needle indentation for Determination of Cartilage Thickness

A needle tip with a diameter of 0.8 mm was used to determine the facet cartilage thickness. The procedure for needle indentation was the same as that described in Section 2.2.13.2 above.

The thickness measurement was determined by observing the difference in position of the needle from when it contacted the cartilage surface to when it reached the subchondral bone.

2.2.14. Degeneration Model of Ovine Facet Cartilage using Chondroitinase ABC

Whole facets dissected as described in Section 2.2.5.2 were transferred into universals containing 12.5 ml antibiotic solution (Section 2.1.2.). The universals were placed on an orbital shaker (120 rpm) at 4 ºC for 18 hours. The solutions were replaced with 12.5 ml 0.05 $U.ml^{-1}$ chondroitinase ABC solution (Section 2.1.2.) and placed on an orbital shaker (120 rpm) at 37 ºC for 16 hours. All facets were washed with PBS twice for 30 minutes on an orbital shaker (rpm 120) at 4 ºC. The facets were stored at -20 ºC on PBS moistened filter paper until analysed.

2.2.15. Statistical Analysis

All numerical data was analysed using GraphPad Prism software, version 6.0 and/or Microsoft Office Excel 2007.

The inter-rater reliability (kappa) test was performed to measure the level of agreement between graders on the assignment of categories of a categorical value (Chapter 3). The resulting value was between 0.1-0.

Kappa	Interpretation
<0	Poor agreement
0.0-0.20	Slight agreement
0.21-0.40	Fair agreement
0.41-0.60	Moderate agreement
0.61-0.80	Substantial agreement
0.81-1.00	Almost perfect agreement

Table 2.9: The interpretation of kappa scores. Kappa measures the level of agreement between graders on the assignment of categories of a categorical value.

All parametric numerical data are presented as means ± standard deviation. One way analysis of variance was used for comparison of data from more than two groups. Significance was accepted when the difference of the means was less than 0.05. The Tukey's multiple comparisons test was used in GraphPad Prism to determine significant differences between the groups.

For percentage data, the data was arcsine transformed in order to fulfil the assumption of normally distributed data, required by analysis of variance. The arcsine transformed values were then averaged and the standard deviation was calculated. The upper and lower limits were then calculated as follows:

- Upper limit = mean + standard deviation
- Lower limit = mean – standard deviation

The mean, upper and lower limits values were then back transformed to percentages for presentation.

For data in the form of grades (analysis of degenerative changes using images and histological sections), the data for different groups was compared using the Kruskal-Wallis test followed by determination of difference between groups ($p<0.05$) using the Dunn's multiple comparisons test.

Correlation coefficients between the age of sheep and parameters analysed were determined using Spearman`s rank correlation (graded data) or Pearson's moment correlation (parametric data). The extent of the correlation from the r values generated from these tests was determined using Table 2.10.

r value	Correlation
0-0.4	No correlation
0.4-0.6	Weak correlation
0.6-0.8	Good correlation
0.8-1.0	Excellent correlation

Table 2.10: The significance of r values generated from the Spearman's rank correlation and Pearson's moment correlation.

2.3 Validation of Methodologies

The majority of the methods used during this study had not been previously applied to ovine tissue or FSU tissue. It was therefore necessary to validate the methods used as indicated below.

2.3.1. Determination of the Working Dilutions of Primary and Secondary Antibodies using Indirect Immunofluorescence and Immunohistochemistry

A range of primary antibody dilutions were tested against a range of secondary antibody dilutions (using the method described in Section 2.2.9.2 and 2.2.10.2) to determine the working concentrations for all primary antibodies used for indirect immunofluorescence and as a guide to the dilution range for immunohistochemistry. The antibodies were tested on FSU cells including facet, CEP, NP and AF cells from a five to six year old sheep. Dilutions of the primary antibody were 1:50, 1:100, 1:150 and 1:200 and dilutions of the secondary antibodies were 1:100, 1:300 and 1:500. A chessboard method of recording the result of each combination was used. Three positives were assigned for very strong fluorescence, two positives were assigned for good fluorescence, one positive was assigned for visible fluorescence and a negative for no fluorescence. An example of the chessboard titration for antibodies to collagen II is shown in Figure 2.8.

A

primary antibody dilution: / secondary antibody dilution:	1:50	1:100	1:150	1:200
1:100	++	++	+++	+++
1:300	++	-	++	+++
1:500	+	+	++	++

B

primary antibody dilution: / secondary antibody dilution:	1:50	1:100	1:150	1:200
1:100	+	+	++	++
1:300	++	+	++	++
1:500	+	-	+	+

C

primary antibody dilution: / secondary antibody dilution:	1:50	1:100	1:150	1:200
1:100	++	+	++	++
1:300	+	-	++	+
1:500	++	+	+++	++

D

primary antibody dilution: / secondary antibody dilution:	1:50	1:100	1:150	1:200
1:100	++	+	++	++
1:300	+	+	++	+
1:500	++	+	+	+

Figure 2.8: Collagen II antibody titrations. Chessboard results A: facet cartilage cells, B: CEP cells, C: NP cells, D: AF cells showing the combinations of 1:50, 1:100, 1:150 and 1:200 dilutions of primary antibody against 1:100, 1:300 and 1:500 diluted secondary antibody. +++: very good fluorescence, ++: good fluorescence, +: positive fluorescence, -: no fluorescence. The tables indicate that the best combination for all cells was a 1:200 primary antibody dilution and 1:100 secondary antibody dilution.

The results of the titrations carried out for all other antibodies used to characterise the FSU cells are summarised in Table 2.11.

Antibody	Primary Antibody Dilution	Secondary Antibody Dilution	Secondary Antibody
CD44	1:50	1:500	Rabbit ant-rat
Chondroitin-6-sulphate	1:200	1:300	Goat anti-mouse
Collagen I	1:50	1:100	Goat anti-mouse
Collagen III	1:100	1:300	Goat anti-rabbit
Collagen V	1:50	1:500	Goat anti-mouse
Collagen VI	1:200	1:500	Goat anti-rabbit
Collagen X	1:50	1:100	Goat anti-mouse
Desmin	1:50	1:300	Goat anti-mouse
Fibronectin	1:200	1:500	Goat anti-mouse
Osteocalcin	1:100	1:300	Goat anti-mouse
SOX-9	1:50	1:300	Goat anti-rabbit

Table 2.11: Summary of all working primary and secondary antibody dilutions. Antibody details are shown in Table 2.1.

2.3.2. Determination of the Effect of Passage Number on Expression of Markers by FSU cells

Before characterising the FSU cells it was important to understand their behavior in monolayer culture and whether expression of certain markers changed with passage number. Previous work carried out on chondrocytes in monolayer culture has shown that it is common for them to dedifferentiate to fibroblasts at passage six (von der Mark, 1977; Nadzir *et al.,* 2011). To investigate this, the FSU cells including AF, NP, CEP and facet cartilage cells from a five to six year old sheep were cultured in monolayer. Tissue was selected from random FSUs to obtain a mixture of different cells types from different levels to investigate. The cells were transferred onto multispot slides and immunostained with antibodies specific for known chondrocyte markers including chondroitin-6-sulphate, CD44, collagen I and II and SOX-9 at passage four, six and eight. This was repeated for each cell type three times. In addition to this, the morphology of the cells in the culture flasks was also monitored for any changes. Examples of this are shown in Figure 2.9.

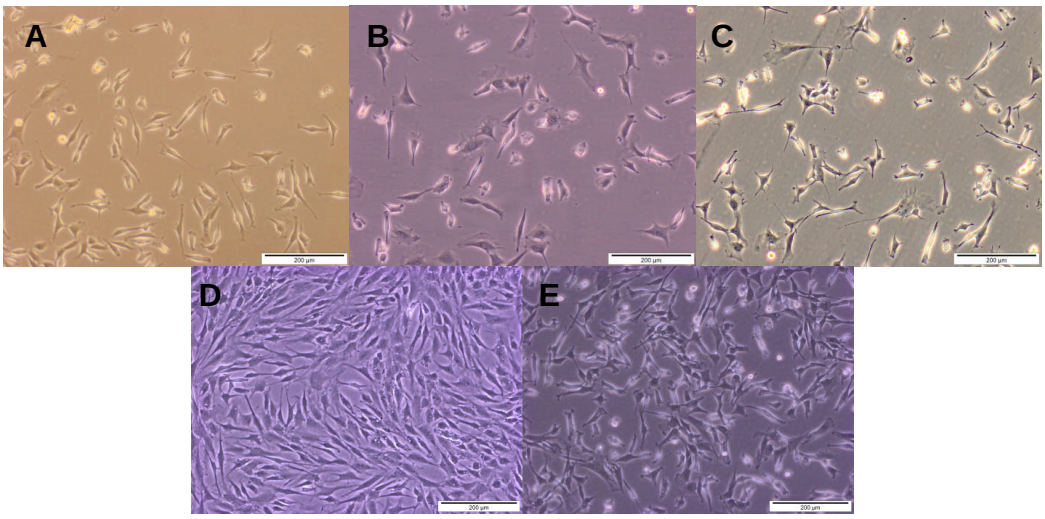


Figure 2.9: Facet cartilage cells in monolayer culture. A: passage two, B: passage three, C: passage four, D: passage five, E: passage six.

The images in Figure 2.9 show that the morphology of the cells remained thin and elongated throughout passaging in monolayer culture. No changes were observed in morphology between the passages.

The results obtained for the expression of various markers by the cells over time in culture are summarised in Table 2.12.

Cell: **Passage:** **Antibody:**	**F** **4**	**F** **6**	**F** **8**	**C** **4**	**C** **6**	**C** **8**	**A** **4**	**A** **6**	**A** **8**	**N** **4**	**N** **6**	**N** **8**
CD44	+++	+++	-	+++	+++	+++	+++	+++	+++	+++	+++	+++
Chondroitin -6-sulphate	++	+	++	++	+	++	++	+	++	++	+	++
Collagen I	-	++	-	-	++	-	-	++	-	-	++	-
Collagen II	++	++	++	++	++	++	++	++	++	++	++	++
SOX-9	++	++	++	++	++	++	++	++	++	++	++	++

Table 2.12: The phenotype of all cell types. F: facet cartilage, C: CEP, A: AF, N: NP, at passage four, six and eight based on immunofluorescent stain intensity: +++: very good, ++: good, +: positive, -: negative.

The results from these studies showed that collagen type II and SOX-9 expression was maintained throughout all the passages. Chondroitin sulphate expression was reduced at passage six but regained expression at passage eight. CD44 expression was lost at passage eight for facet cartilage cells. Collagen type I was not expressed at passage four or eight but was at passage six. As some changes in expression of these markers were apparent at passage six and collagen type I expression was not present at passage four, it was concluded that FSU cells could be analysed reliably for up to four passages.

The original indirect immunofluorescence method used in these preliminary studies differed from that described in Section 2.2.9.1 (Method C). Originally, the washing times between the addition of antibodies to the cells were only three times each for three minutes (once in Tween buffer and twice in TBS). Furthermore, the slides were not washed under running tap water for 10 minutes and the antibodies were diluted in TBS (Method A). Figure 2.10 show examples of images obtained after using method A.

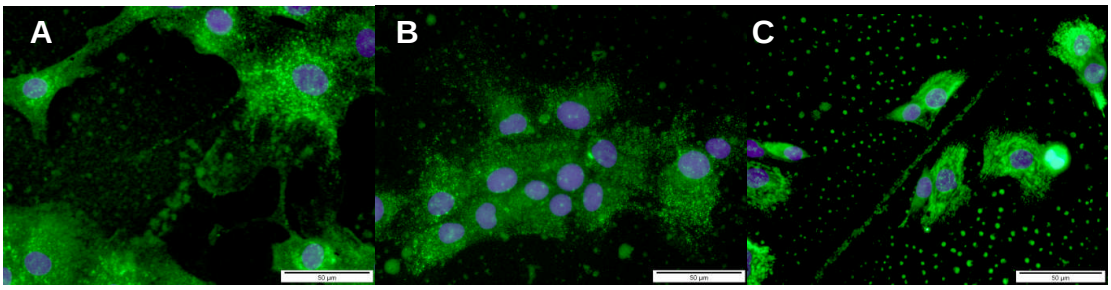


Figure 2.10: CEP cells stained with three different primary antibodies using in direct immunofluorescence using method A. A: Chondroitin-6-sulphate, B: Collagen II, C: Collagen III. CEP: cartilage end plate. Method A was similar to that described in Section 2.2.9.2 except the slides were not washed under running tap water for 10 minutes, the washing times were reduced to three times each for three minutes and the antibodies were diluted in TBS.

Background staining was observed around the cells after using Method A (Figure 2.10). As a result of this, the method was changed to Method B. Method B involved washing the slides initially under running tap water for 10 minutes prior to rinsing in TBS for five minutes. Primary antibodies were diluted in antibody diluent (Section 2.1.2) and the washing steps were altered to two washes with tween buffer for 10 minutes each and two washes in TBS for 10 minutes each. In addition to this, permeabilisation buffer was excluded from the method as it was thought to disturb the morphology of the cells.

Following the revised procedure (Method B), examples of the resulting images are shown in Figure 2.11.

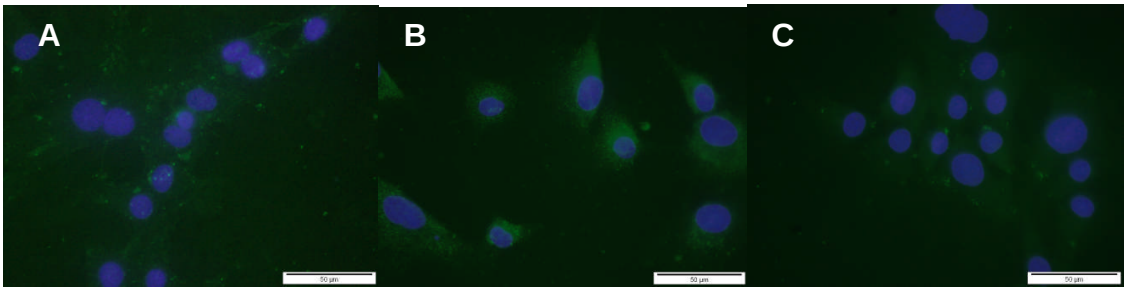


Figure 2.11: AF cells immunostained with three different primary antibodies using in direct immunofluorescence Method B. A: Chondroitin-6-sulphate, B: Collagen II, C: Collagen X. AF: Annulus fibrosus. Method B differed from Method A in that the slides were initially washed under running tap water, antibodies were diluted in antibody diluent, washing times were increased to 10 minutes and permeabilisation buffer was not used.

The images in Figure 2.11 show that the immunofluorescent stain was not sufficiently been taken up by the cells. This was likely due to the elimination of permeabilisation buffer from the staining procedure. As a result, the same method was used in future characterisation experiments but an extra step was included by incubating the slides with permeabilisation buffer for five minutes prior to the addition of the primary antibody (Method C: Section 2.2.9.1).

2.3.3. Validation of Methods for the Immunohistochemical Staining of Tissues Sections

All antibodies were optimised on control tissue sections (Table 2.3.). The initial method used to detect selected tissue markers using antibodies was the Streptavidin-Biotin method (Section 2.2.10.2.). As this did not give rise to any positive staining for all antibodies, the DAKO Envision method was then used (Section 2.2.10.1.).

Collagen II

Detection of collagen II was initially carried out on ovine femoral head cartilage using the DAKO Envision method without antigen retrieval (Figure 2.10A and 2.10B). The resulting images showed that only very faint staining was observed throughout the cartilage in comparison with the isotype control. As a result of this, proteinase K was used for antigen retrieval (Section 2.2.10.3.). The resulting images of this showed much darker staining in comparison to the

isotype control and sections without proteinase K treatment (Figure 2.12). The staining was observed throughout the cartilage as predicted and therefore the antibody was concluded to be validated using this method.

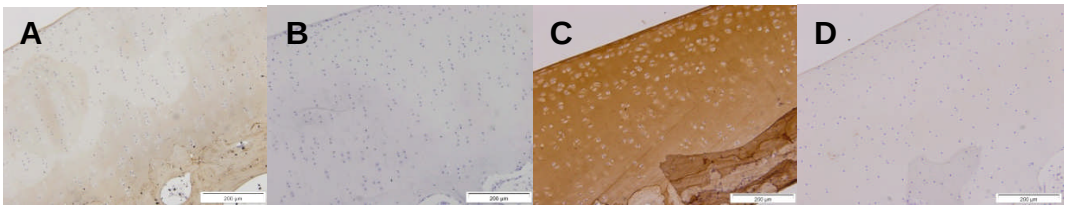


Figure 2.12: The validation of immunohistochemical staining using antibodies to collagen II on ovine femoral head cartilage. A: Collagen II (1:200) labelled ovine femoral head cartilage using the Envision method. B: IgG1 (1:100) labelled ovine femoral head cartilage using the Envision method. C: Collagen II (1:200) labelled ovine femoral head cartilage using the Envision method and proteinase K antigen retrieval. D: IgG1 (1:100) labelled ovine femoral head cartilage using the Envision method and proteinase K antigen retrieval.

Chondroitin-6-Sulphate

Detection of chondroitin-6-sulphate was initially carried out on ovine femoral head cartilage using the DAKO Envision method without antigen retrieval (Figure 2.13A and 2.13B). The resulting images showed that no staining was observed in comparison to the isotype control. As a result of this, proteinase K was used for antigen retrieval (Figure 2.13A and 2.13B). After this, the staining appeared much darker in colour when compared to the isotype control. The staining was present mainly in the superficial, transitional and deep zones. This is where it was expected and therefore the antibody was concluded to be validated using this method.

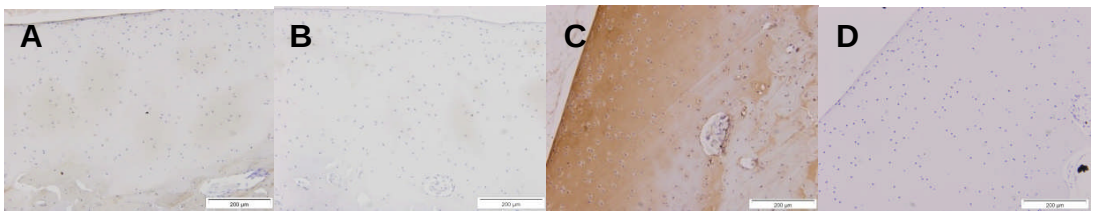


Figure 2.13: The validation of immunohistochemical staining using antibodies to chondroitin-6-sulphate on ovine femoral head cartilage. A: Chondroitin-6-sulphate (1:200) labelled ovine femoral head cartilage using the Envision method. B: IgG1 (neat) labelled ovine femoral head cartilage using the Envision method. C: Chondroitin-6-sulphate (1:200) labelled ovine femoral head cartilage using the Envision method and proteinase K antigen retrieval. D: IgG1 (neat) labelled ovine femoral head cartilage using the Envision method and proteinase K antigen retrieval.

Collagen I

Detection of collagen I was initially carried out on ovine spinous ligament using the DAKO Envision method without antigen retrieval (Figure 2.14A and 2.14B). The resulting images showed no positive staining. As a result, proteinase K antigen retrieval was used to improve this (Figure 2.14C and 2.14D). The results showed that after proteinase K antigen retrieval, the tissue was still not stained positively for collagen I. The primary collagen I antibody was then incubated overnight at 37 ºC to test whether this might give rise to positive staining. The results from this showed that the ligament was intensely stained with collagen I after proteinase K treatment and overnight incubation of the primary antibody at 37 ºC in comparison to the isotype control (Figure 2.14E and 2.14F). Therefore, this was concluded to be the method for collagen I staining was validated for ovine tissues.

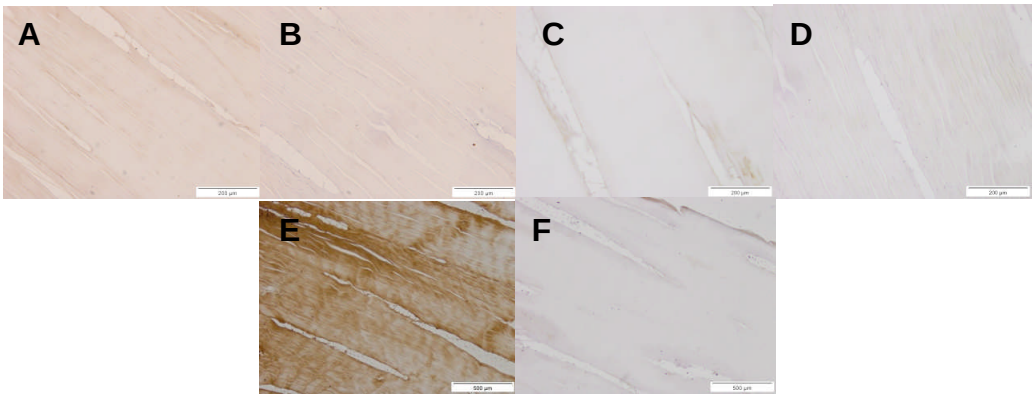


Figure 2.14: The validation of immunohistochemical staining using antibodies to collagen I on ovine spinous ligament. A: Collagen I (1:50) labelled ovine ligament using the Envision method. B: IgG1 (1:5) labelled ovine ligament using the Envision method. C: Collagen I (1:50) labelled ovine ligament using the Envision method and proteinase K antigen retrieval. D: IgG1 (1:5) labelled ovine ligament using the Envision method and proteinase K antigen retrieval. E: Collagen I (1:50) labelled ovine ligament using the Envision method, proteinase K antigen retrieval and 24 hour incubation at 37 ºC. F: IgG1 (1:5) labelled ovine ligament using the Envision method, proteinase K antigen retrieval and 24 hour incubation at 37 ºC.

Collagen III

Detection of collagen III was initially carried out on ovine ligament tissue using the DAKO Envision method without antigen retrieval. With this approach, no positive staining was observed (Figure 2.15A and 2.15B). The procedure was repeated using proteinase K for antigen retrieval (Figure 2.15C and 2.15D) however the results showed a similar negative result. To improve the staining, a lower dilution of 1:50 instead of 1:100 of collagen III was used alongside proteinase K antigen retrieval (Figure 2.15E and 2.15F). The result of this was negative when compared to the isotype control and it was concluded that false positive staining was present in the negative control. To eliminate this, prior to the addition of the primary antibody, the slides were incubated with 20 % (v/v) swine serum in antibody diluent for five minutes before washing in TBS for three minutes. Using this method staining was observed to be positive in the outer regions of the ligament in comparison to the isotype control (Figure 2.15G and 2.15H).

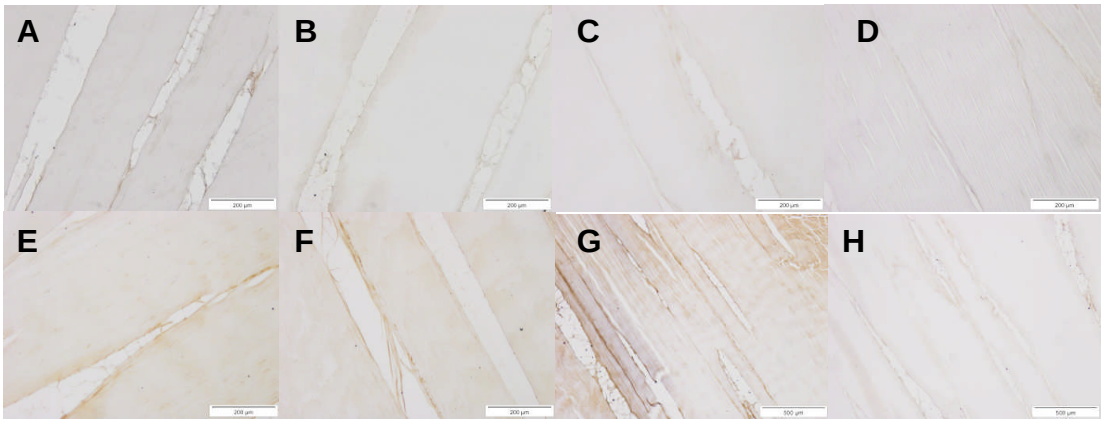


Figure 2.15: The validation of immunohistochemical staining using antibodies to collagen III on ovine spinous ligament. A: Collagen III (1:100) labelled ovine ligament using the Envision method. B: IgG (1:100) labelled ovine ligament using the Envision method. C: Collagen III (1:100) labelled ovine ligament using the Envision method and proteinase K antigen retrieval. D: IgG (1:100) labelled ovine ligament using the Envision method and proteinase K antigen retrieval. E: Collagen III (1:50) labelled ovine ligament using the Envision method and proteinase K antigen retrieval. F: IgG (1:50) labelled ovine ligament using the Envision method and proteinase K antigen retrieval. G: Collagen III (1:50) labelled ovine ligament using the Envision method, proteinase K antigen retrieval and blocking with swine serum. H: IgG (1:50) labelled ovine ligament using the Envision method, proteinase K antigen retrieval and blocking with swine serum.

Collagen VI

Detection of collagen VI was initially carried out on ovine femoral head cartilage using the DAKO Envision method without antigen retrieval. The results using this method showed staining around the lacunae in the cartilage (Figure 2.16A and 2.16B). However, the intensity of the stain was not as strong as expected. Therefore, the method was repeated with proteinase K antigen retrieval. The results from this showed a greater intensity of staining around the lacunae but also staining within the ECM (Figure 2.16C and 2.16D). As the isotype control also gave rise to positive staining within the ECM this was concluded to be due to non-specific binding. As a result, 20 % (v/v) swine serum in antibody diluent was added prior to the addition of primary antibody and incubated for five minutes before washing with TBS for three minutes. Using this method, the staining around the lacunae of the cells was intense and the background staining in the ECM was eliminated in both the antibody and isotype control

samples (Figure 2.16E and 2.16F). Therefore, this method was concluded to be the optimal one for use with collagen VI antibodies.

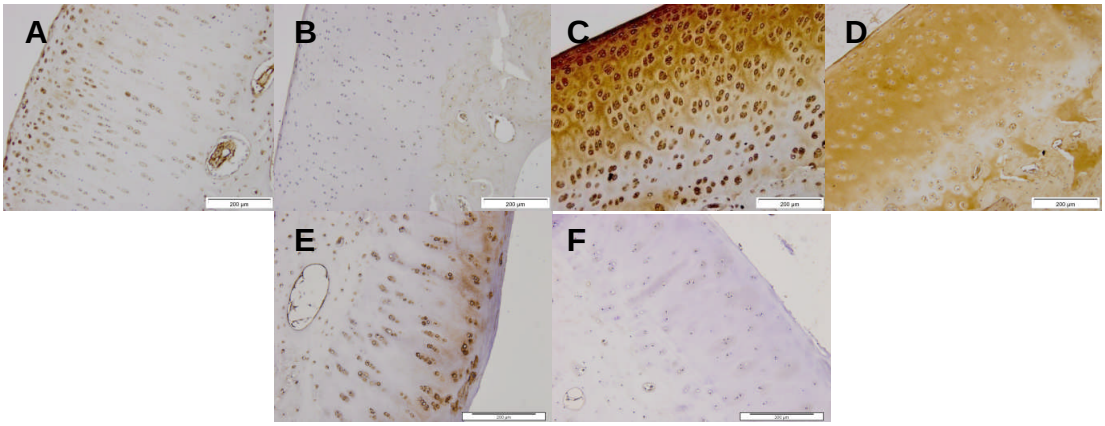


Figure 2.16: The validation of immunohistochemical staining using antibodies to Collagen VI on ovine femoral head cartilage. A: Collagen VI (1:200) labelled ovine femoral head cartilage using the Envision method. B: IgG (1:200) labelled ovine femoral head cartilage using the Envision method. C: Collagen VI (1:200) labelled ovine femoral head cartilage using the Envision method and proteinase K antigen retrieval. D: IgG (1:200) labelled ovine femoral head cartilage using the Envision method and proteinase K antigen retrieval. E: Collagen VI (1:200) labelled ovine femoral head cartilage using the Envision method, proteinase K antigen retrieval and blocking with 20 % (v/v) swine serum for five minutes prior to primary antibody incubation and washing in TBS for three minutes. F: IgG (1:200) labelled ovine femoral head cartilage using the Envision method, proteinase K antigen retrieval and blocking with 20 % (v/v) swine serum for five minutes prior to primary antibody incubation and washing in TBS for three minutes.

Collagen X

Staining for collagen X was initially carried out on ovine femoral head cartilage using the DAKO Envision method without antigen retrieval. The results from this showed faint staining in the calcified zones in comparison to the isotype control (Figure 2.17A and 2.17B). In an attempt to intensify the staining in the calcified zone, proteinase K was used for antigen retrieval. The results from this showed positive staining in the calcified zone in comparison to the isotype control but also staining in the ECM which was not expected (Figure 2.17C and 2.17D). In addition to this, staining was observed around the cells within the cartilage in the isotype control. As a result, the method was repeated with proteinase K antigen retrieval and blocking with 20 % (v/v) swine serum in antibody diluent

for five minutes and washing with TBS for three minutes prior to the addition of primary antibody.

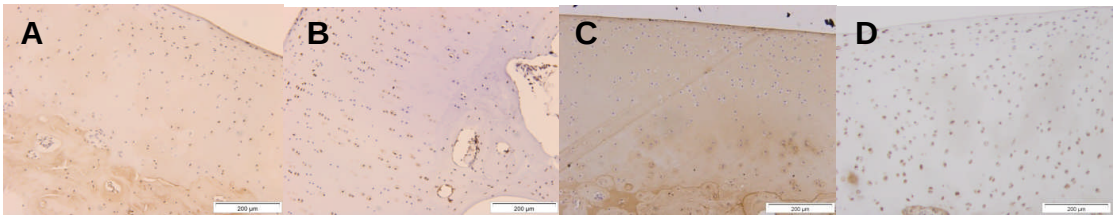


Figure 2.17: The validation of immunohistochemical staining using antibodies to collagen X. on ovine femoral head cartilage A: Collagen X (1:50) labelled ovine femoral head cartilage using the Envision method. B: IgM (1:3) labelled ovine femoral head cartilage using the Envision method. C: Collagen X (1:50) labelled ovine femoral head cartilage using the Envision method and proteinase K antigen retrieval. D: IgM (1:3) labelled ovine femoral head cartilage using the Envision method and proteinase K antigen retrieval.

Desmin

Detection of desmin was initially carried out on ovine spinous muscle using the DAKO Envision method without antigen retrieval. The results using this approach showed no positive staining in comparison with the isotype control (Figure 2.18A and 2.18B). Therefore the method was repeated using proteinase K as antigen retrieval. The results showed intense positive staining in comparison to the isotype control (Figure 2.18C and 2.18D). This method was therefore concluded to be validated for use of desmin antibodies on ovine tissue.

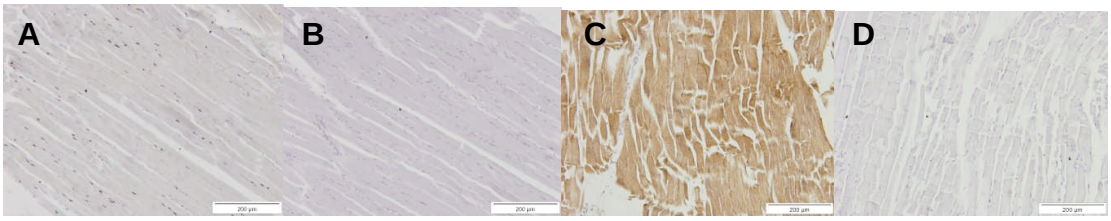


Figure 2.18: The validation of immunohistochemical staining using antibodies to desmin on ovine spinous muscle. A: Desmin (1:50) labelled ovine muscle using the Envision method. B: IgG1 (neat) labelled ovine muscle using the Envision method. C: Desmin (1:50) labelled ovine muscle using the Envision method and proteinase K antigen retrieval. D: IgG1 (neat) labelled ovine muscle using the Envision method and proteinase K antigen retrieval.

Fibronectin

Detection of fibronectin was initially carried out on ovine ligament tissue using the DAKO Envision method without antigen retrieval. The results from this approach showed no positive staining within the ligament tissue (Figure 2.19A and 2.19B). The experiment was repeated using proteinase K antigen retrieval which showed darker staining around the edges of the tissues in comparison to the isotype control (Figure 2.19C and 2.19D). Therefore this method was concluded to be validated for use of fibronectin antibodies on ovine tissues.

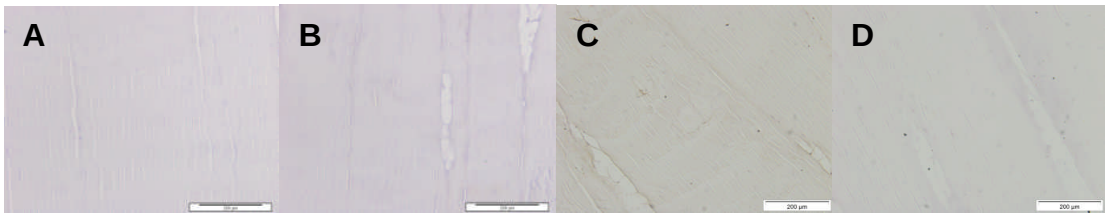


Figure 2.19: The validation of immunohistochemical staining using antibodies to fibronectin on ovine spinous ligament. A: Desmin (1:50) labelled ovine ligament using the Envision method. B: IgG1 (neat) labelled ovine ligament using the Envision method. C: Fibronectin (1:200) labelled ovine ligament using the Envision method and proteinase K antigen retrieval. D: IgG1 (neat) labelled ovine ligament using the Envision method and proteinase K antigen retrieval.

Osteocalcin

Detection of osteocalcin was initially carried out on ovine femoral head bone using the DAKO Envision method without antigen retrieval. The results using this approach showed no positive staining when compared to the isotype control (Figure 2.20A and 2.20B). As a result, proteinase K was used as an antigen retrieval method. This method gave a dark positive stain in comparison to the isotype control (Figure 2.20C and 2.20D). Therefore, this method was concluded to be validated for the use of osteocalcin antibodies on ovine tissue.

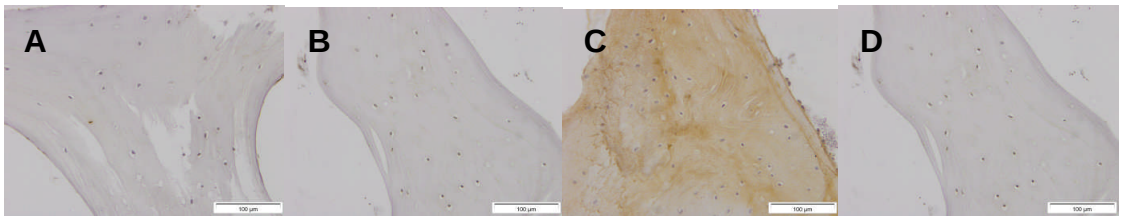


Figure 2.20: The validation optimisation of immunohistochemical staining antibodies to osteocalcin on ovine femoral head bone using. A: Osteocalcin (1:100) labelled ovine bone using the Envision method. B: IgG1 (neat) labelled ovine bone using the Envision method. C: Osteocalcin (1:100) labelled ovine bone using the Envision method and proteinase K antigen retrieval. D: IgG1 (neat) labelled ovine bone using the Envision method and proteinase K antigen retrieval.

2.3.4. Validation of Papain Digestion Method and Diluent for use in the GAG Assay

The assay for determination of sulphated GAGs used in this study had previously been developed for the determination of GAGs in articular cartilage from hip and knee tissues (Section 2.2.11.1). As the surface area of the facets are considerably smaller in comparison to articular surfaces found in the hip and knee, a smaller amount of cartilage was available for the GAG assay to quantify the amount of GAGs present. Therefore, for the GAG assay, it was likely that the sample would not require dilution (Section 2.2.11). However, this in turn meant that the crude papain, used initially to digest the cartilage, might interfere with the absorbance readings. In order to determine whether crude papain interfered with absorbance readings, three standard curves were obtained. The first curve represented standards diluted in GAG assay buffer, the second were standards diluted in neat 50 $U.ml^{-1}$ papain solution and lastly the third curve represented standards diluted in a 1:10 dilution of 50 $U.ml^{-1}$ papain solution. The curves obtained from these studies are shown in Figure 2.21.

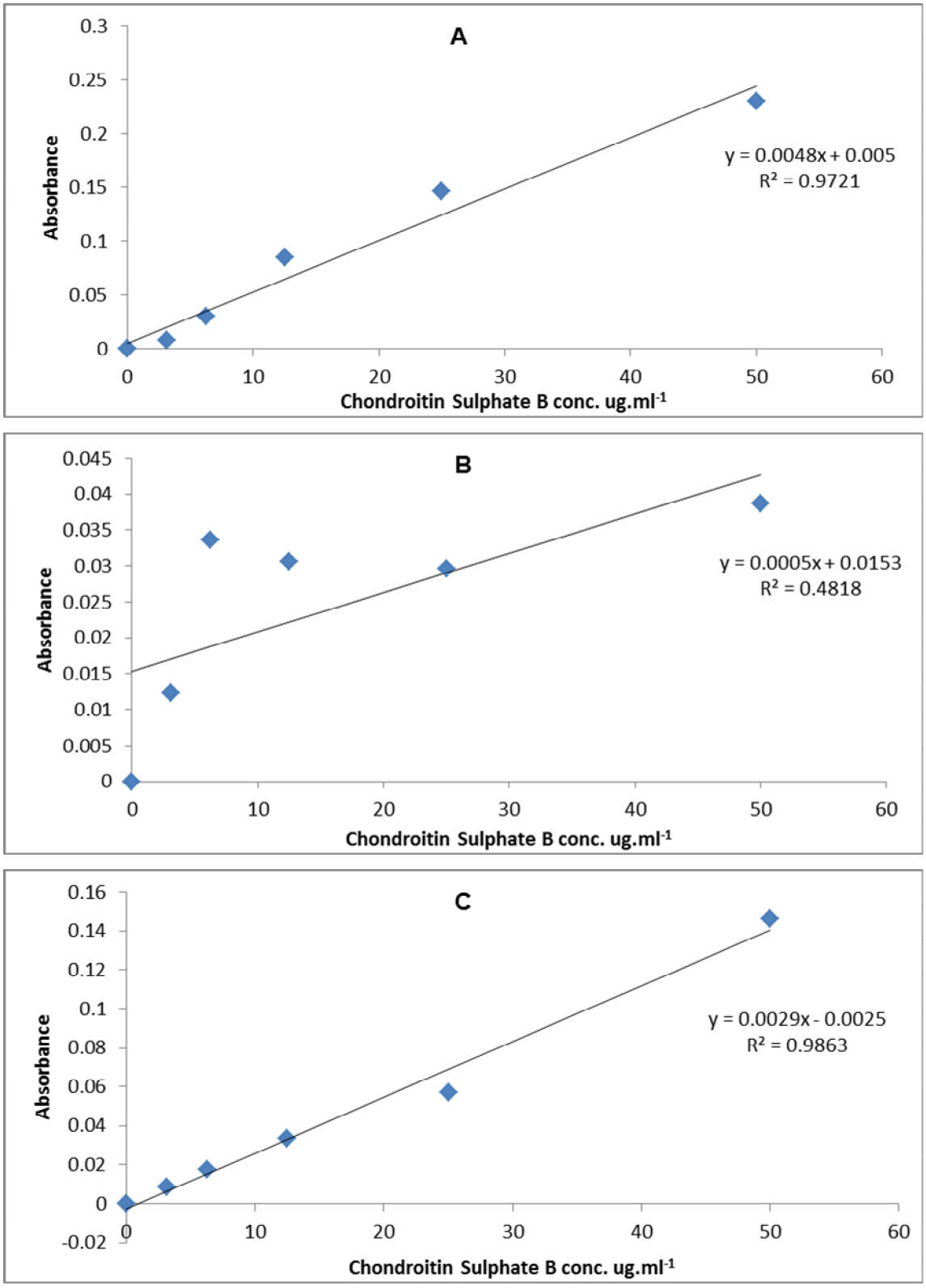


Figure 2.21: Standard curves for chondroitin sulphate B against absorbance at 525 nm. Chondroitin sulphate B was diluted in A: GAG assay buffer, B: neat 50 $U.ml^{-1}$ papain solution, C: 1:10 50 $U.ml^{-1}$ papain solution.

The results from this experiment suggested that neat papain solution had a significant effect on the absorbance readings as shown in Figure 2.21B. As a result, standards were diluted in a 1:10 dilution of 50 $U.ml^{-1}$ papain solution in all future studies to take into account absorbance that may have resulted from the presence of papain.

Lastly, in order to ensure all facet cartilage was fully digested in 50 $U.ml^{-1}$ papain solution, an experiment was carried out using the GAG assay to test facet cartilage that had been digested using 50 $U.ml^{-1}$ and 60 $U.ml^{-1}$ crude papain. Facet cartilage, previously freeze dried from a T3/T4 left inferior facet of a three year old sheep, was digested in 50 $U.ml^{-1}$ and facet cartilage previously freeze dried from a T3/T4 right inferior facet of a three year old sheep, was digested in 60 $U.ml^{-1}$ solution of papain. Both samples were analysed alongside two controls containing 50 $U.ml^{-1}$ and 60 $U.ml^{-1}$ papain only digestion solutions. The results from this experiment indicated that there was no increase in the amount of GAGs from the 60 $U.ml^{-1}$ papain digested cartilage (0.064 $mg.mg^{-1}$) in comparison to the 50 $U.ml^{-1}$ papain digested cartilage (0.071 $mg.mg^{-1}$). In addition to this, remaining undigested tissue was tested by staining with Von Kossa. The staining was positive confirming that any remnants after digestion were due to calcified tissue rather than undigested cartilage.

Chapter 3:

Anatomical Study of Ovine FSUs

Chapter 3: Anatomical Study of Ovine FSUs

3.1. Introduction

Previous work has been carried out to compare ovine and human spines (Alini *et al.*, 2008; Hasler *et al.*, 2010; Sheng *et al.*, 2010; Wang *et al.*, 2010; Bai *et al.*, 2012). Due to the similarities between these species, as discussed in Section 1.7, the sheep is an ideal animal model for the human spine. Ovine spines can be obtained from animals of different ages. This offers the potential to ultilise spines from animals of different ages as models for healthy and degenerate FSUs and facet cartilage. In addition, a variety of sheep breeds exist which may exhibit differences in spinal tissues due to variations in size and shape.

The sheep breeds analysed in this study included the breeds which could be obtained from the local abattoir. These were the Charollais, Suffolk, Texel and Hebridean breeds as shown in Figure 3.1.

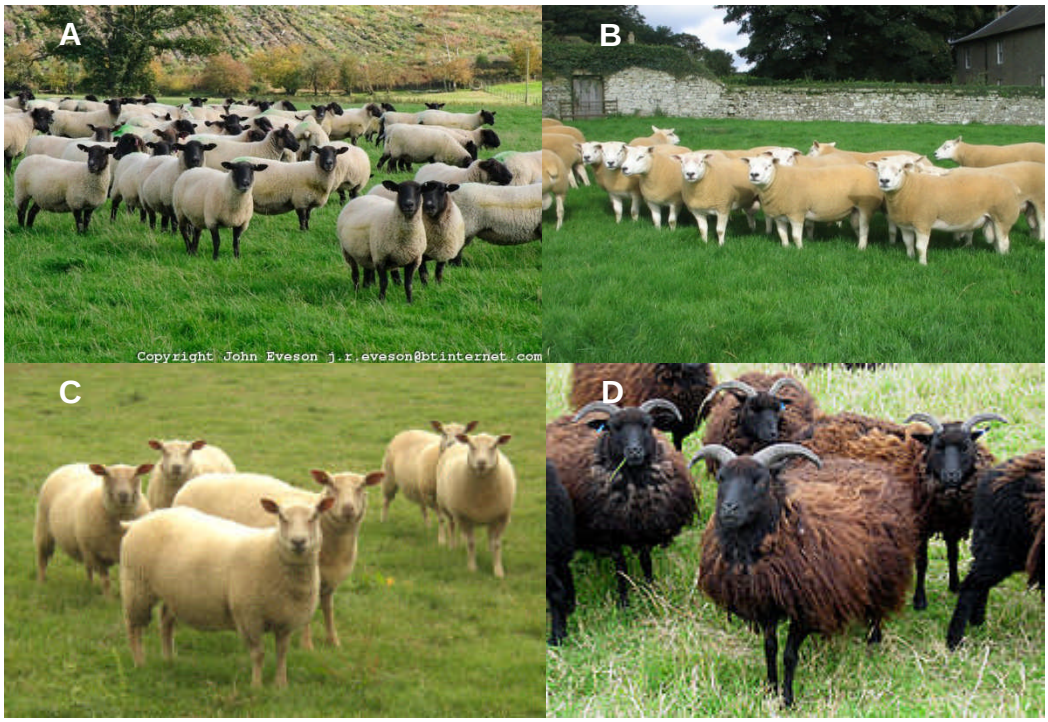


Figure 3.1: Four different breeds of sheep used in the study. A: Suffolk, B: Texel, C: Charollais, D: Hebridean (http://www.nationalsheep.org.uk/sheep-breeds.php).

The Suffolk, Texel and Charollais breeds are of similar size weighing between 85-95 kg at maturity. The Texel and Suffolk sheep are bred for meat production with the Suffolk also being used for wool. The Texel sheep produce lean meat. The Charollais breed, originating from France, is used primarily for cross breeding ewes and rams to produce quality meats. The Hebridean breed sheep are considerably smaller than the Suffolk, Texel and Charollais sheep with an average weight of 40 kg at maturity. They are not used for their meat but instead to maintain grassland. For this reason, they are kept longer and are generally older than the other three breeds.

The initial stage of the study was to determine the age of sheep which would provide healthy tissue and that which would provide degenerate tissue. This would enable a detailed characterisation study of healthy ovine facet cartilage and IVD tissue to be carried out (Chapter 4).

3.2. Aims and Objectives

The aim of the work described in this chapter was to analyse ovine FSUs of different ages and breeds to determine whether age and breed have an effect on the health of facet cartilage, CEP, IVD and bone within FSUs. The ultimate aim was to determine the age of animal which would provide healthy tissues and that which would provide degenerated tissues for the future development of *in vitro* models.

Specific Objectives:

- Analyse the morphology of FSUs from cervical, thoracic and lumbar regions of different ages and breeds of sheep including the whole FSU, IVD and facet joints.
- Analyse and grade degeneration using H&E stained transverse sections of IVDs from cervical, thoracic and lumbar regions of different ages and breeds of sheep.
- Analyse and grade degeneration using H&E stained sagittal sections of IVDs from cervical, thoracic and lumbar regions of different ages and breeds of sheep.
- Analyse and grade the morphological degeneration of facets from cervical, thoracic and lumbar regions of different ages and breeds of sheep.
- Analyse and grade degeneration using H&E stained sections of facet cartilage from cervical, thoracic and lumbar regions of different ages and breeds of sheep.
- Scan whole FSUs from cervical, thoracic and lumbar regions of different ages and breeds of sheep to determine the properties of the bone, IVD height and facet joint space distance.

3.3. Experimental Approach

The sheep spines included in this study were limited by the availability of spines from sheep of different ages and breeds. The sheep spines used in the study were divided into four age groups. These were 0-1, 3-4, 5-6 and 8-10 years of age. For each group, other than the three to four year group (n=9), three spines of the appropriate age were analysed. Various breeds of ovine spines were in the age groups. In the 0-1 year age group, the spines were all from the Charollais breed. In the 3-4 year age group, replicates one to three were from Charollais sheep, replicates four, eight and nine from Suffolk sheep and replicates five to seven were from Texel sheep. In the 5-6 year age group, replicate one was a Suffolk, two was a Texel and three was a Suffolk. In the 8-10 year age group all spines were obtained from Hebridean sheep. For the 3-4 year old age group, the effect of sheep breed was investigated. This involved analysing three Charollais, Texel and Suffolk spines giving a total of nine for the group. It was important to determine whether the characteristics of the tissue changed with breed as well as age.

For each spine, the cervical, thoracic and lumbar regions were analysed. FSUs C4/C5, T8/T9 and L3/L4 were selected for H&E staining of transverse IVD sections and photography of the whole FSU, dissected FSU and IVD. These FSUs were dissected and fixed immediately after obtaining the spine (approximately one day after slaughter). FSUs C6/C7, T11/T12 and L1/L2 were selected for µCT scanning, H&E staining of sagittal IVD and facet sections and photography of the facet surfaces. These FSUs were dissected whole and immediately stored at -20 ºC until being thawed for µCT scanning. They underwent another freeze/thaw cycle in order to cut 2 mm sagittal IVD slices followed by dissection of the left inferior facet to cut 2 mm facet slices. The grading systems used to grade all histological sections and images of the facets have been described in Section 2.2.7.8. Details of histology have been described in Section 2.2.7.1-2.2.7.5 and µCT analysis in Section 2.2.12.

As the grading data was non-parametric and divided into six unmatched groups (each with n=3), the Kruskal-Wallis test was used to assess whether there was any significant variation in the data, followed by post hoc testing using Dunn`s

test to determine individual difference between group means ($p < 0.05$). If significant variation was not found in the data for the three breeds in the 3-4 year age group, data from the different breeds of sheep were combined. Spearman's rank correlation was chosen to identify the strength of the relationship between grade and age and whether any correlations were present.

For the parametric µCT data including HA concentration, IVD height and facet joint space, analysis of variance was used to determine any significant variation in the data from the different age groups and breeds groups. This was followed by calculation of the minimum significant difference between means ($p<0.05$; $p<0.01$). For this data correlations between age and the parameter measured were determined using the Pearson`s moment correlation.

For BV/TV, as this data was a proportion and therefore did not meet the assumptions of analysis of variance the data was subject to arcsine transformation and analysis of variance of the transformed data. Since the BV/TV data was not parametric, correlation with age analysis was by Spearman`s rank correlation.

3.4. Results

3.4.1. Morphological Analysis of FSUs using Photography

The FSUs C4/C5, T8/T9 and L3/L4 were photographed intact and separated for each sheep spine. The facets and IVDs were then photographed separately. Examples of the images captured from the cervical, thoracic and lumbar regions of a three year old Texel sheep are shown in Figure 3.2.

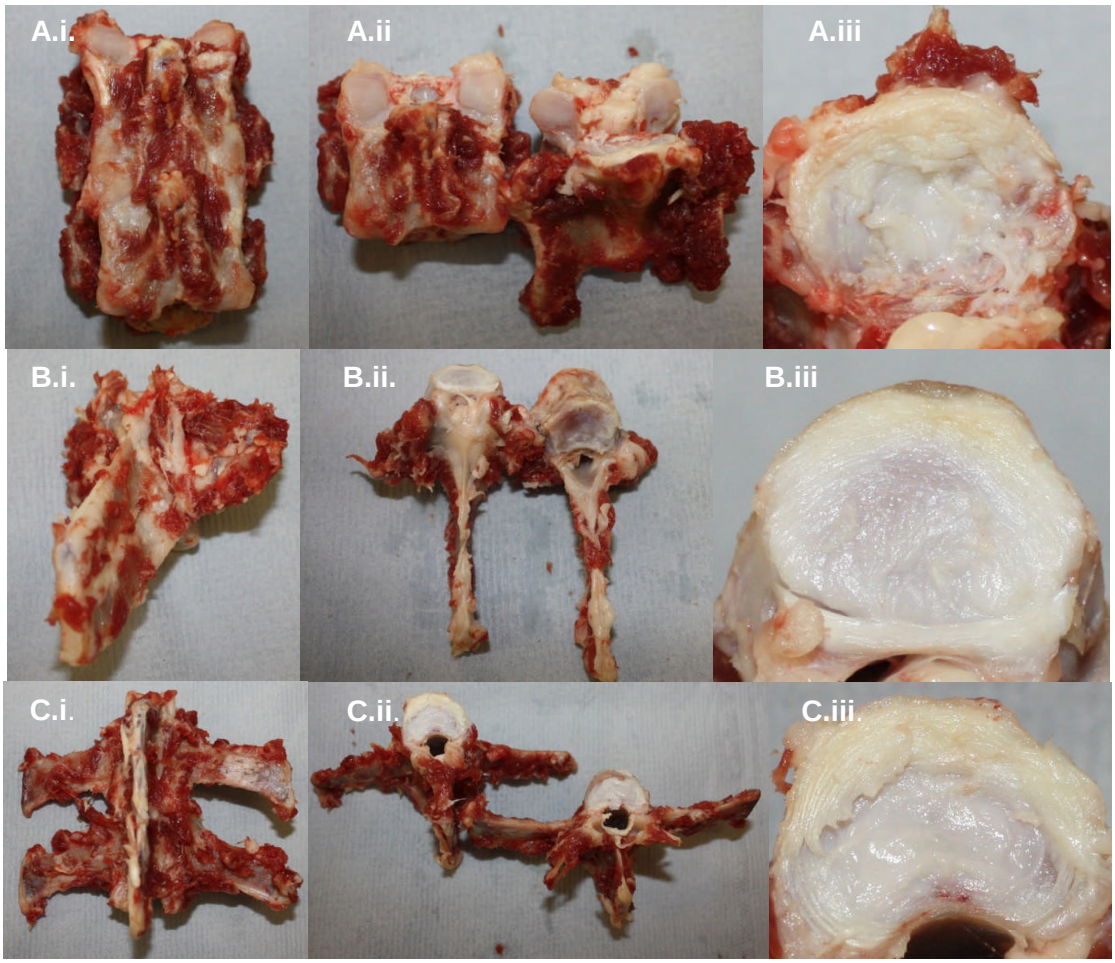


Figure 3.2: Images of FSUs from a three year old Texel sheep. A: C4/C5, B: T8/T9, C: L3/L4, i: Intact FSU, ii: separated FSU, iii: IVD. FSU: Functional spinal unit, IVD: Intervertebral disc.

In general, differences were observed between cervical, thoracic and lumbar FSUs from all ages and breeds of sheep. In the cervical region, the FSUs appeared straight and had no transverse processes. The vertebrae and surrounding pedicles were bulky and thick. The spinous processes were short. The facets were round and flat with a large surface area. The cervical IVDs were curved around the vertebrae and were thick in comparison to both the

thoracic and lumbar IVDs. The thoracic FSUs were much shorter in vertebral height and contained long spinous processes. The transverse processes were replaced with ribs which extended outwards and had been removed from the tissue during dissection as shown in Figure 3.2.B.ii. The pedicles and laminal arches were less bulky in comparison to cervical FSUs. The facets appeared much smaller and had an arch-like shape that was curved. The IVDs appeared flat, smaller and thinner in appearance in comparison to those in the cervical FSUs. The lumbar FSUs by comparison were larger containing long, flat transverse processes. The vertebrae also appeared long and the spinous processes short but flat and thick. The inferior facets were bulky and appeared tall and slightly curved. The superior facets were observed to be completely curved all the way around the inferior facets. As with the thoracic facets there was no flat surface. The lumbar IVDs were very similar to the thoracic IVDs in that they were flat but had a larger surface area and were thicker. Lumbar FSUs of different age groups are shown for comparison in Figure 3.3.

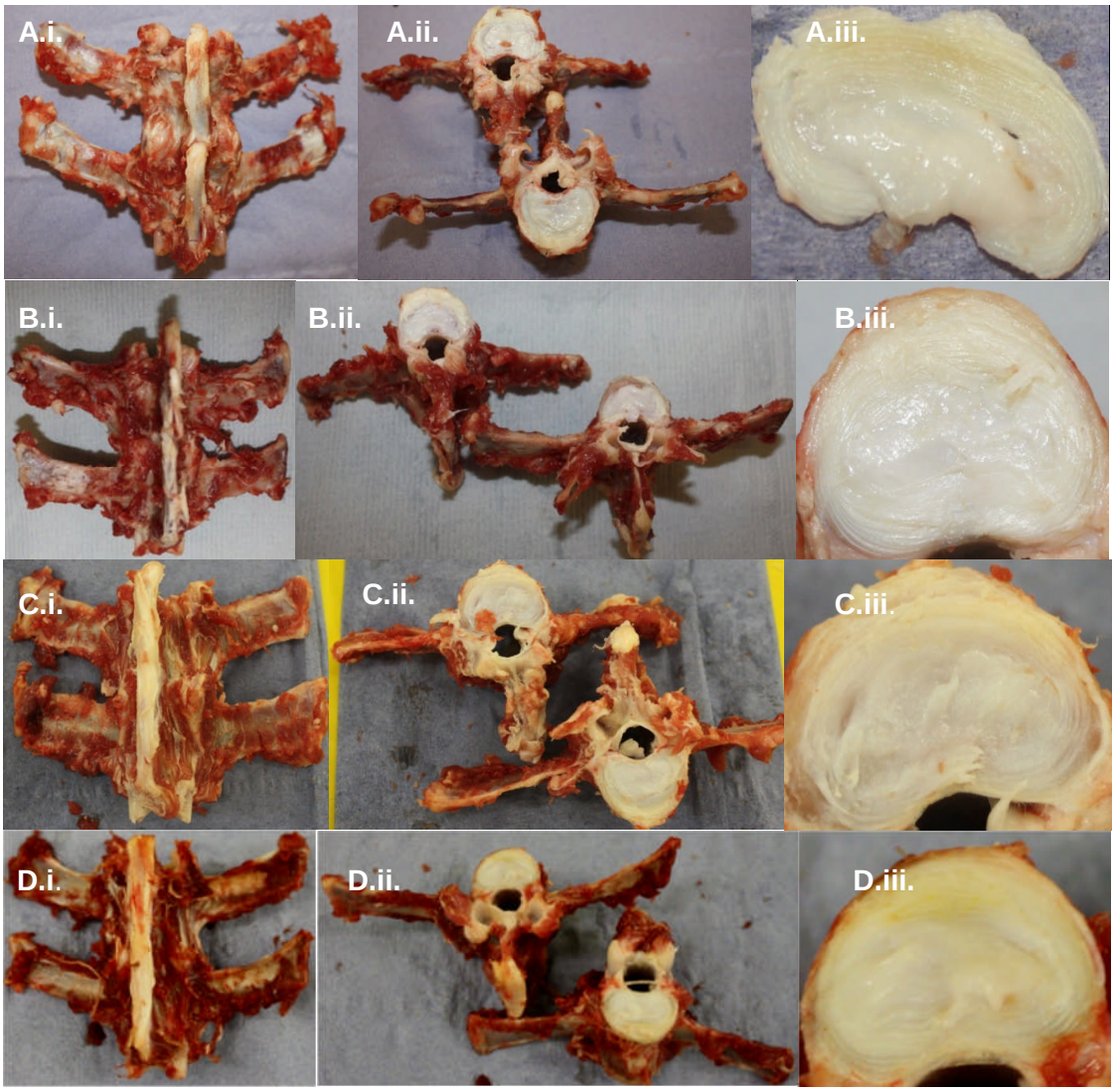


Figure 3.3: Images of lumbar L3/L4 FSUs from 0-1, 3-4, 5-6 and 8-10 year old sheep. A: 0-1 year old (Charollais), B: 3-4 years old (Charollais), C: 5-6 years old (Texel), D: 8-10 years old (Hebridean), i. intact FSU, ii. separated FSU, iii. transverse IVD. FSU: Functional spinal unit, IVD: Intervertebral disc.

No morphological differences were observed in the intact and separated FSUs between the ages in the three different regions. However, differences were observed in the IVDs. In all regions, 0-1 year old IVDs appeared thick enough to be removed from their vertebral body with the NP white and gelatinous in appearance. With age, the NP became more fibrous and yellow in colour. At five to six years of age, the IVD became too thin to be removed from the vertebral body as an intact tissue.

3.4.2. Grading of Haematoxylin and Eosin Stained Sections of Transverse IVDs for Degeneration

Whole intact IVDs were removed from the FSUs C4/C5, T8/T9 and L3/L4. These were then prepared by fixing, tissue processing, embedding, sectioning and staining with H&E (Section 2.2.7.5). All transverse sections of each IVD were observed and graded blindly (Section 2.2.7.8) by two independent trained graders. The inter-rater reliability (kappa) test was performed on all the data from both graders. The kappa score was 0.04 (p=0.716), showing there was slight agreement between the two graders.

The degeneration grading results for the transverse sections of cervical IVD are shown in Figure 3.4.

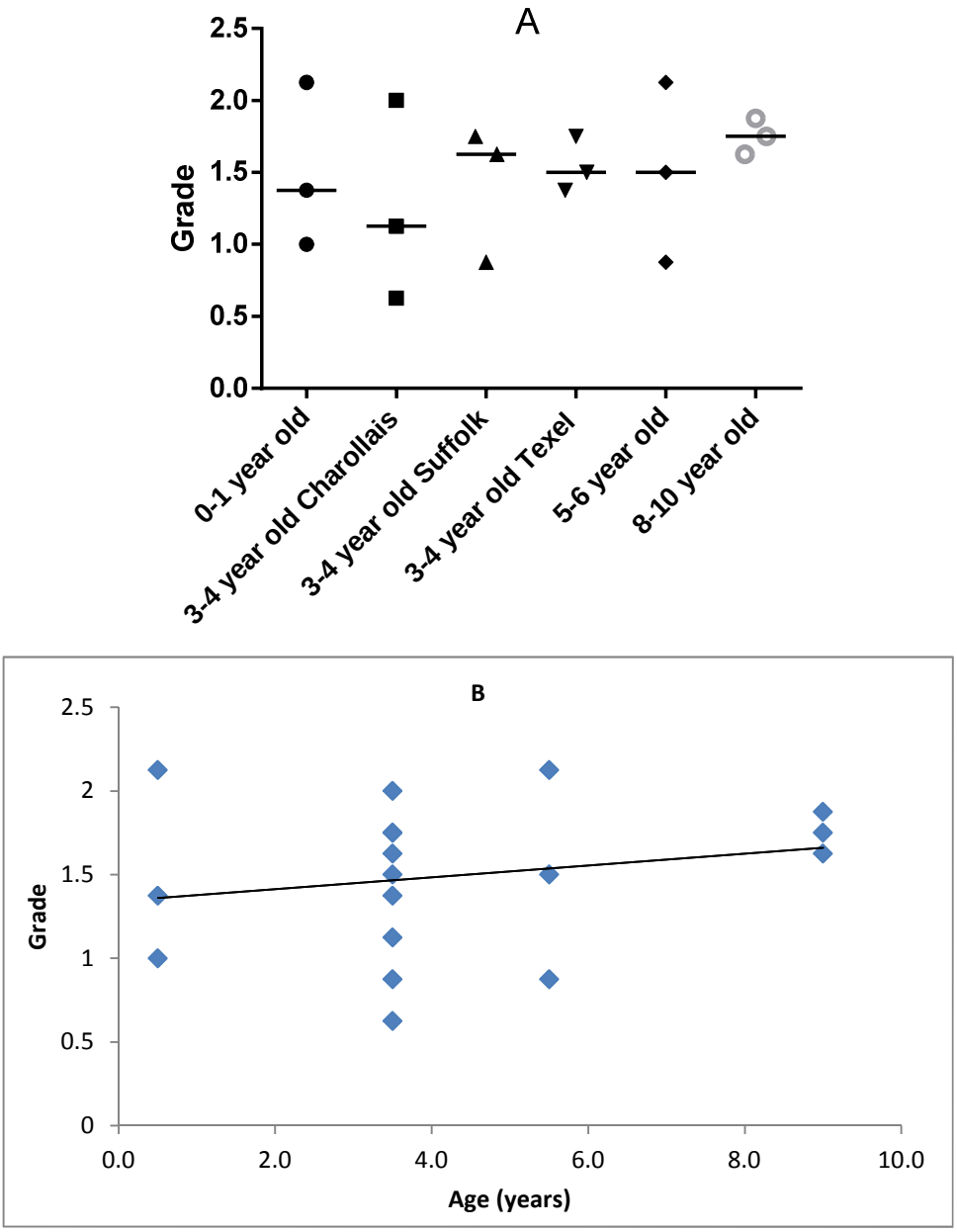


Figure 3.4: The distribution of grading scores for H&E stained sections of ovine cervical (C4/C5) transverse IVDs in four age groups and three breeds of 3-4 year old sheep. A: The distribution of grades for each age and breed group (n=3). The age/breed group data was analysed using the Kruskal-Wallis test (p=0.8814) which found no significant variation in the data. B: The distribution of grades for each age group. The data was analysed using Spearman's rank correlation (r=0.2699) which found no correlation between the grade and age of sheep. H&E: Haematoxylin and eosin, IVD: Intervertebral disc.

No variation was found in the degeneration grade of the transverse sections of the cervical IVDs from sheep of different ages or between the breeds of the 3-4 year age group (Kruskal-Wallis test p=0.88). There was no correlation between

the degeneration grade and age (r=0.27; Spearman`s rank correlation). The data was evenly spread and high grades (above 1.5) were assigned to the degeneration in the transverse sections of the IVDs across the age groups. As a result, no trend was observed.

The degeneration grading results for the transverse sections of thoracic IVDs are shown in Figure 3.5.

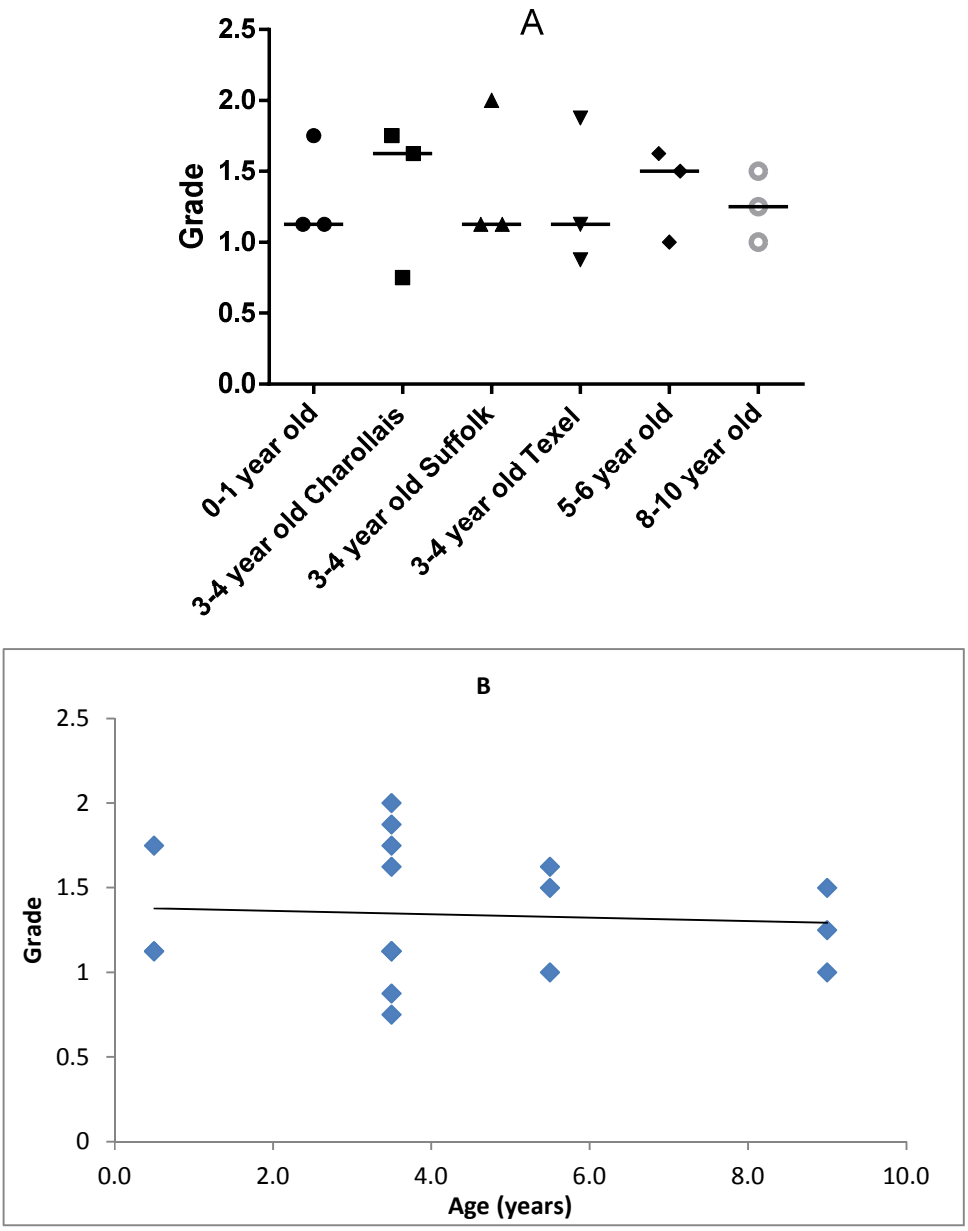


Figure 3.5: The distribution of degeneration grading scores for H&E stained sections of ovine thoracic (T8/T9) transverse IVDs in four age groups and three 3-4 year old breeds of sheep. A: The distribution of grades for each age and breed group (n=3). The age/breed group data was analysed using the Kruskal-Wallis test (p=0.9951) which found no significant variation between the age and breed groups. B: The distribution of grades for each age group. The data was analysed using Spearman's rank correlation (r=-0.0495) which found no correlation between grades and age. H&E: Haematoxylin and eosin, IVD: Intervertebral disc.

No significant variation was found in the degeneration grades of the transverse sections of the thoracic IVDs between the age groups or between the breeds of the 3-4 year age group (Kruskal-Wallis test p=0.10). There was no correlation

between degeneration grade of the histological sections of the transverse sections of the IVDs (r= -0.05). Similarly to the cervical sagittal IVD sections, the data was spread relatively evenly across all age groups. The data in the 3-4 year age group was particularly spread across the different grades from 0.75 to 2.00.

The degeneration grading results for the transverse sections of the lumbar IVDs are shown in Figure 3.6.

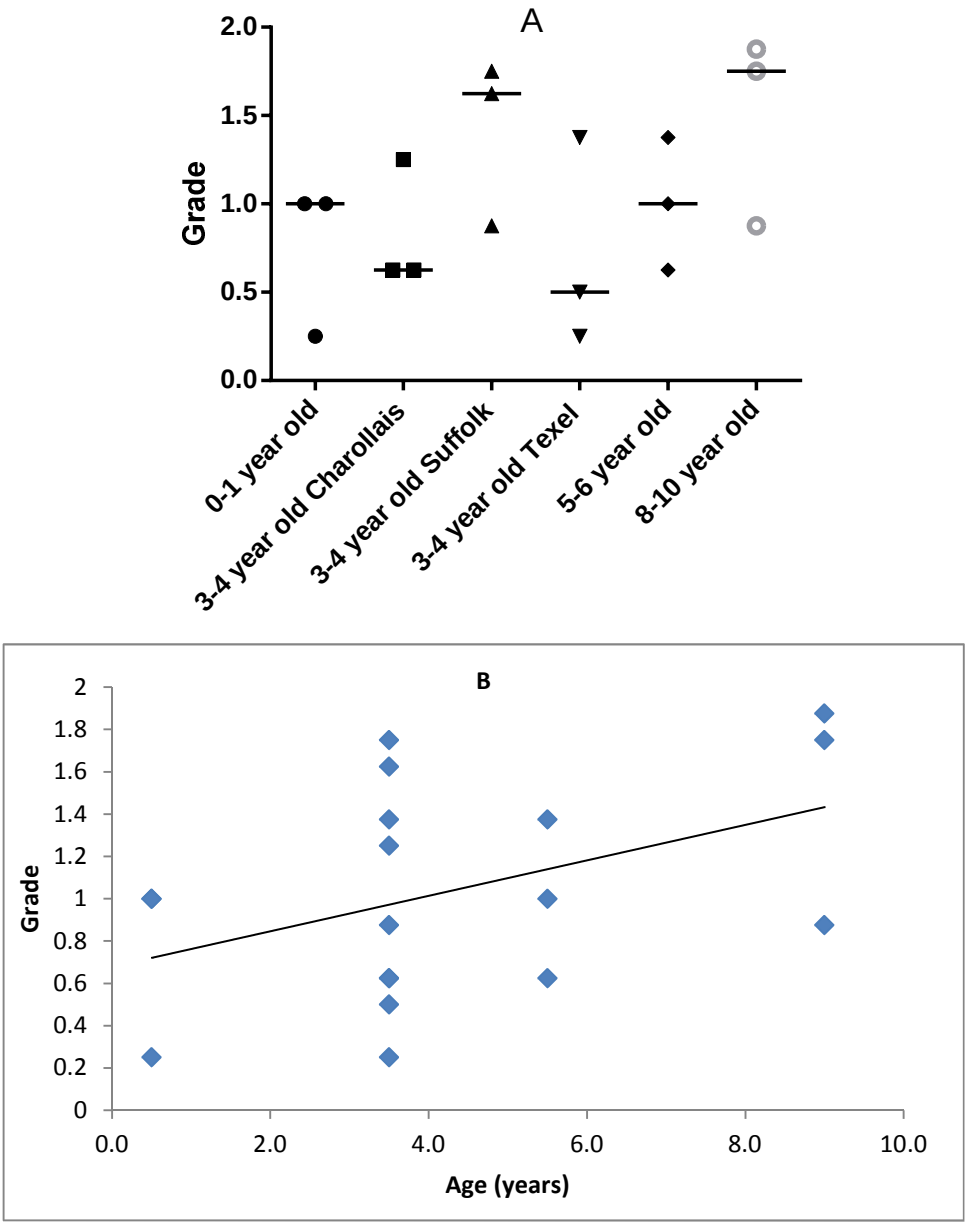


Figure 3.6: The distribution of degeneration grading scores for H&E stained sections of ovine lumbar (L3/L4) transverse IVDs in all four age groups and three 3-4 year old breeds of sheep. A: The distribution of grades for each age and breed group (n=3). The age/breed group data was analysed using the Kruskal-Wallis test (p=0.3211) which found no variation between the age and breed groups B: The distribution of grades for each age group. The data was analysed using Spearman's rank correlation (r=0.4226) which indicated a weak positive correlation between age and grade. H&E: Haematoxylin and eosin, IVD: Intervertebral disc.

No variation was observed between the degeneration grades of the transverse sections of the lumbar IVDs of different age groups or between the breeds of the 3-4 year age group (Kruskal-Wallis test; p=0.32). The grades were generally

more spread between the grades than those in the cervical and thoracic IVDs with grades in the 0-1 and 3-4 year age groups as low as 0.25. There was a weak positive correlation of increasing grade with age (r=0.42; Spearman`s rank correlation). The grade increased at 5-6 years of age with the lowest grades in the older age groups increasing from 0.25 to 0.625.

3.4.3. Grading of Haematoxylin and Eosin Stained Sections of Sagittal IVDs for Degeneration

Sagittal sections (2 mm thick) were obtained from FSUs C6/C7, T11/T12 and L1/L2 from each age group. These were fixed overnight before being decalcified in 12.5 % (v/v) EDTA for two weeks. The samples were then tissue processed, embedded in paraffin wax, sectioned at 5 μm and stained with H&E. Each section was graded (Section 2.2.7.8) blind by two independent trained graders. The inter-rater reliability (kappa) test was performed on all the data from both graders. The kappa score was 0.278 (p=0.007), showing there was fair agreement between the two graders.

The degeneration grading results for the cervical sagittal IVDs are shown in Figure 3.7.

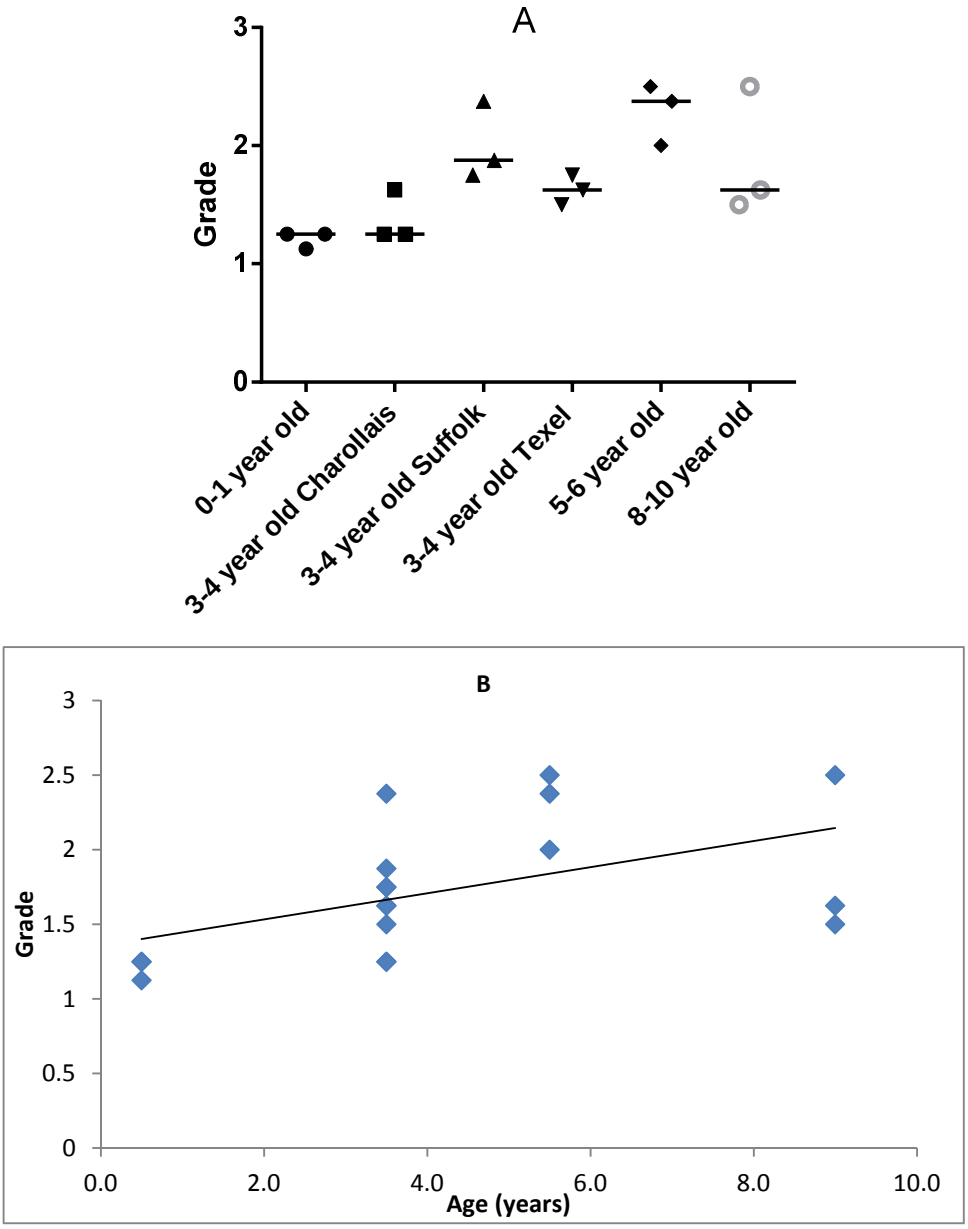


Figure 3.7: The distribution of degeneration grading scores for H&E stained ovine cervical (C6/C7) sagittal IVD sections in four age groups and three 3-4 year old breeds of sheep. A: The distribution of grades for each age and breed group (n=3). The age/breed group data was analysed using the Kruskal-Wallis test (p=0.0254) which revealed a significant difference between the 0-1 year and 5-6 year age group. B: The distribution of grades for each age group. The data was analysed using Spearman's rank correlation (r=0.6285) which showed a good positive correlation between the grades and age. H&E: Haematoxylin and eosin, IVD: Intervertebral disc.

There was a significant difference between the degeneration grade of the 0-1 and 5-6 year old age group sagittal sections of the cervical IVDs (Kruskal-Wallis test), indicating an increase in grade with age. However, no significant

differences were found between the 8-10 year old age group and the other five groups. No significant differences were observed between the three breeds in the 3-4 year age group. There was a good positive correlation of increasing grade with age (r=0.63; Spearman`s rank correlation).

The degeneration grading results for the sagittal sections of the thoracic IVDs are shown in Figure 3.8.

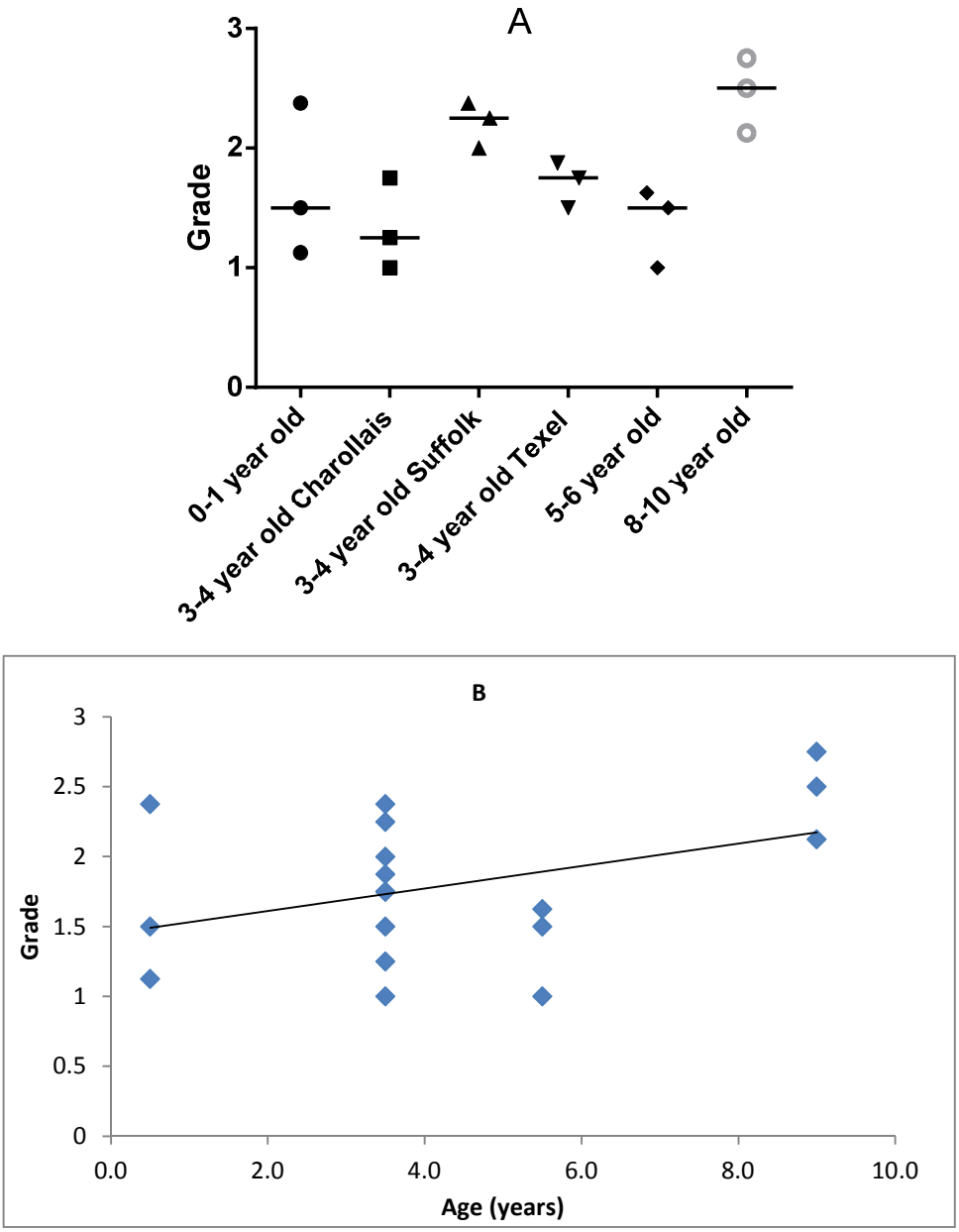


Figure 3.8: The distribution of degeneration grading scores for H&E stained ovine thoracic (T11/T12) sagittal IVD sections in four age groups and three 3-4 year old breeds of sheep. A: The distribution of grades for each age and breed group (n=3). The age/breed group data was analysed using the Kruskal-Wallis test (p=0.0546) which found no differences between the age and breed groups. B: The distribution of grades for each age group. The data was analysed using Spearman's rank correlation (r=0.3117) which found no correlation between the grades and age groups. H&E: Haematoxylin and eosin, IVD: Intervertebral disc.

No significant differences were found in the degeneration grading of the sagittal sections of the thoracic IVDs between the age groups or between the breeds of the 3-4 year old age group (Kruskal-Wallis test). There were no significant

differences in the grades of the 3-4 year old age groups of different breeds Generally, the score appeared to increase with age however no correlation was found between age and grade (r= 0.31; Spearman`s rank correlation). In comparison to the sagittal sections of the cervical IVDs, the degeneration grades were slightly lower particularly for the 5-6 year age group whose lowest grades decreased from 2.00 in the cervical sagittal sections to 1.00 in the thoracic sagittal sections. The grades in the 8-10 year age group appeared to be particularly high in comparison to the other three age groups.

The degeneration grading results for the sagittal sections of the lumbar IVDs are shown in Figure 3.9.

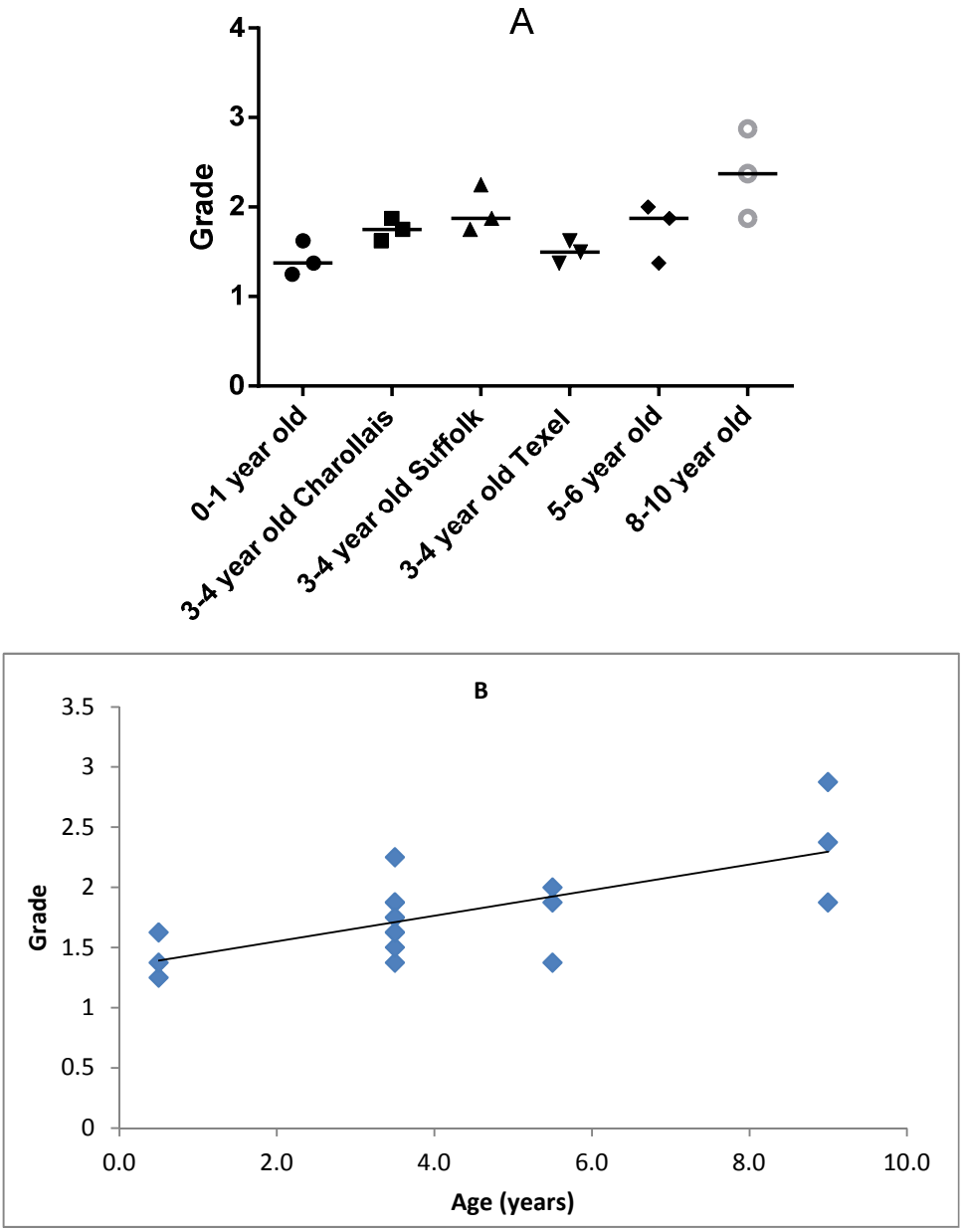


Figure 3.9: The distribution of degeneration grading scores for H&E stained ovine lumbar (L1/L2) sagittal IVD sections in four age groups and three 3-4 year old breeds of sheep. A: The distribution of grades for each age and breed group (n=3). The age/breed group data was analysed using the Kruskal-Wallis test (p=0.0464) which found no differences between the age and breed groups. B: The distribution of grades for each age group. The data was analysed using Spearman's rank correlation (r=0.6775) which found a good positive correlation between the grades and age groups. H&E: Haematoxylin and eosin, IVD: Intervertebral disc.

There were no significant differences found in the degeneration grading of the sagittal sections of the thoracic IVDs between the age groups or between the breeds of the 3-4 year old age group (Kruskal-Wallis test). However, a good

positive correlation was observed in grade with increasing age (r=0.68; Spearman`s rank correlation). The grades were in similar ranges to the cervical and thoracic samples, between 1.00 and 3.00. Similarly to the sagittal sections of the thoracic IVDs the degeneration grades of the 8-10 year age group appeared higher in comparison to the other age groups.

The change in tissue morphology with age was most visible in the CEP tissue of the lumbar sagittal sections. Examples of H&E stained sections in the CEP of lumbar IVDs from the four age groups is shown in Figure 3.10.

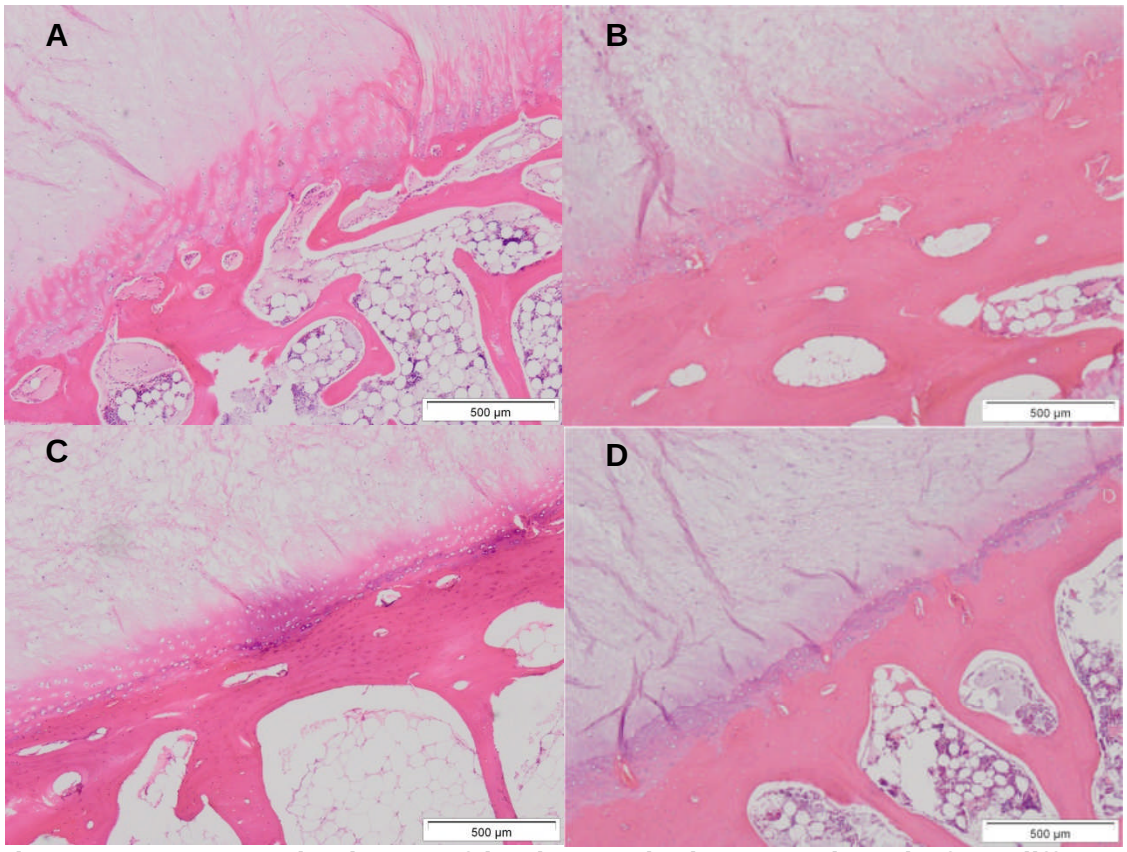


Figure 3.10: H&E stained CEP of lumbar sagittal IVD sections in four different age groups. A: 0-1 year old (Charollais), B: 3-4 year old (Charollais), C: 5-6 year old (Suffolk), D: 8-10 year old (Hebridean). H&E: Haematoxylin and eosin, CEP: Cartilage end plate, IVD: Intervertebral disc.

In sagittal sections of the IVDs of the 0-1 year old age group, the CEP was at its thickest and had an organised structure with no visible fissures. The cells appeared randomly dispersed and there were no empty lacunae. No calcification could be seen. In the sagittal sections of the IVDs of 3-4 year olds, the structure was similar except for the occasional empty lacunae. For IVDs

from 5-6 year old sheep, the cartilage was thinner and had a much greater number of empty lacunae. The CEP showed evidence of calcification. At 8-10 years old, the CEP had lost most of its structure, had no visible cells and was thinner than that in the 5-6 year old group. Extensive calcification was visible.

3.4.4. Morphological Grading of Facets Using Photography

Left superior and inferior facets from FSUs C6/C7, T11/T12 and L1/L2 were dissected and photographed. Examples from the cervical, thoracic and lumbar regions across all four age groups are shown in Figure 3.11.

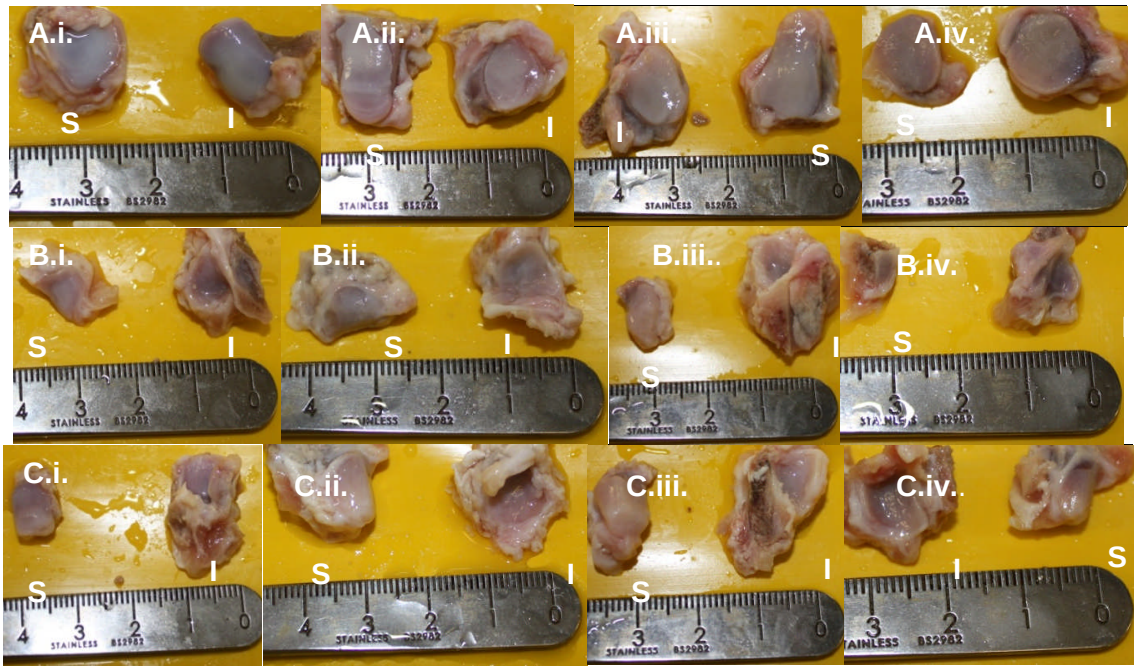


Figure 3.11: Images of ovine cervical (C6/C7), thoracic (T11/T12) and (L1/L2) lumbar left superior (S) and inferior (I) facets from one, three to four, five to six and eight to 10 year old sheep. A: Cervical inferior and superior facets. B: Thoracic inferior and superior facets. C: Lumbar inferior and superior facets. i. one year, ii. Three to four years, iii. Five to six years, iv. Eight to 10 years.

Each of the left inferior and superior facets were graded using the degeneration grading system described (Section 2.2.7.8) by two independent trained graders. The inter-rater reliability (kappa) test was performed on all the data from both graders. The kappa score was 0.567 ($p<0.0001$), showing there was moderate agreement between the two graders.

The final grades for the inferior and superior facets were combined by calculating their mean to give a final score. The mean score from both graders was determined and plotted for each of the cervical, thoracic and lumbar regions. The results from the cervical facets degeneration grading is shown in Figure 3.12.

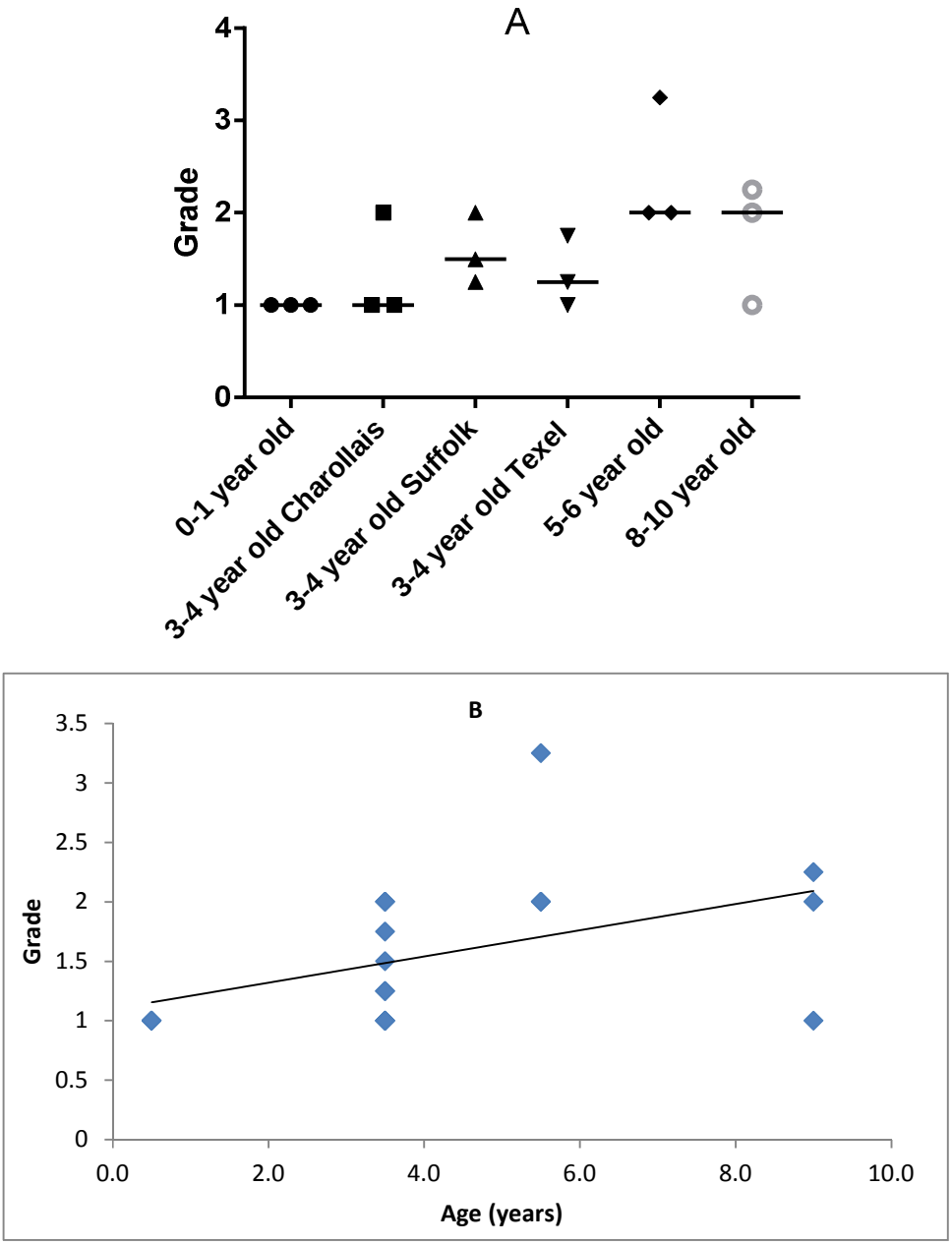


Figure 3.12: The distribution of grading scores for the macroscopic left ovine cervical (C6/C7) facets in four age groups and three 3-4 year old breeds of sheep. A: The distribution of grades for each age and breed group (n=3). The age/breed group data was analysed using the Kruskal-Wallis test (p=0.1113) which found no differences between the age and breed groups. B: The distribution of grades for each age group. The data was analysed using Spearman's rank correlation (r=0.6553) which found a good positive correlation between the grades and age groups.

There were no significant differences found for the morphological grading of the cervical facets between the age groups and between the different breeds in the 3-4 year old age group (Kruskal-Wallis test). However, a good positive

correlation was found in grade with increasing age (r=0.66; Spearman`s rank correlation). The grading scores for the 0-1 year age group were low with all grades at 1.0 whilst the ranges of grades in the 3-4 and 8-10 year age groups were similar. The grades in the 5-6 year age group were considerably higher in comparison to the other three age groups.

The results for the morphological grading of thoracic facets are shown in Figure 3.13.

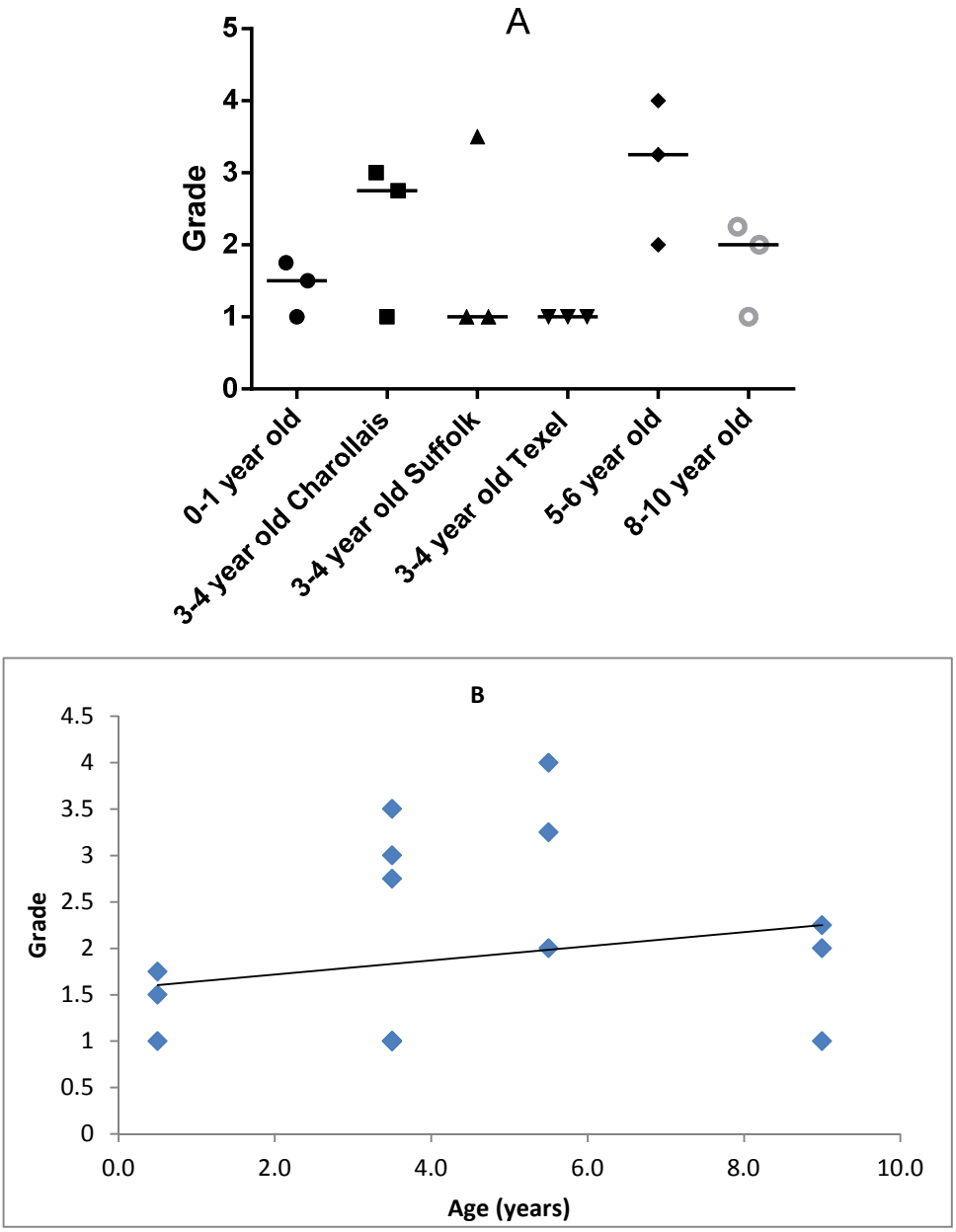


Figure 3.13: The distribution of grading scores for the macroscopic left ovine thoracic (T11/T12) facets in all four age groups and three 3-4 year old breeds of sheep. A: The distribution of grades for each age and breed group (n=3). The age/breed group data was analysed using the Kruskal-Wallis test (p=0.1983) which found no differences between the age and breed groups. B: The distribution of grades for each age group. The data was analysed using Spearman's rank correlation (r=0.3762) which found no correlation between the grades and age groups.

No differences were observed between the age and breed groups of the macroscopic cervical facet grading scores (Kruskal-Wallis test). There was no correlation between age and grade (r=0.38; Spearman`s rank correlation).

Overall, the grades for each group appeared to fluctuate showing no obvious trend or pattern. The highest grade was in the 5-6 year old group which had a mean score of 3.08. The grades were higher than those observed for the cervical facets.

The results for the morphological grading of the lumbar facets are shown in Figure 3.14.

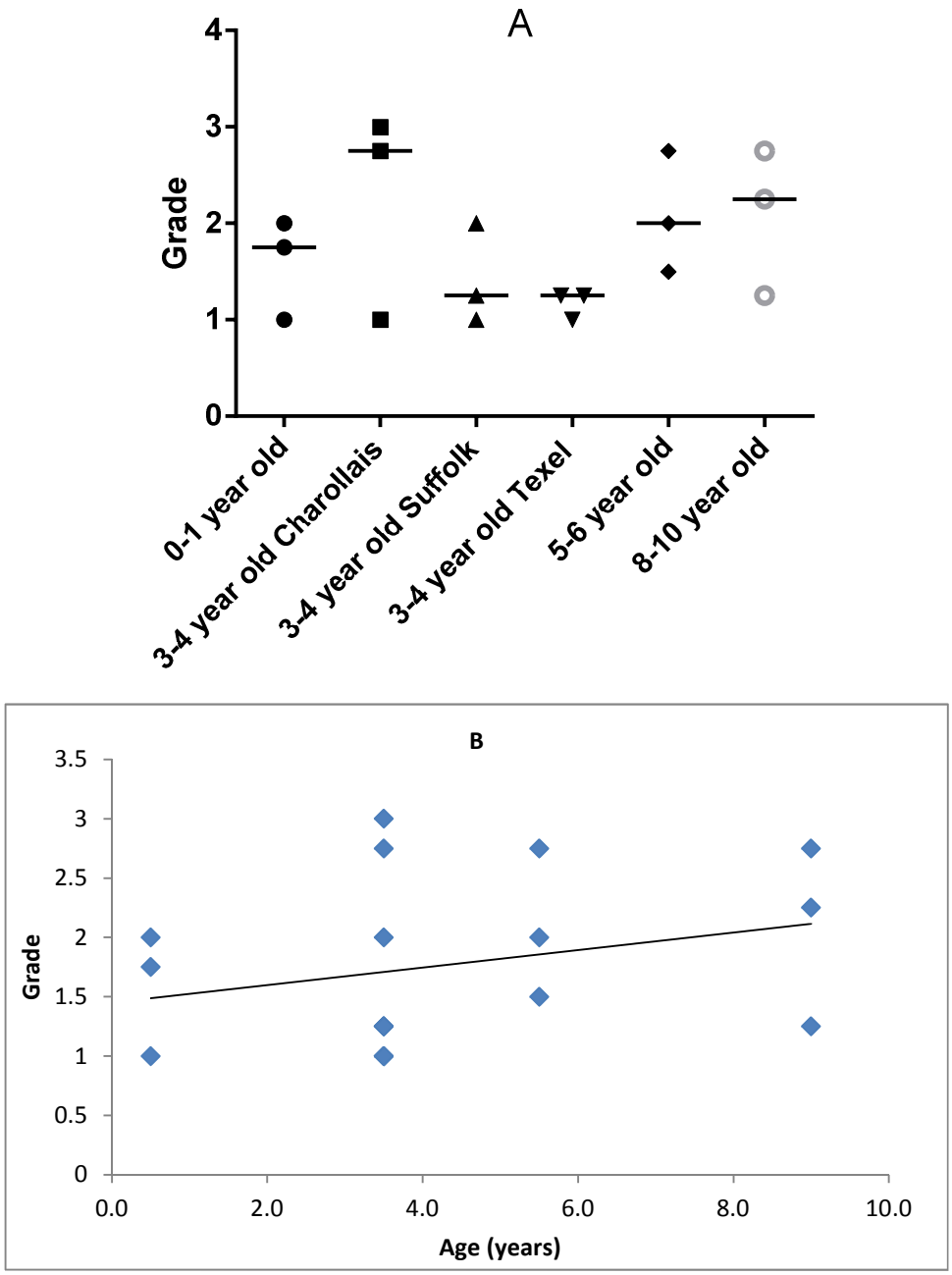


Figure 3.14: The distribution of grading scores for the macroscopic left ovine lumbar (L1/L2) facets in all four age groups and three 3-4 year old breeds of sheep. A: The distribution of grades for each age and breed group (n=3). The age/breed group data was analysed using the Kruskal-Wallis test (p=0.3784) which found no differences between the age and breed groups B: The distribution of grades for each age group. The data was analysed using Spearman's Rank Correlation (r=0.3669) which found no correlation between the grades and age groups.

No differences were observed between the age and breed groups of the macroscopic lumbar facet grading scores (Kruskal-Wallis test). There was no

correlation between age and grade (r=0.37; Spearman`s rank correlation). The range of grades was similar to those of the thoracic facets and fluctuated with age. The range of grades fell between 1.00-3.50, lower than both the cervical and thoracic facets.

3.4.5. Grading of Haematoxylin and Eosin Stained Sections of Facets for Degeneration

Left inferior facets from the FSUs C6/C7, T11/T12 and L1/L2 were fixed in 10 % (v/v) neutral buffered formalin before being cut at the centre to give rise to 2 mm thick cross-sections. These were decalcified in 12.5 % (w/v) EDTA for two weeks, tissue processed (Section 2.2.7.2.), sectioned using a microtome at 5 µm and stained with H&E. A grading system was used (Section 2.2.7.8.) by two independent graders to grade each stained section blind. The inter-rater reliability (kappa) test was performed on all the data from both graders. The kappa score was 0.515 ($p<0.0001$), showing there was moderate agreement between the two graders.

The results of the degeneration grading of H&E stained sections of cervical facet cartilage are shown in Figure 3.15.

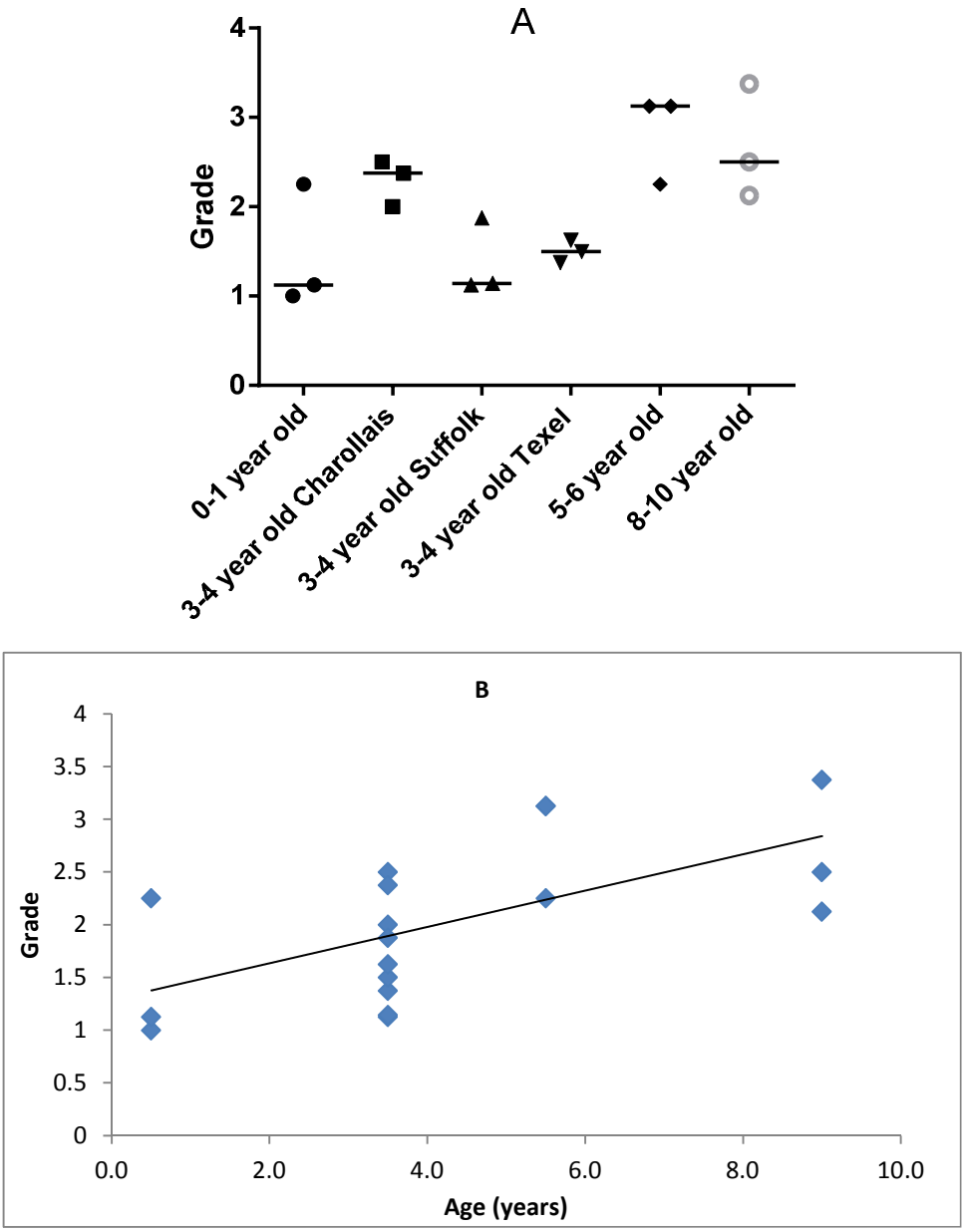


Figure 3.15: The distribution of degeneration grading scores for H&E stained ovine cervical (C6/C7) left inferior facet cartilage sections in four age groups and three 3-4 year old breeds of sheep. A: The distribution of grades for each age and breed group (n=3). The age/breed group data was analysed using the Kruskal-Wallis test (p=0.0377) which found no differences between the age and breed groups. B: The distribution of grades for each age group. The data was analysed using Spearman's rank correlation (r=0.6744) which found a good positive correlation between the grades and age groups. H&E: Haematoxylin and eosin.

No differences were observed in the degeneration grade for the cervical facet cartilage sections between the age and breed groups (Kruskal-Wallis test). However a good positive correlation was found between grade with increasing

age (r=0.67; Spearman`s rank correlation). There was an obvious increase in the range of degeneration grading score from 3-4 years to 5-6 years. The grades in the 0-4 year old samples were lower in comparison to the 5-10 year samples.

The results of the degeneration grading of H&E stained sections of thoracic facet cartilage are shown in Figure 3.16.

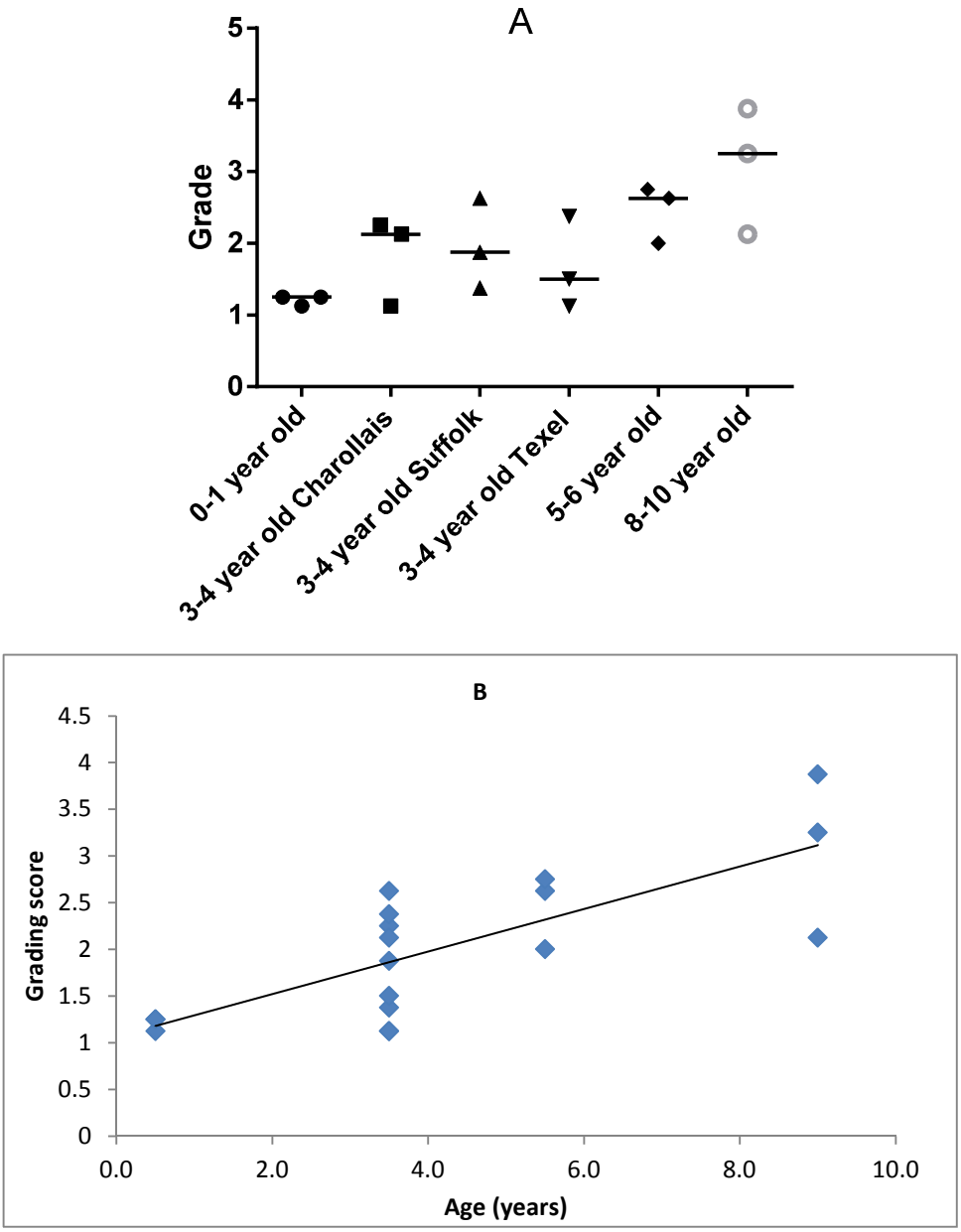


Figure 3.16: The distribution of degeneration grading scores for H&E stained ovine thoracic (T11/T12) left inferior facet cartilage sections in four age groups and three 3-4 year old breeds of sheep. A: The distribution of grades for each age and breed group (n=3). The age/breed group data was analysed using the Kruskal-Wallis test (p=0.1042) which found no differences between the age and breed groups. B: The distribution of grades for each age group. The data was analysed using Spearman's rank correlation (r=0.7595) which found a good positive correlation between the grades and age groups. H&E: Haematoxylin and eosin.

No differences were observed in the degeneration grade for the thoracic facet cartilage sections between the age and breed groups (Kruskal-Wallis test). However a good positive correlation was found between grade and increasing

age (r=0.76; Spearman`s rank correlation). The range of grades was generally lower in comparison to the cervical facet sections. Similarly to the cervical sections, there was an obvious increase in grades from the 3-4 year to 5-6 year age groups. The grades in the 0-4 year old samples were lower in comparison to the 5-10 year samples.

The results of the degeneration grading of H&E stained sections of lumbar facet cartilage are shown in Figure 3.17.

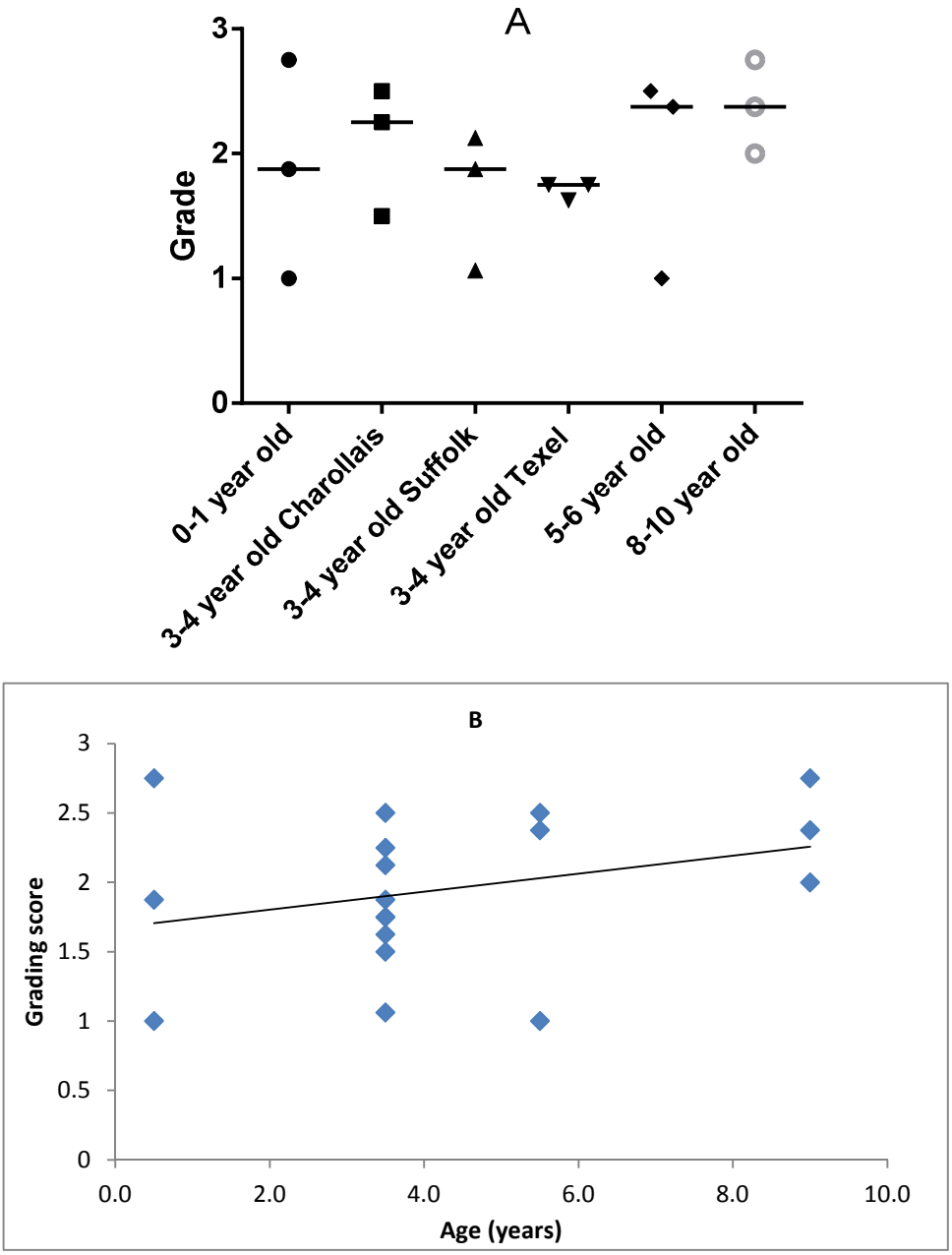


Figure 3.17: The distribution of degeneration grading scores for H&E stained ovine lumbar (L1/L2) left inferior facet cartilage sections in four age groups and three 3-4 year old breeds of sheep. A: The distribution of grades for each age and breed group (n=3). The age/breed group data was analysed using the Kruskal-Wallis test (p=0.5897) which found no differences between the age and breed groups. B: The distribution of grades for each age group. The data was analysed using Spearman's rank correlation (r=0.3731) which found no correlation between the grades and age groups. H&E: Haematoxylin and eosin.

No differences were observed in the degeneration grade for the lumbar facet cartilage sections between the age and breed groups (Kruskal-Wallis test). In

contrast to the cervical and thoracic sections, no correlation was found between grade and age (r=0.37; Spearman`s rank correlation). In general, the grades were lower than those in the cervical and thoracic sections but the range of grades in the 0-1 year age group were more spread reaching as high as 2.75.

The most visible signs of aging were present in the histological sections of cervical facet cartilage. Examples of this are shown in Figure 3.18.

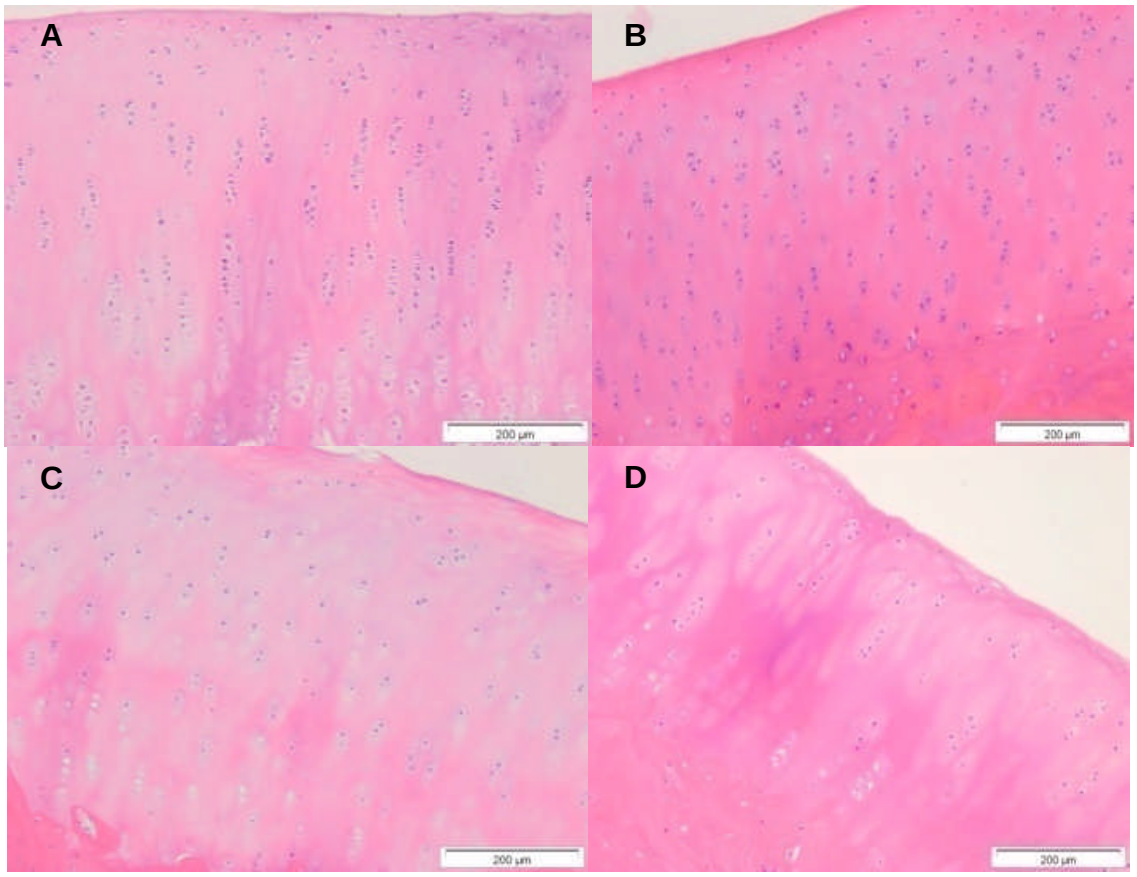


Figure 3.18: H&E stained sections of ovine cervical (C6/C7) facet cartilage from four different age groups. A: 0-1 year old (Charollais), B: 3-4 year old (Charollais), C: 5-6 year old (Suffolk), D: 8-10 year old (Hebridean). H&E: Haematoxylin and eosin.

The structure of facet cartilage in the 0-1 year and 3-4 year old samples was very similar with an organised thick structure and minimal calcification. In both the 5-6 year and 8-10 year old samples, the cartilage began to lose its structure with fewer cells, calcification and fissures on its surface.

3.4.6. Analysis of the Bone in Ovine FSUs

FSUs C6/C7, T11/T12 and L1/L2 from each age and breed of sheep were scanned whole in a µCT scanner (Section 2.2.12). After scanning was complete, software was used to calculate BV/TV and hydroxyapatite (HA) concentration as a measure of BMD (Section 2.2.12).

3.4.6.1. Bone Volume/Total Volume of Ovine FSUs

The results of BV/TV analysis of cervical FSUs are shown in Figure 3.19.

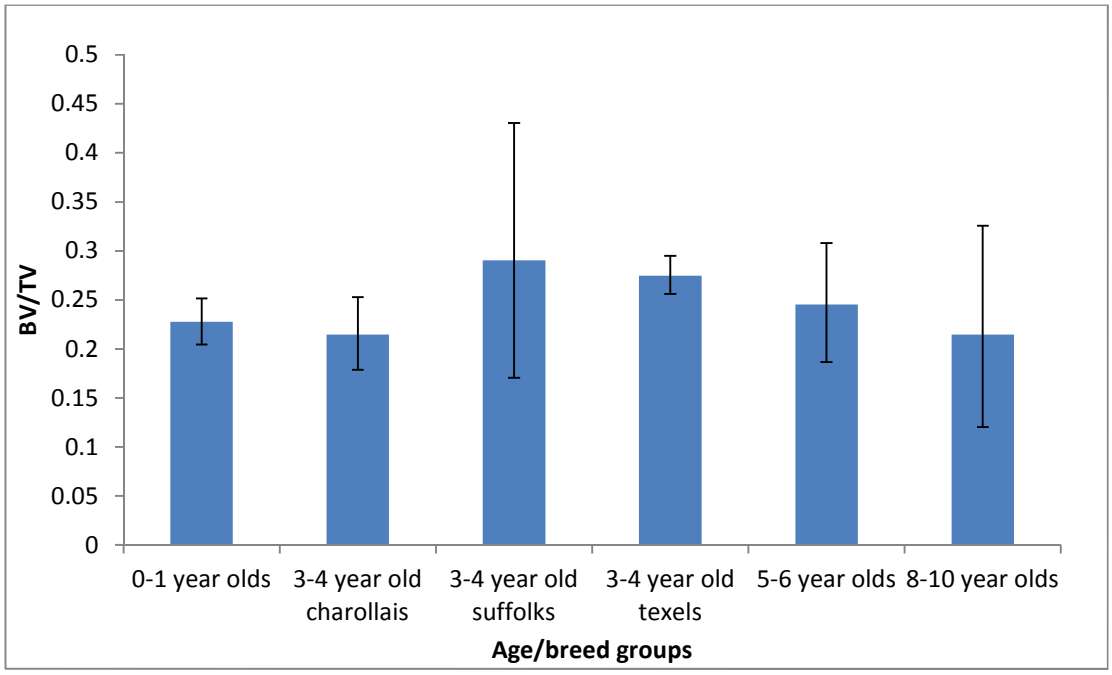


Figure 3.19: The mean BV/TV of ovine cervical (C6/C7) FSUs from four age groups and three 3-4 year old breeds of sheep. Data was transformed by arcsine transformation, the means (n=3) and SDs calculated and analysed by one-way ANOVA which revealed no significant differences between any of the groups (p=0.7340). The data was then back transformed to proportions for presentation purposes. BV/TV: Bone volume/total volume, FSU: Functional spinal unit, SD: Standard deviation, ANOVA: Analysis of variance.

There was no significant variation in the data for the BV/TV of cervical FSUs of sheep in the different age groups or between the three breeds in the 3-4 year age group (analysis of variance; p=0.7340) . The BV/TV values were relatively constant with age and breed lying between 0.2 and 0.3, or 20-30 %. The Charollais breed in the 3-4 year old age group had lower BV/TV than that of the Texel and Suffolk breeds. However, this was not significant. The data (age vs

BV/TV) was therefore analysed using Spearman's rank correlation which showed no correlation (r=-0.0206) between the BV/TV and age of the animals

The results of BV/TV analysis of thoracic FSUs are shown in Figure 3.20.

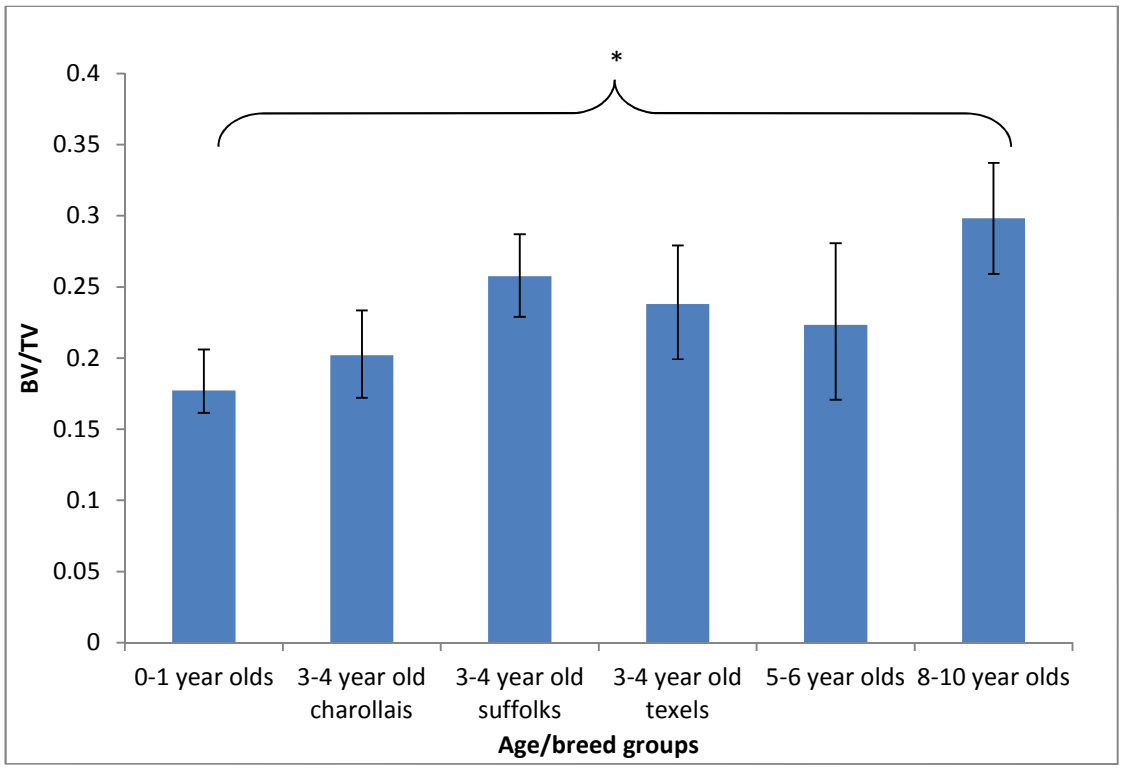


Figure 3.20: The mean BV/TV of ovine thoracic (T11/T12) FSUs from four age groups and three 3-4 year old breeds of sheep. Data was transformed by arcsine transformation, the means (n=3) and SDs calculated and analysed by one-way ANOVA which revealed significant variation amongst the groups (p=0.0301). Calculation of the minimal significant difference between means showed a significant difference between the 0-1 and 8-10 year age groups ($p < 0.05$). The data was then back transformed to proportions for presentation purposes. *p<0.05. BV/TV: Bone volume/total volume, FSU: Functional spinal unit, SD: Standard deviation, ANOVA: Analysis of variance.

The BV/TV of FSUs from sheep in the 0-1 age group was significantly lower than the BV/TV of FSUs in the 8-10 year old age group ($p< 0.05$; ANOVA). There were no differences in the BV/TV of the FSUs from the three breeds in the 3-4 year old age groups. The data (age vs BV/TV) was therefore analysed using Spearman's rank correlation which showed a good positive correlation (r=0.6171) between an increase in BV/TV with age in the thoracic FSUs. The increase in BV/TV was from 0.18 in 0-1 year old samples to 0.30 in the 8-10 year old samples. The samples from the four other age/breed groups had mean

values which lay within this range. In comparison to the cervical FSUs, all BV/TV values lay in a similar range (0.2-0.3) with the exception of the 0-1 year age group (0.18).

The results of BV/TV analysis of lumbar FSUs are shown in Figure 3.21.

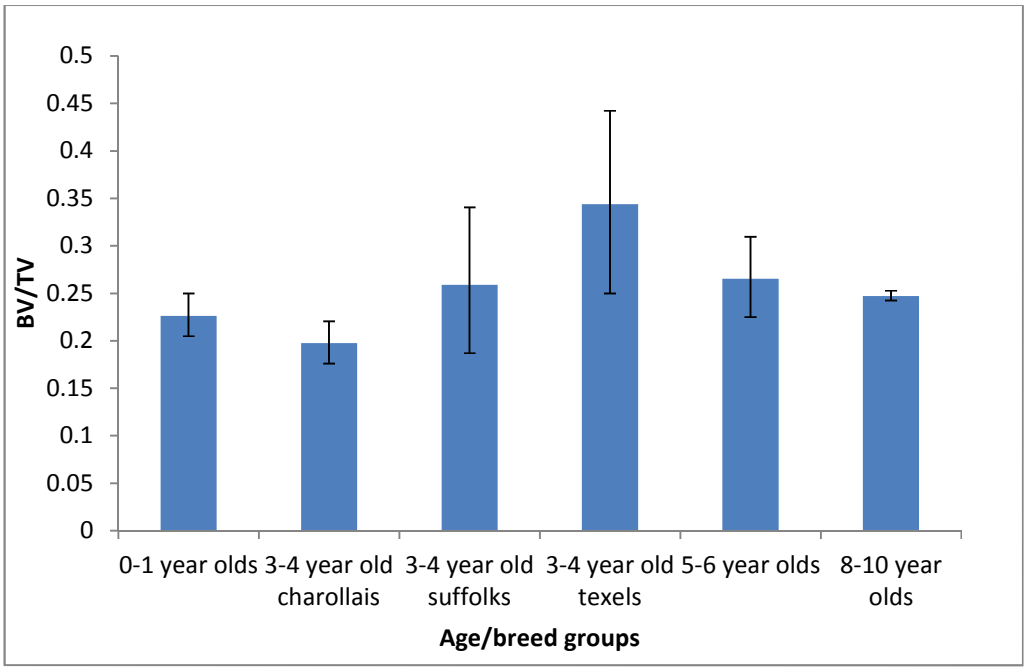


Figure 3.21: The mean BV/TV of ovine lumbar (L1/L2) FSUs from four age groups and three 3-4 year old breeds of sheep. Data was transformed by arcsine transformation, the means (n=3) and SDs calculated and analysed by one-way ANOVA which revealed no significant differences between any of the groups (p=0.1146). The data was then back transformed to proportions for presentation purposes. BV/TV: Bone volume/total volume, FSU: Functional spinal unit, SD: Standard deviation, ANOVA: Analysis of variance.

There was no significant variation in the data for the BV/TV values of the lumbar FSUs of sheep of different ages or breeds (analysis of variance; p=0.12). The data (BV/TV vs age) was therefore analysed using Spearman's rank correlation which showed no correlation between BV/TV and age (r=0.2162). The values appeared to fluctuate with age and breed. In comparison to the cervical and thoracic samples, the range of BV/TV values was higher lying between 0.20 and 0.34.

3.4.6.2. Hydroxyapatite Concentration

The results of HA concentrations in the bone from cervical FSUs are shown in Figure 3.22.

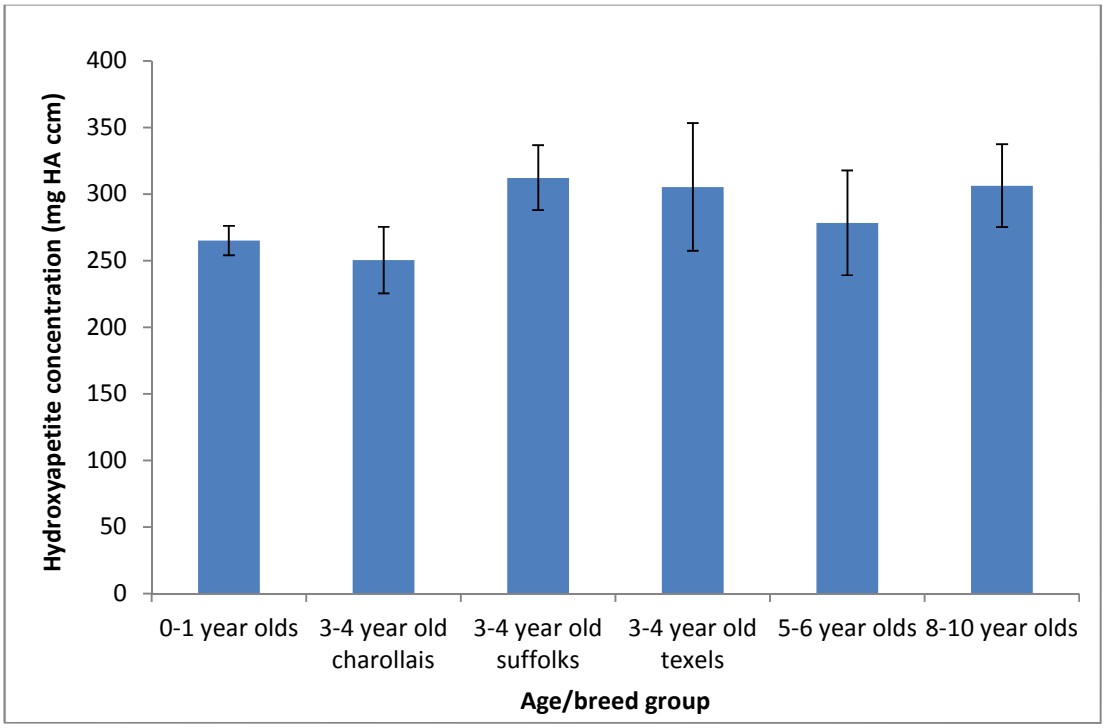


Figure 3.22: The mean HA concentration in ovine cervical (C6/C7) FSUs from four age groups and three 3-4 year old breeds of sheep. Data is presented as the mean (n=3) ± SD. Data was analysed by one-way ANOVA which revealed no significant variation between the groups (p=0.3424). HA: Hydroxyapatite concentration, FSU: Functional spinal unit, SD: Standard deviation, ANOVA: Analysis of variance.

The mean HA concentration in the ovine cervical FSUs showed no variation between the different age groups or breed of sheep (analysis of variance; p=0.34). The data (HA concentration vs age) was therefore analysed using the Pearson's moment correlation which showed no correlation between HA concentration of the FSUs and age (r=0.2574). The range of values was fairly constant amongst all ages and breeds of sheep. The mean values ranged from 250 mg HA/ccm (3-4 year old Charollais) to 312 mg HA/ccm (3-4 year old Suffolk).

The results of HA concentrations in the bone of thoracic FSUs are shown in Figure 3.23.

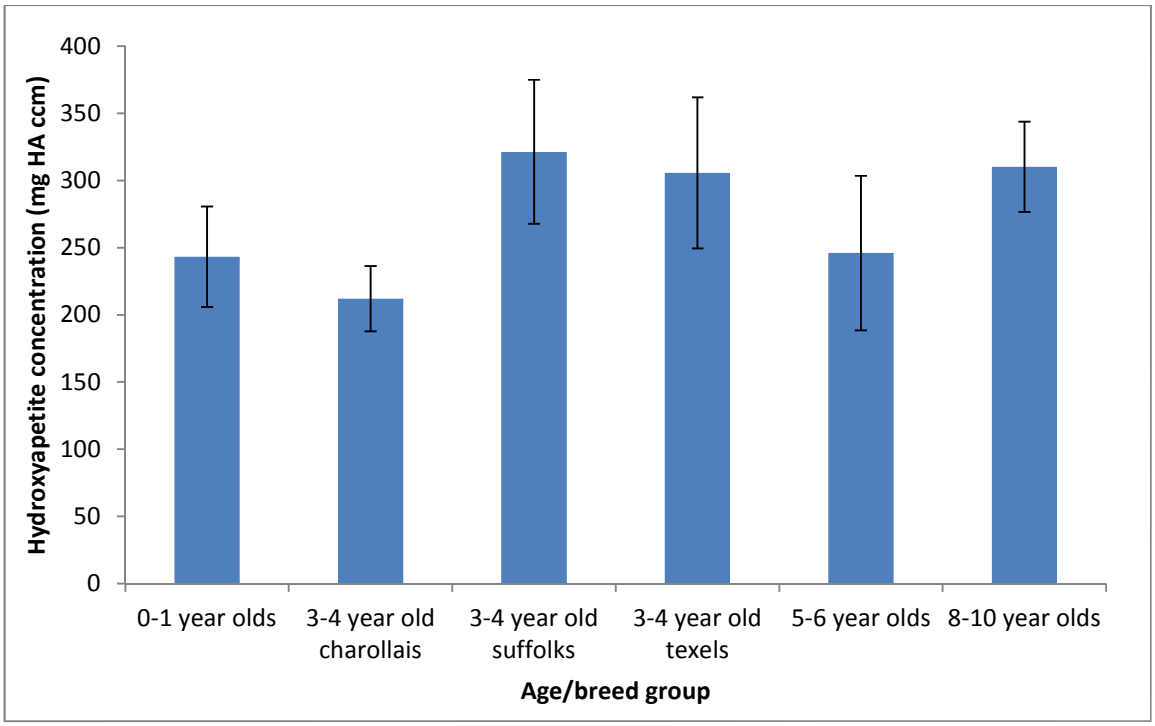


Figure 3.23: The mean HA concentration in ovine thoracic (T11/T12) FSUs from four age groups and three 3-4 year old breeds of sheep. Data is presented as the mean (n=3) ± SD. Data was analysed by one-way ANOVA which revealed no significant variation between the groups (p=0.0592). HA: Hydroxyapatite concentration, FSU: Functional spinal unit, SD: Standard deviation, ANOVA: Analysis of variance.

There was no significant variation in the concentrations of HA in the bone of thoracic FSUs from sheep of different ages or breeds (analysis of variance; p=0.06). The values fluctuated between age and breed groups. The data (HA concentration vs age) was therefore analysed using the Pearson's moment correlation which showed no correlation between age and HA concentration in the bone of the thoracic FSUs (r=0.2799). In comparison to the cervical FSUs, the range of values was wider lying between 212 mg HA/ccm (3-4 year old Charollais) and 321 mg HA/ccm (3-4 year old Suffolk). As with the cervical FSUs the Charollais breed showed the lowest values with the Suffolk breed showing the highest values. However, this was not statistically significant.

The results of HA concentrations in the bone of lumbar FSUs are shown in Figure 3.24.

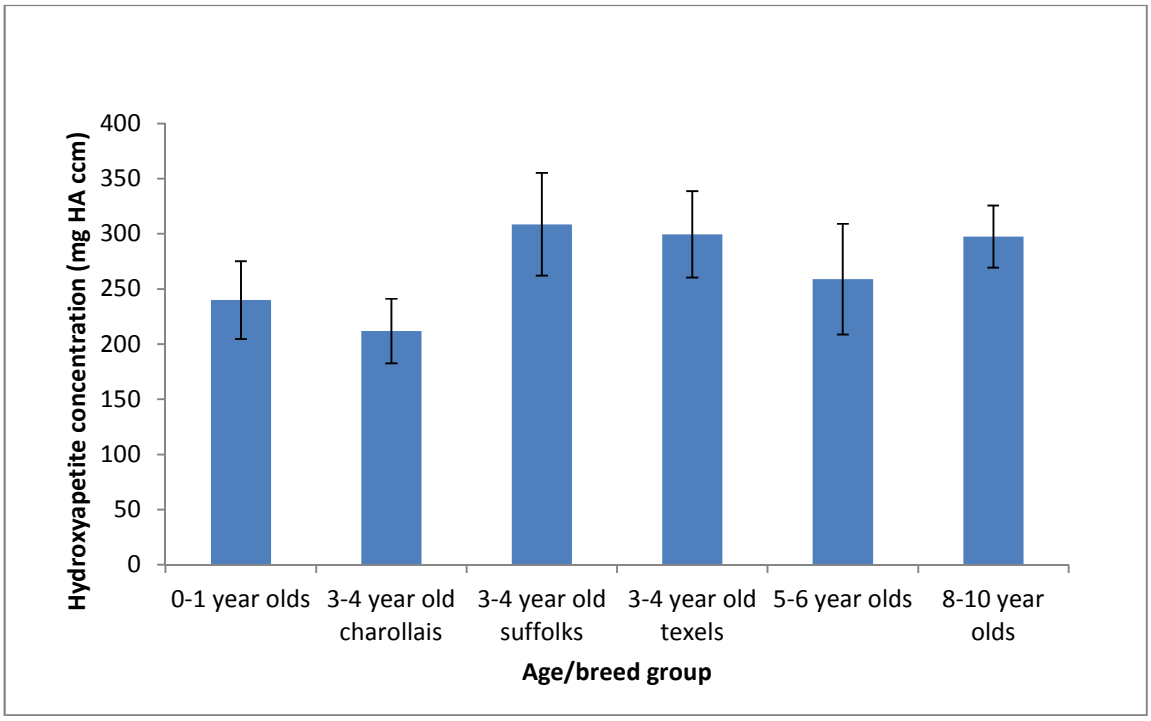


Figure 3.24: The mean HA concentration in ovine lumbar (L1/L2) FSUs from four age groups and three 3-4 year old breeds of sheep. Data is presented as the mean (n=3) ± SD. Data was analysed by one-way ANOVA which revealed no significant variation in the data between the groups (p=0.0563). HA: Hydroxyapatite concentration, FSU: Functional spinal unit, SD: Standard deviation, ANOVA: Analysis of variance.

No significant variation was found in the HA concentration in the bone of lumbar FSUs from the different age groups or breeds of the lumbar FSUs. The values fluctuated between all age and breed groups. The data (HA concentration vs age) was therefore analysed using the Pearson's moment correlation which showed no correlation between HA concentration and age (r=0.3015). In comparison to the cervical and thoracic FSUs, the values lay in a similar range from 212 mg HA/ccm (3-4 year old Charollais) and 309 mg HA/ccm (3-4 year old Suffolk). As with both the cervical and thoracic FSUs the Charollais breed showed the lowest values with the Suffolk breed showing the highest values. However, this was not statistically significant.

3.4.7. IVD Height and Facet Spacing Measurements of Ovine FSUs

The µCT scans were used to measure the thickness of the IVD (including the CEP). Three equally spaced points along the IVD were chosen to take

measurements from (Section 2.2.12). The µCT scans were also used to measure the space between the facet joints in the FSU as a measure of cartilage thickness. Three equally spaced points were chosen along both the left and right facet joint. Three measurements were taken along each facet at three equally spaced depths which were averaged out to give one measurement along each facet and averaged out again to give one measurement for both inferior and superior facets (Section 2.2.12).

3.4.7.1. IVD Height

The results of IVD height in cervical FSUs of sheep of different ages and breeds are shown in Figure 3.25.

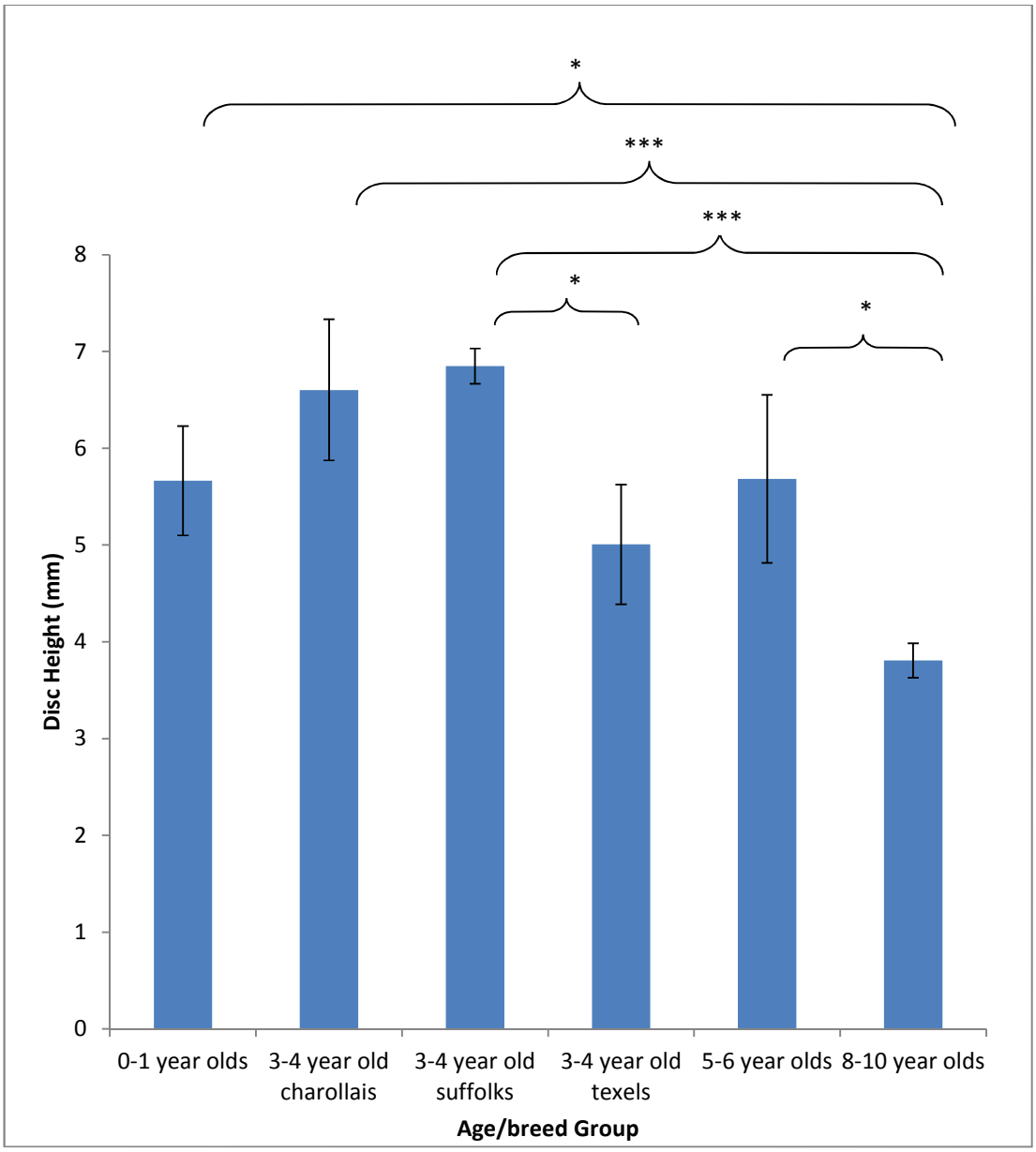


Figure 3.25: The IVD height in ovine cervical (C6/C7) FSUs from four age groups and three 3-4 year old breeds of sheep. Data is presented as the mean (n=3) ± SD. Data was analysed by one-way ANOVA which revealed significant variation in the data (p= 0.0004). Calculation of the minimum significant difference revealed significant differences between the 0-1 and 8-10 year age groups, 3-4 Charollais and 8-10 year age groups, 3-4 Suffolk and 3-4 year old Texel groups, 3-4 Suffolk and 8-10 year age groups and 5-6 and 8-10 year age groups (p=0.0004).*p<0.05, ***p<0.001. IVD: Intervertebral disc, FSU: Functional spinal unit, SD: Standard deviation, ANOVA: Analysis of variance.

Significant differences in cervical IVD height were found between 0-1 and 8-10 year age groups, 3-4 Charollais and 8-10 year age groups, 3-4 Suffolk and 8-10 year age groups and 5-6 and 8-10 year age groups. A significant difference was

also found between the 3-4 year old Suffolk and Texel breeds with the Suffolks having a greater cervical IVD height. Analysis of the data using Pearson's moment correlation showed a weak negative correlation between age and IVD height (r=0.3015). This showed that the IVD height within cervical FSUs decreased with age.

The results of IVD height in thoracic FSUs are shown in Figure 3.26.

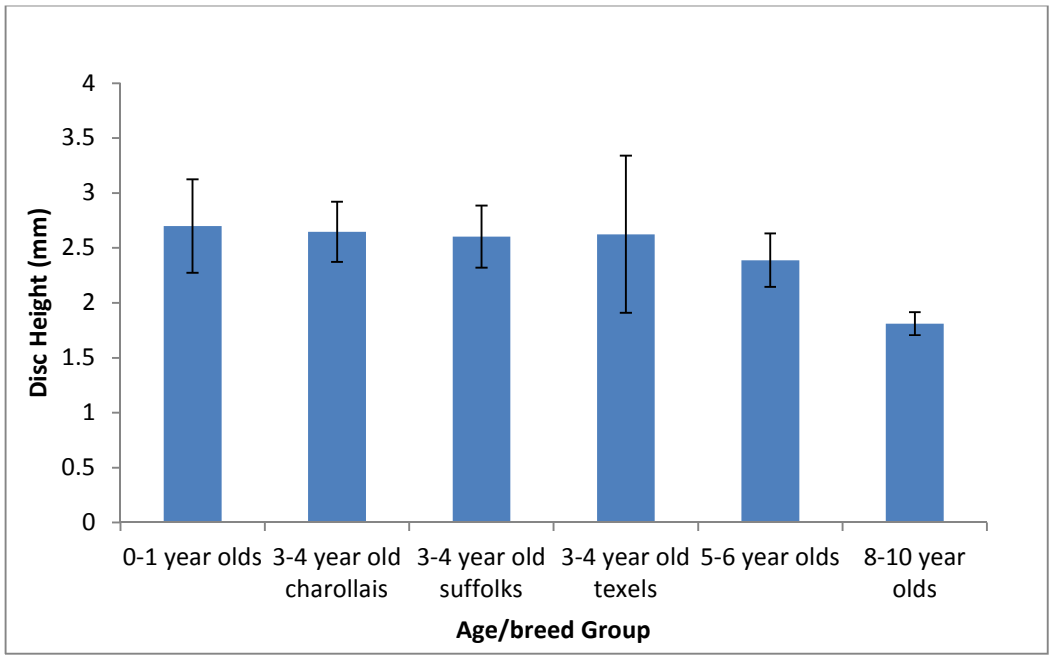


Figure 3.26: The mean IVD height in ovine thoracic (T11/T12) FSUs from four age groups and three 3-4 year old breeds of sheep. Data is presented as the mean (n=3) ± SD. Data was analysed by one-way ANOVA which revealed no significant variation between the age and breed groups (p=0.1188. IVD: Intervertebral disc, FSU: Functional spinal unit, SD: Standard deviation, ANOVA: Analysis of variance.

There was no significant variation in the data for thoracic FSU IVD height between the age groups and breeds of sheep (analysis of variance; p= 0.1188). Although the mean IVD height in the 8-10 year old age group appeared to be lower than in the other five groups, this was not significant. No differences were found between the three different breeds in the 3-4 year old age group. The data (IVD height vs age) was analysed using the Pearson's moment correlation which revealed a good negative correlation (r=-0.65) indicating a decrease in IVD height with age. In comparison to the cervical FSU disc height which

ranged from 3.8 mm to 6.9 mm, the thoracic values were much lower ranging from 1.8 mm to 2.7 mm.

The results for IVD height in lumbar FSUs are shown in Figure 3.27.

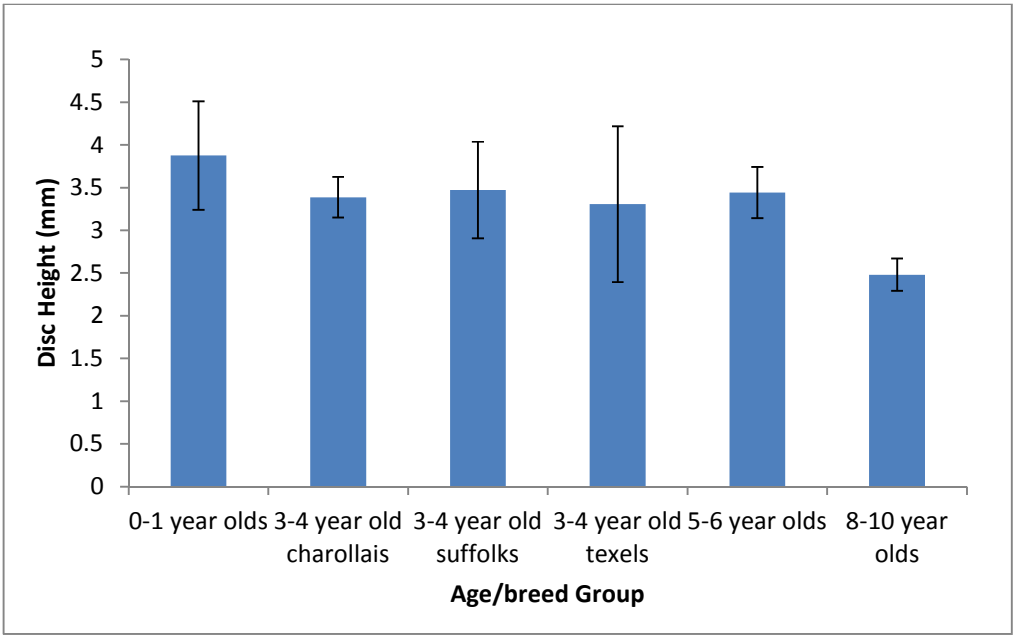


Figure 3.27: The mean IVD height in ovine lumbar (L1/L2) FSUs from four age groups and three 3-4 year old breeds of sheep. Data is presented as the mean (n=3) ± SD. Data was analysed by one-way ANOVA which revealed no significant variation between the age and breed groups (p=0.1241). IVD: Intervertebral disc, FSU: Functional spinal unit, SD: Standard deviation, ANOVA: Analysis of variance.

There was no significant variation in the lumbar FSU IVD height between the age groups or breed of sheep (analysis of variance; p=0.1241). Although the mean IVD height in the 8-10 year old age group appeared to be lower than in the other five groups, this was not significant. No differences were found between the three different breeds in the 3-4 year old age group. The data (IVD height vs age) was analysed by Pearson`s moment correlation which revealed a good negative correlation indicating a decrease in IVD height with age. In comparison to both the cervical and thoracic IVD height, the lumbar IVD height was higher (2.48-3.88 mm) than that of the thoracic samples (1.81-2.70 mm) but lower than the cervical samples (3.81-6.85 mm).

3.4.7.2. Facet Joint Spacing Measurements

The results of facet joint spacing in cervical FSUs of sheep of various ages and breeds are shown in Figure 3.28.

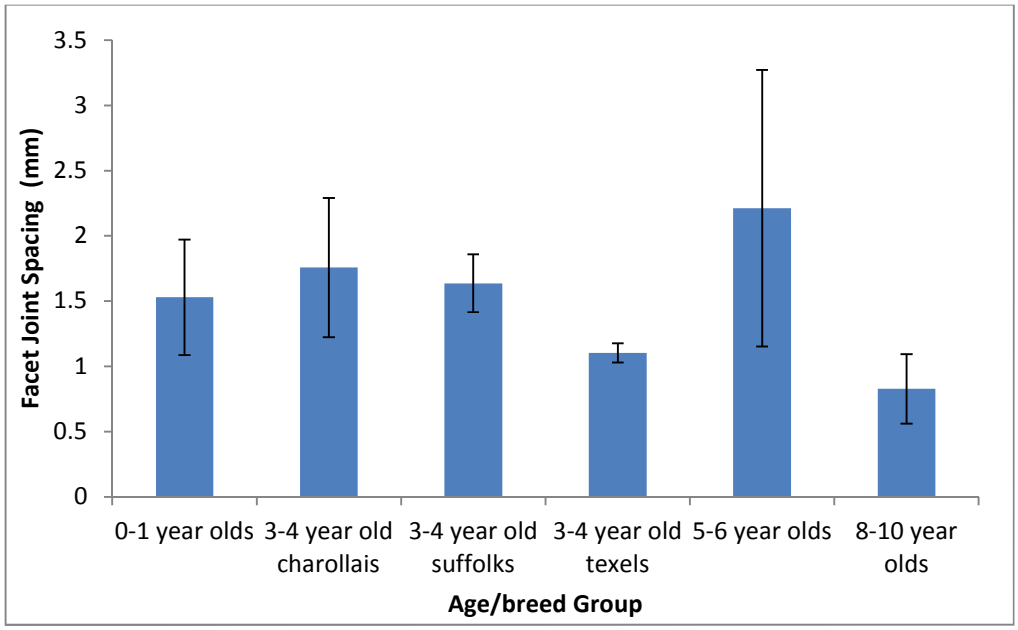


Figure 3.28: The mean facet joint spacing in ovine cervical (C6/C7) FSUs from four age groups and three 3-4 year old breeds of sheep. Data is presented as the mean (n=3) ± SD. Data was analysed by one-way ANOVA which revealed no significant variation between the data for the different age and breed groups (p=0.0895). FSU: Functional spinal unit, SD: Standard deviation, ANOVA: Analysis of variance.

There was no significant variation in the data for the facet joint spacing measurements in the cervical FSUs from sheep of different ages or breed (analysis of variance; p=0.09). No differences in facet joint spacing were found between the age groups in the cervical FSUs. No differences were present between the three breeds in the 3-4 year old age group. The data (facet joint space vs age) was analysed using Pearson`s moment correlation which showed no correlation with age.

The results of facet joint spacing in thoracic FSUs are shown in Figure 3.29.

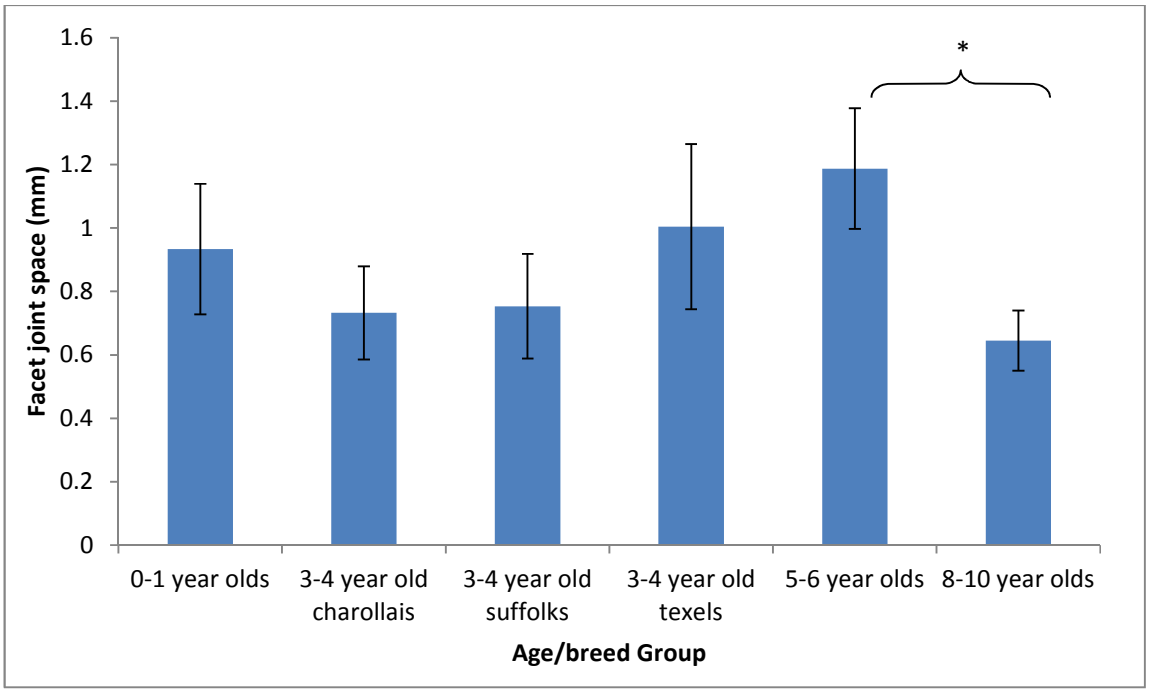


Figure 3.29: The mean facet joint spacing in ovine thoracic (T11/T12) FSUs from four age groups and three 3-4 year old breeds of sheep. Data is presented as the mean (n=3) ± SD. Data was analysed by one-way ANOVA which revealed significant variation amongst the data. The minimum significant difference between means was therefore calculated and this revealed a significant difference between the 5-6 year and 8-10 year age groups ($p < 0.05$). *$p<0.05$. FSU: Functional spinal unit, SD: Standard deviation, ANOVA: Analysis of variance.

Analysis of the data using ANOVA revealed significant variation in the data and this was found to be due to a significantly smaller facet joint spacing ($p<0.05$) in thoracic FSU`s in the 8-10 years age group compared to the 5-6 year old group. This showed that the facet joint space decreased with age after 5-6 years. No difference was found in facet joint space between the three breeds in the 3-4 year old age group. The data (facet joint spacing vs. age) was analysed using Pearson`s moment correlation which revealed no correlation between facet joint space and age ($r= 0.22$). In comparison to the facet joint space in the cervical FSUs, the space between the facet joints was smaller.

The results of facet joint spacing in lumbar FSUs are shown in Figure 3.30.

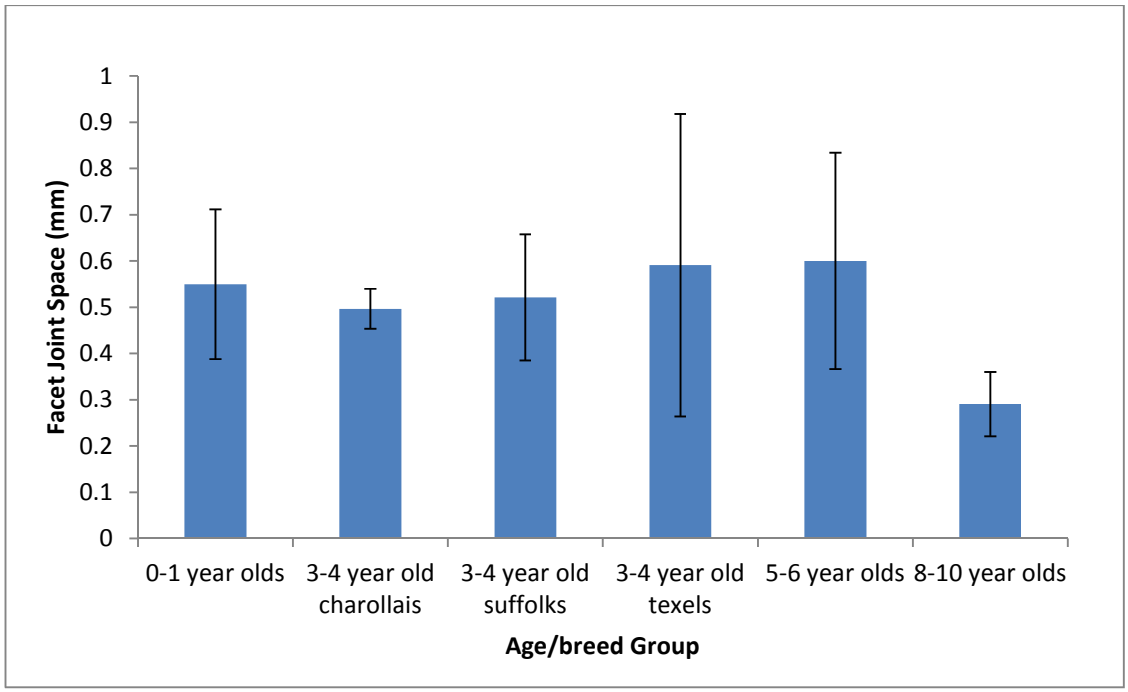


Figure 3.30: The mean facet joint spacing in ovine lumbar (L1/L2) FSUs from four age groups and three 3-4 year old breeds of sheep. Data is presented as the mean (n=3) ± SD. Data was analysed by one-way ANOVA which revealed no significant variation in the data for the different age and breed groups (p=0.4130). FSU: Functional spinal unit, SD: Standard deviation, ANOVA: Analysis of variance.

There was no significant variation in the data for the facet joint spacing between the age groups and breeds of the lumbar FSUs. The facet joint space in the 8-10 year old age group appeared to be smaller in comparison to the other age groups however this was not significant. No differences were present in facet joint space between the three breeds in the 3-4 year old age group. The data (facet joint space vs age) was analysed using Pearson`s moment correlation which showed a weak negative correlation between facet joint space in lumbar FSUs and age (r= -0. 4). In comparison to both the cervical (0.83-2.21) and thoracic (0.65-1.19) mean values, the facet joint space in the lumbar FSUs (0.29-0.60) was smaller.

A summary of all the data collected in this part of the study is presented in Tables 3.1-3.3.

	0-1 year old	3-4 year old Charollais	3-4 year old Suffolk	3-4 year old Texel	5-6 year old	8-10 year old	Significant difference between breeds?	Significant difference between age groups?	Correlation?
Transverse IVD grading	1.38	1.13	1.63	1.50	1.50	1.75	No	No (p=0.8814)	No (r=0.2699)
Sagittal IVD grading	1.25*	1.25	1.88	1.50	2.38*	2.38	No	Yes* (0-1 & 5-6)	Good (r=0.6285)
Morphological facet grading	1.00	1.00	1.50	1.25	2.00	2.00	No	No (p=0.1113)	Good (r=0.6553)
Facet section grading	1.13	2.38	1.14	1.50	3.13	2.50	No	No (p=0.0377)	Good (r=0.6744)
BV/TV	0.2277	0.2146	0.2903	0.2746	0.2455	0.2146	No	No (p=0.7340)	No (r=-0.0206)
HA concentration	265.10	250.55	312.32	305.34	278.29	306.29	No	No (p=0.3424)	No (r=0.2574)
IVD height	5.66* (8-10)	6.60*** (8-10)	6.85*** (8-10)	5.01* (3-4suffolk)	5.68* (8-10)	3.81***	Yes*	Yes***	Weak (r=-0.5718)
Facet joint space	1.53	1.76	1.64	1.10	2.21	0.827	No	No (p=0.0895)	No (r=-0.2489)

Table 3.1: A summary of the data for the cervical FSUs. Each value for the grading data represents the median and each value for the measurement data represents the mean (n=3). Grading data were analysed using the Kruskal-Wallis test and Spearman's rank correlation. BV/TV data were calculated using one-way ANOVA on arcsine transformed data. HA concentration, IVD height and facet joint height data were analysed using one-way ANOVA and determination of the minimal significant difference between group means and Pearson`s moment correlation coefficient. *p<0.05, **p<0.005. BV/TV: Bone volume/total volume, HA: Hydroxyapatite, IVD: Intervertebral disc, ANOVA: Analysis of variance.

	0-1 year old	3-4 year old Charollais	3-4 year old Suffolk	3-4 year old Texel	5-6 year old	8-10 year old	Significant difference between breeds?	Significant difference between age groups?	Correlation?
Transverse IVD grading	1.13	1.63	1.13	1.13	1.50	1.25	No	No (p=0.9951)	No (r=-0.0495)
Sagittal IVD grading	1.50	1.25	2.25	1.75	1.63	2.50	No	No (p=0.0546)	No (r=0.3117)
Morphological facet grading	1.50	2.75	1.00	1.00	3.25	2.00	No	No (p=0.1983)	No (r=0.3762)
Facet section grading	1.25	2.13	1.88	1.50	2.75	3.25	No	No (p=0.1042)	Good (r=0.7595)
BV/TV	0.1773*	0.2019	0.2576	0.2380	0.2233	0.2982*	No	Yes* 0-1 & 8-10	Good (0.6171)
HA concentration	242.21	212.06	321.42	305.69	246.04	310.28	No	No (p=0.0592)	No (r=0.2799)
IVD height	2.70	2.65	2.60	2.63	2.39	1.81	No	No (p=0.1188)	Good (r=-0.6484)
Facet joint space	0.933	0.733	0.753	1.00	1.19*	0.645*	No	Yes* 5-6 & 8-10	No (r=-0.2217)

Table 3.2: A summary of the data for the thoracic FSUs. Each value for the grading data represents the median and each value for the measurement data represents the mean (n=3). Grading data were analysed using the Kruskal-Wallis test and Spearman's rank correlation. BV/TV data were analysed using one-way ANOVA on arcsine transformed data. HA concentration, IVD height and facet joint height data were analysed using one-way ANOVA followed by determination of the minimum significant difference between group means and Pearson's moment correlation coefficient. *p<0.05. BV/TV: Bone volume/total volume, HA: Hydroxyapatite, IVD: Intervertebral disc, ANOVA: Analysis of variance.

	0-1 year old	3-4 year old Charollais	3-4 year old Suffolk	3-4 year old Texel	5-6 year old	8-10 year old	Significant difference between breeds?	Significant difference between age groups?	Correlation?
Transverse IVD grading	1	0.63	1.63	0.50	1.00	1.75	No	No (p=0.3211)	Weak (r=0.4226)
Sagittal IVD grading	1.38	1.75	1.75	1.63	1.88	2.38	No	No (p=0.0464)	Good (r=0.6775)
Morphological facet grading	1.75	2.75	1.25	1.25	2.00	2.25	No	No (p=0.3784)	No (r=0.3669)
Facet section grading	1.88	2.25	1.88	1.75	2.38	2.38	No	No (p=0.5897)	No (r=0.3731)
BV/TV	0.2262	0.1977	0.2591	0.3438	0.2653	0.2470	No	No (p=0.1146)	No (r=0.2162)
HA concentration	239.97	211.90	308.65	299.49	258.92	297.48	No	No (p=0.0563)	No (r=0.3015)
IVD height	3.88	3.39	3.47	3.31	3.44	2.48	No	No (p=0.1241)	Good (r=-0.6460)
Facet joint space	0.550	0.497	0.522	0.591	0.600	0.291	No	No (p=0.4130)	Weak (r=-0.3960)

Table 3.3: A summary of the data for the lumbar FSUs. Each value for the grading data represents the median and each value for the measurement data represents the mean (n=3). Grading data were analysed using the Kruskal-Wallis test and Spearman's rank correlation. BV/TV data were analysed using one-way ANOVA on arcsine transformed data. Data on HA concentration, IVD height and facet joint height were analysed using one-way ANOVA and Pearson`s moment correlation coefficient. BV/TV: Bone volume/total volume, HA: Hydroxyapatite, IVD: Intervertebral disc, ANOVA: Analysis of variance.

3.5. Discussion and Conclusions

The aim of this part of the study was to analyse ovine FSUs from cervical, thoracic and lumbar regions to determine at what age the ovine spine begins to show signs of degeneration. This included analysing the morphology of the FSUs and facet surfaces, the micro-detail of the facet cartilage and IVD whilst also determining some bone properties of the vertebral body, IVD height and space between the facet joints. As aging has been frequently reported in the literature to be linked to the degeneration of the IVD, facet joint and bone structure, the analyses focused on these tissues (Miller *et al.*, 1988; Gong *et al.*, 2005; Tischer *et al.*, 2006; Urban and Roberts, 2006; Melrose *et al.*, 2009; Varlotta *et al.*, 2011A). In addition, due to the difficulties in obtaining ovine spines from a single breed, three breeds were analysed using the same methods to determine whether there were differences between different breeds and therefore whether the study was valid using a range of breeds. Currently, no such study exists in the literature.

The results with regard to the different breeds in the 3-4 year old age range showed only one significant difference between the Suffolk and Texel breeds in the cervical FSU and this was for the IVD height. No significant differences were observed between thoracic and lumbar FSUs in IVD height. In addition there were no significant differences in cervical, thoracic and lumbar FSUs between the three breeds in the histological grading of the transverse IVD sections, sagittal IVD sections, facet photography and facet histology grading or the other µCT measurements. As a result, the breed of sheep within an age group, with the exception of the Hebridean breed in the 8-10 year age group, was not relevant and was not considered to be important and taken into consideration whilst discussing the results.

The FSU morphology results showed changes in the macrostructure of the IVD with age. The common features observed within an aging IVD were observed including loss of water within the NP and loss of demarcation. However, the results from the grading of the histological sections of the transverse IVD showed no significant differences between the age groups and only one weak

correlation of increasing grade with age in the lumbar sections. This did not reflect the macroscopic appearance. This may have been due to the other factors in the transverse IVD grading system that was not visible to the naked eye. These included both the presence of cell clusters and fissures. As a result, this meant that although the loss of demarcation and haematoxophilia increased with age, the presence of cell clusters and fissures within these samples did not. The results showed that a great deal of variation existed between samples within the age groups. This may explain the absence of correlations in the grading of the cervical and thoracic transverse IVD sections. The results of the grading of the histological sections of the lumbar transverse IVD did not show any significant differences between the age groups; however, there was a noticeable trend with the grade for the 0-1 year age group being lower than that of the 8-10 year age group and the overall data showing a weak correlation between age and grade. Previous studies have found that the disc degenerates with age (Urban and Roberts, 2003; An *et al.*, 2006). Despite the absence of differences in degeneration with age in the transverse histological sections, significant differences were observed in the grades of the cervical sagittal IVD sections. This was between the 0-1 year and 5-6 year old samples. In addition a good positive correlation was present in cervical and lumbar sagittal sections showing increasing grade with age. These results showed that generally the grades given to histological sections increased with age. This difference between the sagittal and transverse section histological grading systems may have been due to the fact that the CEP and subchondral bone were taken into consideration when analysing the sagittal sections as well as the IVD itself. In addition, the grading of the sagittal IVD sections involved closer examination of both the AF and NP. This included not only analysing fissures but detail of widening of the matrix, vessels, disorganisation of attachment, cystic degeneration and chondrone formation. For this reason it was apparent that the grading system for the sagittal IVD sections was more reliable than that of the grading system for the transverse IVD sections. No significant difference in grades were observed between the 0-1 year and 3-4 year age groups suggesting that degeneration had not yet begun at this age and therefore began at 5-6 years of age in the IVD.

The grading data for the facet cartilage grading from both photographs and H&E stained sections, showed no statistical differences between the age and breed groups. However, good correlations between degeneration and age were observed in grading of both the morphology and histological sections of cervical facets. In addition, a good correlation was present between degeneration and age in the grading of thoracic facet histological sections. More correlations between age and degeneration were observed for the facet histology sections than for the photographs. This may have been because the facet histology grading system was more detailed than that for the facet photographs. Previous work to investigate the changes in facet cartilage with age was restricted to human samples rather than ovine (Taylor and Twomey, 1986; Gries *et al.*, 2000; Tischer *et al.*, 2006; Kettler *et al.*, 2007). In comparison to the macroscopic appearance of degenerated human facets shown in the literature, the ovine facets analysed here were in general much healthier. Most of the samples, including those in the 8-10 year age group, did not show major signs of degeneration such as eburnation of cartilage from the underlying bone. This may have explained the lack of significant differences between the age groups. It may be that more extensive features exist in older sheep.

Only one significant difference was observed for BV/TV in the bone of all FSU samples. This was between the 0-1 year and 8-10 year age group in the thoracic FSUs. A correlation was also found showing an increase in BV/TV with age for thoracic FSUs. It is not known whether this was due to variations in the Hebridean breed of sheep or their older age. However, despite the lack of statistical differences and correlations for the cervical and lumbar FSUs, it was observed that BV/TV generally increased with age in some FSUs. Some studies have previously reported this for human vertebrae (Simpson *et al.*, 2001; Briggs *et al.*, 2004). However, other studies since have found that BV/TV decreases with age in human vertebrae due to increased bone resorption (Gong *et al.*, 2005; Chen *et al.*, 2008; Wilke *et al.*, 2012). The change in BV/TV with age in ovine vertebrae has not previously been reported. The findings here were most likely due to the lack of biomechanical support within the IVDs as the amount of GAGs decreased affecting resistance to axial loads. As a result, the bone within

the vertebral body may have restructured to deal with this increase loading force by synthesising bone.

No significant differences or correlations were observed in HA concentration between age groups. HA deposition in the degenerated human lumbar IVD has previously been reported (Feinberg *et al.*, 1990). Another study found calcium deposits present in the IVDs of 11 year old sheep which contained a reduced amount of PGs in the absence of any morphological signs of degeneration (Melrose *et al.*, 2009). Further studies will need to be carried out to determine whether there is a link between HA concentration and age. This may involve using a larger sample size.

In the cervical FSUs the IVD height in the 8-10 year old group was significantly smaller than all other age groups. Although, there were no significant differences in the IVD heights of FSUs from the thoracic and lumbar regions between the different age groups and breeds, negative correlations were found in cervical, thoracic and lumbar FSUs indicating a decrease in IVD height with age. As the Hebridean breed were considerably smaller than the other breeds used in this study, it is likely that this change in IVD height was due to the smaller animal and therefore smaller spine. Due to the limitations in obtaining 8-10 year old tissue of Charollais, Suffolk or Texel breed it was not possible to investigate this further. Therefore, whether IVD height decreases with age is not known.

A major limitation of this study was the number of replicates. For each age group, with the exception of the 3-4 year age group, there were only three replicates. A greater n value could have resulted in more evident trends, correlations and significant differences. However, overall, the results from this study showed that in comparison to 0-1 year old samples which did not show signs of degeneration, 3-4 year old FSU samples also did not show significant signs of degeneration. Significant changes were observed in 5-6 and 8-10 year old samples with regards to degeneration and therefore it was concluded from this work that degeneration began at 5 years of age. As issues may arise from using 0-1 year old samples for characterisation as bone does not mature in

sheep until approximately 15-18 months (Hasler *et al.*, 2010), tissue from 3-4 year old sheep was regarded as “healthy” tissue and used for characterisation studies. As the most easily obtained sheep breed was the Texel and would most likely be used in future studies, this breed was used in the characterisation studies reported in the following chapter.

Chapter 4: Biological Characterisation of the Ovine Functional Spinal Unit and Biomechanical Evaluation of the Facet Joint Cartilage

Chapter 4: Biological Characterisation of the Ovine Functional Spinal Unit and Biomechanical Evaluation of the Facet Joint Cartilage

4.1 Introduction

The results presented in Chapter 3 demonstrated that healthy ovine FSU tissue suitable for histological, immunohistochemical, biochemical and biomechanical characterisation could be obtained from sheep aged three to four years. Tissue from sheep of this age was therefore used for characterisation. The longer term aim was to enable direct comparison with normal and pathological human tissue and allow for similarities and differences to be identified.

The approach taken was to firstly determine the biological characteristics of the three to four year old ovine tissue from the IVD, including the outer AF, inner AF and NP, and facet cartilage. This was carried out by histology and immunohistological evaluation of key extracellular matrix components and cellular markers. In order to determine the phenotype of the cells from the different FSU tissues the cells were isolated and phenotyped in primary cell culture.

In addition to the major collagens (types I, II, III, V, VI and X; Section 1.2.1.) and aggrecan (Section 1.2.1.), which have been widely documented in the FSU tissues, other key cellular markers and extracellular markers including SOX-9, CD44 and fibronectin were included in the study due to their reported expression by the tissues/cells as outlined below.

Immunohistochemical staining for aggrecan within tissues/cells is problematic due to the epitopes of the protein being masked by the associated GAGs. It was

therefore decided to determine the presence of chondroitin sulphate in tissues/cells as an indication of proteoglycan/GAG content/expression.

Chondroitin sulphate is a naturally sulphated GAG (Section 1.2.1.2.). It is commonly sulphated at the fourth and sixth position making chondroitin-4-sulphate and chondroitin-6-sulphate the most common forms. It is highly anionic and forms a major part of aggrecan which binds to collagen. Its main functions when covalently linked to the aggrecan core protein are to maintain structural integrity of cartilage as well as providing resistance to compression (Henrotin, 2010). In addition, by affecting matrix integrity and bone mineralisation, chondroitin sulphate has also been reported to play a role in articular and bone metabolism (Bali *et al.*, 2001).

*Sox*9 is a gene that regulates chondrogenesis in mammals. This process involves mesenchymal cells which condense and differentiate to form chondrocytes initiating endochondral bone formation during the development of the vertebrate skeleton. The process of skeletal development is regulated and controlled by many factors such as signalling molecules and transcription factors including SOX-9 (Ng *et al.*, 1997).

SOX-9 is a transcription factor involved in regulating developmental events including cartilage development. The gene is highly expressed in proliferating and prehypertrophic chondrocytes but this decreases greatly in hypertrophic chondrocytes. It has also been found to be a negative regulator of cartilage vascularisation, cartilage resorption and formation of trabecular bone in the growth plate (Hattori *et al.*, 2010).

CD44 is a single-pass transmembrane receptor expressed by chondrocytes and other cell types. It is the primary receptor that allows hyaluronan binding. As hyaluronan is associated with many PG monomers attached non-covalently via link proteins, CD44 allows the highly charged protein aggregates to be present at the chondrocyte surface as illustrated in Figure 4.1 (Knudson and Loeser, 2002).

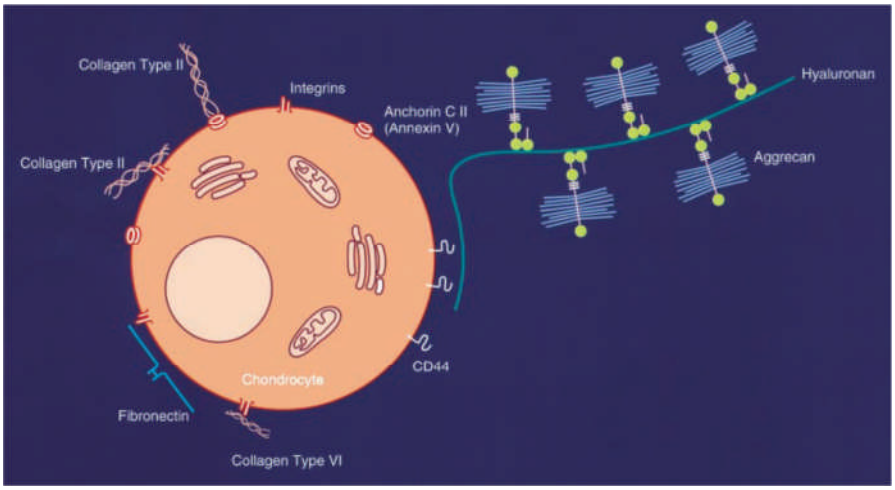


Figure 4.1: A human chondrocyte making multiple interactions with different macromolecules. The image shows the attachment of a large hyaluronan/PG aggregate at the surface of a chondrocyte. PG: Proteoglycan (Knudson and Loeser, 2002).

As well as providing attachment of hyaluronan to the chondrocyte, CD44 has also been shown to be involved in the internalisation of hyaluronan resulting in its catabolism (Hua *et al.*, 1993). CD44 expression by chondrocytes is believed to be essential for maintaining healthy cartilage metabolism (Knudson and Loeser, 2002).

Fibronectin is a multifunctional glycoprotein within the ECM of articular cartilage. Its main function is to provide a site for the attachment of chondrocytes via integrins (Figure 4.1) which is important to allow cellular responses to physical forces in the ECM. It also binds to other components of the ECM. Fibronectin has been shown to be present at low levels in normal articular cartilage. However, it is expressed at higher levels in osteoarthritic cartilage (Chevalier, 1993).

Several potential roles for fibronectin in healthy cartilage have been suggested. The first possibility is that it is part of a cell substrate-adhesion complex alongside cell surface proteoglycans. Chondrocytes are capable of binding fibronectin and fibronectin has been shown to bind to chondroitin sulphate and dermatan sulphate (Ruoslahti, 1988). Another role involves regulating the organisation of the ECM. This is due to the common multiple binding sites that are shared between fibronectin and other ECM molecules. This would suggest

an important role in organising the collagen and aggrecan network (Brown and Jones, 1990). In addition to this, fibronectin has been shown to protect collagen from collagenases (Menzel and Borth, 1983).

Osteocalcin is a non-collagenous protein expressed in bone and is thought to regulate bone matrix formation (Ducy *et al.*, 1996). It is involved in the mineralisation process of bone via its three γ-carboxyglutamic acid residues which bind to calcium and hydroxyapetite (Hauschka and Reid, 1978; Poser *et al.*, 1980). Osteocalcin can be used as a marker for mature and fully differentiated osteoblasts. Osteocalcin mRNA has been identified in osteoarthritic articular cartilage from human knees (Pullig *et al.*, 2000).

Since a major focus of this study was to characterise the facet joint cartilage, which has received little attention in the literature, additional characterisation of this tissue was carried out. This was mainly to assess the biomechanical properties of the cartilage using unconfined indentation testing. The compressive behaviour of cartilage is determined mainly by physical interactions between solid and fluid phases of the tissue during loading. This is mainly controlled by the GAG content of the tissue (Katta *et al.*, 2008A). Hence the GAG content was determined using the DMB assay.

4.2. Aims and Objectives

The aim of this chapter was to analyse cells and tissue of the three year old ovine FSU including inner AF, outer AF, NP and facet cartilage to determine the biological characteristics. In addition, the biomechanical properties of the facet cartilage was investigated and the total GAG content.

Specific objectives:

- Isolate outer AF, inner AF, NP and facet cartilage cells from cervical, thoracic and lumbar FSUs of a three year old sheep.
- Culture the cells in monolayer culture.
- Phenotype the cells using a panel of selected antibodies.
- Analyse three year old ovine facet cartilage and IVD tissue from cervical, thoracic and lumbar regions histologically.
- Analyse three year old ovine facet cartilage and IVD tissue from cervical, thoracic and lumbar regions immunohistochemically.
- Determine the indentation properties of three year old ovine cervical facet cartilage.
- Quantify the amounts of GAGs in three year old ovine facet cartilage from the thoracic region.

4.3. Experimental Approach

A three year old Charollais sheep (third replicate of the three to four year old age group in the anatomical study (Figure 4.2)) was dissected as previously described (Section 2.2.5.3.) Tissue from the outer AF, inner AF, NP and facet cartilage (from all facets) from the FSUs C2/C3, T5-T7 and L5/L6 were removed for cell isolation (Section 2.2.8). The isolated cells were transferred to monolayer culture to establish 12 primary cell cultures including outer and inner AF, NP and facet cartilage from cervical, thoracic and lumbar regions. After two passages each cell type was transferred to multispot slides at a density of approximately 800 cells per spot. Cells from the CEP were excluded due to the technical difficulties in isolating the tissue.

In order to determine the phenotype of the FSU cells, indirect immunofluorescence was carried out. This technique made it possible to identify which chondrocyte-specific markers were being expressed and allowed a qualitative assessment by the level of intensity of the fluorescent signal (Section 2.2.9.1.). Primary antibodies to the following markers (Section 2.1.3.1.) were used:

- Collagen I
- Collagen II
- Collagen III
- Collagen V
- Collagen VI
- Collagen X
- Chondroitin-6-sulphate
- CD44
- Fibronectin
- SOX-9

The tissues of the ovine FSU including the left inferior facet cartilage, IVD and CEP were analysed using the DAKO Envision method of immunohistochemistry (Section 2.2.10.1) and histology (Section 2.2.7). This was carried out on the FSUs C6/C7, T11/T12 and L1/L2 of replicates five, six and seven from the three

to four year old age group in the natural history study (Figure 4.2). These were used because the sheep were all of the Texel breed which is the most accessible breed and thus available for use as a pre-clinical model. Antibodies to the following markers were used for immunohistochemistry:

- Collagen I
- Collagen II
- Collagen III
- Collagen VI
- Chondroitin Sulphate
- Fibronectin
- Osteocalcin

For histological analysis, H&E, alcian blue, picro-sirius red and Miller's elastin stains were used to determine the structure and distribution of GAGs, collagen and elastic fibres in facet cartilage, CEP and the IVD.

In order to explore some biomechanical properties of ovine facet cartilage, indentation studies were carried out (Section 2.2.13). This was performed on 4 mm pins from the C6/C7 facets of a three year old Texel sheep including the left and right of both superior and inferior facets.

The GAG content of ovine facet cartilage was quantified using the DMB assay (Section 2.2.11.1). This was carried out on ovine facet cartilage from the T2/T3 facets remaining from the natural history study. This included the second replicate of the one year old age group; replicates one, four, five, six, seven, eight and nine from the three to four year old age group; the second replicate from the five to six year age group; and the second and third replicates of the eight to 10 year old age group (Figure 4.2). The focus was on the three year old samples and the samples from the 0-1, 5-6 and 8-10 year age groups were analysed for comparative purposes only. Cartilage from the left inferior facet of T2/T3 was used for the GAG assay.

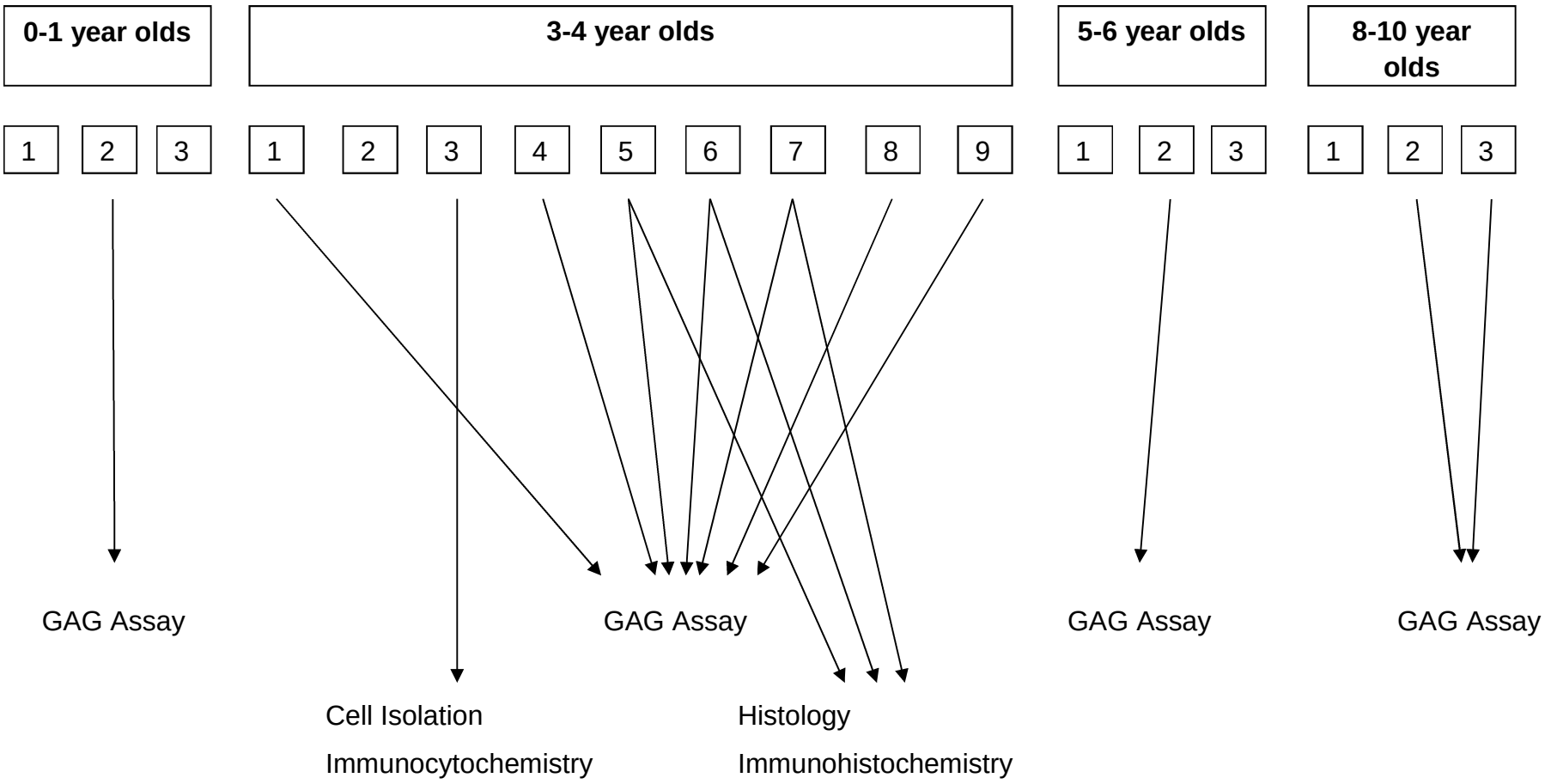


Figure 4.2: The allocation of tissue for each analysis. Tissue from the natural history study in Chapter 3 was used (Section 3.3). Each number represents the replicate spine number for each age group.

4.4 Results

4.4.1. Growth Characteristics of Isolated Cells

Outer AF, inner AF, NP and facet cartilage cells were isolated from C2/C3, T5-T7 and L5/L6 of a three year old Charollais sheep and were cultured in monolayer (Section 2.2.9). All cells appeared to grow at different rates. Facet cartilage cells from the cervical region grew the fastest reaching confluency after 12 days in culture. The outer AF cells from both cervical and lumbar regions grew at the slowest rate. Images of the cells in monolayer culture 12 days after isolation are shown in Figure 4.3.

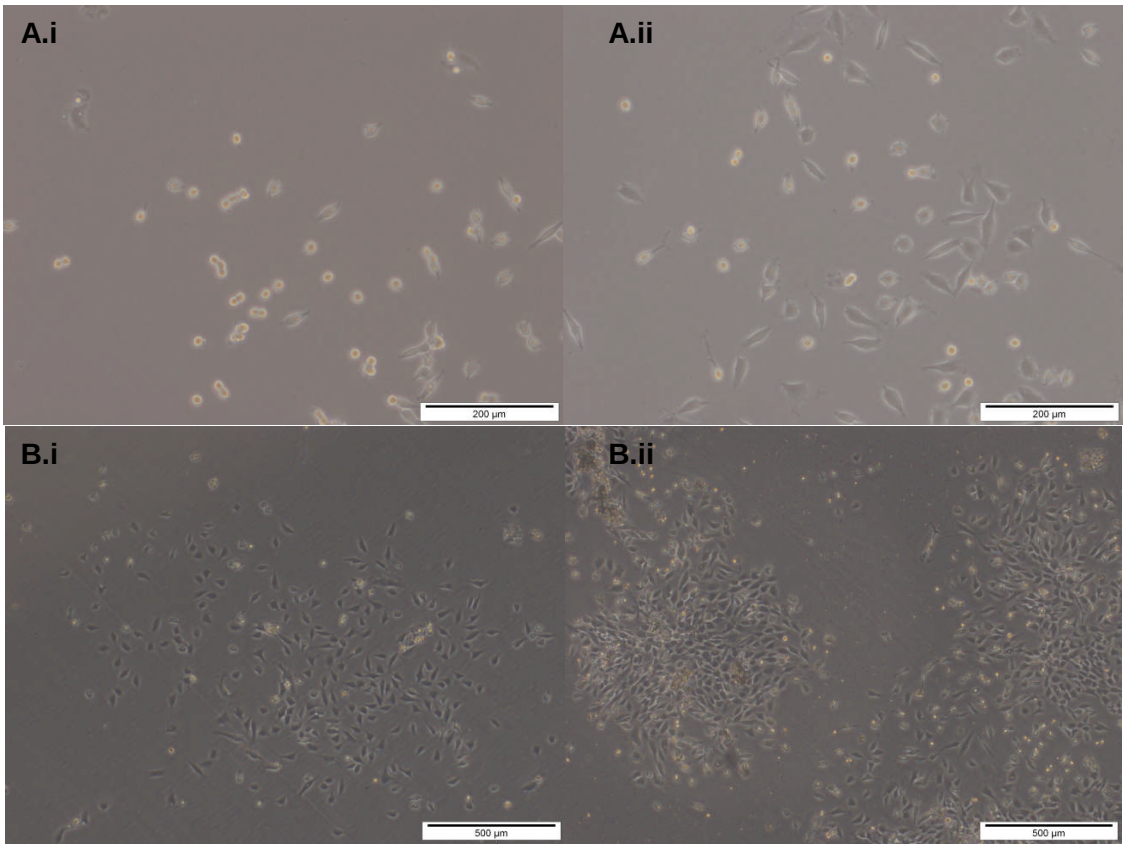


Figure 4.3: Light microscope images of FSU cells growing 12 days after isolation and before passage. A: **i**. Outer AF cells (cervical) 10x magnification, **ii**: NP cells (thoracic) 10x magnification. **B**: **i**. NP cells (cervical) 4x magnification, **ii**: Facet cells (lumbar) 4x magnification. FSU: functional spinal unit, AF: annulus fibrosus, NP: nucleus pulposus.

The cells appeared rounded during the initial stages. As the cells divided and became more confluent they formed colonies. The cells also became elongated and spindle shaped as they adhered to the plastic of the culture flask.

4.4.2. Phenotype of FSU cells

Once the cells had reached confluency after approximately three weeks, they were passaged and split into two flasks. Once the cells had reached confluency for a second time they were transferred to multispot slides and phenotyped at passage two (Section 2.2.9.2).

The cells were analysed for their expression of collagen types I, II, III, V, VI and X, chondroitin-6-sulphate, CD44, fibronectin and SOX-9 in outer and inner AF, NP and facet cartilage cells. The level of expression was measured as a level of intensity of the immunofluorescent stain. The following system was used to describe the levels of marker expression:

- - No expression
- + Positive expression
- ++ Good expression
- +++ Very good expression

Each cell and antibody combination was assessed. Across the different cell types the expression of the different markers appeared to be relatively similar. The markers which were highly expressed in the FSU cells were collagen types II, III and VI, CD44, chondroitin-6-sulphate, fibronectin and SOX-9. Markers which were not expressed or expressed at a low level by the ovine FSU cells were collagen types I, V and X. The results obtained using antibodies to collagens are shown in Table 4.1 and results for the other antibodies are shown in Table 4.2.

Cell Type	Collagen I	Collagen II	Collagen III	Collagen V	Collagen VI	Collagen X
C.F	++	++	++	-	++	+
C.NP	+	++	+++	-	++	+
C.IAF	+	+++	+++	-	++	-
C.OAF	+	+	+	-	+	+
T.F	+	+	-	-	+++	+
T.NP	+	++	+	-	+++	+
T.IA	+	++	+	-	+	-
T.OA	+	+++	++	-	+	-
L.F	++	++	++	-	++	-
L.NP	+	++	-	-	+++	-
L.IAF	+	+++	++	-	++	-
L.OAF	-	+	-	-	+++	+

Table 4.1: Expression of collagens and levels of collagen expression in FSU cell types at passage two. C: Cervical, T: Thoracic, L: Lumbar cells, F: Facet, IAF: inner AF, OAF: outer AF, AF: annulus fibrosus, NP: nucleus pulposus, FSU: Functional spinal unit. **-**: No expression, +: positive expression, ++: good expression, +++: very good expression.

Cell Type	CD44	Chondroitin-6-sulphate	Fibronectin	SOX-9
C.F	+	++	++	+
C.NP	+++	++	+++	++
C.IAF	+++	++	+++	+++
C.OAF	+	+	+	+++
T.F	++	++	+++	+++
T.NP	+	++	+++	++
T.IA	+	++	++	+
T.OA	++	++	++	+++
L.F	+	++	++	++
L.NP	++	++	++	++
L.IAF	++	+++	+++	++
L.OAF	++	++	+	+

Table 4.2: The expression of non-collagenous markers and the level of expression in FSU cell types at passage two. C: cervical, T: thoracic, L: lumbar cells. F: Facet, IAF: inner AF, OAF: outer AF, AF: annulus fibrosus, NP: nucleus pulposus, FSU: Functional spinal unit. **-**: No expression, +: positive expression, ++: good expression, +++: very good expression.

4.4.2.1. Collagen Type I

Collagen I expression was found to vary with cell type. For the cervical region, staining was positive in cells from all regions of the FSU but particularly good in the facet cartilage cells where it was present in the cytoplasm and nucleus and appeared granular. In the inner AF and NP cells most of the staining was nuclear. In the outer AF, the staining was largely cytoplasmic. For the thoracic region the facet cartilage and NP cells showed little expression. In both the inner and outer AF however there was good positive expression. This is illustrated in Figure 4.4. The majority of the positive staining was found in the cytoplasm but some was present within the nucleus. The staining was generally uniform within the cells. Lastly in the lumbar region, the facet cartilage cells displayed the most staining. This was found uniformly throughout the cytoplasm and nucleus and appeared granular. The NP and inner AF cells showed positive

staining of less intensity which was largely present as granular staining in the nucleus. No staining was observed in the outer AF cells.

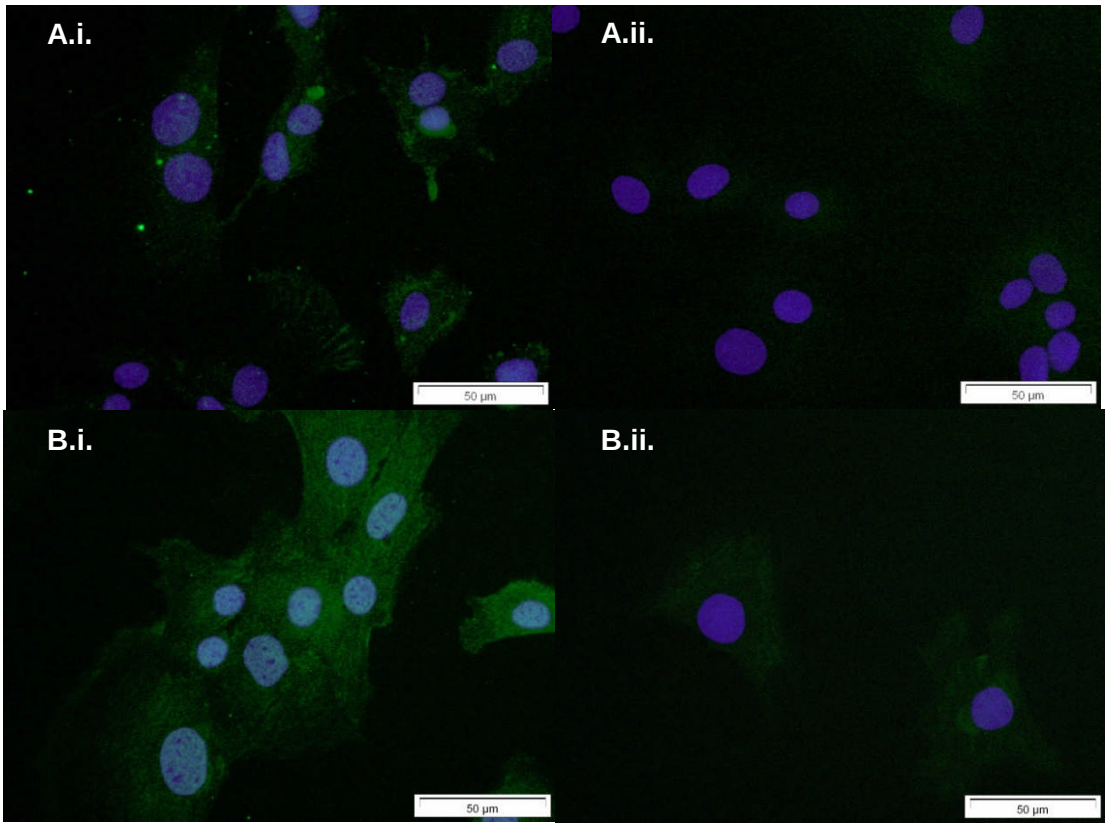


Figure 4.4: Ovine thoracic (T5-T7) facet cartilage (A) and outer AF (B) cells stained with mouse anti-sheep collagen type I monoclonal antibody (i) and mouse IgG1 isotype control (ii) together with rabbit anti-mouse FITC-conjugated secondary antibodies. 40x magnification. AF: Annulus fibrosus.

4.4.2.2. Collagen Type II

Collagen II expression varied between different cell types. For the cervical region, the greatest staining intensity was seen in the inner AF cells (Figure 4.5B). The staining was located within the cytoplasm and was granular. There were some areas within the nucleus which also contained granular staining. The staining was less intensive but evidently positive within the facet cartilage cells (Figure 4.5A). The pattern of staining was similar to the inner AF cells. The same was observed for the NP cells. The outer AF cells in the cervical region had the lowest intensity of collagen II staining.

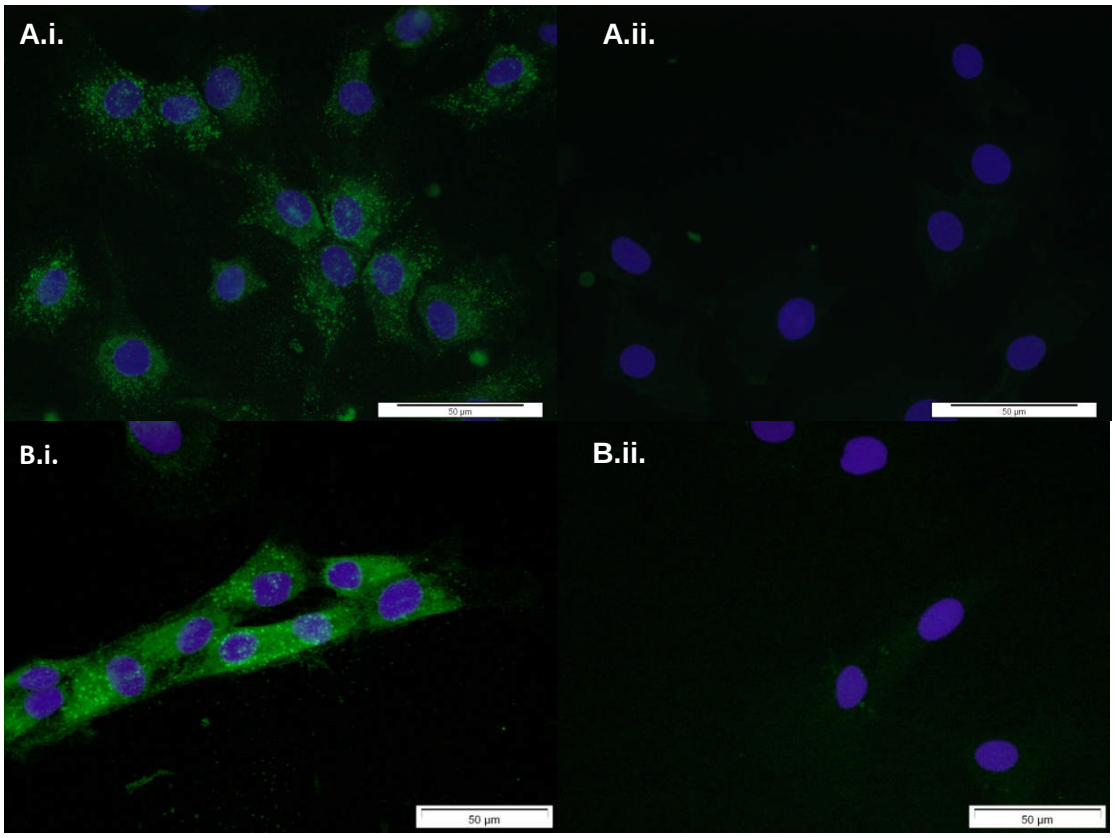


Figure 4.5: Ovine cervical (C2/C3) facet cartilage (A) and inner AF (B) cells stained with mouse anti-sheep collagen type II monoclonal antibody (i) and mouse IgG1 isotype control (ii) together with rabbit anti-mouse FITC-conjugated secondary antibodies. 40x magnification. AF: Annulus fibrosus.

In the thoracic region, a different pattern of staining was observed between the cells. Very little staining was observed in the facet cartilage cells. The difference between the collagen II staining and the isotype control was the presence of small concentrated granules in the cytoplasm. The outer AF cells showed the highest level of staining which appeared as concentrated granules similar to that seen in the cervical facet cartilage cells but of greater intensity. The staining was mainly in the cytoplasm but was also observed in the nucleus.

4.4.2.3. Collagen Type III

Collagen III staining varied between different cell types. In the cervical region, the most intense staining was found in the NP and inner AF cells in comparison to the isotype control. The facet cartilage cells showed good staining intensity whilst the outer AF cells stained positive. The staining was present in the cytoplasm and was generally uniform in the different cell types. No staining was

found in the nucleus. An example of collagen III staining within the inner AF and outer AF cells in the cervical region is shown in Figure 4.6.

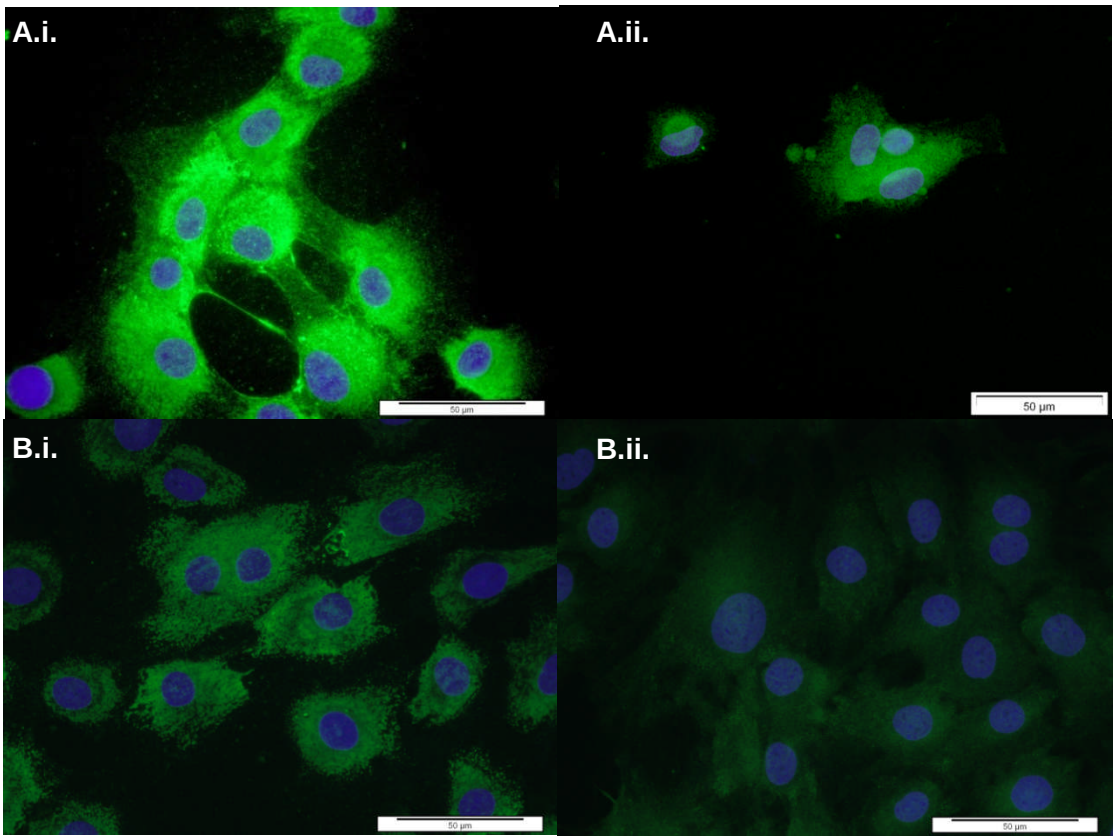


Figure 4.6: Ovine cervical (C2/C3) inner AF (A) and outer AF (B) cells stained with rabbit anti-sheep collagen type III rabbit polyclonal antibody (i) and rabbit IgG isotype control (ii) together with Goat anti-rabbit FITC-conjugated secondary antibodies. 40x magnification. AF: Annulus fibrosus.

In the thoracic region, the facet cartilage cells did not express collagen III. The NP and inner AF cells showed positive expression and the outer AF cells showed good expression. As with the cervical region, the staining was limited to the cytoplasm and no staining was present within the nucleus. In the lumbar region, the staining was good in the facet cartilage cells and inner AF cells but negative in the NP and outer AF cells. The staining patterns were the same as observed in the cervical and thoracic cells.

4.4.2.4. Collagen Type V

Collagen type V staining was absent in all cell types. An example of cervical and lumbar outer AF cells stained with antibodies to collagen type V is shown in Figure 4.7.

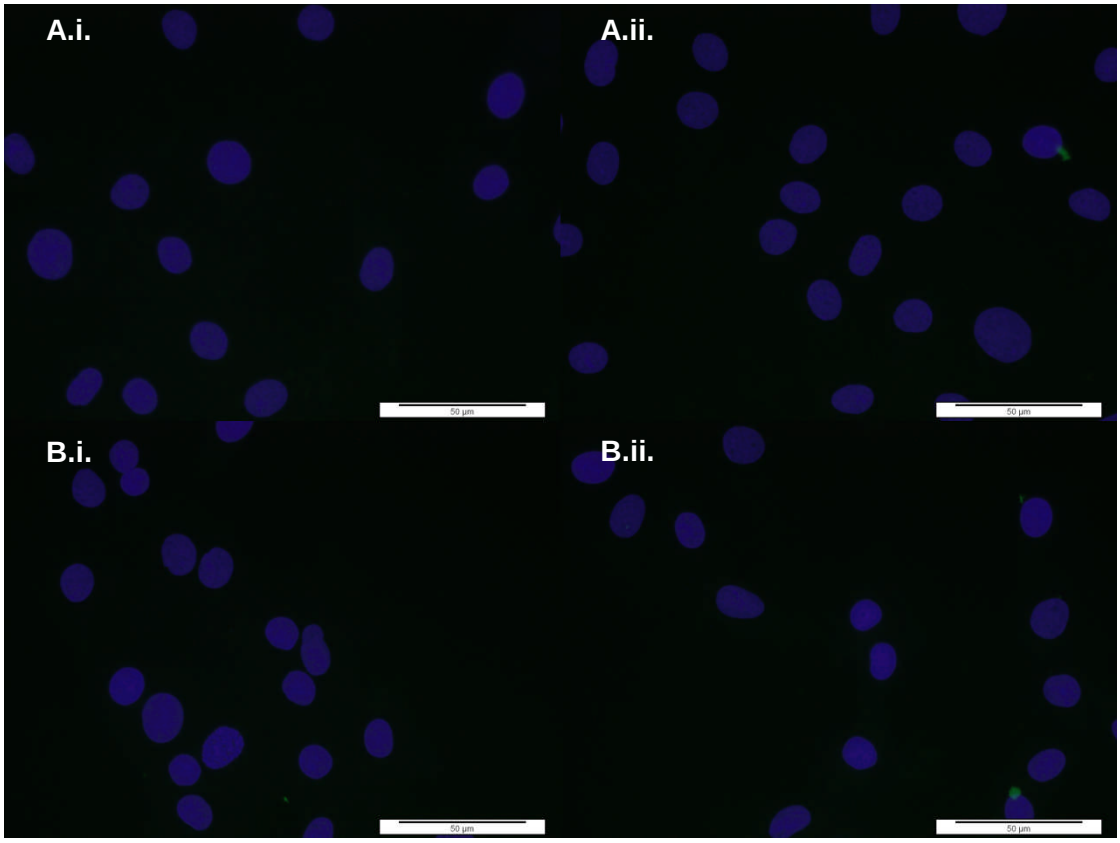


Figure 4.7: Ovine cervical (C2/C3) outer AF (A) and lumbar (L5/6) outer AF (B) cells stained with mouse anti-sheep collagen type V monoclonal antibody (i) and mouse IgG2a isotype control (ii) together with Goat anti-mouse FITC-conjugated secondary antibodies. 40x magnification. AF: Annulus fibrosus.

4.4.2.5. Collagen Type VI

Collagen type VI staining varied amongst the different cells types. In the cervical region, good staining was observed for the facet cartilage, NP and inner AF cells. Staining in the outer AF cells was just positive. In the thoracic region, good staining was found in the facet cartilage and NP cells but only positive in the inner and outer AF cells. In the lumbar region, very good staining was observed in the NP and outer AF cells and good staining in the facet cartilage and inner AF cells. An example of the staining in lumbar outer AF cells and thoracic inner AF cells is shown in Figure 4.8.

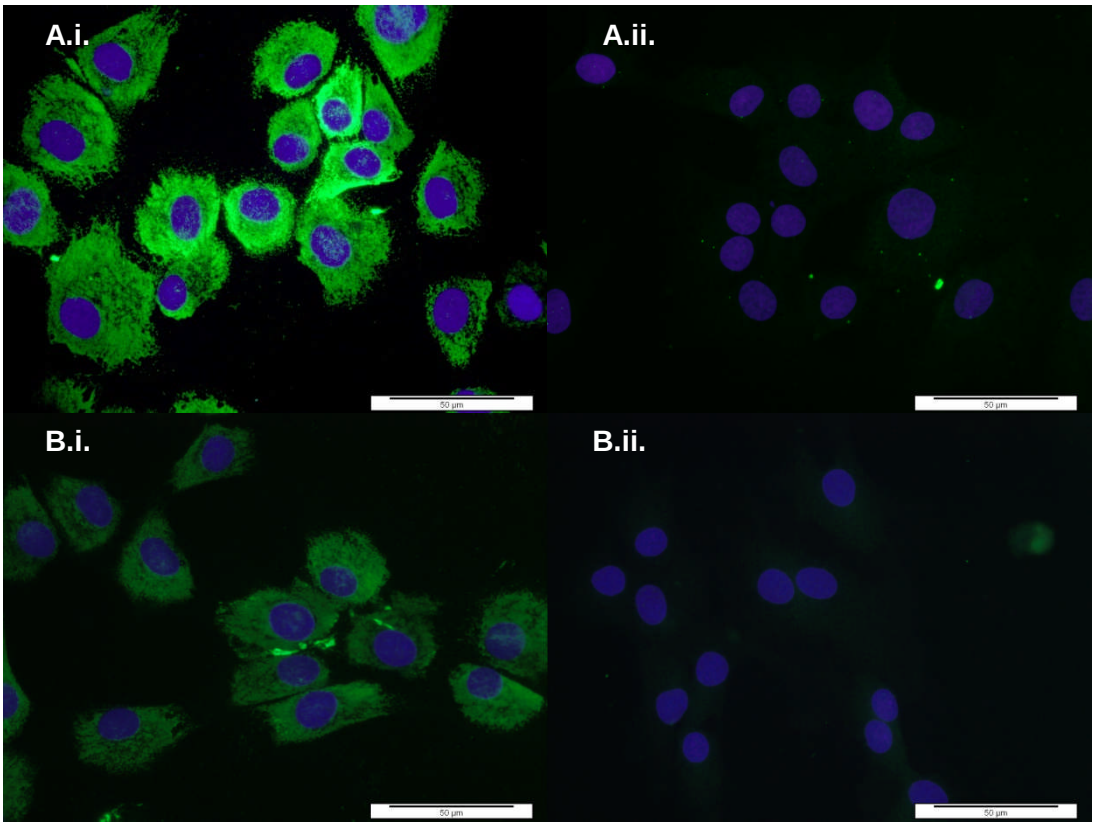


Figure 4.8: Ovine lumbar (L5/L6) outer AF (A) and thoracic (T5-T7) inner AF (B) cells stained with rabbit anti-sheep collagen type VI polyclonal antibody (i) and rabbit IgG isotype control (ii) together with Goat anti-rabbit FITC-conjugated secondary antibodies. 40x magnification. AF: Annulus fibrosus.

The staining distribution patterns within the cells were the same across all cervical, thoracic and lumbar regions. The staining was within the cytoplasm outside the nucleus and was uniform without any accumulation in particular areas.

4.4.2.6. Collagen Type X

The staining intensities of collagen type X in the FSU cells were either positive or negative. In the cervical region, the cells of the inner AF were negative whilst the cells in the facet cartilage, NP and outer AF were positive in comparison to the isotype controls. The staining distribution within the positive cells was confined to the cytoplasm with no staining in the nucleus. The staining was not uniform and appeared more intense in some areas than others giving a speckled appearance. In the FSU cells from the thoracic region, facet cartilage and NP cells stained positively whilst AF cells, both in the inner and outer

regions were negative. In the lumbar region, all cells were negative for collagen type X with the exception of the outer AF cells which were positive. An example of the immunofluorescence in cervical outer AF cells and thoracic facet cartilage cells is shown in Figure 4.9.

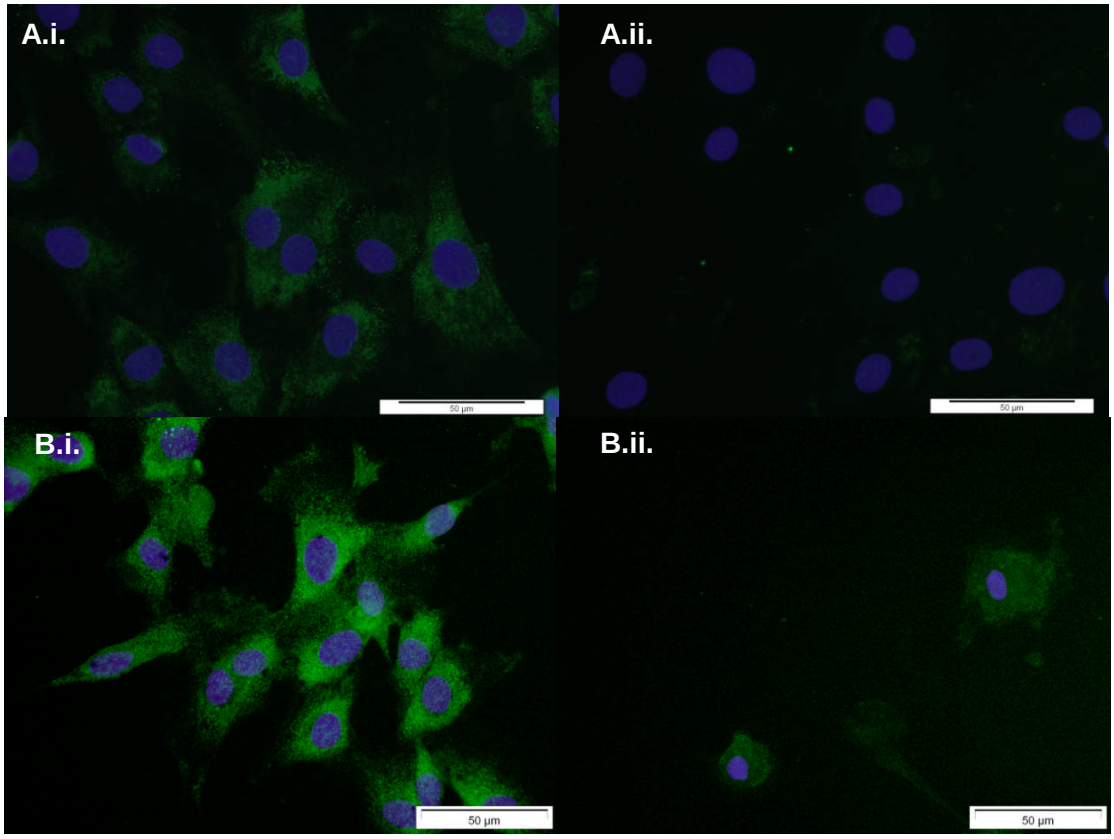


Figure 4.9: Ovine cervical (C2/C3) outer AF (A) and thoracic (T5-T7) facet (B) cells stained with mouse anti-sheep collagen type X monoclonal antibody (i) and mouse IgM isotype control (ii) together with Goat anti-mouse FITC-conjugated secondary antibodies. 40x magnification. AF: Annulus fibrosus.

The staining distributions in the thoracic and lumbar cells were the same as observed in the cervical FSU cells.

4.4.2.7. Chondroitin-6-sulphate

FSU cells in all regions were positive for chondroitin-6-sulphate with staining intensity ranging from good to very good in comparison to the isotype control. In the cervical region, facet cartilage, NP and inner AF cells showed good staining patterns with outer AF cells showing just a positive result. In the thoracic region, all FSU cells showed good staining. In the lumbar region, facet cartilage, NP and outer AF cells showed good staining and inner AF cells showed very good

staining. An example of chondroitin-6-sulphate staining in thoracic facet cartilage cells and lumbar inner AF cells is shown in Figure 4.10.

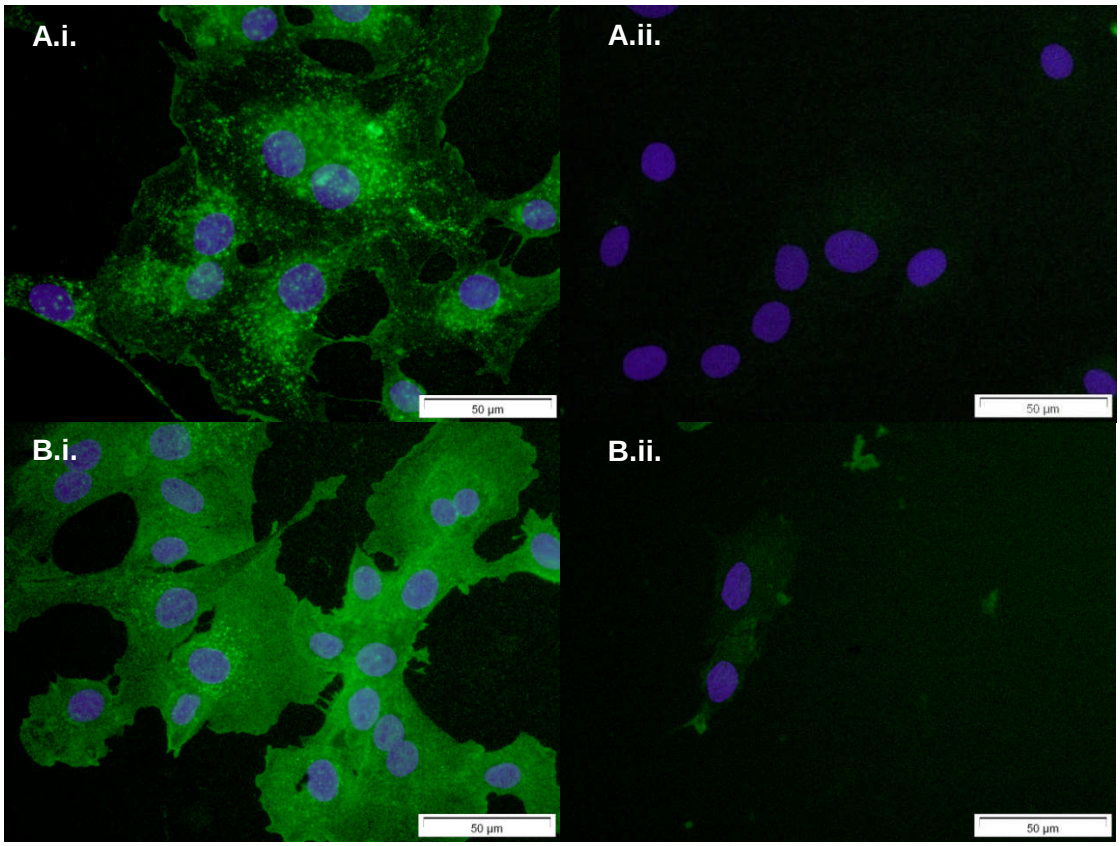


Figure 4.10: Ovine thoracic (T5-T7) facet cartilage (A) and lumbar (L5/L6) inner AF (B) cells stained with mouse anti-sheep chondroitin-6-sulphate monoclonal antibody (i) and mouse IgG1 isotype control (ii) together with goat anti-mouse FITC-conjugated secondary antibodies. 40x magnification. AF: Annulus fibrosus.

The staining patterns within the FSU cells immunofluorescently stained with antibodies to chondroitin-6-sulphate were both cytoplasmic and nuclear. Most areas of staining were granular in appearance with intensely stained regions showing more uniform staining. Most intense staining appeared to be located near the nucleus of the cells. In the nucleus, the staining was randomly distributed and granular.

4.4.8. CD44

CD44 staining was positive in all the FSU cells from different regions and intensities varied. In the cervical region, the NP and inner AF cells showed very good staining whilst the facet cartilage and outer AF cells were only positively stained. In the thoracic region, the facet cartilage and outer AF cells showed

good staining and the NP and inner AF cells were only positive. In the lumbar region, the facet cartilage cells showed positive staining whilst the NP, inner and outer AF cells showed good staining. An example of the staining patterns in cervical inner AF cells and lumbar facet cartilage cells is shown in Figure 4.11.

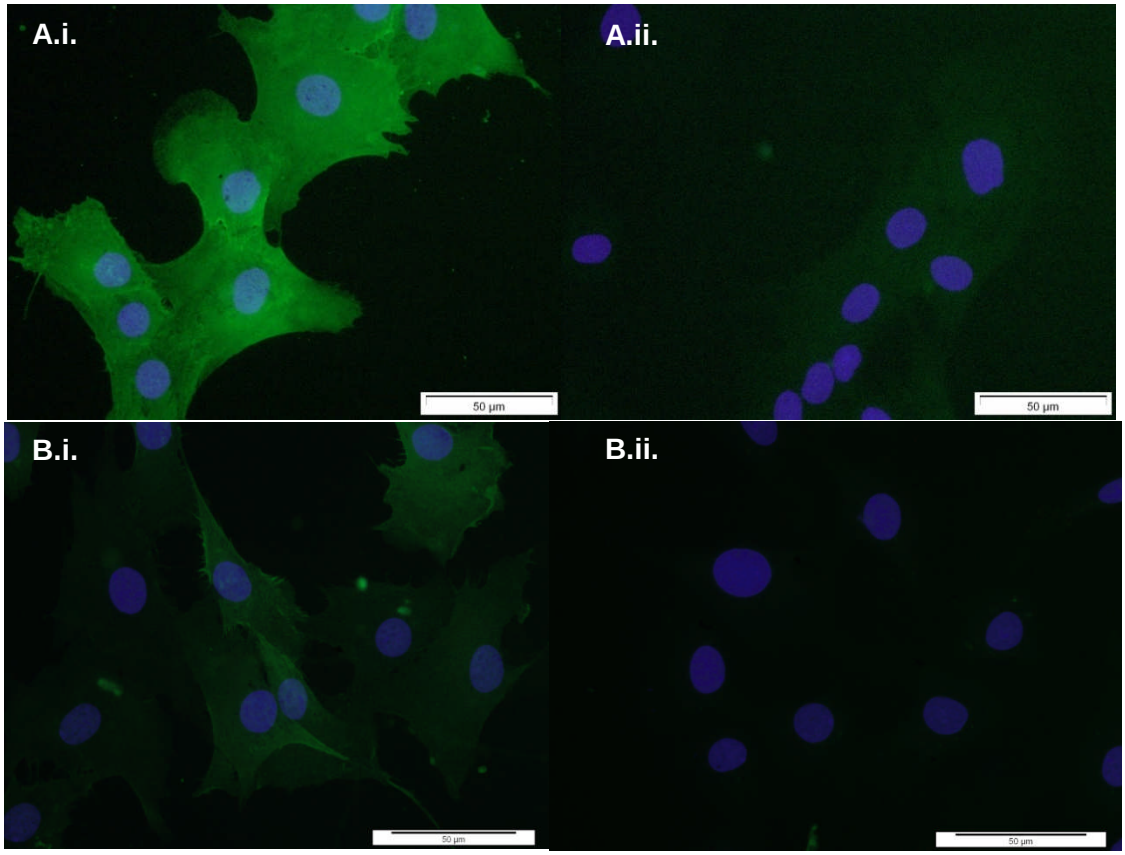


Figure 4.11: Ovine cervical (C2/C3) inner AF (A) and lumbar (L5/L6) facet cartilage (B) cells stained with rat anti-sheep CD44 monoclonal antibody (i) and rat IgG1 isotype control (ii) together with rabbit anti-rat FITC-conjugated secondary antibodies. 40x magnification. AF: Annulus fibrosus.

The staining patterns within the FSU cells appeared to be mainly cytoplasmic and slightly nuclear. Most of the expression appeared more intense around the nucleus of the cell and around the membrane. Staining within the nucleus was generally uniform; however, in some areas the staining was slightly speckled evenly throughout the nucleus.

4.4.2.9. Fibronectin

All the FSU cells stained positively for fibronectin and the level of intensities varied amongst the cells across the different regions. In the cervical region, the NP and inner AF cells showed very good expression whilst the facet cartilage

cells showed good expression and outer AF cells stained positively. In the thoracic region, facet cartilage and NP cells had very good expression of fibronectin whilst inner and outer AF cells showed good expression. In the lumbar region, the inner AF cells showed very good expression. The facet cartilage and NP cells showed good expression and the outer AF cells gave a positive result. An example of fibronectin staining in lumbar facet cells and cervical NP cells is shown in Figure 4.12.

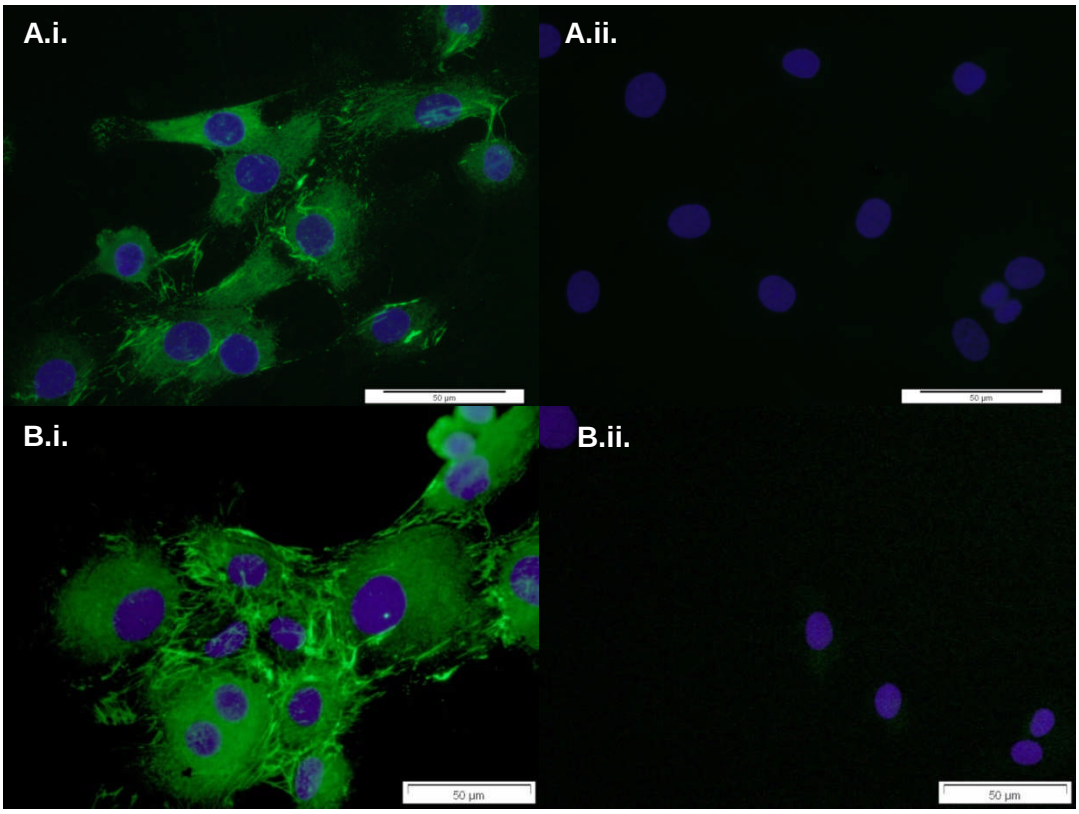


Figure 4.12: Ovine lumbar (L5/L6) facet (A) and cervical (C2/C3) NP cartilage (B) cells stained with mouse anti-sheep fibronectin monoclonal antibody (i) and mouse IgG1 isotype control (ii) together with goat anti-mouse FITC-conjugated secondary antibodies. 40x magnification. NP: Nucleus pulposus.

The staining patterns of the cells were largely pericellular and cytoplasmic with slight staining in the nucleus. Long, thin patterns were seen distributed in the intercellular space and pericellular. The highest level of intensities was seen in these regions. The cells appeared to make connections to one another through these thin projections. Some staining was observed in the nuclear space and this appeared mostly diffuse and random with few speckled regions.

4.4.2.10. SOX-9

All FSU cells across the different regions expressed different levels of SOX-9. In the cervical region, facet cartilage cells showed positive expression and NP cells showed good expression. Both inner and outer AF cells showed very good expression. In the thoracic region, both facet and outer inner AF cells showed very good expression. NP cells showed good expression whilst inner AF cells showed only positive expression. In the lumbar region, facet cartilage, NP and inner AF cells showed good expression whilst the outer AF cells only showed positive expression. Examples of SOX-9 staining in cervical outer AF cells and lumbar facet cartilage cells are shown in Figure 4.13.

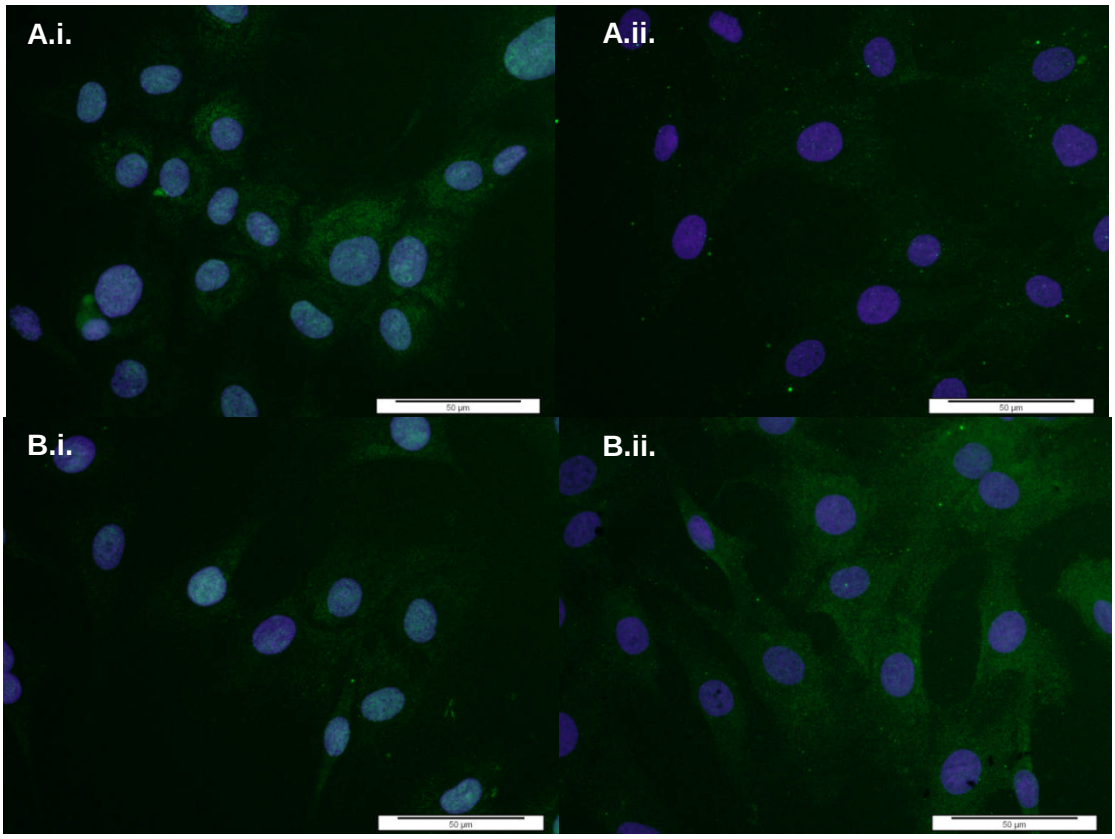


Figure 4.13: Ovine cervical (C2/C3) outer AF (A) and lumbar (L5/L6) facet cartilage (B) cells stained with rabbit anti-sheep SOX-9 polyclonal antibody (i) and rabbit IgG isotype control (ii) together with goat anti-rabbit FITC-conjugated secondary antibodies. 40x magnification. AF: Annulus fibrosus.

In comparison to the isotype controls, the staining in all cell types was confined to the nucleus. The staining was diffuse and covered all parts of the nucleus with some speckled areas containing a higher concentration of the fluorescence.

4.4.3. Characterisation of the IVD and Facet Cartilage using H&E Stained Histological Sections of Ovine FSU tissue

H&E was used to stain ovine facet cartilage and IVD tissues to determine the organisation and distribution of the cells and ECM in cervical, thoracic and lumbar regions.

The cervical AF tissue in all three replicates of the three to four year old age group showed intact lamellae with minimal fissures. The cells were randomly distributed. The thickness of the lamellae layers varied across the section of the AF. Dense fibrous tissue was present in between the layers and occasionally passed across them. The NP tissue in the three cervical replicates appeared homogenous. The colour of the eosin stain was light pink and no dense fibrous tissue or fissures were present. The cells were contained within their lacunae and the haematoxylin stain was confined to the nuclei. The cells were randomly distributed and no clusters were present. The cervical CEPs were relatively thick in comparison to the thoracic and lumbar regions and contained randomly distributed cells confined within lacunae. The eosin stain became darker towards the deeper layers of the CEP where it met the subchondral bone. The thickness of the CEP remained constant along the length of the AF/NP section. The CEP followed a curved path along the length of the AF/NP section in comparison to the thoracic and lumbar CEPs which were relatively straight.

The cervical facet sections showed articular cartilage which was thicker in comparison to the thoracic and lumbar regions. The cartilage was divided into four zones. The top superficial layers contained flat chondrocytes randomly distributed. The middle and deep zones were comparably thicker and contained chondrocytes randomly arranged in groups within lacunae of approximately four cells. The deep zone contained chondrocytes which were stacked on top of each other. Each zone within the articular cartilage was thicker than that of the thoracic and lumbar regions. The calcified zone was present near the subchondral bone and was stained more darkly with eosin than the upper layers particularly around the lacunae. The thickness of the calcified zone was relatively constant along the length of the cartilage. The cells that were present within the calcified zone appeared more stacked in comparison to the upper

zones. The subchondral bone within cervical facet cartilage was relatively uniform and budded into the calcified zone. The middle zone of cervical facet cartilage was less intensely stained by eosin in comparison to the other zones. Examples of H&E stained sections of cervical AF, NP, CEP and facet cartilage are shown in Figure 4.14.

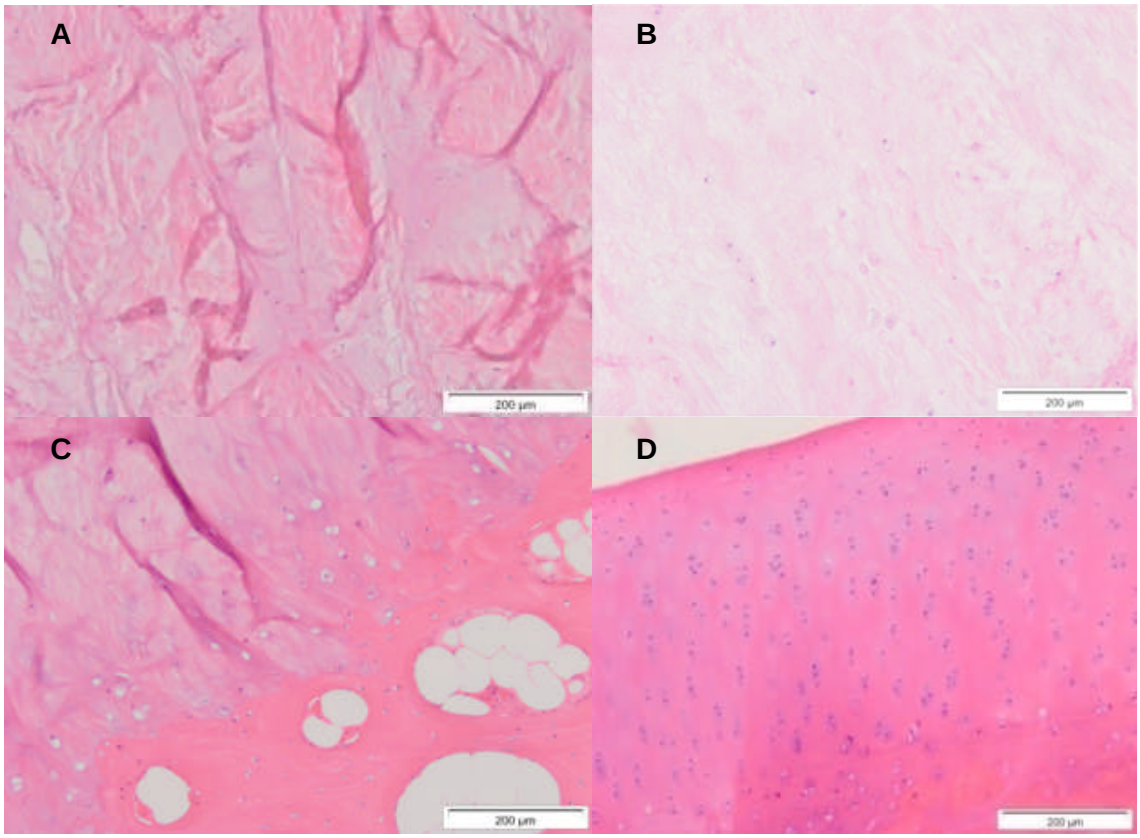


Figure 4.14: H&E stained facet cartilage and IVD sagittal sections from C6/C7. A: AF, B: NP, C: CEP, D: Facet cartilage. H&E: Haematoxylin and eosin, AF: Annulus fibrosus, NP: Nucleus pulposus, CEP: Cartilage end plate.

The thoracic AF tissue showed dense tissue arranged in lamellae as in the cervical and lumbar regions. The thickness of the lamellae layers appeared to differ throughout the length of the AF section, similar to that of the cervical AF. The layers appeared thin in comparison to the cervical lamellae. The colour of the eosin stain within the lamellae was constant; however, the colour in between in the layers was much lighter in comparison. Small amounts of fibrous tissue ran between the layers and occasionally across the lamellae layers as seen in the cervical AF. The cells within the AF were randomly distributed and minimal cell clustering was observed. The haematoxylin stain was confined to the nuclei and did not extend to the lacunae. The thoracic NP tissue appeared

similar to that of the cervical NP and was homogenous. The eosin stain was a light pink colour and occasional deepening of the colour was observed indicating the presence of a few fibres. The cells were randomly distributed and no cell clustering was observed. The thoracic CEP appeared thin in comparison to the cervical CEP and its thickness was constant along the AF/NP section. Eosin stained the CEP darker pink in comparison to the IVD tissue. The cells were randomly distributed within the CEP and contained within lacunae. Occasional lacunae were observed which contained no cells. The haematoxylin stain appeared to spread from some of the cells to the surrounding lacunae. The boundary between the CEP and subchondral bone was relatively flat. Some small, transverse fissures were present.

The histology sections of the facet cartilage in the three thoracic replicates showed that the cartilage was arranged into four zones similar to the cervical facet cartilage but had less depth. Few cells were seen in the superficial layer but the ones that were observed were flat and randomly distributed over a small depth. The cells in the middle and deep zones were stacked on top of one another and arranged in lacunae of approximately three cells. Many lacunae were present in the calcified zone with some containing no cells. The boundary between the calcified zone and subchondral bone was relatively constant along the length of the cartilage. The cells in the subchondral bone were randomly distributed. The darkness of the eosin stain appeared to vary along the depth of the cartilage. The superficial, deep and calcified zones were more intensely stained in comparison to the middle zone. The same was observed for cervical facet cartilage. Examples of some H&E stained FSU tissue sections from the thoracic region are shown in Figure 4.15.

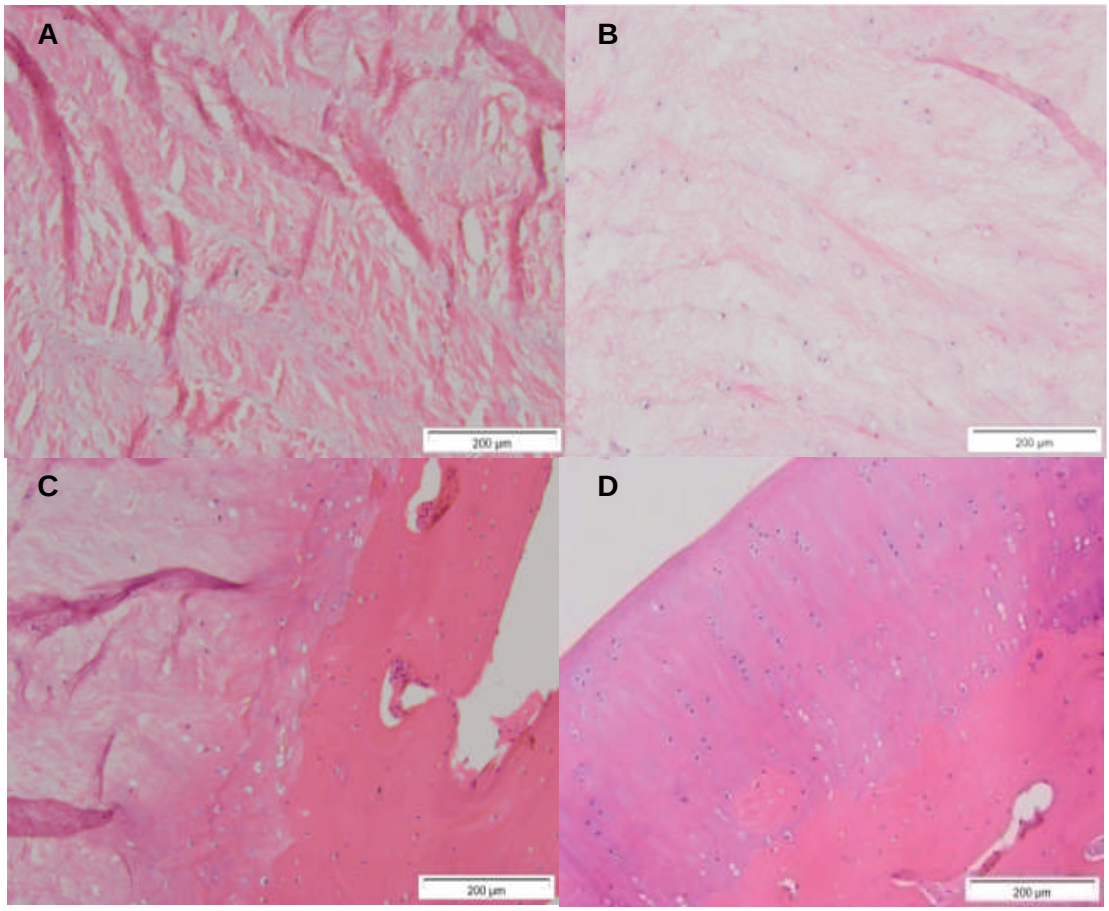


Figure 4.15: H&E stained facet cartilage and IVD sagittal sections from T11/T12. A: AF, B: NP, C: CEP, D: Facet cartilage. H&E: Haematoxylin and eosin, AF: Annulus fibrosus, NP: Nucleus pulposus, CEP: Cartilage end plate.

The lumbar AF showed many similarities to both the cervical and thoracic AF. Dense fibrous tissue was arranged into lamellae. The lamellae layers were slightly thinner in comparison to the cervical lamellae. The thickness of the layers across the section of AF appeared to vary. Again as with the thoracic AF, the colour of the eosin stain within the lamellae was constant; however, the colour in between in the layers was much lighter in comparison. Thin fibrous tissue lined the lamellae layers and also passed through them occasionally throughout the AF structure. The cells within the lumbar AF showed similar characteristics to that of the cervical and thoracic AF and were randomly distributed. The haematoxylin stain was confined to the nuclei and did not spread to the lacunae. The lumbar NP tissue showed the same characteristics as that of both cervical and thoracic NPs. The NP tissue was homogenous and was stained a light pink colour by eosin. The cells were randomly distributed and contained within their lacunae. No cell clusters were present. The

haematoxylin stain of the NP cells was confined to the nuclei and did not spread to the lacunae. There were occasional areas of darkening indicating the presence of few fibres. The lumbar CEP had similar features of that of the thoracic region. The CEP was thin and constant along the length of the AF/NP section. The colour of the eosin stain was darker in comparison to the IVD tissue. There were many randomly distributed lacunae some containing no cells. The subchondral bone was more darkly stained with eosin and budded into the CEP but at a constant level and thickness throughout the length of the CEP. Very few fissures were present.

The three lumbar facet cartilages were not as thick in comparison to the cervical and thoracic cartilage. The cartilage was still divided into four zones; however, these had less depth in comparison to those of the cervical and thoracic facet cartilage. Few cells were seen in the superficial zone and these were not as flat as those seen in the cervical and thoracic sections. The cells in the middle and deep zones contained stacked cells in lacunae containing approximately two cells, less than both the cervical and thoracic sections. The calcified zone contained similar stacking patterns of chondrocytes in lacunae. The haematoxylin stain around the cells appeared to spread into the lacunae in this zone. The subchondral bone showed similar patterns to that of the cervical and thoracic region and remained relatively constant along the length of the cartilage in the three lumbar replicates. The colour of the eosin stain varied across the depth of the cartilage with the superficial and calcified zones appearing more intensely stained compared to the middle and deep zones. Similar patterns were observed in both the cervical and thoracic sections. An example of some H&E stained FSU tissue sections from the thoracic region are shown in Figure 4.16.

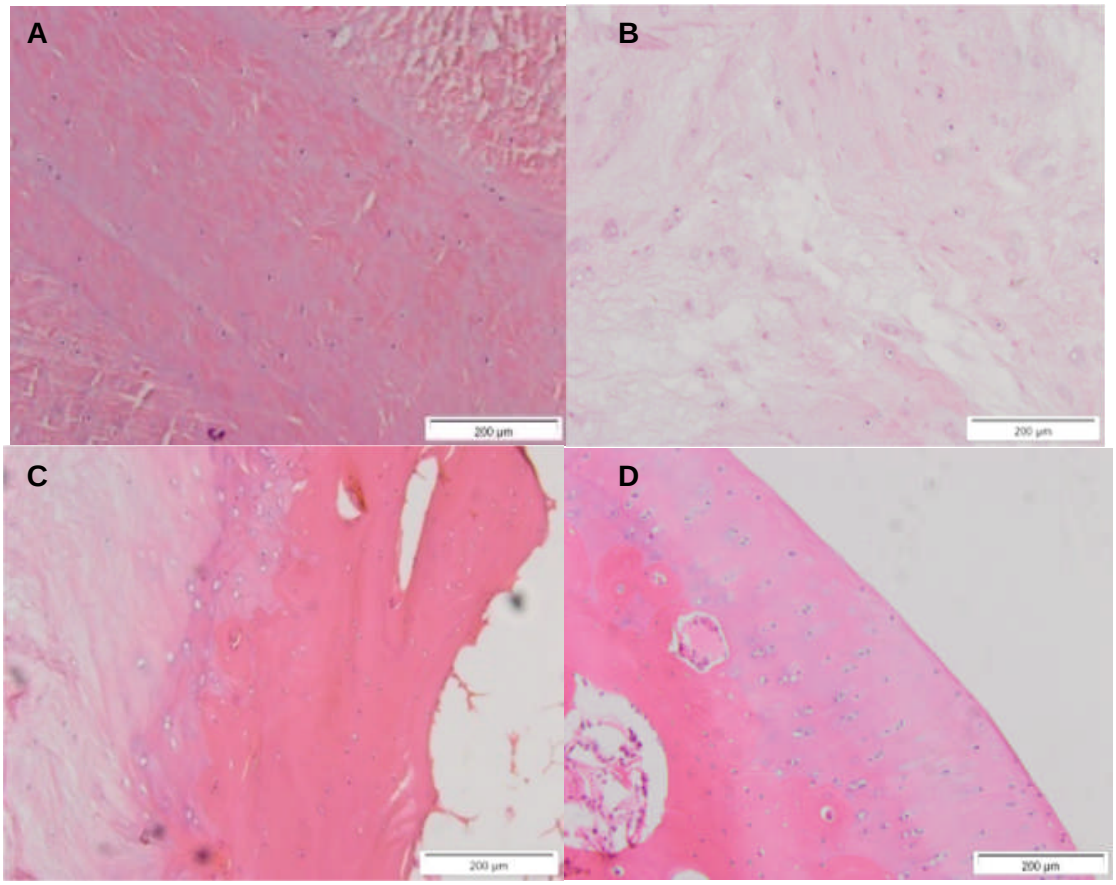


Figure 4.16: H&E stained facet cartilage IVD sagittal sections from L1/L2. A: AF, B: NP, C: CEP, D: Facet cartilage. H&E: Haematoxylin and eosin, AF: Annulus fibrosus, NP: Nucleus pulposus, CEP: Cartilage end plate.

4.4.4. Characterisation of the IVD and Facet Cartilage using Alcian Blue Stained Histological Sections of Ovine FSU tissue

Alcian blue was used to stain sections of all three replicates of cervical, thoracic and lumbar facet cartilage and IVD tissue to determine the distribution of GAGs.

The cervical AF was deeply stained with alcian blue in all three replicates. The intensity of the stain was found to increase from the outer AF to the inner AF. The fibres running in between the lamellae layers stained more intensely than the fibres within the lamellae. The cells and surrounding lacunae of the AF did not stain. The NP tissue was less intensely stained than the AF but varied in the three replicates. The stain was distributed in patches throughout the ECM with the cells appearing to capture more of the stain than the ECM. Alcian blue intensely stained the cells within the NP and this appeared to spread out to the surrounding lacunae. The CEP appeared to capture more of the stain than the

NP. The distribution of the stain throughout the CEP appeared constant and stopped at the subchondral bone where the colour became a lighter blue/pink. The staining intensity within the cells and surrounding lacunae appeared the same as that of the ECM. However, in one of the three replicates the stain was less intense with areas of light blue/pink stain distributed randomly.

The facet cartilage in all three cervical samples was intensely stained with alcian blue. This appeared relatively constant throughout most of the cartilage with the superficial layer being the most intense. The stain became lighter in some parts of the calcified region. The stain became light blue/pink at the subchondral bone. Examples of alcian blue stained sections of the cervical AF, NP, CEP and facet cartilage is shown in Figure 4.17.

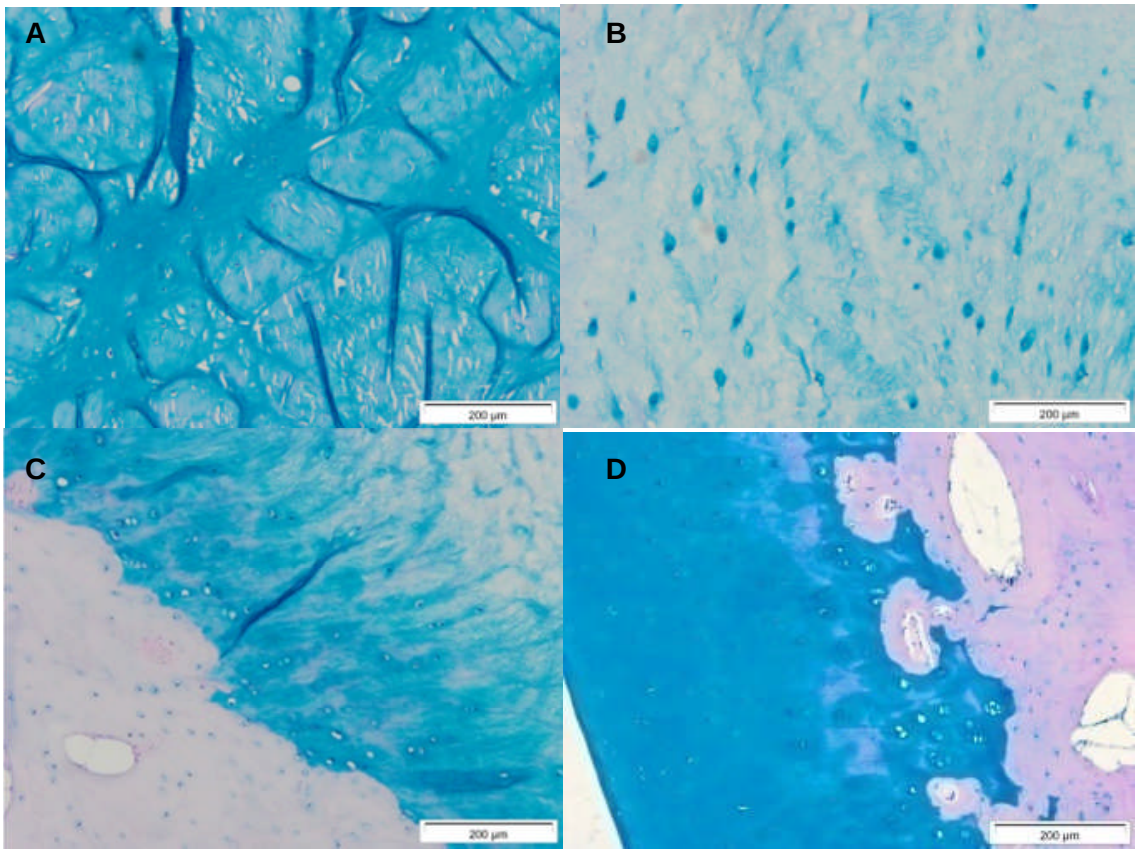


Figure 4.17: Alcian blue stained facet cartilage and IVD sagittal sections from C6/C7. A: AF, B: NP, C: CEP, D: Facet cartilage. IVD: Intervertebral disc, AF: Annulus fibrosus, NP: Nucleus pulposus, CEP: Cartilage end plate.

Alcian blue stained sections of the thoracic AF showed similar patterns to that of the cervical AF. The intensity of the stain increased from the outer AF to the inner AF. The stain intensity was greater in between the lamellae layers than

within them. This was true for all three replicates. The staining patterns within the NP were similar to that in the cervical region. The stain was less intense than the AF and distributed randomly in patches. Alcian blue intensely stained the NP cells and the surrounding lacunae. This was observed for all three replicates. The staining within the thoracic CEP varied with some parts showing a pink/purple colour within the ECM. These variations were seen in all three replicates. The cells and their surrounding lacunae also took up the stain and appeared bluer in comparison to the ECM. The blue colour was absent in the subchondral bone with the colour becoming light pink.

The facet cartilage in all thoracic samples did not show as much intensity as the cervical samples. The superficial layer showed the deepest blue staining and both the middle and deep zones were more lightly stained in comparison. The distribution of colour within the middle and deep zones was random with some parts more deeply stained than others. The colour in the calcified zone was pink/purple however, the cells and their lacunae were deeply stained blue. Less intense staining was observed in the calcified zone in comparison to the cervical samples. The colour was lighter in the subchondral bone. The same observations were recorded for all replicates in the thoracic region. Examples of alcian blue stained sections of the AF, NP, CEP and facet cartilage in the thoracic region are shown in Figure 4.18.

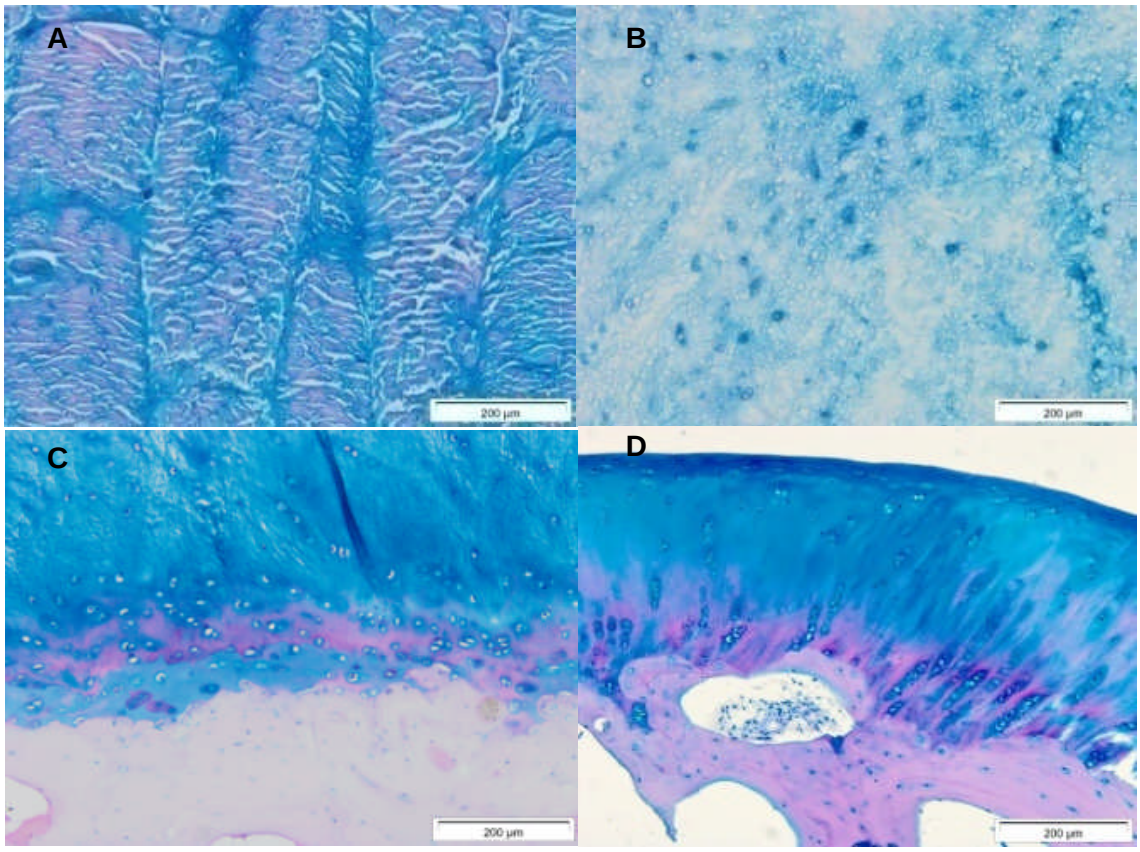


Figure 4.18: Alcian blue stained facet cartilage and IVD sagittal sections from T11/T12. A: AF, B: NP, C: CEP, D: Facet cartilage. IVD: Intervertebral disc, AF: Annulus fibrosus, NP: Nucleus pulposus, CEP: Cartilage end plate.

The sections of the lumbar AF showed similar alcian blue staining patterns to that of the cervical and thoracic sections. The intensity of the stain increased from the outer to inner AF and greater staining was observed between the lamellae layers rather than within them. Similar trends were seen in all three replicates. The lumbar NP also showed similar patterns to that of the cervical and thoracic samples. The stain was less intense than that in the AF and was distributed randomly in patches. The cells of the NP had taken up the stain and were found to spread to the surrounding lacunae. Similar to the thoracic CEP, the distribution of the alcian blue stain in the lumbar CEP varied throughout the length of the AF/NP section with some patches of pink/purple staining. The colour of the stain abruptly changed from a deep blue colour to light pink at the subchondral bone. The lacunae of the cells appeared more intensely stained than the surrounding ECM. In general, the colour of the CEP was bluer in comparison to the IVD tissue surrounding it. The lumbar CEP samples showed similar features to that of the thoracic samples. The most intense staining was

observed in the superficial layer. This intensity decreased but was still strong in the middle and deep zones. In the calcified zone, the ECM stained pink/purple with only the cells and their lacunae staining a deep blue colour. The colour of the subchondral bone was light pink.

Similarly to the thoracic facet cartilage sections, the distribution of the stain within the middle and deep zones appeared patchy with some areas more intense than others. The lacunae in these zones were less intensely stained than those in the calcified zones. These observations were present in all three replicate samples. Examples of alcian blue stained sections of the AF, NP, CEP and facet cartilage are shown in Figure 4.19.

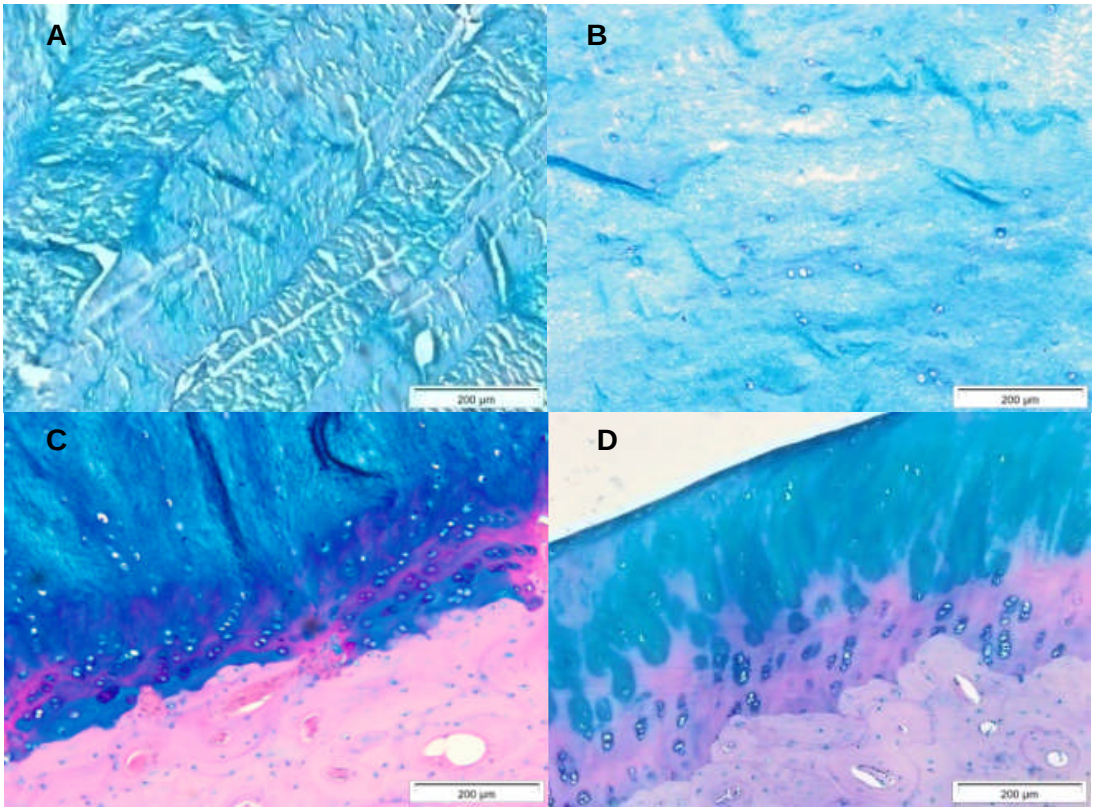


Figure 4.19: Alcian blue stained facet cartilage and IVD sagittal sections from L1/L2. A: AF, B: NP, C: CEP, D: Facet cartilage. IVD: Intervertebral disc, AF: Annulus fibrosus, NP: Nucleus pulposus, CEP: Cartilage end plate.

4.4.5. Characterisation of the IVD and Facet Cartilage using Sirius Red Stained Histological Sections of Ovine FSU tissue

Sirius red staining was viewed under polarised light and was used to stain FSU tissue to determine the distribution of collagen. The cervical AF stained

positively for Sirius red throughout all the sections of all three replicates. The colour of the stain within the AF was red and orange indicating the presence of large mature collagen fibres. The staining intensity between different lamellae layers appeared to alternate throughout the length of the AF. The most intense staining appeared to be within the lamellae layers rather than between them. These collagen staining patterns appeared constant throughout the length of the AF in the section and did not vary. No staining was observed in the cervical NPs. The staining within the cervical CEP appeared random but consistent throughout the AF/NP sections in all three replicates. The colour of the staining in the CEP was largely red/orange indicating the presence of large mature collagen fibres. The staining became greener in colour towards the surface of the CEP. Gaps in the staining were seen where the cells were situated.

In the cervical facet cartilage, the collagen distribution appeared organised. The collagen was confined to the superficial, deep and calcified zones. The staining within these regions was patchy with some parts showing more intensity than others. The colour of the staining was largely red/orange in most parts but green in the upper deep zone. The staining intensity was greatest in the calcified zone. The staining was visible within the lacunae of cells. There was no staining in the middle zones. Examples of Sirius red stained sections of the cervical AF, NP, CEP and facet cartilage are shown in Figure 4.20.

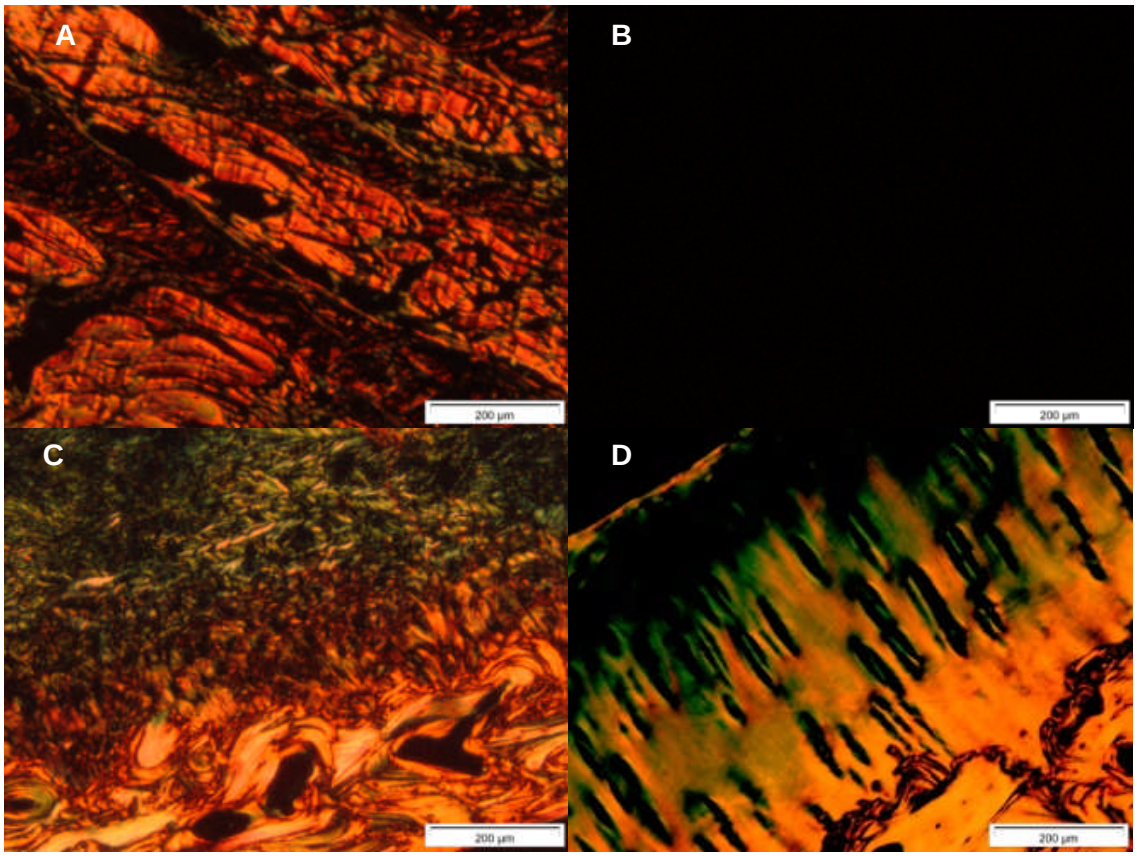


Figure 4.20: Sirius Red stained facet cartilage and IVD sagittal sections from C6/C7. A: AF, B: NP, C: CEP, D: Facet cartilage. IVD: Intervertebral disc, AF: Annulus fibrosus, NP: Nucleus pulposus, CEP: Cartilage end plate.

The staining within the thoracic AF showed similar characteristics to that of the cervical AF. The intensity of the stain remained constant throughout the length of the AF. The lamellae layers themselves were highly stained rather than the tissue in between them as is seen in the cervical AF. The colour of stain was red and orange. Small traces of stain were observed in the thoracic NP and this was white/green in colour indicating the presence of thin, perhaps newly formed collagen fibres. Very little staining was observed in the thoracic CEP in comparison to the cervical CEP. As with the cervical CEP the staining within the tissue was random and patchy with some areas showing more intensity than others. The intensity of the staining was much higher in the underlying subchondral bone. The colour of the staining in the CEP was largely red and orange.

The thoracic facet cartilage showed similar patterns to the cervical facet cartilage with the superficial, deep and calcified zones staining positively for

collagen. The staining within these zones varied between samples and was patchy. The colour of the staining was red and orange. Very little staining was observed in the middle zone. In some replicates, the superficial zone was less intensely stained in comparison to that in the cervical facet cartilage. Examples of Sirius red stained sections of the AF, NP, CEP and facet cartilage are shown in Figure 4.21.

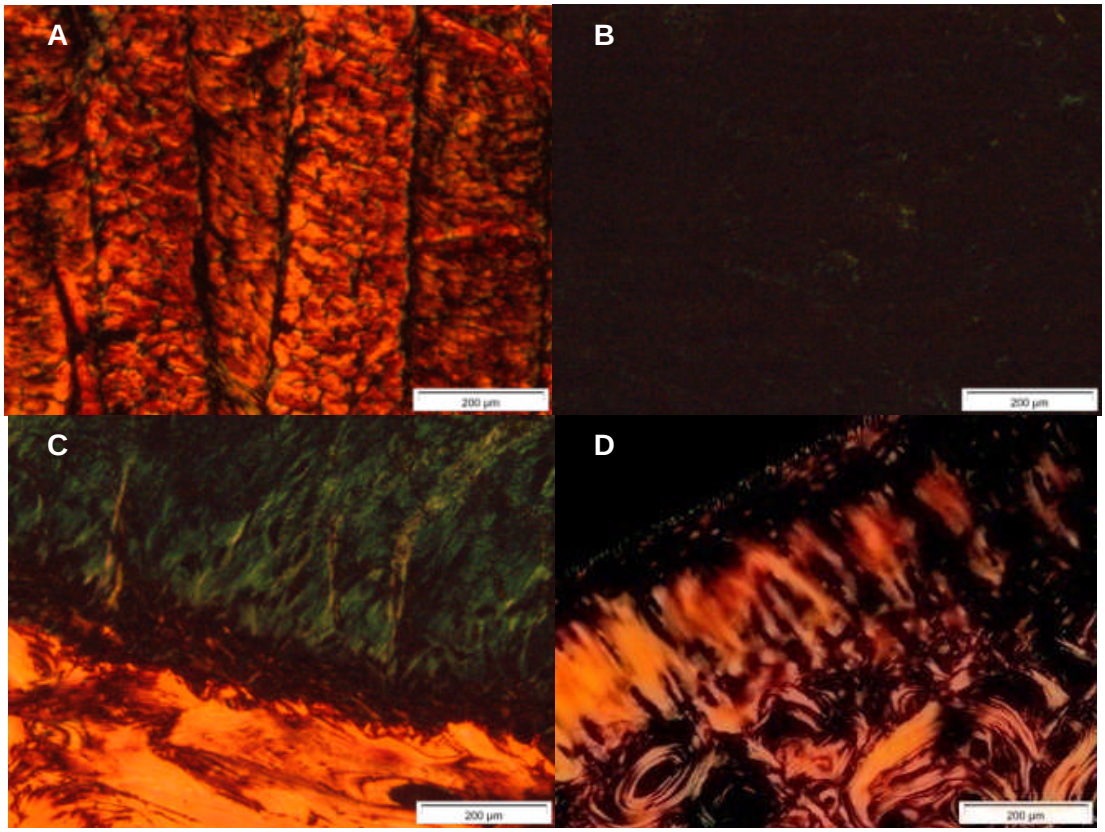


Figure 4.21: Sirius Red stained facet cartilage and IVD sagittal sections from T11/T12. A: AF, B: NP, C: CEP, D: Facet cartilage. IVD: Intervertebral disc, AF: Annulus fibrosus, NP: Nucleus pulposus, CEP: Cartilage end plate.

The staining of Sirius red within the lumbar AF showed similar staining patterns to that in both the cervical and thoracic AF. The level of staining throughout the structure from the outer to inner AF remained constant. The stain was confined to within the densely packed lamellae layers and not in between them. The colour of the staining was red/orange. No staining was observed in the NP samples. The staining in the lumbar CEP was similar to that observed in the cervical and thoracic CEPs. Along the depth and length of the AF/NP it was constant. The collagen fibres appeared to be randomly orientated in all three replicates. The intensity of the stain greatly increased at the subchondral bone.

The colour of the staining was red/orange but green above its surface, similar to the thoracic sections. The staining patterns in the facet cartilage were similar to those observed in the cervical and thoracic samples. The most intensely stained zones were the superficial, deep and calcified zones. As with the cervical and thoracic samples, the staining in these regions was distributed randomly. Some staining in the middle zones was observed in some of the replicates. The colour of the staining in the lumbar facet cartilage was similar to that in the thoracic samples with large amounts of red/orange stain with no green staining as seen in the cervical samples. Examples of Sirius red stained sections of the lumbar AF, NP, CEP and facet cartilage are shown in Figure 4.22.

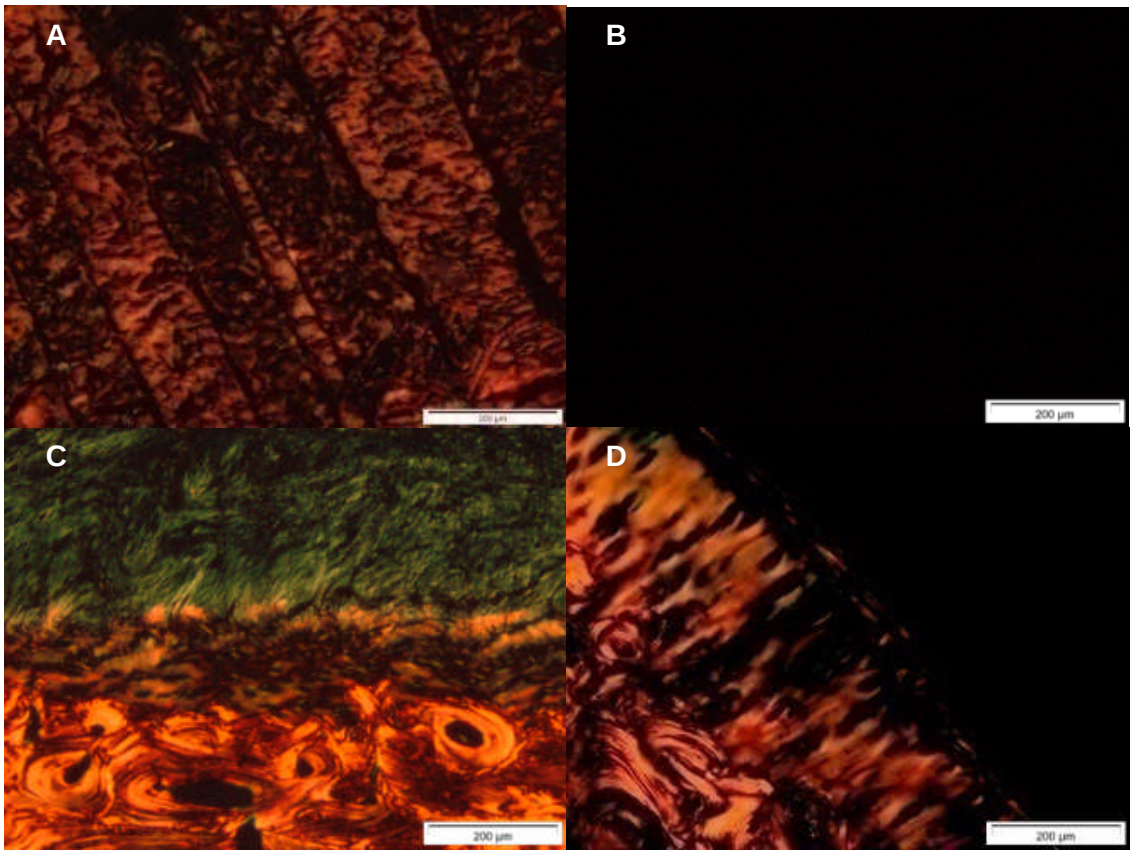


Figure 4.22: Sirius red staining of facet cartilage and IVD sagittal sections from L1/L2. The AF, NP and CEP in cervical, thoracic and lumbar regions were stained. **A**: C6/C7, **B**: T11/T12, **C**: L1/L2. IVD: Intervertebral disc, AF: annulus fibrosus, NP: nucleus pulposus, CEP: cartilage end plate.

4.4.6. Characterisation of the IVD and Facet Cartilage using Miller`s Elastin Stained Histological Sections of Ovine FSU tissue

Miller's elastin staining was used to stain FSU tissue sections to determine the distribution of elastin. The cervical AF appeared to stain positively for elastin within and between the lamellae layers. Elastin fibres were observed passing in between the red lamellae layers of the AF and were thin and blue in colour. This was found along the whole length of the AF and in all three replicates. In the cervical NP, blue staining was found to be present within the cells and the surrounding lacunae. The ECM was very faintly stained red. Small traces of blue stain were found randomly distributed in the ECM. The sections of the cervical CEP showed positive staining around the lacunae of the cells with the presence of blue staining. The ECM was largely stained red. Some positive blue/black staining was also observed randomly throughout the ECM. This was found along the length of the CEP in all three replicate samples. The staining within the ECM of the CEP was random. The facet cartilage was largely stained red. Some positive blue staining was observed around the lacunae of cells. Examples of Miller's elastin stained sections of the cervical AF, NP, CEP and facet cartilage are shown in Figure 4.23.

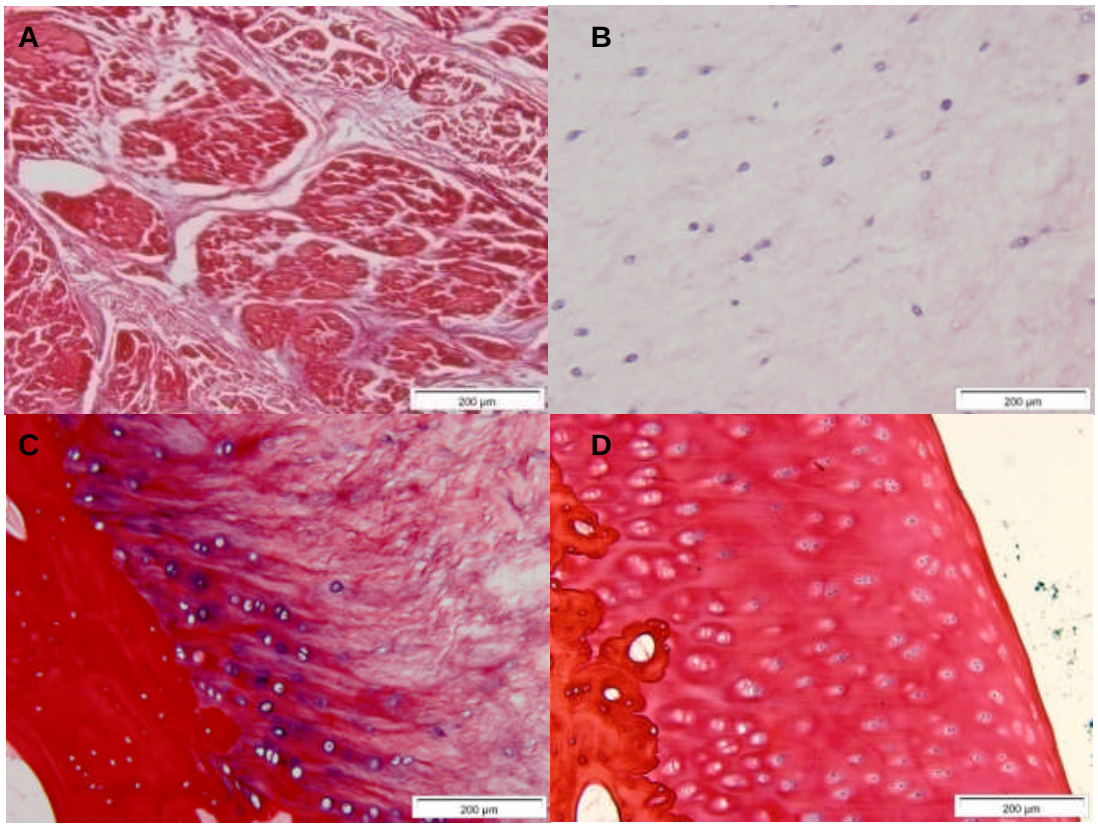


Figure 4.23: Miller's elastin stained facet cartilage and IVD sagittal sections from C6/C7. The AF, NP and CEP in cervical, thoracic and lumbar regions were stained. **A**: C6/C7, **B**: T11/T12, **C**: L1/L2. IVD: Intervertebral disc, AF: annulus fibrosus, NP: nucleus pulposus, CEP: cartilage end plate.

Miller's elastin staining within the thoracic tissues was the same as that observed in the cervical AF. Red/blue staining was observed in between the red lamellae layers and in fibrous tissues crossing over between the layers. The red/blue fibres in between the lamellae were thin in appearance. This was consistent along the entire length of the AF section in all three replicates. Staining in the thoracic NP was also similar to that observed in the cervical NP. Most of the blue staining was found to be located around the lacunae of the cells. Some traces of positive blue staining was also found randomly distributed in the ECM. Much of the faint staining within the ECM however was red. This was observed in all three replicate samples. Staining of the thoracic CEP varied between the three replicate samples. In two of the replicates, the staining was found to be random and located largely around the lacunae of the cells with small amounts distributed in the ECM. In one of the replicates, a band of positive blue staining was observed in the upper half of the CEP structure and a

band of red staining was found in the lower half (Figure 4.24C). The staining here was found to be largely red but with some trace of blue staining throughout the ECM and around the lacunae of the cells. Some small amounts of positive blue staining were observed in the lacunae of facet cartilage in all replicate samples as was observed in the cervical samples however the staining here was largely red. Examples of Miller's elastin stained sections of the thoracic AF, NP, CEP and facet cartilage are shown in Figure 4.24.

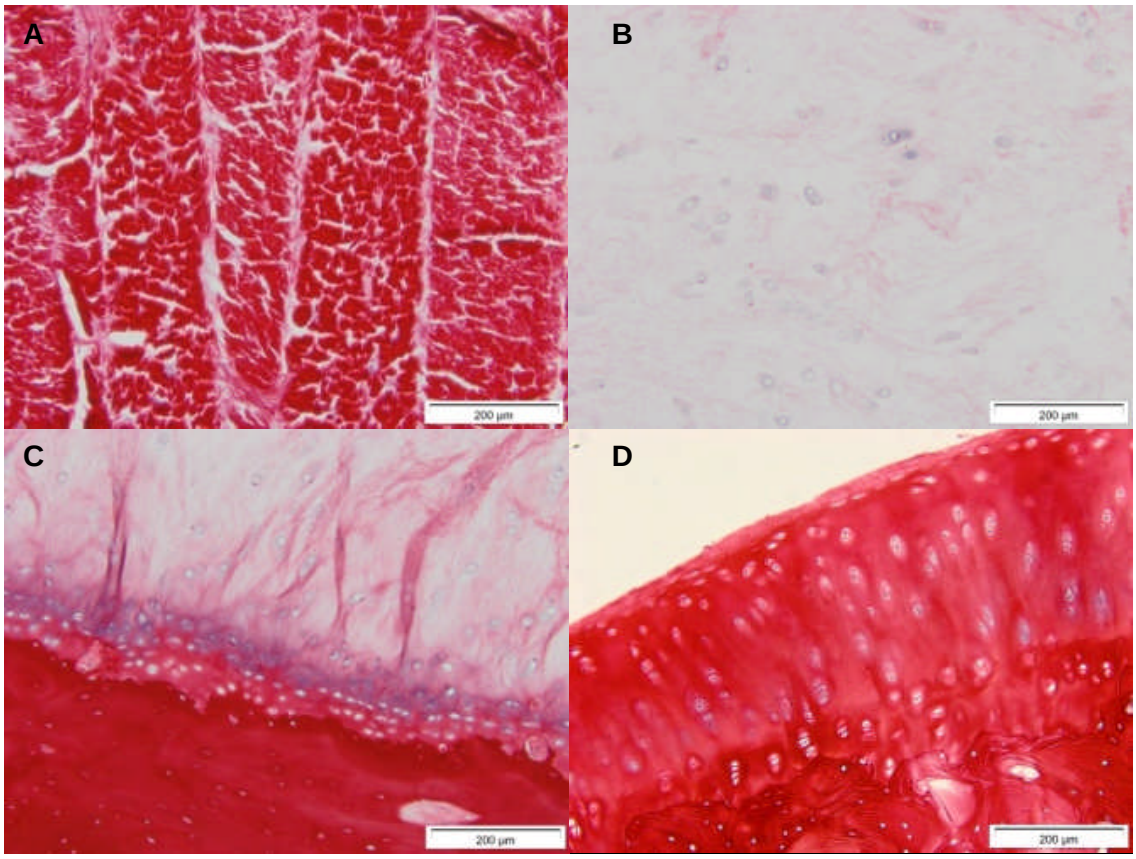


Figure 4.24: Miller's elastin stained facet cartilage and IVD sagittal sections from T11/T12. The AF, NP and CEP in cervical, thoracic and lumbar regions were stained. **A**: C6/C7, **B**: T11/T12, **C**: L1/L2. IVD: Intervertebral disc, AF: annulus fibrosus, NP: nucleus pulposus, CEP: cartilage end plate.

Miller's elastin staining within the lumbar AF showed the same characteristics as that of the cervical and thoracic samples. Positive blue staining was observed between the layers of the lamellae, which stained red, and in fibres crossing between the layers. The blue fibres were thin in appearance. This was observed along the entire length of the AF and in all three replicates. The NP cells in the lumbar sections did not contain as much blue stain as those in the cervical and thoracic NP sections. This was an observation for all three replicate

samples. Some traces of blue staining were observed in the ECM of the lumbar NP samples however it was mostly red in colour. The lumbar CEP showed the same characteristics as those observed in the cervical and thoracic samples. The stain, which was largely red in colour, was found randomly distributed in the ECM and around the lacunae of cells. Blue staining was also present around some lacunae. Similarly to the cervical and thoracic facet cartilage samples, minimal blue staining was observed around the lacunae of cells in the lumbar facet cartilage which was largely stained red. A band of dark red staining was observed in the deep zone in one of the replicates (Figure 4.25D). Examples of Miller's Elastin stained sections of the lumbar AF, NP, CEP and facet cartilage are shown in Figure 4.25.

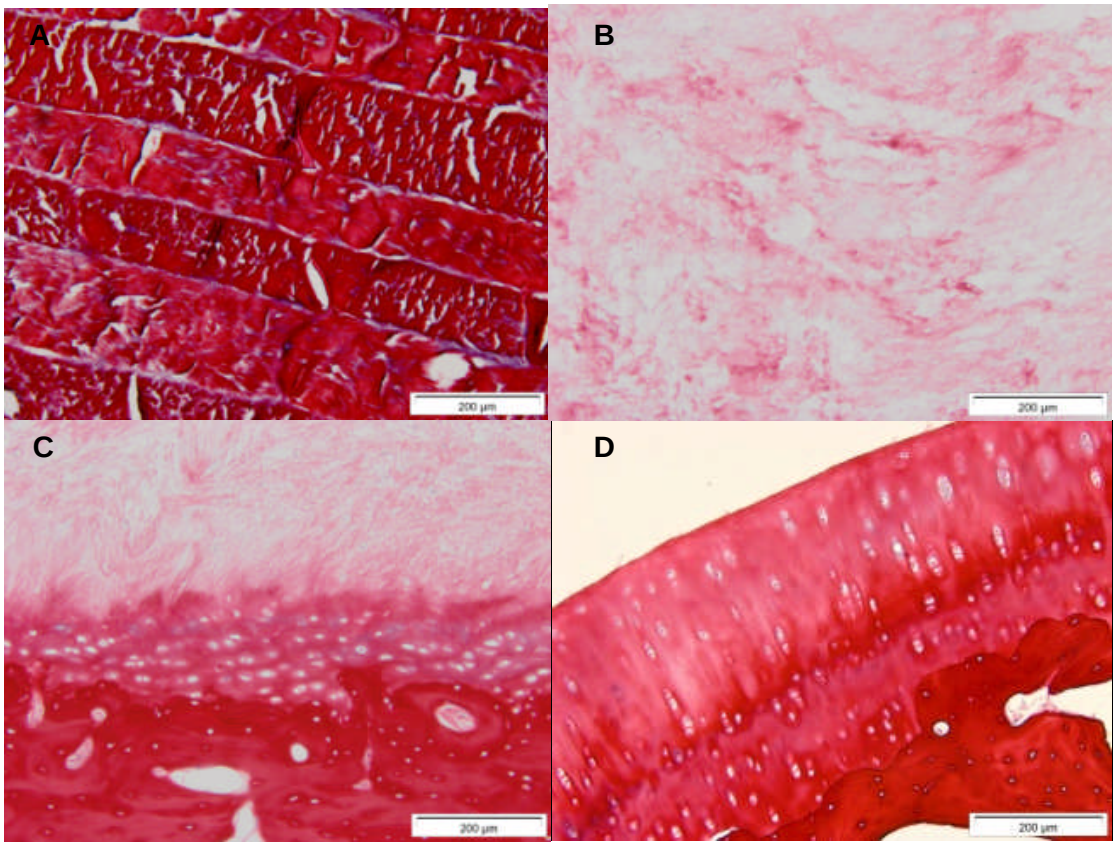


Figure 4.25: Miller's elastin stained facet cartilage and IVD sagittal sections from L1/L2. The AF, NP and CEP in cervical, thoracic and lumbar regions were stained. **A**: C6/C7, **B**: T11/T12, **C**: L1/L2. IVD: Intervertebral disc, AF: annulus fibrosus, NP: nucleus pulposus, CEP: cartilage end plate.

4.4.7. Localisation of Specific Markers within the Ovine IVD and Facet Cartilage

A selection of antibodies used to phenotype the FSU cells were also used to identify the location of specific markers in three year old Texel ovine FSU tissue from replicates five, six and seven from the natural history study (Chapter 3).

4.4.7.1. Collagen Type I

Facet cartilage from all replicates and all regions including cervical, thoracic and lumbar facet cartilage did not positively stain in any of the four zones of cartilage in the ECM, lacunae or cells with antibodies to collagen type I. The underlying subchondral layer of cartilage was stained positively in all samples. An example of collagen type I staining within a section of facet cartilage is shown in Figure 4.26.

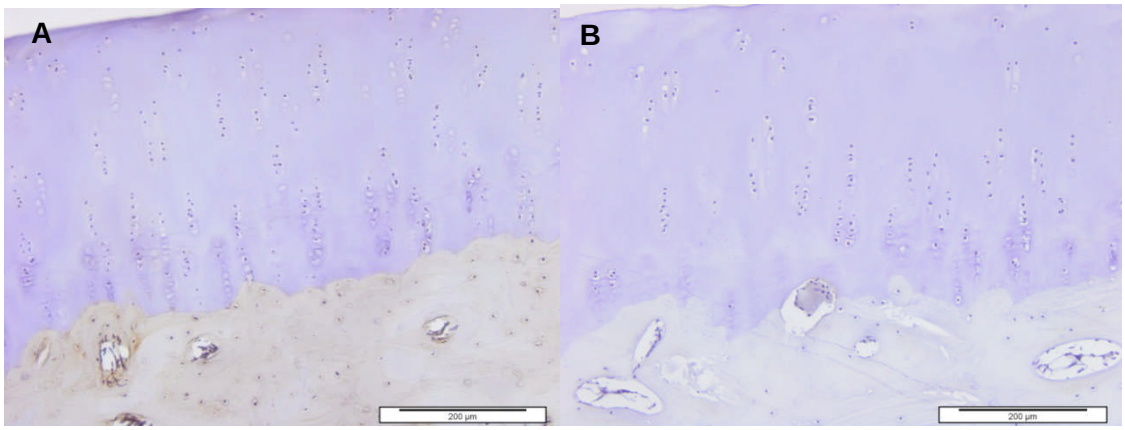


Figure 4.26: Ovine cervical (5.C6/C7) facet cartilage stained with mouse anti-sheep collagen type I monoclonal antibody (A) and mouse IgG1 isotype control (B). 40x magnification.

Collagen type I staining was visible throughout most of the AF in all replicate samples in cervical, thoracic and lumbar regions. It was particularly evident within the outer AF where the intensity of the stain was at its highest. Within the AF, the staining was distributed randomly. Some lamellae were more intensely stained than others. The edges of each lamella were, in general, more intensely stained than within the layers. Staining was seen around some of the cells within the AF structure. Similarly to the facet cartilage, no staining was visible in the CEP only in the underlying subchondral bone. This was observed in all replicate samples from cervical, thoracic and lumbar regions. In the majority of the samples, no staining was observed in the NP. However, for three samples

in the cervical, thoracic and lumbar region, some staining was visible around the lacunae of the NP cells. The intensity of the stain in these samples varied. Examples of IVD sections stained with antibody to collagen type I are shown in Figure 4.27.

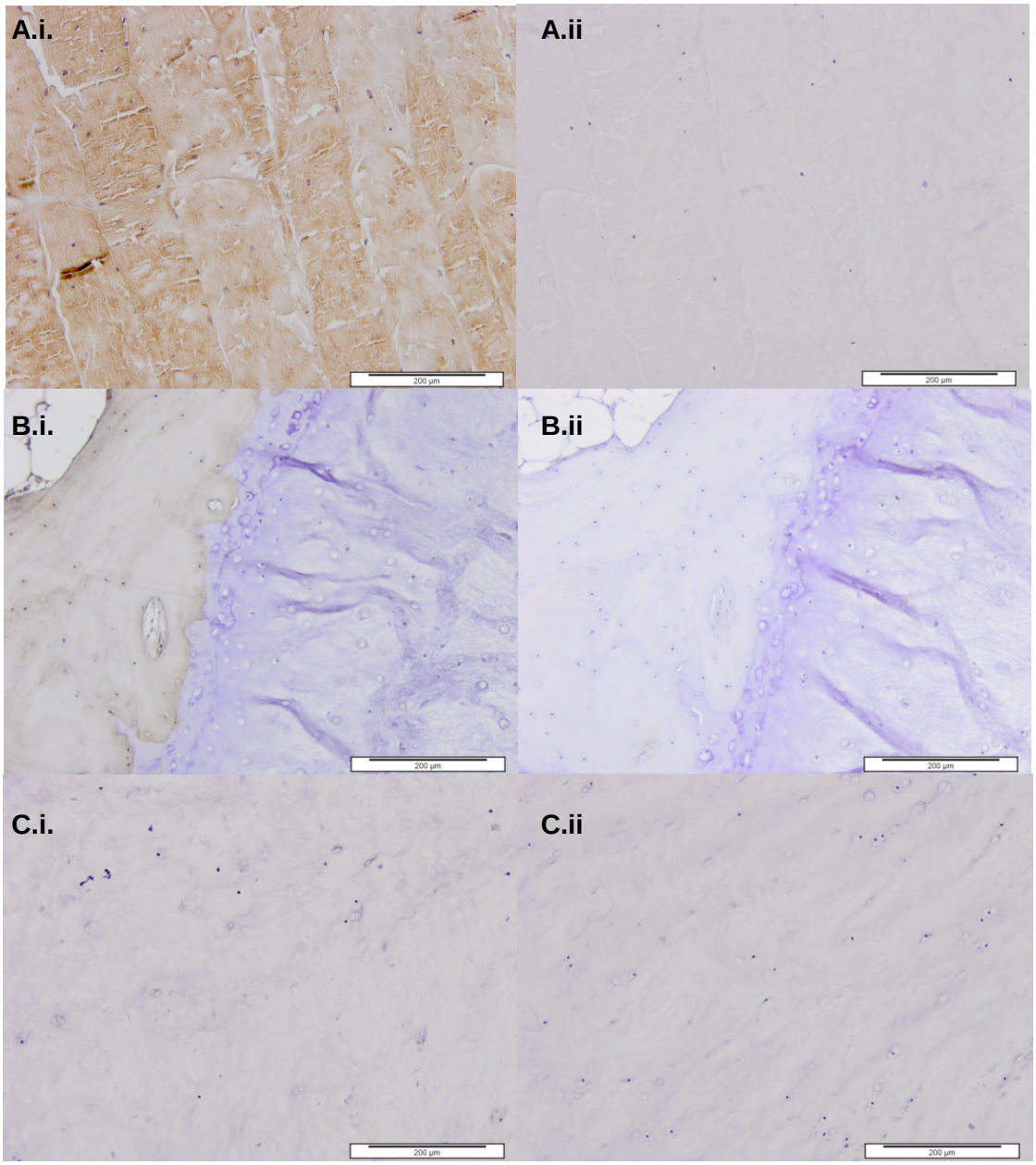


Figure 4.27: Ovine lumbar (6.L1/L2) AF (A), thoracic (6.T11/T12) CEP (B) and lumbar (7.L1/L2) NP (C) sections stained with mouse anti-sheep collagen type I monoclonal antibody (i) and mouse IgG1 isotype control (ii). 40x magnification. AF: Annulus fibrosus, CEP: cartilage end plate, NP: Nucleus pulposus.

4.4.7.2. Collagen Type II

Facet cartilage in all replicates and regions stained positively for collagen type II. In general, all zones of cartilage and underlying subchondral bone were stained. The superficial, middle and calcified zones were more intensely stained than the deep zone. This was observed for all replicate samples from all three regions. The stain within these zones was randomly distributed. The intensity of the stain did not increase around the chondrocytes or lacunae. An example of staining within facet cartilage is shown in Figure 4.28.

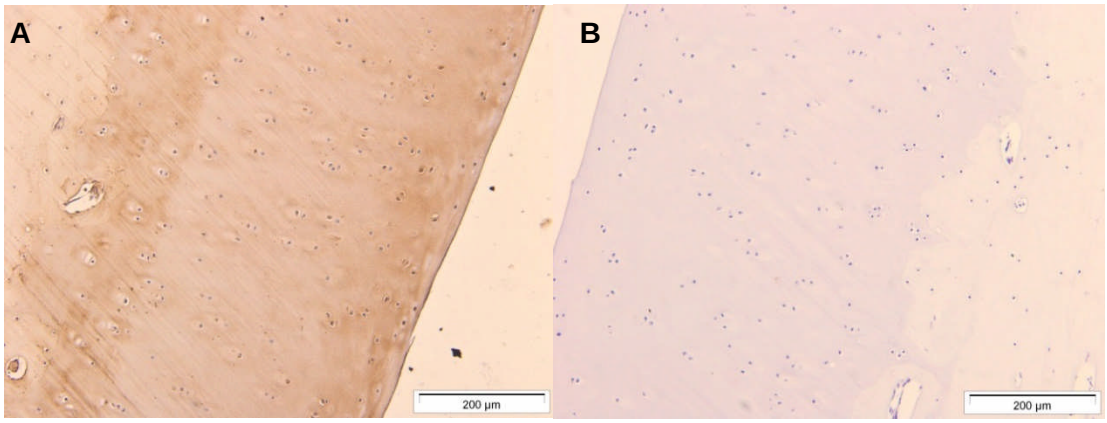


Figure 4.28: Ovine cervical (6.C6/C7) facet cartilage sections stained with mouse anti-sheep collagen type II monoclonal antibody (A) and mouse IgG1 isotype control (B). 40x magnification.

The tissues of the ovine IVD stained positively for collagen type II. The majority of the collagen type II stain within the AF was found in the inner AF, however, the whole structure stained positively. Similarly to the facet cartilage, the stain did not intensify around the cells. Within the inner AF, the stain intensified around the edges of the lamellae layers. This was observed in all replicate samples from all three regions. In the CEP, the stain was distributed randomly in all replicates and regions. The stain was dispersed throughout the ECM. In some samples, there was some accumulation of the stain around the lacunae of the cells. Some samples stained more positively than others. Collagen type II staining continued through to the subchondral bone as was observed in facet cartilage. Collagen type II staining was dispersed randomly throughout all NP samples. There was no accumulation of the stain around the lacunae of the cells. Some samples stained more positively than others. Examples of IVD sections stained with antibody to collagen type II are shown in Figure 4.29.

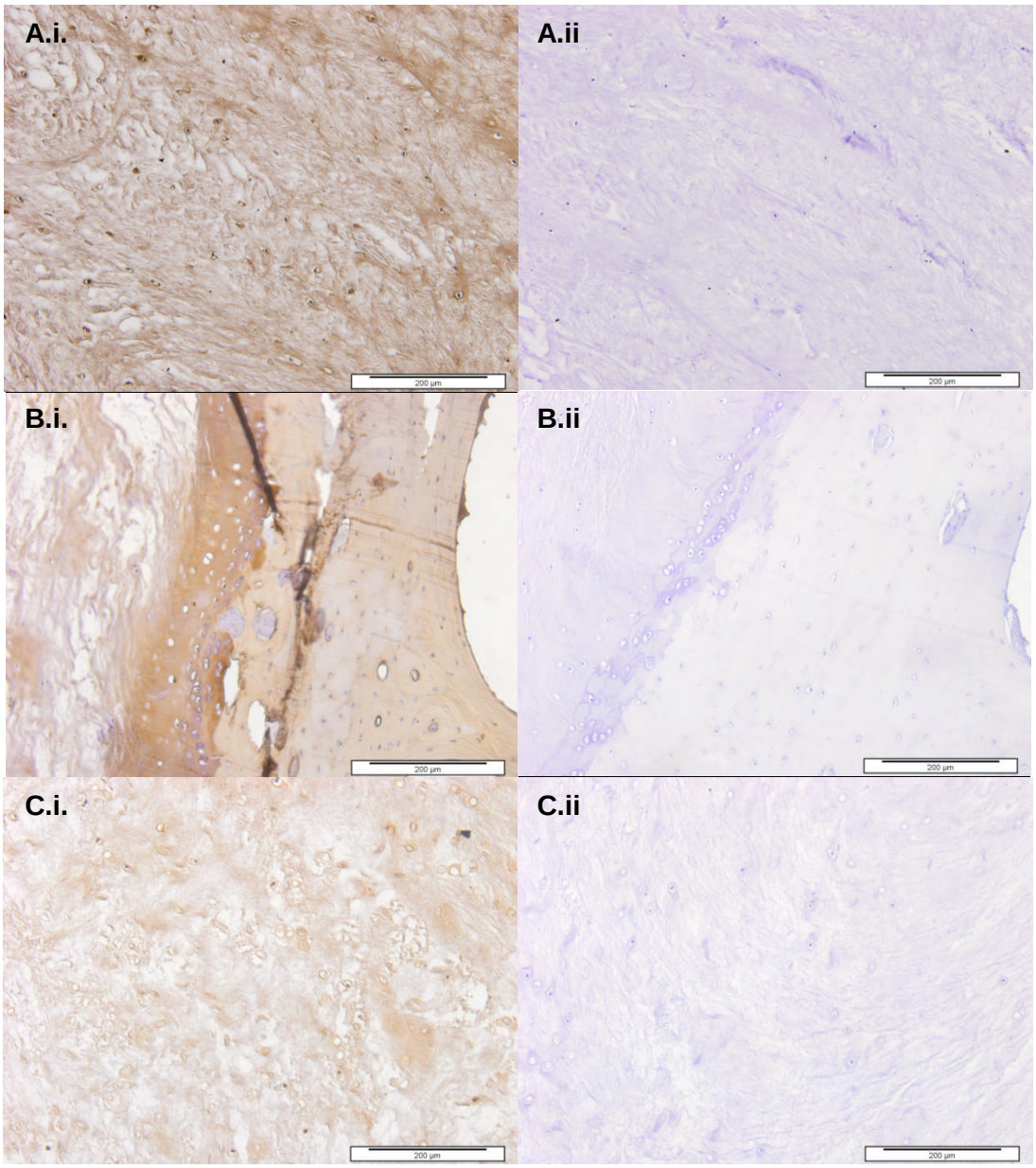


Figure 4.29: Ovine cervical (6.C6/C7) AF (A), lumbar (7.L1/L2) CEP (B) and thoracic (5.T11/T12) NP (C) sections stained with mouse anti-sheep collagen type II monoclonal antibody (i) and mouse IgG1 isotype control (ii). 40x magnification. AF: Annulus fibrosus, CEP: cartilage end plate, NP: Nucleus pulposus.

4.4.7.3. Collagen Type III

Facet cartilage in all replicate samples from all three regions stained positively for collagen type III. The stain accumulated in lacunae and the surrounding space around them in all four zones of the cartilage including the subchondral bone. This was observed in all replicate samples from all cervical, thoracic and lumbar regions. An example of collagen type III staining in facet cartilage is shown in Figure 4.30.

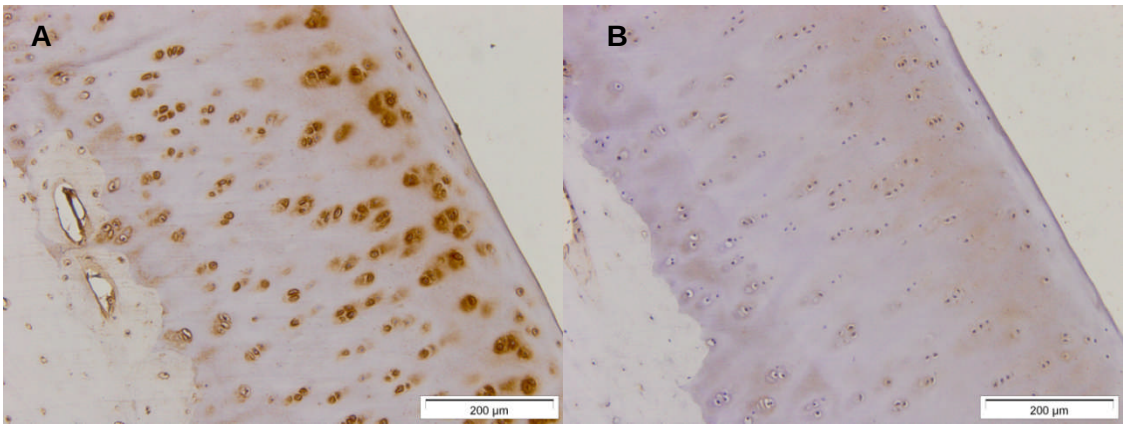


Figure 4.30: Ovine cervical (6.C6/C7) facet cartilage sections stained with rabbit anti-sheep collagen type III polyclonal antibody (A) and rabbit IgG isotype control (B). 40x magnification.

The tissues of the IVD stained positively for collagen type III in all replicate samples from all three regions. The whole AF was positively stained. The stain appeared to accumulate between the lamellae layers and around the cells of the AF. This was observed in all samples and no differences were found between the three regions. Staining within the CEP was mostly found around the cells and their lacunae. Some very faint staining was also observed in the ECM. The intensity of the stain varied between the samples but the same observations were made. Similar observations were made within the NP where most of the positive staining was confined to the cells and their surrounding lacunae. Very faint staining was also observed randomly throughout some parts of the ECM. Again, the level of intensity varied between the sample but no differences were observed between the cervical, thoracic and lumbar regions. Examples of IVD sections stained with antibody to collagen type III are shown in Figure 4.31.

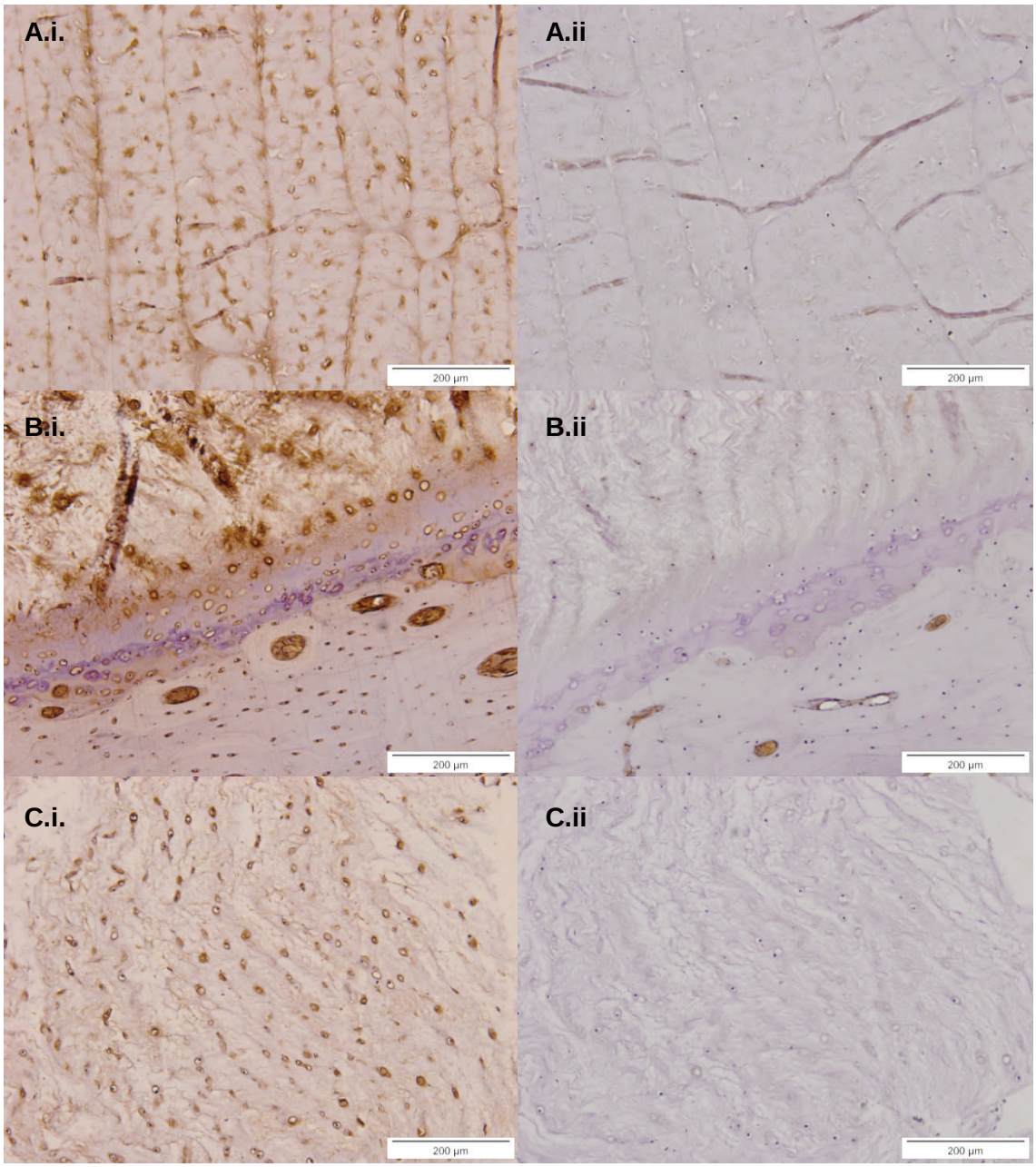


Figure 4.31: Ovine lumbar (6.L1/L2) AF (A), thoracic (7.T11/T12) CEP (B) and lumbar (6.L1/L2) NP (C) sections stained with rabbit anti-sheep collagen type III polyclonal antibody (i) and rabbit IgG isotype control (ii). 40x magnification. AF: Annulus fibrosus, CEP: cartilage end plate, NP: Nucleus pulposus.

4.4.7.4. Collagen Type VI

Facet cartilage in all replicates samples from all three regions stained positively for collagen type VI. The staining patterns within facet cartilage were similar to that observed for collagen type III. The stain was present around the lacunae of each cell. In contrast to collagen type III, the stain was not dispersed around the lacunae and the surrounding space but was located close to the lacunae and

cells. In some of the replicate samples, the stain was found randomly dispersed amongst the ECM in all four zones. The middle zone appeared to be more intensely stained in comparison to the other zones. An example of collagen type VI staining in facet cartilage is shown in Figure 4.32.

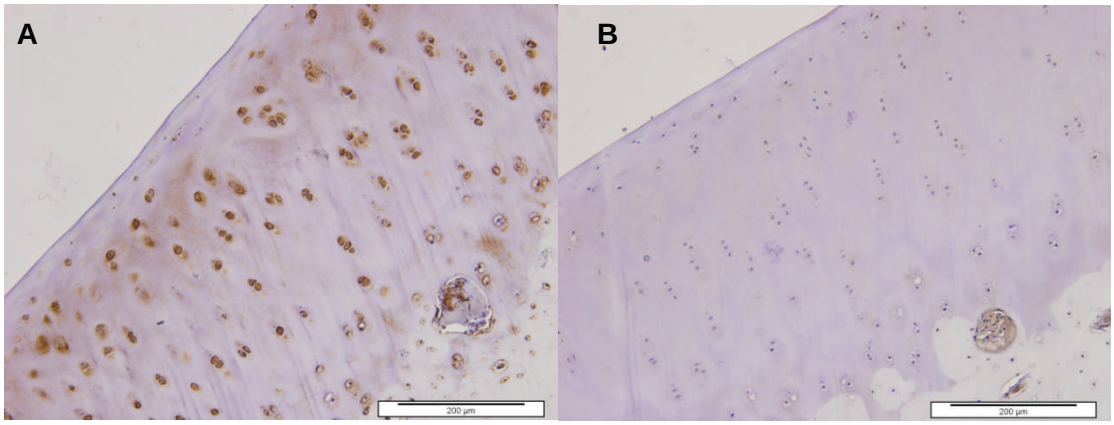


Figure 4.32: Ovine cervical (6.C6/C7) facet cartilage sections stained with rabbit anti-sheep collagen type VI polyclonal antibody (A) and rabbit IgG isotype control (B). 40x magnification.

AF tissue in all replicate samples from all regions stained positively for collagen VI. Most of staining was present around lacunae and cells and along the fibres in between the lamellae layers. Some staining was also found distributed randomly within the lamellae layers. There were no differences in staining between cervical, thoracic and lumbar samples. Within the CEP tissue samples, positive staining was found largely around the lacunae of the cells. This was confined to the lacunae and did not spread to the surrounding areas. In some samples small traces of staining was found randomly among the ECM. This was observed in samples from all three regions. The intensity of the staining within the NP varied between samples. As with the other FSU tissues, most of the staining was confined to the lacunae of the cells. However, in most samples there was staining present in the ECM. This was distributed randomly. Examples of IVD sections stained with antibody to collagen type VI are shown in Figure 4.33.

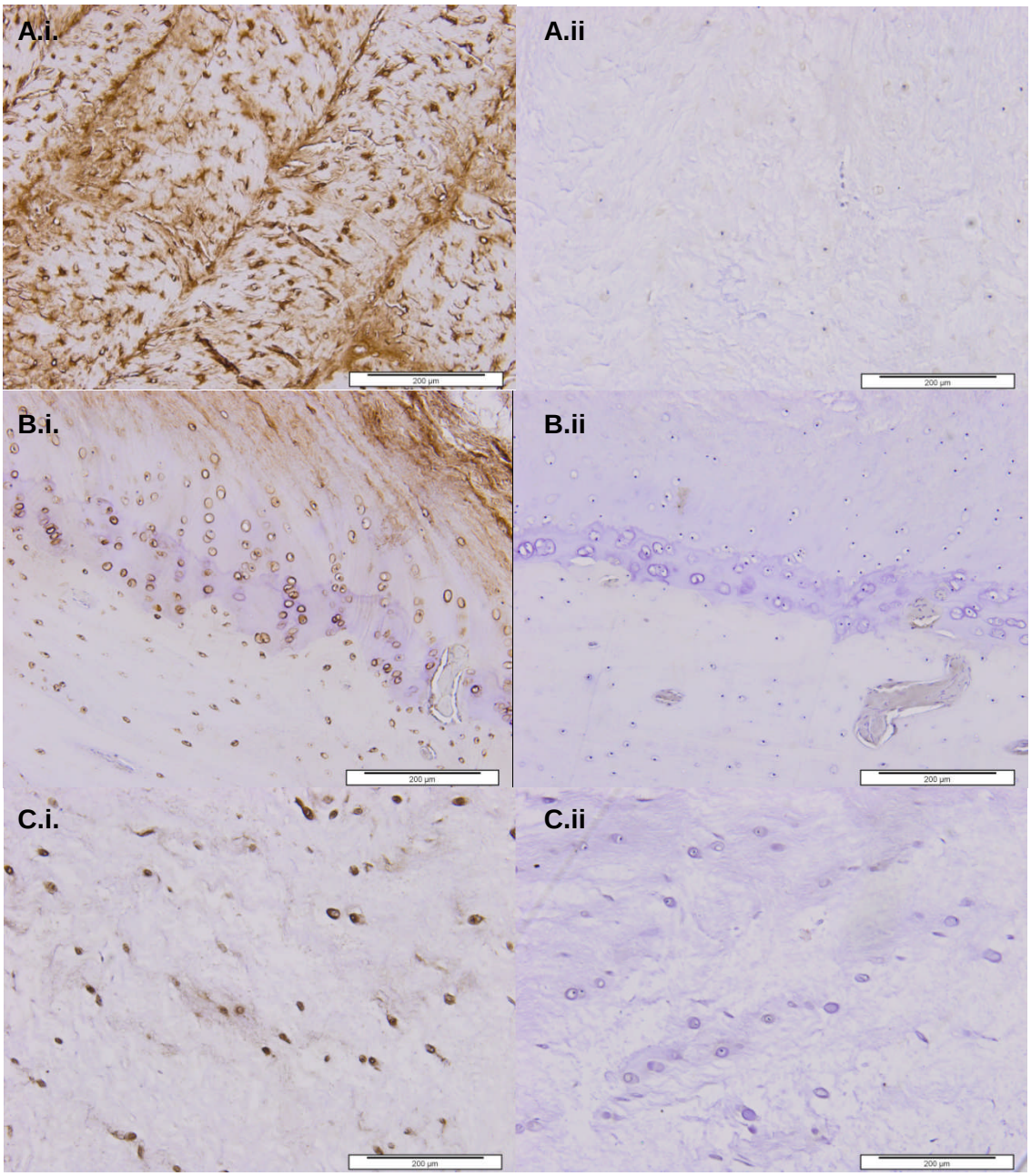


Figure 4.33: Ovine thoracic (5.T11/T12) AF (A), lumbar (7.L1/L2) CEP (B) and cervical (6.C6/C7) NP (C) sections stained with rabbit anti-sheep collagen type VI polyclonal antibody (i) and rabbit IgG isotype control (ii). 40x magnification. AF: Annulus fibrosus, CEP: cartilage end plate, NP: Nucleus pulposus.

4.4.7.5. Chondroitin Sulphate

All facet cartilage in all replicate samples from all three regions stained positively for chondroitin sulphate. The intensity of the stain varied between different replicate samples. In all samples staining was present in the middle and deep zones. The staining was distributed relatively evenly in the ECM and around the lacunae of the cells. Staining around the lacunae was slightly more

intense than that in the ECM. No key differences were highlighted between cervical, thoracic and lumbar samples. An example of chondroitin sulphate staining in facet cartilage is shown in Figure 4.34.

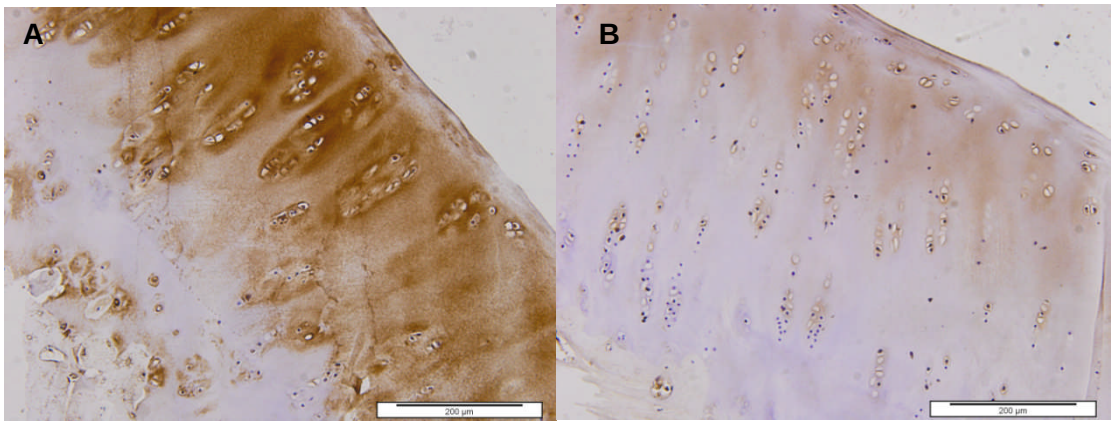


Figure 4.34: Ovine cervical (7.C6/C7) facet cartilage sections stained with rabbit anti-sheep chondroitin sulphate polyclonal antibody (A) and rabbit IgG isotype control (B). 40x magnification.

All IVD tissues from all replicate samples and regions stained positively for chondroitin sulphate. Staining in the AF was very intense but varied between samples. The staining was found distributed relatively evenly within the tissue between the lamellae layers and within them. No differences were observed between cervical, thoracic and lumbar samples. Staining for chondroitin sulphate in the CEP was random and varied between different samples. In most of the samples there was notably less stain within the ECM in comparison to the AF/NP tissue. Minimal staining was present in most samples and was distributed randomly within the ECM and around some lacunae. The NP tissue was intensely stained in all replicate samples from all regions. The stain was evenly distributed in the ECM and lacunae of cells. No differences were observed between cervical, thoracic and lumbar regions. Examples of IVD sections stained with antibody to chondroitin sulphate are shown in Figure 4.35.

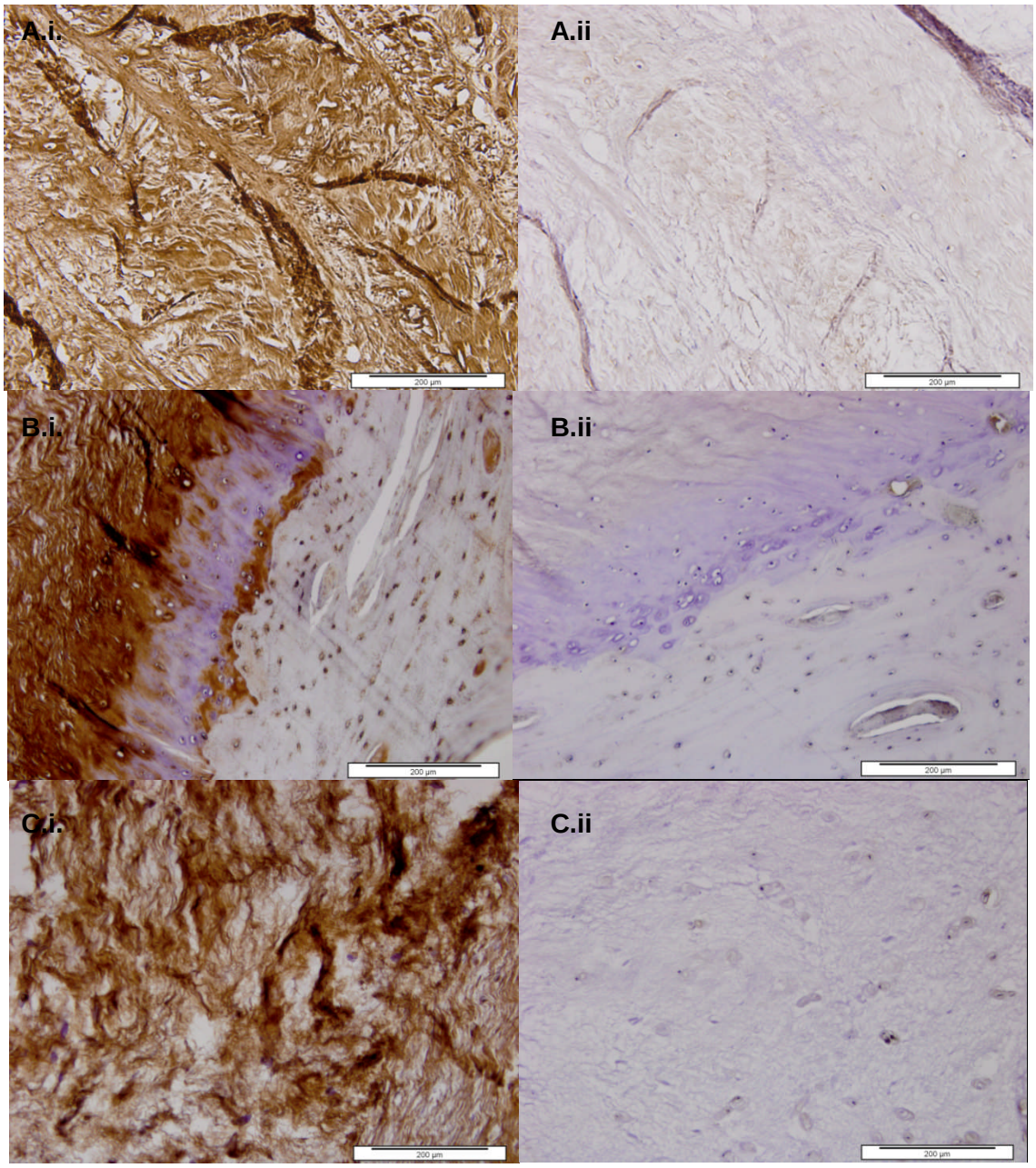


Figure 4.35: Ovine cervical (7.C6/C7) AF (A), cervical (5.C6/C7) CEP (B) and cervical (5.C6/C7) NP (C) sections stained with rabbit anti-sheep chondroitin sulphate polyclonal antibody (i) and rabbit IgG isotype control (ii). 40x magnification. AF: Annulus fibrosus, CEP: cartilage end plate, NP: Nucleus pulposus.

4.4.7.6. Fibronectin

Facet cartilage from all replicate samples and regions stained positively for fibronectin. The intensity of the staining varied from sample to sample. In general, the staining was found distributed randomly in the ECM and some lacunae in all four zones of the cartilage. The calcified zone was more intensively stained than the other three zones. There was no positive staining

past the calcified zone in the subchondral bone. An example of fibronectin staining within ovine facet cartilage is shown in Figure 4.36.

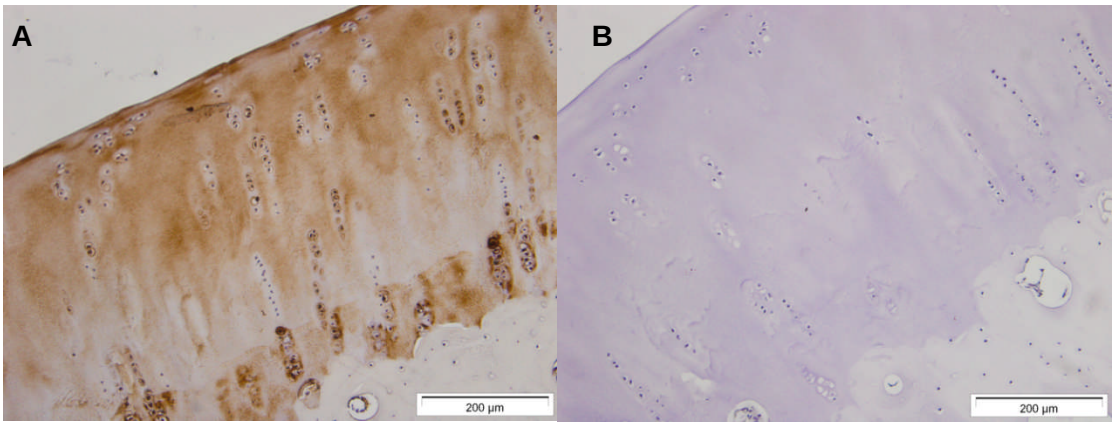


Figure 4.36: Ovine cervical (7.C6/C7) facet cartilage sections stained with mouse anti-sheep fibronectin monoclonal antibody (A) and rabbit IgG1 isotype control (B). 40x magnification.

All IVD tissue in replicate samples from all regions stained positively for fibronectin. The intensity of staining within the AF varied between samples. In general, the stain randomly distributed throughout the lamellae layers. Staining in between the layers was more intense than that within them. The lacunae around the cells were also intensely stained. No differences were observed between cervical, thoracic and lumbar sections. Staining in the CEP was mainly observed in the top layer and was randomly distributed within the ECM and lacunae. The lower layer of the CEP contained much less of the stain in comparison and in most samples only some lacunae were positively stained with some very small traces of stain within the ECM. No differences were observed between regions. The NP was lightly stained in all samples. The stain was distributed randomly in the ECM and in some instances around the lacunae. Examples of IVD sections stained with antibody to fibronection are shown in Figure 4.37.

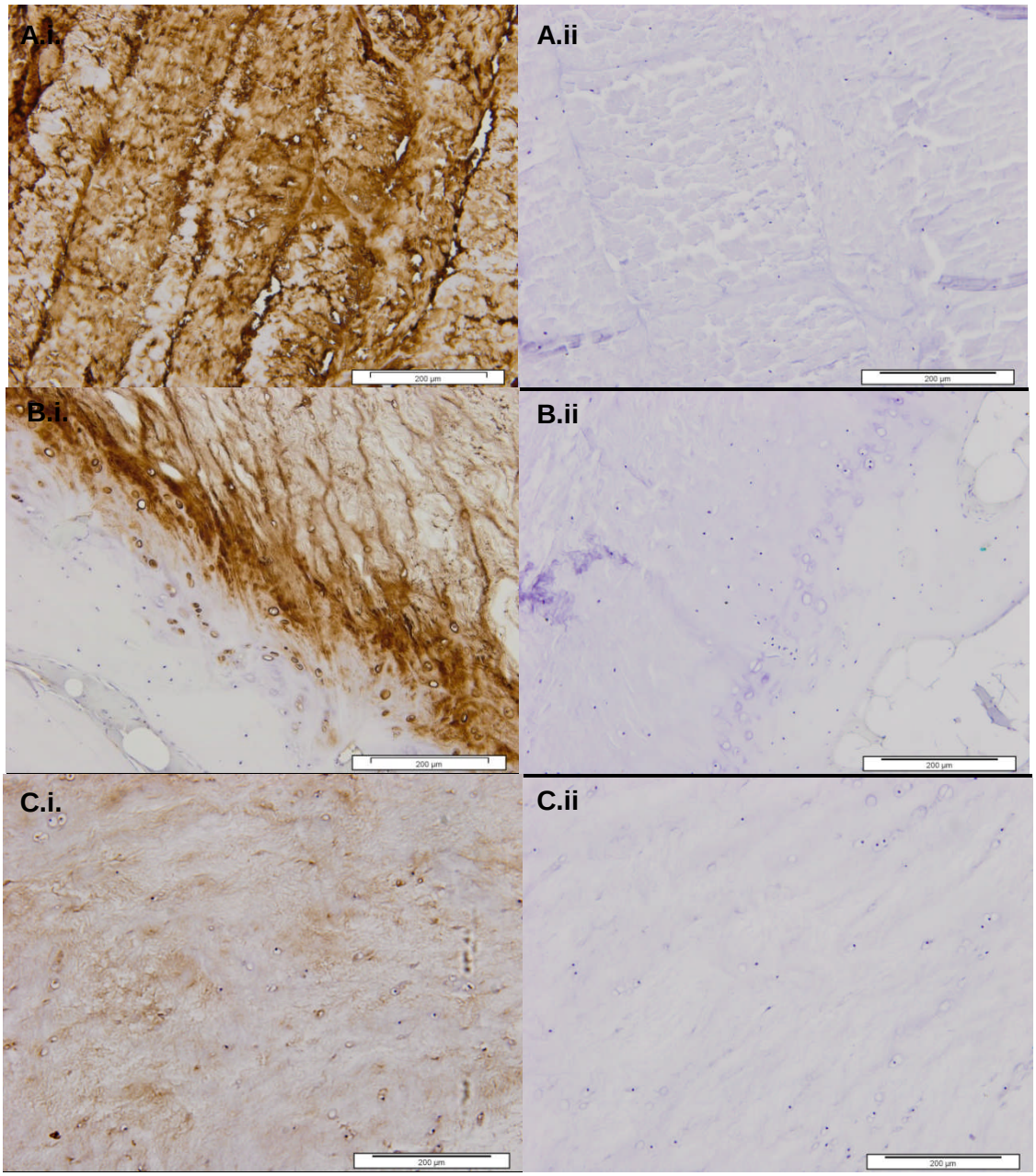


Figure 4.37: Ovine lumbar (5.L1/L2) AF (A), cervical (5.C6/C7) CEP (B) and lumbar (7.L1/L2) NP (C) sections stained with mouse anti-sheep fibronectin monoclonal antibody (i) and mouse IgG1 isotype control (ii). 40x magnification. AF: Annulus fibrosus, CEP: cartilage end plate, NP: Nucleus pulposus.

4.4.7.7. Osteocalcin

Facet cartilage in all sample replicates in three regions showed very little positive staining for osteocalcin. In all samples positive staining was found in the subchondral bone. In some samples, traces of stain were found randomly distributed in the ECM and lacunae of the calcified zone. An example of osteocalcin staining in ovine facet cartilage is shown in Figure 4.38.

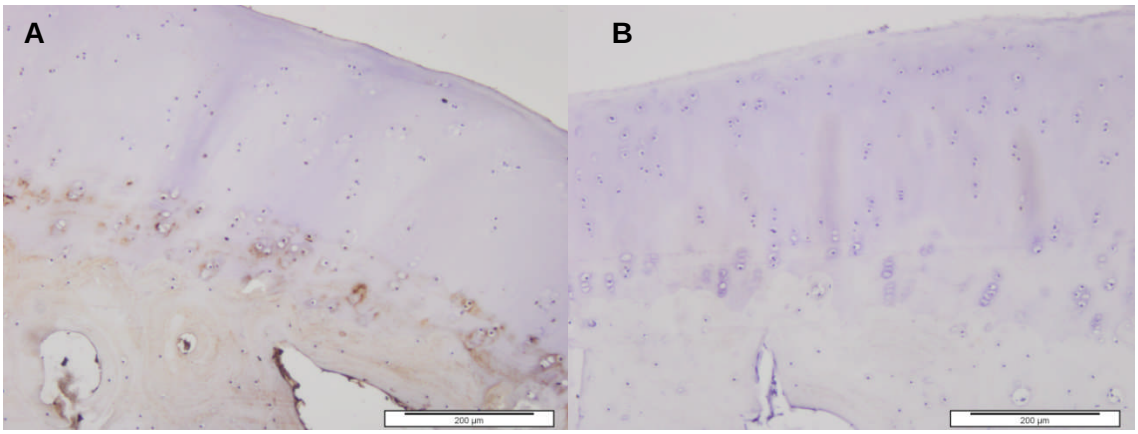


Figure 4.38: Ovine thoracic (5.T11/T12) facet cartilage sections stained with mouse anti-sheep osteocalcin monoclonal antibody (A) and mouse IgG2a isotype control (B). 40x magnification.

Staining for osteocalcin in the AF and NP tissue in all samples from three regions was negative. In the CEP, the underlying subchondral bone was positively stained and this was distributed evenly within the matrix and strongly around the cells. Examples of IVD sections stained with antibody to osteocalcin areshown in Figure 4.39.

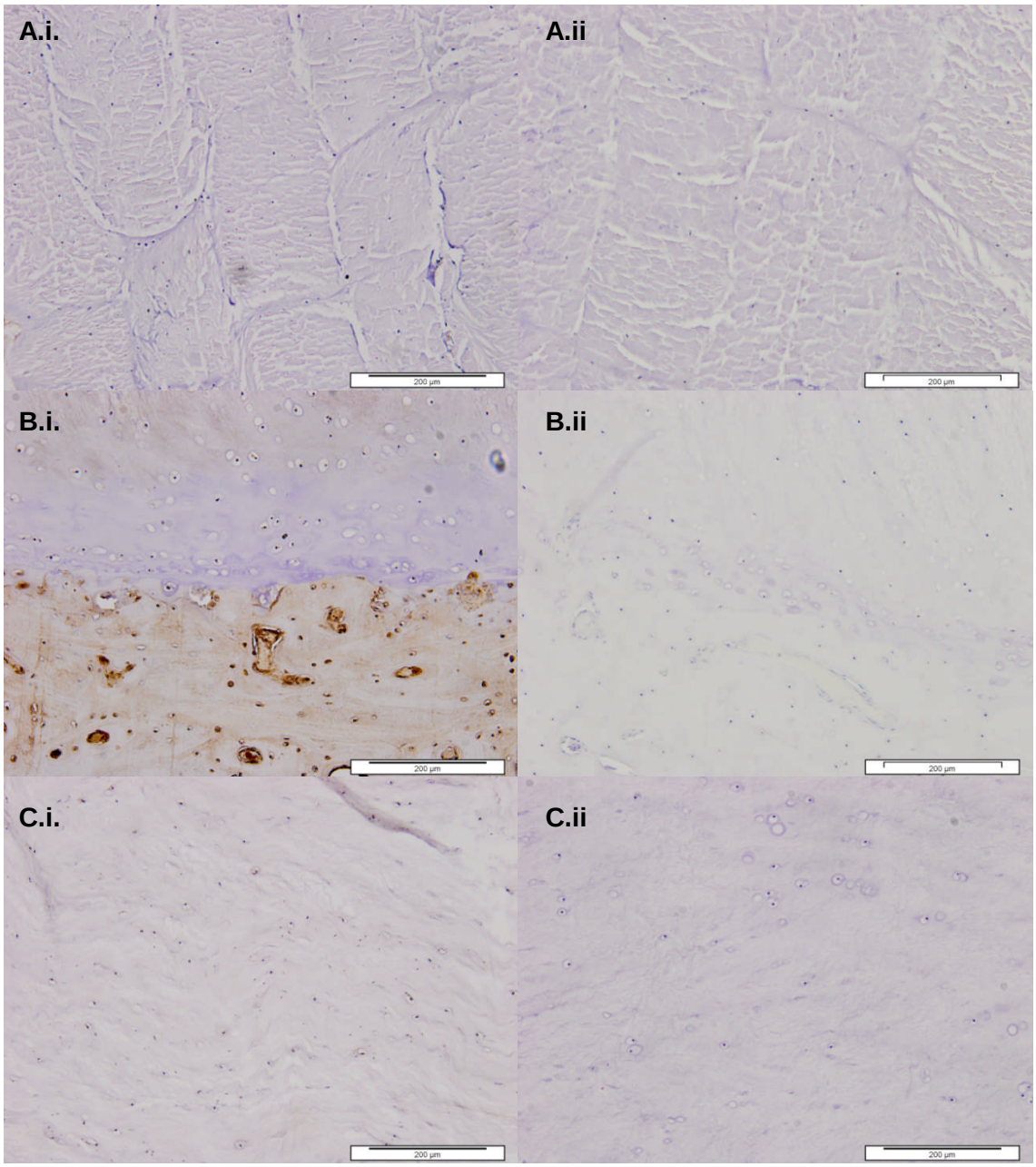


Figure 4.39: Ovine thoracic (5.T11/T12) AF (A), lumbar (5.L1/L2) CEP (B) and lumbar (7.L1/L2) NP (C) stained with mouse anti-sheep osteocalcin monoclonal antibody (i) and mouse IgG2a isotype control (ii). 40x magnification. AF: Annulus fibrosus, CEP: cartilage end plate, NP: Nucleus pulposus.

4.4.8. Deformation Characteristics of Facet Cartilage

Indentation tests were carried out on C6/C7 facets including both left and right inferior and superior facets from a three year old Texel sheep. The thickness of the cartilage on each facet was determined using a needle indenter (Figure 4.40).

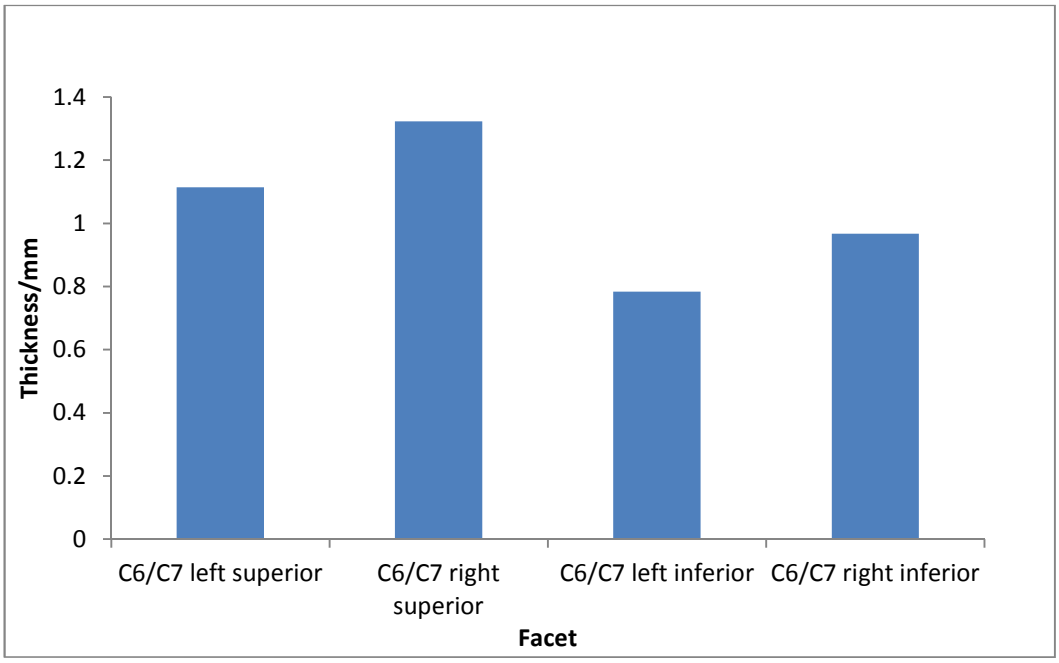


Figure 4.40: The thickness of the cartilage on all four C6/C7 ovine facets.

The thickness of the cartilage of the C6/C7 facets varied between approximately 0.8 mm and 1.4 mm. The right superior facet contained the thickest cartilage whilst the left inferior facet had the thinnest.

The strain values of facet joint cartilage determined over time when subject to indentation are shown in Figure 4.41.

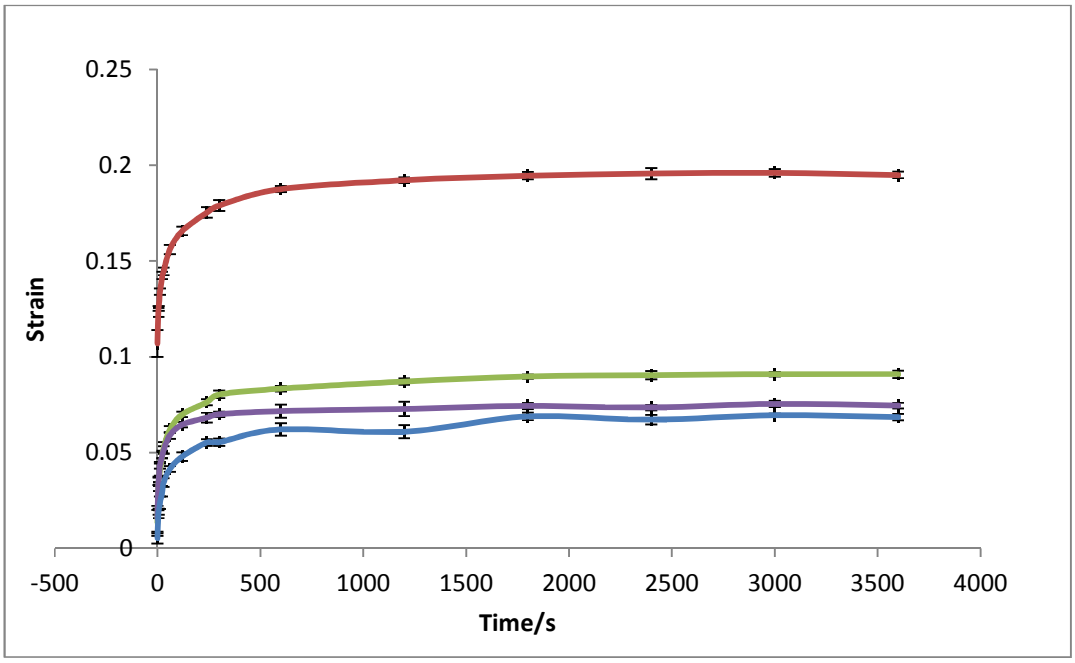


Figure 4.41: Strain curves for four C6/C7 ovine facets. Red: right superior facet, Green: right inferior facet, Purple: Left superior facet, Blue: left inferior facet. Errors bars plotted as standard deviation.

The deformation properties of the right superior facet cartilage were considerably higher than that of the other three facet cartilage samples. All samples reached equilibrium at similar time points. The final deformation measurements for C6/C7 right superior facet cartilage (1.323mm) was 0.195, 0.091 for right inferior facet cartilage (0.967mm), 0.075 for left superior facet cartilage (1.114mm) and 0.069 for left inferior facet cartilage (0.783mm). The mean of all four curves was plotted and is presented in Figure 4.42.

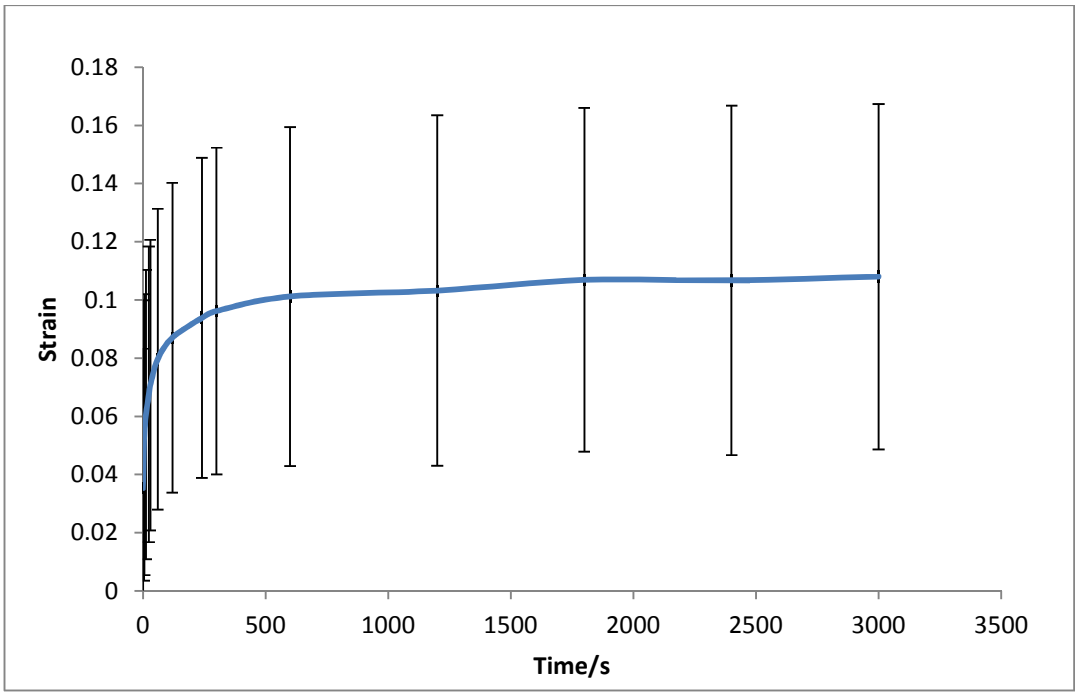


Figure 4.42: Strain curve of the mean for all four C6/C7 ovine facets. Errors bars plotted as standard deviation.

Great variation was observed between the four samples as can be seen from the large error bars in Figure 4.42. The average strain after deformation was approximately 0.1.

4.4.9. Quantification of GAG Content in Facet Cartilage

The amount of GAGs in thoracic facet cartilage was quantified using the GAG assay (Section 2.2.11.1 and 2.2.11.2). Thoracic cartilage from the left inferior facet of the FSU T2/T3 was removed from all the remaining tissue from the natural history study. Due to tissue restrictions, each age group contained a different sample number and some groups including the one and five to six year age group had only one sample available for analysis. The results from the analysis of GAG content are shown in Figure 4.43.

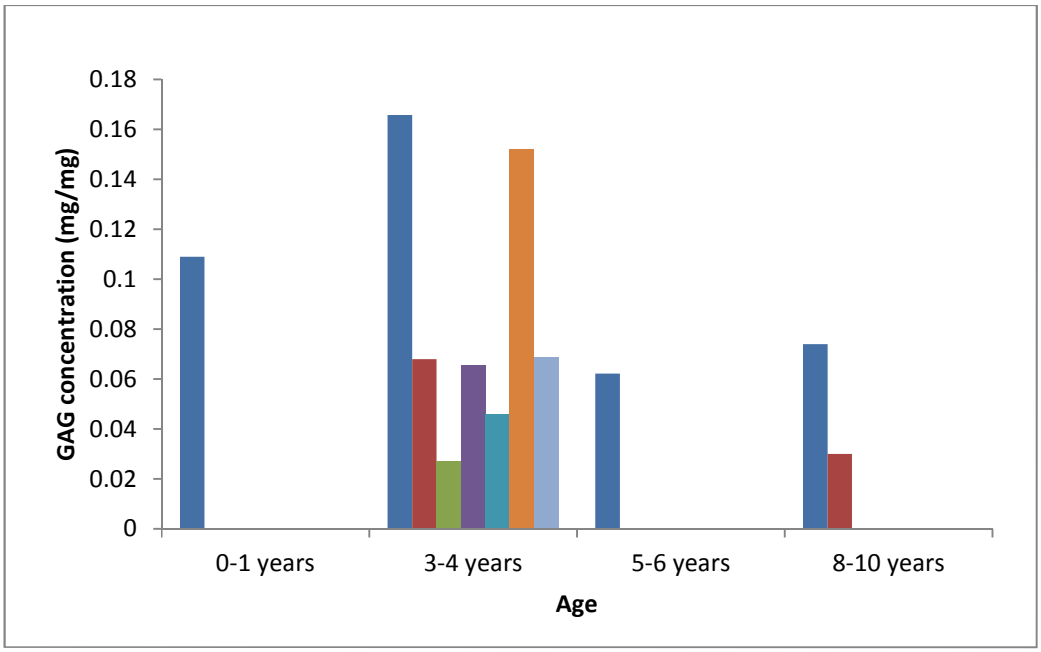


Figure 4.43: GAG concentration (mg/ml dry weight) in ovine thoracic facets across four age groups. Thoracic cartilage from the left inferior facet of T2/T3 in 0-1, 3-4, 5-6 and 8-10 year old sheep of different breeds was analysed. Each bar represents a replicate value for the specific age group. GAG: Glycosaminoglycan.

The results from the analysis of GAG content of the ovine facet cartilages showed a great deal of variation between the quantities of GAGs in different samples. In general, there was a trend towards decrease in GAG content with age as the mean levels appeared to decrease within the replicate groups. The mean values plotted for each age group are presented in Figure 4.44.

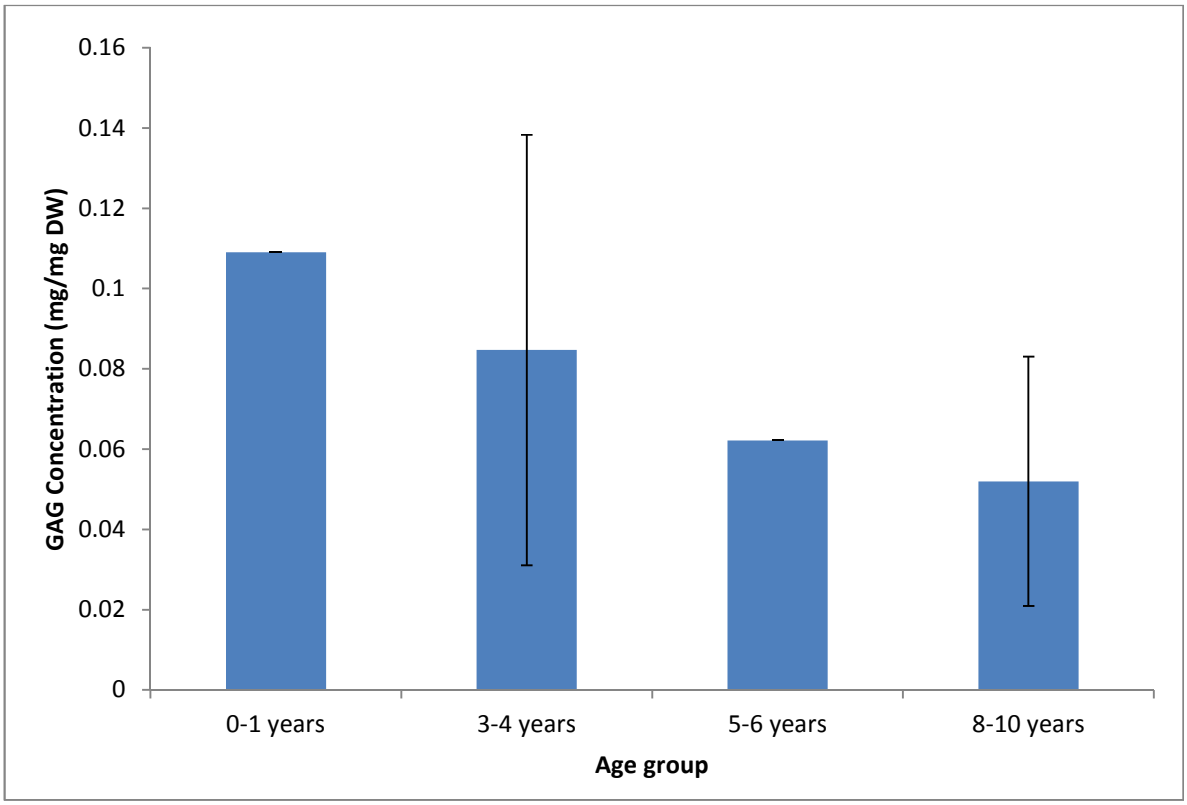


Figure 4.44: GAG concentration (mg/ml dry weight) in ovine thoracic facets across four age groups. Thoracic cartilage from the left inferior facet of T2/T3 in 0-1, 3-4, 5-6 and 8-10 year old sheep of different breeds was analysed. GAG: Glycosaminoglycan. Errors bars plotted as standard deviation.

In general, the facet cartilage from sheep in the healthy age groups, one year olds and three to four year olds had a mean percentage GAG content of 9.69 % (v/v dry weight). This was reduced to 5.54 % in the 8-10 year old age group. The percentage GAG content in the 0-1 year old and 5-6 year old sheep facet cartilages was determined for one replicate from each age group. The data for these two samples, however, followed the trend of decreasing GAG content with age.

4.5. Discussion and Conclusions

This aim of this chapter was to analyse ovine FSU tissue including facet cartilage, AF, NP and CEP tissue from healthy three year old sheep. Literature on the facet cartilage is currently limited and mainly focused on the biomechanical aspects rather than its biology. There are currently no biological studies characterising three year old ovine facet cartilage and IVD tissue reported in the literature. It was important to gain knowledge of the biology of ovine FSU tissue, since in the longer term this will be used to model human FSU tissue. As a result, knowledge of their similarities and differences will be essential.

The previous chapter showed that there were no statistical differences between the different breeds of sheep including Charollais, Suffolk and Texel. Therefore, using sheep of different breeds for comparison studies was not a limitation. In the work outlined in this chapter, a three year old Charollais sheep was used for isolation and analysis of cell phenotype in the FSU tissues whilst three, three year old Texel sheep were used for tissue analysis.

The histological study using H&E stained sections showed that ovine facet cartilage in all cervical, thoracic and lumbar regions exhibit the typical four zones of cartilage as found in articular cartilage from other joints (Broom, 1984; Buckwalter and Mankin, 1997). This finding has been previously reported for canine facet cartilage (Elder *et al.*, 2009). The cartilage on the cervical facets was thicker than that on the thoracic and lumbar facets and the four zones were more defined. This may be due to the greater range of movement in the neck region in sheep. As a result, the cartilage will need to be thicker to account for increased loading in comparison to the thoracic and lumbar regions which do not undergo as much movement. The CEPs in the cervical FSU`s were also found to be curved and thicker in comparison to thoracic and lumbar CEPs. Similarly, this may be due to the increase in biomechanical movement which results in differences in shape in order to cope with the extra demand.

The analysis of alcian blue stained sections showed an increase in positive staining from the AF towards the NP as has been previously reported (Roberts *et al.*, 1994). The staining within the ECM of the NP did not appear as intense as that in the AF however, the lacunae were strongly stained. This suggests that the GAGs are more densely populated around the cells than randomly within the ECM of the NP. This may be due to active secretion of GAGs from the cells. Another interesting observation was the increase in intensity of the alcian blue stain in between the lamellae of the AF. This may help the lamellae layers expand easily during loading whilst allowing them to recover their structure after loading. The facet cartilage in all three regions was intensely stained in the top layer of the superficial zone in comparison to the rest of the structure. This is an interesting and novel finding as previous studies have suggested the superficial zone in typical articular cartilage from other joints contains a higher amount of collagen running parallel to the surface and GAG content increases with depth (Mow *et al.*, 1984; Buckwalter and Mankin, 1997; Eyre, 2002). However, the results of the Sirius red staining also showed the presence of collagen in the superficial zone. This was particularly evident in the cervical facet cartilage sections in comparison to the thoracic and lumbar facet cartilage sections which had less Sirius red staining in the superficial zone. Again, this could be due to the large range of motions in the cervical region. It may be that in the thoracic and lumbar regions, protection of the facet cartilage surface by hydration is more important than protection from tensile forces afforded by collagen. The calcified zone of facet cartilage was also more intensely stained in the facets from the cervical region compared to the facets from the thoracic and lumbar regions. These findings are novel as there are currently no histological studies using alcian blue staining of ovine facet cartilage from cervical, thoracic and lumbar regions reported in the literature.

Sirius red staining within the FSU tissues showed that collagen was present in the AF, NP, CEP and facet cartilage as previously reported for IVDs and articular cartilage from other joints (Roberts *et al.*, 1989; Urban *et al.*, 2000; Eyre, 2002; Roberts *et al.*, 2006; Becerra *et al.*, 2010). This has also been previously reported in canine facet cartilage (Elder *et al.*, 2009). Collagen within the AF was densely distributed and relatively even throughout the structure in

the majority of samples. The size and the colours of the staining indicated that the fibres were large and fully mature. This suggests that they provide the AF with great structural support that is essential for its function as previously reported (Urban *et al.*, 2000; Roberts *et al.*, 2006). The staining within the NP was very different with thinner fibres which were green and white in appearance suggesting that they were thin fibres or perhaps newly formed. This supports previous findings in the literature that collagen is distributed randomly within NP tissue (Beard *et al.*, 1980; Eyre, 1979; Roughley, 2004). Collagen within the CEP was randomly distributed. The fibres were thin but mature. In comparison to the cervical samples, in both thoracic and lumbar samples the staining for collagen within the subchondral bone was much more intense than in the CEP suggesting a greater and more supportive network of collagen in the underlying bone. It has been reported that the attachment of the CEP to the underlying subchondral bone is poor due to the attachment of collagen fibrils between these two areas (Inoue, 1981). This may explain the lack of overlap in collagen structure observed here. The collagen within facet cartilage largely consisted of dense and mature fibres. The patterns were similar to that reported for articular cartilage from other joint areas (Eyre, 2002). Some newly formed fibres were present in the middle zone of cervical facet cartilage. The increased loading in the cervical region may therefore mean that collagen is actively being synthesised in facet cartilage. This may also indicate a greater turnover of collagen in the mid-zone of cervical facet cartilage.

Elastin was sparsely present in all four tissues. In the AF, the presence of elastin in between the lamellae layers allows the AF to retain its structure after deformation during loading. This may also be linked to the increase in GAGs in between the lamellae layers of the AF. Studies carried out in human and bovine AF tissue have also reported this distribution of elastin (Yu *et al.*, 2002; Yu *et al.*, 2005). Miller's elastin staining in the NP, CEP and facet cartilage showed that the elastin content was largely present around the cells and lacunae. Previous studies in bovine IVD tissue have reported an extensive network of elastin (Yu *et al.*, 2002). A limitation of Miller's elastin staining for identifying elastin fibres is that they are easily masked by GAGs and collagen in the ECM. This may explain the lack of positive staining within the ECM of these tissues. A

more reliable method that could be used for future analysis of the elastin network in ovine FSU tissues would be to pre-treat the tissues with hyaluronidase and collagenases to unmask elastin from GAGs and collagen (Yu *et al.*, 2002).

Collagen type I staining within ovine facet cartilage tissue was negative but positive within the underlying subchondral bone. This indicated that the cartilage samples were healthy and not undergoing degeneration. The variation of staining of collagen type I along with its presence within facet cartilage and NP cells may have been the result of the being cultured in monolayer. Although collagen type I staining of the FSU cells at passage four were negative in Section 2.3.2 (Table 2.10), the phenotype at passage two may be different. In addition, the cells were from a different age and breed of sheep and therefore variations may occur. The presence of collagen type I in the subchondral bone indicated its function to provide the essential biomechanical properties of bone including load bearing and tensile strength (Gelse *et al.*, 2003). This is also likely to apply to the positive staining observed in the subchondral bone underlying the CEP. In the AF, the outer region was densely stained with collagen type I in both cells and tissue indicating its presence as has been previously reported for AF tissue from other species (Eyre and Muir, 1977; Beard *et al.*, 1980; Antoniou *et al.*, 1996; Schollmeier *et al.*, 2000). This suggested that the outer AF in ovine tissue is more fibrous and stronger in comparison to the inner AF. The presence of osteocalcin staining indicated where the bone underlying the facet cartilage and the CEP began.

Collagen type II and chondroitin sulphate staining was present in all ovine AF, NP, CEP and facet cartilage tissue and cells. Within the AF, the most intense staining for both of these markers was present in the inner region as has been previously reported for AF tissue from other species (Eyre and Muir, 1977; Antonoiu *et al.*, 1996; Schollmeier *et al.*, 2000). This suggested that the inner AF is subject to more mechanical movement than the outer AF. This is due to compression from the adjacent NP. The NP was also positively stained for collagen type II and chondroitin sulphate. This has been previously reported for NP tissue from other species (Antonoiu *et al.*, 1996; Urban *et al.*, 2000; Gan *et*

al., 2003A). The presence of collagen type II and chondroitin sulphate within tissues of the IVD and cartilage is very important for their function and is widely documented in the literature. Although the qualitative distribution of these markers has been documented in the IVD for various species, it has not been previously carried out in facet cartilage.

Collagen III expression was evident in all FSU tissues and cells analysed here. Interestingly, the pattern of staining within FSU tissue was very similar to that of elastin. This may therefore suggest that collagen type III and elastin are co expressed together and have a structure/function relationship. This has not been previously reported in the literature. A previous study concluded that collagen type III co-localises with collagen type II (Young *et al.*, 2000). However, in this study differences were observed in the staining patterns. Collagen III and VI were highly expressed around the cells in the tissues as well as by the cells identified by immunofluorescence in comparison to other collagen types other than collagen type II. Collagen type III is a fibril forming collagen whilst collagen type VI is associated with fibrocartilage. This may suggest that the cells within both the facet cartilage and intervertebral disc are protected by a fibrous barrier. Collagen VI has also been previously reported to make connections to the ECM (Pullig *et al.*, 1999). This enables the cells to be anchored into the matrix. These observations have been previously reported for IVD tissue and articular cartilage but not for facet cartilage (Wu *et al.*, 1987; Roberts *et al.*, 1991A; Roberts *et al.*, 1991B; Wotton and Duance, 1994). The relationship between collagen III and VI has been previously considered (Koller *et al.*, 1989; Chu *et al.*, 1990; Roberts *et al.*, 1991A). Studies suggest that the homologous repeats on the three polypeptide chains of collagen type VI may be capable of interacting with collagen type III through the microfilaments on collagen type VI. The elastin network present around the cells in the tissues analysed here may provide further protection by allowing the structure to be maintained after loading. The staining of collagen types III and VI around the cells in the IVD suggest that they sit in pericellular capsules like chondrocytes in articular cartilage as reported in previous work (Roberts *et al.*, 1991A).

The expression of fibronectin within the ECM of facet cartilage tissue and cells showed that it was present within all zones of the cartilage which was consistent with previous reports on articular cartilage from other joints which suggest that it plays an important role in binding GAGs and organising components of the ECM including collagen and aggrecan (Ruoslahti, 1988; Brown and Jones, 1990; Chevalier, 1993). This may also apply to IVD tissue and cells which also showed high expression. Previous studies have indicated that high expression of fibronectin may reflect degeneration in the IVD and articular cartilage (Lust *et al.,* 1987; Homandberg and Wen, 1998; Oegema *et al.*, 2000). However, the results from Chapter 4 have shown that the tissue analysed here was not degenerate. It may be that analysing tissue of an older age group such as between eight and 10 years of age may result in more intense staining for fibronectin.

Some facet cartilage, NP and outer AF cells showed positive staining for collagen type X. Collagen type X has been reported to be expressed in the calcified zone of articular cartilage and the IVD (Mayne, 1989; Gannon *et al.*, 1991; Aigner *et al.*, 1998; Eyre, 2002). Collagen type X has been shown to be present within the human NP at a young age and expressed in older tissue when the IVD undergoes degeneration (Boos *et al.*, 1997). This may explain this expression in some of the IVD cells in this study. Most of the cells in the current work also expressed CD44 and SOX-9 as expected from the results of previous studies (Sive *et al.*, 2002).

The average GAG concentration in 3-4 year old ovine thoracic facet cartilage was 7.44 % (w/w). This was within the range of GAG concentration for articular cartilage. Only one pervious study has quantified GAG content in facet cartilage (Elder *et al.*, 2009). This study analysed lumbar facet cartilage of 2-4 year old dogs. They found an average GAG content (dry weight) of 14.9 %. The difference in values may be a result of differences in species and spinal region. The indentation testing carried in the current work showed that ovine cervical facet cartilage displayed biphasic properties as previously reported for ovine cervical facet cartilage in 5-6 year old specimens (Latif *et al.*, 2012).

There were limitations to some of the methods used in this part of the study. The process of cell isolation from cartilage and IVD tissue was particularly difficult due to the low cell densities within cartilage and the NP. However, the challenges were overcome and a large number of cells were obtained. All cell phenotyping was, however, performed on cells which were cultured in monolayer. FSU cells, in particular chondrocytes have been widely reported in the literature to change phenotype in culture by dedifferentiating into fibroblasts (von der Mark *et al.*, 1977; Archer *et al.*, 1990). However, studies described in Chapter 2 showed that the cells from ovine facet cartilage, AF, NP and CEP maintained collagen type II expression up to passage eight. As previous work suggests that chondrocyte phenotype can be confirmed with collagen type II expression, it can be assumed that the true phenotype was observed and that this data was reliable for comparing the phenotype of the different cells (Zaucke *et al.*, 2001; Hoffman *et al.*, 2010).

Another limitation was the lack of tissue available for GAG analysis. In some age groups, including the 0-1 and 5-6 age groups, there was only one sample. This therefore meant that statistical comparisons could not be made between the age groups. However, as there were seven replicates in the 3-4 year old group this allowed for a relatively accurate analysis of the percentage of GAGs in healthy ovine facet cartilage and fulfilled the objective of this chapter. Similarly, there was a lack of tissue was available for the indentation testing. As whole cervical facets were needed to obtain cartilage pins for testing this was a limitation as only one pin could be obtained per facet. As only four facets from a 3-4 year old Texel sheep could be obtained for this analysis, only four facet cartilage pins were tested. The indentation test results could have been analysed further to provide more information with regards to the biphasic properties of facet cartilage. Finite-element (FE) modelling could have been used to determine the permeability and elastic modulus of the cartilage. However, due to time restrictions this was not possible.

In conclusion, the results from this chapter showed that, generally, facet cartilage showed similar characteristics to that of articular cartilage from other joint areas. The next stage of this study was to determine whether it was

possible to treat ovine facet cartilage to produce a tissue which mimicked the biomechanical properties of degenerate human facet cartilage. Since the strain properties of healthy ovine facet cartilage had been determined this would allow direct comparisons to be made.

Chapter 5: A Degeneration Model of Ovine Facet Cartilage

Chapter 5: A Degeneration Model of Ovine Facet Cartilage

5.1. Introduction

The work carried out in Chapter 4 investigated the characteristics of healthy ovine facet cartilage and IVD tissue. The aim of this chapter was to utilise healthy ovine facet cartilage, from the 3-4 year age group and develop a method of treating the cartilage such that it mimicked the features of degenerated human facet cartilage. The model of the degenerated ovine facet cartilage would have the potential to be used as in an *in vitro* pre-clinical model to test novel cartilage substitution therapies such as biomaterials and therapies produced via tissue engineering.

Chondroitinase ABC is an enzyme which depletes GAGs from tissue. It has been previously used to deplete GAGs in bovine knee cartilage at a concentration of 0.1 $U.ml^{-1}$ (Katta *et al.*, 2007; Katta *et al.*, 2008B). Studies have also shown that chondroitinase depletes GAGs and alters the friction and deformation properties of articular cartilage (Schmidt *et al.*, 1990; Sasada *et al.*, 2005; Basalo *et al.*, 2006). Another study, however, reported that chondroitinase ABC did not alter frictional properties of bovine articular cartilage (Pickard *et al.*, 1998). This method of treatment was investigated for use with ovine facet cartilage.

By depleting GAGs from facet cartilage, the osmotic pressure and biphasic properties should, theoretically, be depleted resulting in cartilage that is less able to resist compression forces. As a result, the cartilage would have reduced capacity to resist deformation under load. This may result in damage to the other ECM components such as the collagen network when cartilage is subject to loading. These changes have been observed in degenerated articular cartilage (Rieppo *et al.*, 2003; Basalo *et al.*, 2005).

5.2. Aims and Objectives

The aim of this chapter was to develop a method for reproducing the biomechanical characteristics of human degenerative facet cartilage in ovine facet cartilage. The approach taken was to reduce the GAG content.

Specific Objectives:

- Determine a suitable method for treatment of ovine cervical facet cartilage with chondroitinase ABC.
- Treat ovine cervical facets with chondroitinase ABC using the established method.
- Determine the macroscopical features of treated ovine cervical facets.
- Determine the quantity of GAGs within the cartilage of chondroitinase ABC treated ovine cervical facets.
- Determine the indentation properties of chondroitinase ABC treated ovine cervical facets.
- Determine the organisation of ECM and cells and distribution of GAGs, collagen and elastin of chondroitinase ABC treated ovine cervical facets using histology.
- Determine the distribution of chondroitin sulphate and collagen type II in chondroitinase ABC treated ovine cervical facets using immunohistochemistry.

5.3. Experimental Approach

Initially it was necessary to determine a suitable method for the treatment of ovine facet cartilage with chondroitinase ABC. This was carried out using thoracic facets from a three year old spine. The devised method was then applied to cervical facet cartilage from a three year old Texel spine (to ensure that the treated facets could be tested using indentation tests). The treated cervical facets were then subject to analysis using histology, indentation testing and evaluation of GAG content.

5.4. Methods

5.4.1. Determination of the Method of Chondroitinase ABC Treatment

Chondroitinase ABC is an enzyme previously used to degrade osteochondral pins by removing the GAGs within the cartilage (Katta *et al.* 2008B). As the original method was designed for 9 mm osteochondral pins from bovine condyles, the concentration of the enzyme and incubation time required investigation for use on the ovine facets. The original method involved incubating the pins in 25 ml antibiotic solution (Section 2.1.2) for 16-18 hours at 4 ºC with agitation at 120 rpm. Pins were then incubated with 25 ml chondroitinase ABC solution (0.1 $U.ml^{-1}$) at 37 ºC with agitation at 120 rpm for 24 hours. Finally, the pins were washed in PBS at 20 ºC with agitation at 240 rpm twice for 20 minutes each.

To develop the method for facet cartilage, eight thoracic facets including left and right inferior facets from levels T3/T4 to T6/T7 of a three year old spine (spine one from the anatomical study in Chapter 3) were washed in antibiotic solution (Section 2.1.2) for 16-18 hours before incubating in solutions of varying concentrations of chondroitinase ABC using two incubation times as shown in Table 5.1.

Chondroitinase ABC concentration ($U.ml^{-1}$)	**8 hour incubation**	**24 hour incubation**
0	Right T3/T4	Left T3/T4
0.025	Right T4/T5	Left T4/T5
0.05	Right T5/T6	Left T5/T6
0.1	Right T6/T7	Left T6/T7

Table 5.1: Thoracic facets incubated with a range of chondroitinase ABC concentrations and incubation times.

The same conditions were used during the incubations as described in the original method (Section 2.2.14). When the treatment was complete, the facet cartilage was removed, freeze dried to constant weight, digested in papain and analysed using the GAG assay (Section 2.2.11.1).

5.4.2 Treatment of Ovine Cervical Facet Cartilage with Chondroitinase ABC

A cervical section of an ovine three year old Texel spine was obtained and stored at -20 °C. Three months later the cervical spine was allowed to thaw overnight at 4 °C. FSUs C4/C5 and C5/C6 were removed and their eight facets including both left and right superior and inferior facets were dissected, using the method described in Section 2.2.5.2 and photographed (Section 2.2.6).

Six of the facets including the left inferior and superior facets of C4/C5 and all four C5/C6 facets were treated with chondroitinase ABC as described in Section 2.2.14. The right inferior facet of C4/C5, the frozen negative control, was immediately stored at -20 °C in a PBS-moist container after being photographed whilst the six facets were undergoing treatment. The right superior facet of C4/C5, the buffer negative control, was placed into chondroitinase ABC solution without the chondroitinase ABC enzyme (Section 2.1.2) as a negative control. Following treatment, all facets were re-photographed and the right inferior facet of C4/C5 was allowed to thaw.

Pins were removed from each facet as described in Section 2.2.13.1 and were indented as described in Section 2.2.13.2 to determine the indentation properties of the chondroitinase ABC treated facet cartilage and both negative controls. Each facet was then indented with a needle indenter to determine the cartilage thickness as described in Section 2.2.13.3.

A 2 mm slice from the top of each facet was removed using a bone saw as described in Section 2.2.5.2 and the slice was fixed, decalcified, tissue processed and embedded in wax as described in Section 2.2.7. Sections were obtained and stained with H&E, alcian blue, Sirius red and Miller's elastin (Section 2.2.7).

The facet cartilage was scraped from each remaining facet and placed into pre weighed bijous. The cartilage was freeze-dried to constant weight and papain

digested for 48 hours at 60 °C. The GAG content was quantified using the GAG assay (Section 2.2.11.1).

5.5. Results

5.5.1 Determination of the Method of Chondroitinase ABC Treatment for Facet Cartilage.

Following treatment of the ovine thoracic facets with different concentrations of chondroitinase ABC, the GAG concentrations were determined. The values obtained from each facet are shown in Figure 5.1.

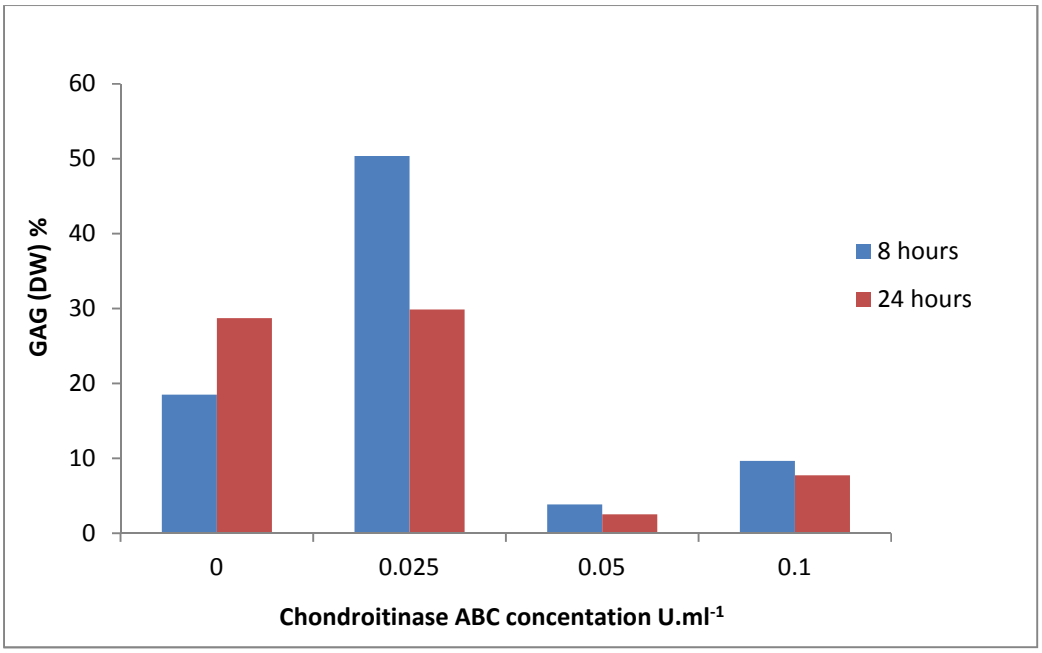


Figure 5.1: The GAG concentration (as a percentage of dry weight) in facets treated with various concentrations of chondroitinase ABC. Each bar represents one result from one facet. DW: Dry weight.

Without enzyme treatment the GAG concentrations in the facet cartilage were 18-28 % (w/w). The results showed that treatment of the facets with 0.025 $U.ml^{-1}$ chondroitinase ABC for eight or 24 hours had little effect on the GAG concentration. Following treatment with 0.05 $U.ml^{-1}$ of chondroitinase ABC, the GAG concentrations in the facet cartilage reduced to less than 5 % (w/w) after eight hours of incubation. The concentration did not reduce further after 24 hours of incubation. Treatment with the higher concentration of enzyme (0.1 $U.ml^{-1}$) did not lead to a further reduction in GAG concentration. Therefore, in the subsequent experiments to reduce the GAG concentration of the facets, they were incubated in 0.05 $U.ml^{-1}$ of chondroitinase ABC for approximately 16 hours.

5.5.2. Morphology of Chondroitinase ABC Treated Ovine Facet Cartilage

A cervical section of an ovine Texel spine which had been stored in the freezer for approximately three months was allowed to thaw overnight. The following day, FSUs C4/C5 and C5/C6 were dissected and all eight facets including the left and right superior and inferior facets from both FSUs were removed. Photographs of all eight cervical facets from FSUs C4/C5 and C5/C6 were taken before and after chondroitinase (or control) treatment. The right inferior facet of C4/C5 was used as a negative control and was stored at -20 °C until used for analysis. The right superior facet of C4/C5 was treated with buffer alone as a negative control.

All C4/C5 facets had similar features before chondroitinase ABC treatment. The soft tissue surrounding the facets was red and white in appearance. The cartilage on the surface of all the facets was white, shiny and smooth in appearance. No major defects were present on the surface with the exception of the C4/C5 right superior facet. The facets after chondroitinase ABC treatment appeared much paler and white in appearance. The soft tissue surrounding the facets had lost any pink or red colour that it had had before treatment. This was true for the facet cartilage of all samples. The surfaces of the cartilage on all facets after treatment appeared to retain their macroscopical structure. The cartilage was still smooth and appeared to have gained no defects. Photographs' of the C4/C5 facets before and after treatment (with the exception of the right inferior facet which was photographed before being stored at -20 °C) are shown in Figure 5.2.

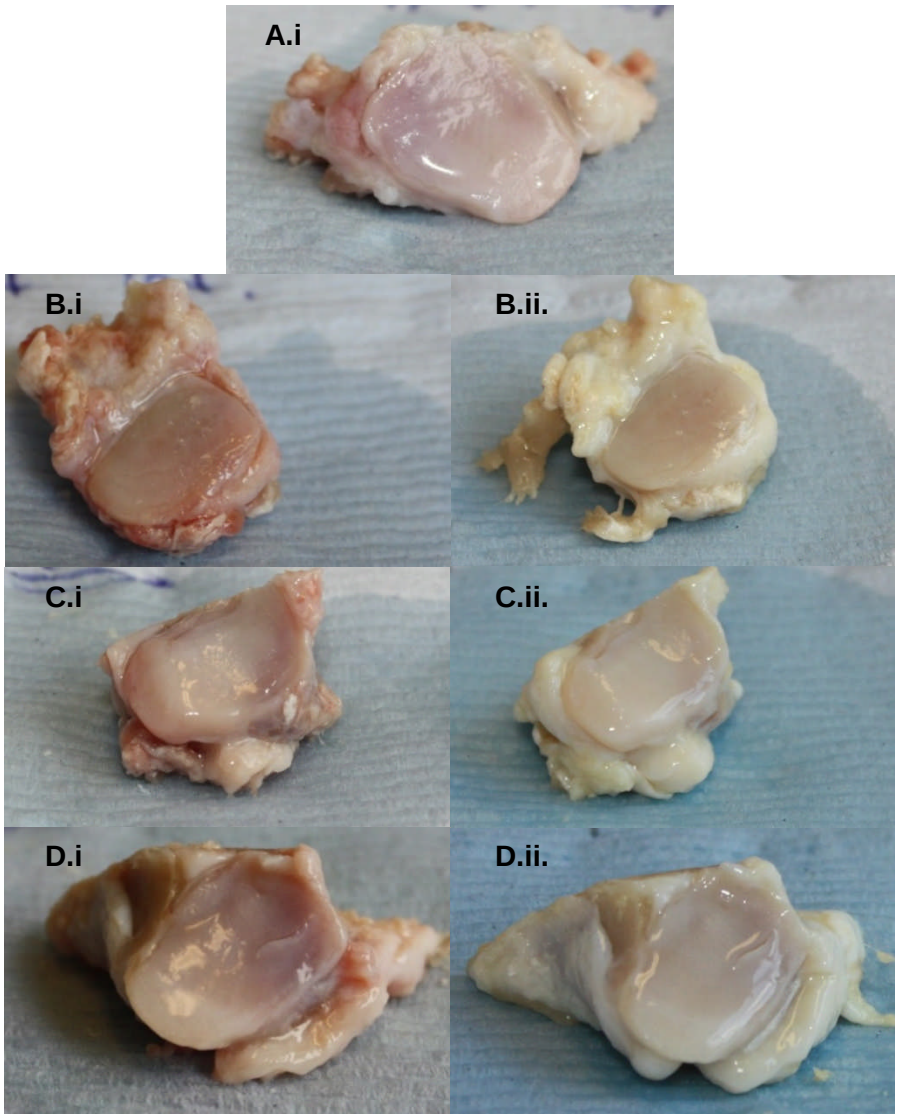


Figure 5.2: C4/C5 facets before and after chondroitinase ABC treatment. A: C4/C5 right inferior facet, B: C4/C5 left inferior facet, C: C4/C5 left superior facet, D: C4/C5 right superior facet before (i) and after (ii) chondroitinase ABC treatment. The C4/C5 right inferior facet was not treated and was stored at -20 °C immediately before being treated. The C4/C5 right superior facet was treated with buffer alone (control).

All C5/C6 facets had similar features before chondroitinase ABC treatment. The soft tissue surrounding the facets was red and white in appearance. The cartilage on the surface of all the facets was white, shiny and smooth in appearance. No major defects were present on the surface. The facets after chondroitinase ABC treatment appeared much paler and white in appearance. The soft tissue surrounding the facets had lost any pink or red colour it had had before treatment. This was true for the facet cartilage of all samples. The surface of the cartilage on all facets after treatment appeared to retain their

macroscopical structure. The cartilage was still smooth and appeared to have gained no defects. Photographs of the C5/C6 facets before and after treatment are shown in Figure 5.3.

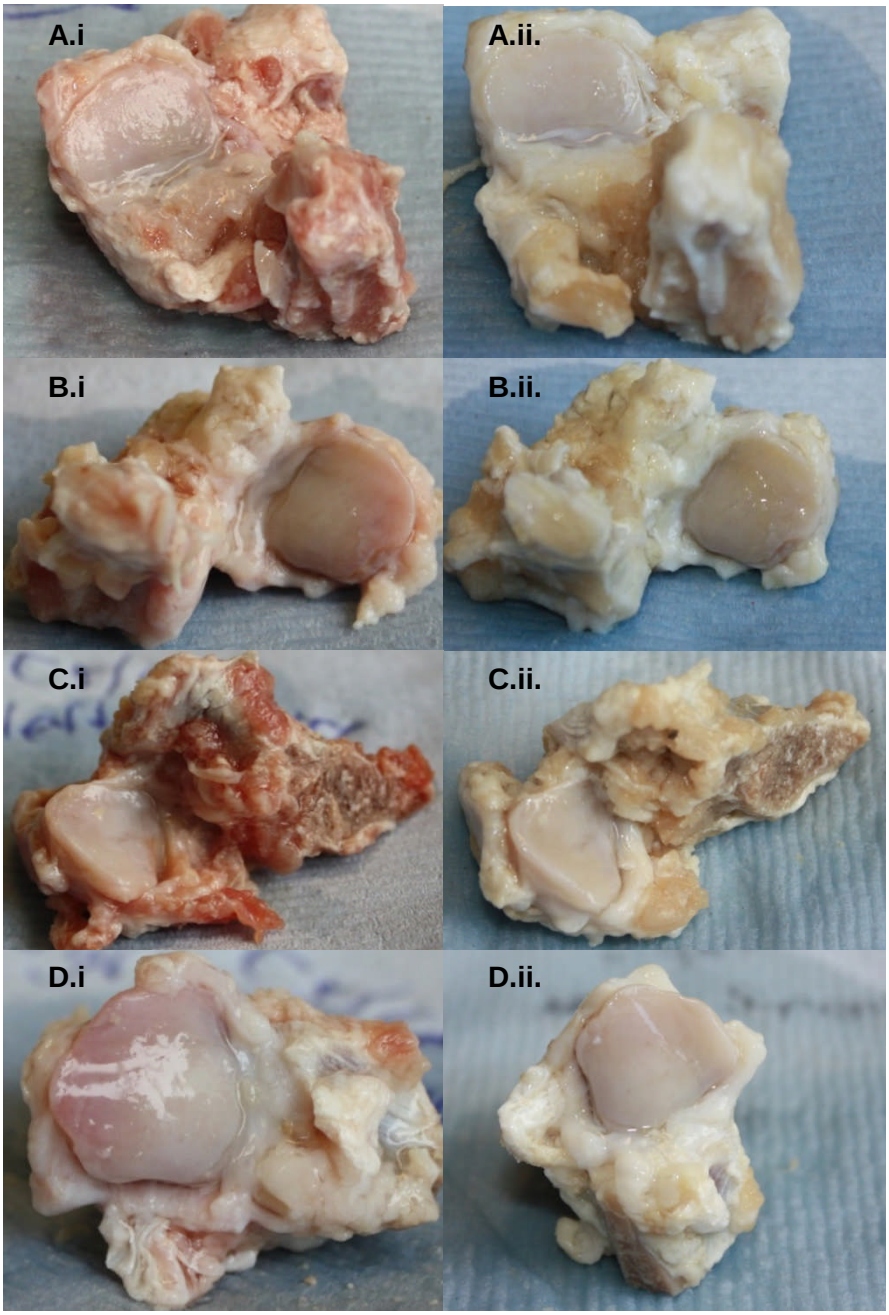


Figure 5.3: C5/C6 facets before and after chondroitinase ABC treatment. A: C5/C6 left inferior facet, B: C5/C6 right inferior facet, C: C5/C6 left superior facet, D: C5/C6 right superior facet before (i) and after (ii) chondroitinase ABC treatment.

5.5.3. Quantification of GAG Content in Chondroitinase ABC Treated Ovine Facet Cartilage

Facet cartilage from each of the eight facets was removed, freeze dried and analysed using the GAG assay. The results from this are shown in Figure 5.4.

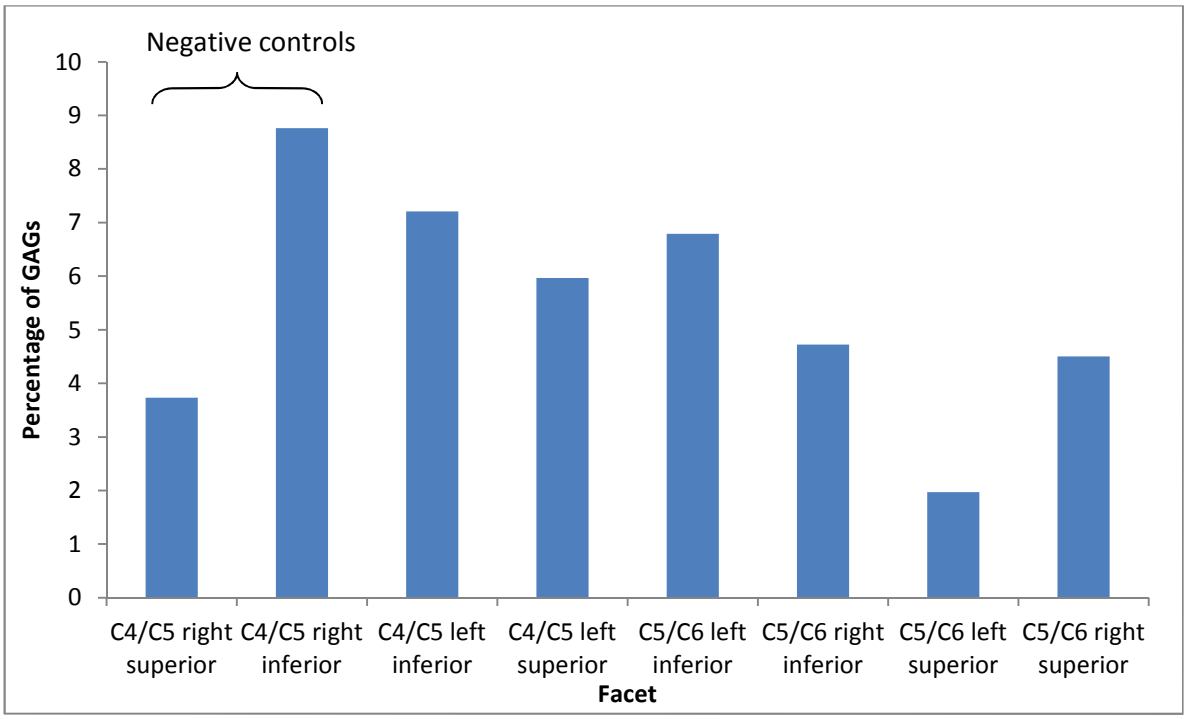


Figure 5.4: The percentage of GAGs (dry weight) in facet cartilage after chondroitinase ABC treatment including negative controls. C4/C5 right inferior facet did not undergo treatment (frozen negative control) and C4/C5 right superior facet only underwent treatment in enzyme buffer without chondroitinase ABC (buffer negative control). GAG: Glycosaminoglycan.

The quantity of GAGs in the frozen negative control (8.76 % w/w) was much higher than that in the buffer negative control (3.73 % w/w). The chondroitinase treated facet cartilage samples fell below that of the frozen negative control. The quantity of GAGs within cartilage of C4/C5 and C5/C6 chondroitinase ABC treated facets varied between 2-7 % (w/w) in samples. The lowest GAG percentage of 1.97 % (w/w) was seen in the cartilage of the C5/C6 left superior facet, lower than both negative controls. The highest GAG percentage was observed in the cartilage of the C4/C5 left inferior facet (7.21 % w/w) lower than the frozen negative control but higher than the buffer negative control.

5.5.4. Indentation Testing of Chondroitinase ABC treated ovine Facet Cartilage

All C4/C5 and C5/C6 4 mm facet pins were indented following chondroitinase ABC treatment including both negative controls. A needle indenter was used to determine the facet cartilage thickness and is plotted in Figure 5.5.

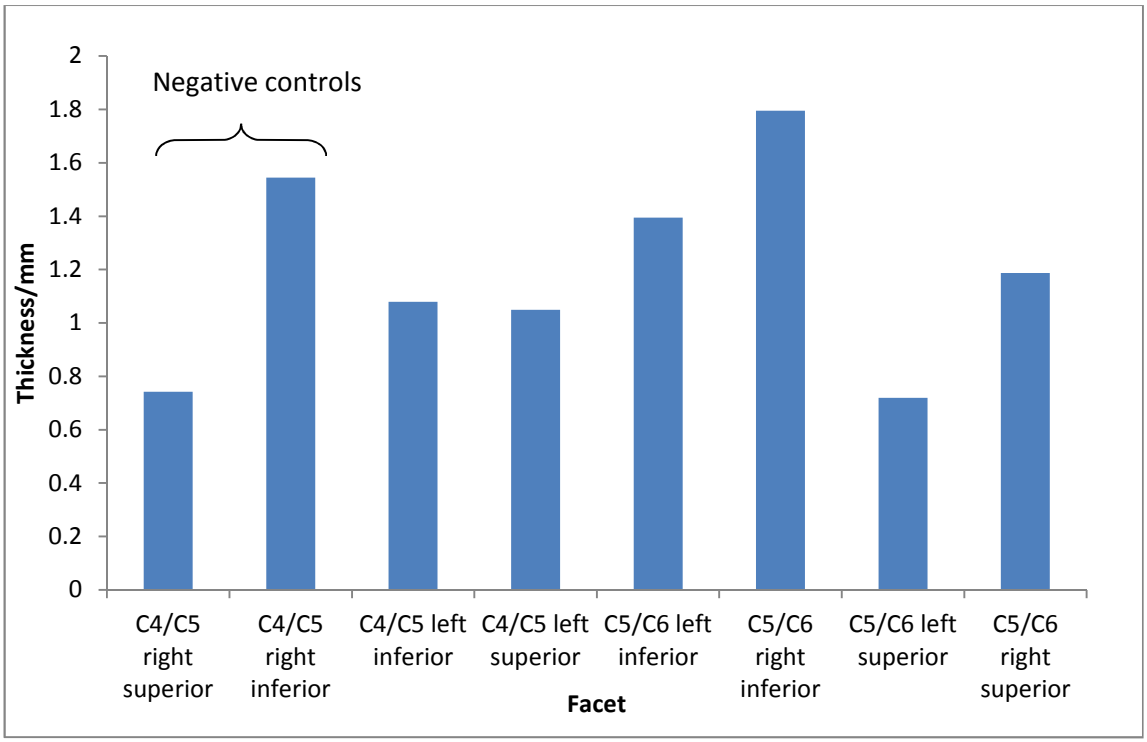


Figure 5.5: The thickness of the cartilage on all eight C4/C5 and C5/C6 ovine facets. C4/C5 right inferior facet did not undergo treatment (frozen negative control) and C4/C5 right superior only underwent treatment in enzyme buffer without chondroitinase ABC (buffer negative control).

The thickness of the cartilage on all the facets after chondroitinase ABC treatment varied between approximately 0.8 mm and 1.8 mm. The C5/C6 right inferior had the thickest cartilage whilst the C5/C6 left superior facet had the thinnest. In comparison to the GAG assay data obtained from all the C4/C5 and C5/C6 facets in Figure 5.5, there appeared to be a similar trend in cartilage thickness; with thicker cartilage having a higher GAG content.

The strain was deduced from the displacement values obtained from indentation testing and plotted for each sample as shown in Figure 5.6.

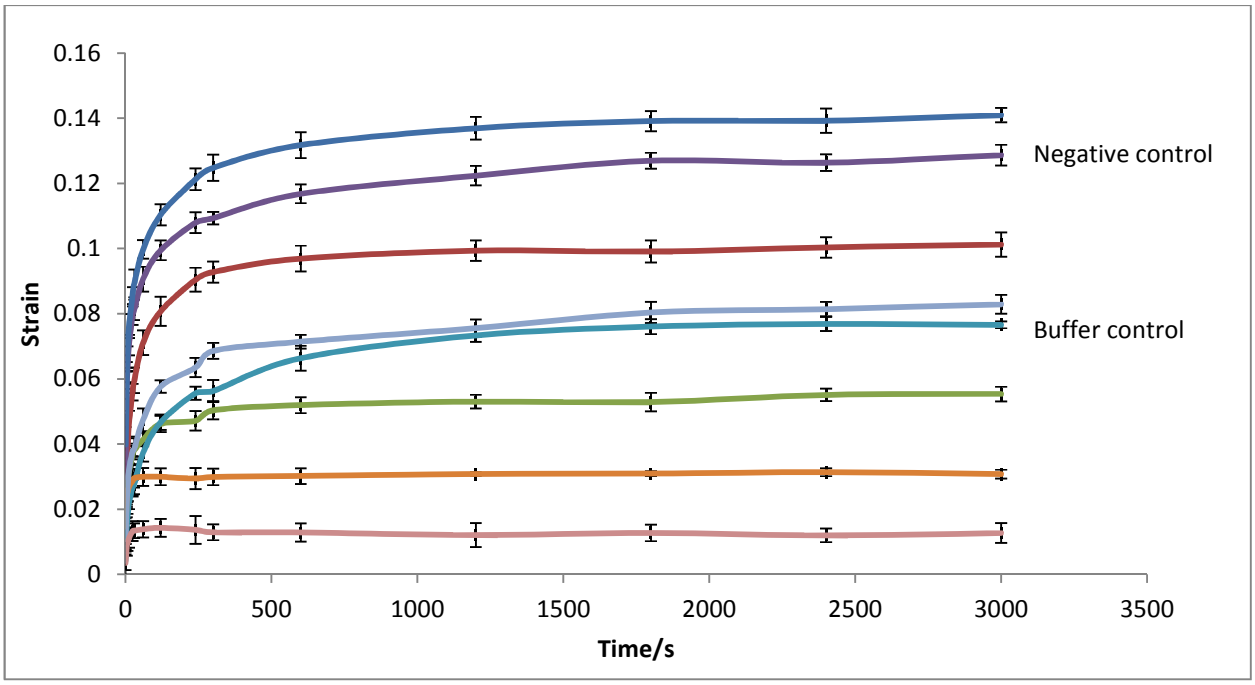


Figure 5.6: The indentation data for ovine C4/C5 and C5/C6 facet cartilage with and without treatment with chondroitinase ABC. Dark blue: C5/C6 right superior, Purple: C4/C5 right inferior (frozen control), Red: C4/C5 left inferior, Cyan: C5/C6 left superior, Turquoise: C4/C5 right superior (buffer only control), Green: C4/C5 left superior, Orange: C5/C6 left inferior, Pink: C5/C6 right inferior.

There was a large degree of variation in the strain exhibited by the C4/C5 and C5/C6 facet cartilage samples. This was also true of the C5/C6 right superior, C4/C5 left inferior and C5/C6 left superior facets. All of these samples showed typical biphasic responses to load. The other facets however, appeared to reach equilibrium within 500 seconds and did not display biphasic responses, reaching equilibrium at much lower strains. The final strain measurement for the C4/C5 left inferior facet was 0.101 (1.0791 mm), 0.0553 for the left superior facet (1.0498 mm), 0.129 for the right inferior facet (1.545 mm) and 0.0765 for the right superior facet (0.743 mm). The final strain measurement for the C5/C6 left inferior facet was 0.0307 (1.395 mm), 0.0829 for the left superior facet (0.720 mm), 0.0127 for the right inferior facet (1.795 mm) and 0.141 for the right superior facet (1.187 mm). The mean of all six treated facets alongside the negative controls is shown in Figure 5.7.

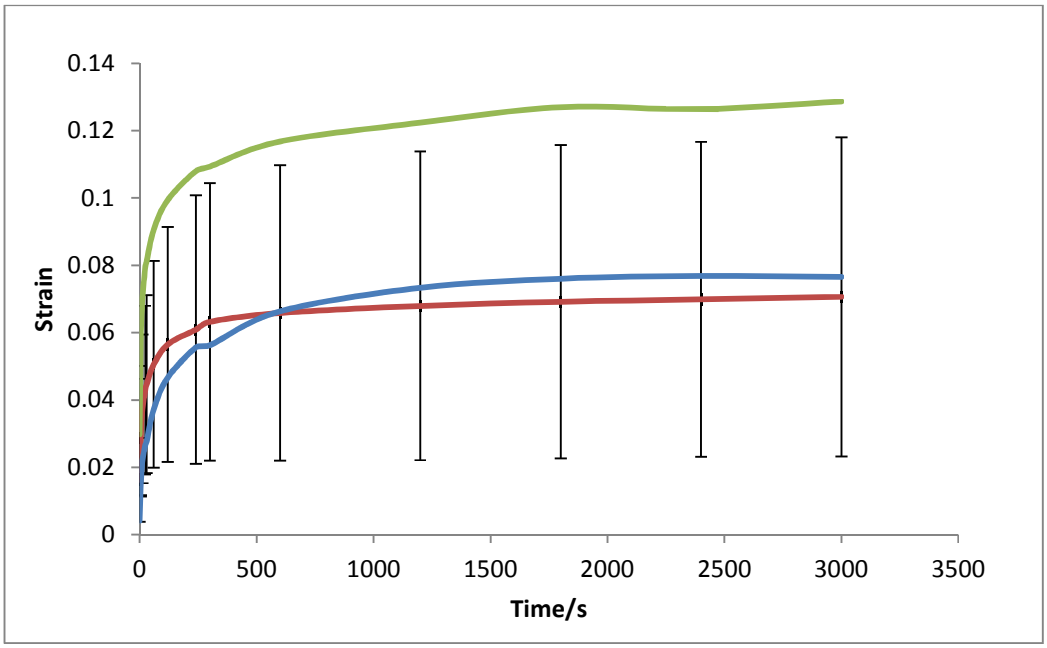


Figure 5.7: The indentation data for ovine C4/C5 and C5/C6 chondroitinase ABC treated facet cartilage including negative controls. Green: C4/C5 right inferior facet (frozen negative control), Blue: C4/C5 right superior facet (buffer negative control), Red: the mean deformation of all six chondroitinase ABC treated facets. Error bars represent the standard deviation of the mean for the six chondroitinase treated facets.

In comparison to both negative controls, the chondroitinase ABC treated facets appeared to deform more quickly reaching equilibrium more quickly. The chondroitinase ABC treated facets and the buffer negative control did not deform as much as the frozen negative control. The frozen negative control showed deformation values similar to that in the C5/C6 facets in Chapter 4 (Section 4.4.8). The C5/C6 values reached equilibrium at approximately 0.11 whilst the negative control of the left inferior C4/C5 facet reached it at approximately 0.13.

5.5.5. Histological Characterisation of Chondroitinase ABC Treated Ovine Facet Cartilage

Sections of the facet cartilage for each of the eight facets were obtained after treatment with chondroitinase ABC, fixation, decalcification, processing and wax embedding. The sections were stained with H&E and photographed.

The frozen negative control, C4/C5 right inferior facet, (Figure 5.8A) showed an organised cartilage structure including the four zones of articular cartilage. The

surface was smooth, intact and did not contain any fissures. The buffer negative control, C4/C5 right superior facet, (Figure 5.8B) also showed a neat cartilage structure with the presence of four zones, however, some fissures were present on the surface.

The chondroitinase ABC treated C4/C5 and C5/C6 facet cartilage samples (Figure 5.8C) appeared to also retain the normal four zone structure of articular cartilage. In all samples, a clear superficial, middle, deep and calcified zone was observed. No major differences could be seen between the negative controls in comparison to the other facets. However, the frozen negative control appeared to have a more intact surface in comparison to the other samples. In some chondroitinase ABC treated samples the surface of the cartilage appeared torn in some areas and had some visible fissures. However, the superficial layer was not lost in these samples. The organisation of the cells was consistent in all chondroitinase ABC treated samples and again no differences were observed in comparison to both negative controls. Images of all eight facets stained with H&E are shown in Figure 5.8.

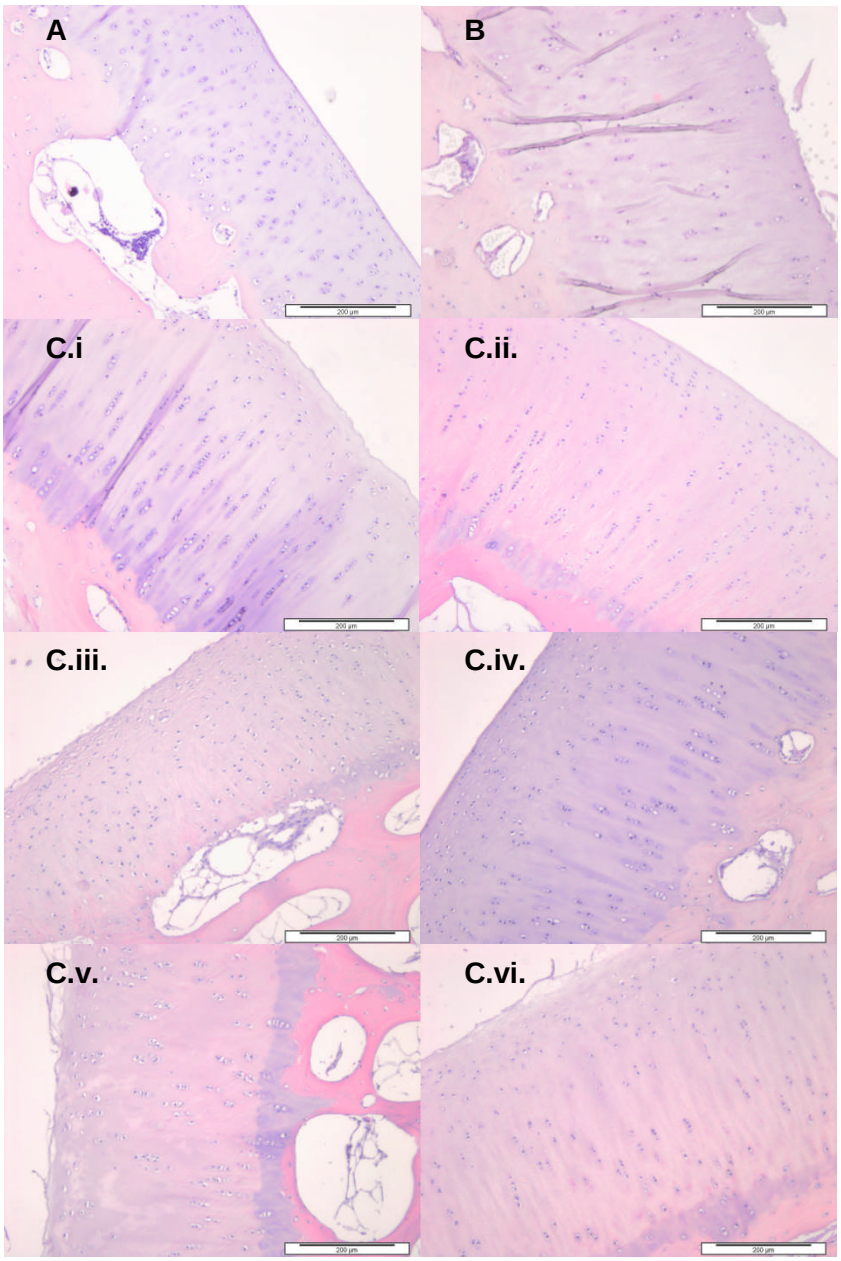


Figure 5.8: C4/C5 and C5/C6 facet sections stained with H&E after chondroitinase ABC treatment including negative controls. A: C4/C5 right inferior facet, frozen negative control, B: C4/C5 right superior facet, buffer negative control, C.i: C4/C5 left inferior facet, C.ii: C4/C5 left superior facet, C.iii: C5/C6 right inferior, C.iv: C5/C6 right superior facet, C.v: C5/C6 left inferior facet, C.vi: C5/C6 left superior facet. H&E: Haematoxylin and eosin.

5.5.6. Characterisation of Chondroitinase ABC Treated Ovine Facet Cartilage sections stained with Alcian Blue

Sections of the facet cartilage for each of the eight facets were obtained after treatment with chondroitinase ABC, fixation, decalcification, processing and wax embedding. The sections were stained with alcian blue and photographed.

The frozen negative control, C4/C5 right inferior facet, (Figure 5.9A) showed positive staining in all four zones. Traces of stain were found in the ECM but largely around the lacunae of the chondrocytes. The deep zone stained more intensely than the other zones. In the buffer negative control, C4/C5 right superior facet, (Figure 5.9B) positive staining was distributed randomly in all four zones of the cartilage but mainly in the superficial and deep zones. Considerably less staining was observed in the frozen negative control in comparison to the buffer negative control.

All facets which had been chondroitinase ABC treated (Figure 5.9C) showed less staining in comparison to both negative controls. Facet cartilage from C4/C5 left superior, C5/C6 left inferior, C5/C6 right inferior and C5/C6 left superior facets showed low levels of GAGs. Blue staining was absent from superficial, middle and deep zones. A band of blue staining was present in the calcified zone. The C4/C5 left inferior and C5/C6 right superior facet samples appeared to still contain some positive alcian blue staining in some of the cartilage zones. This was present mainly in the deep and calcified zones. Images of all eight facets stained with alcian blue are shown in Figure 5.9.

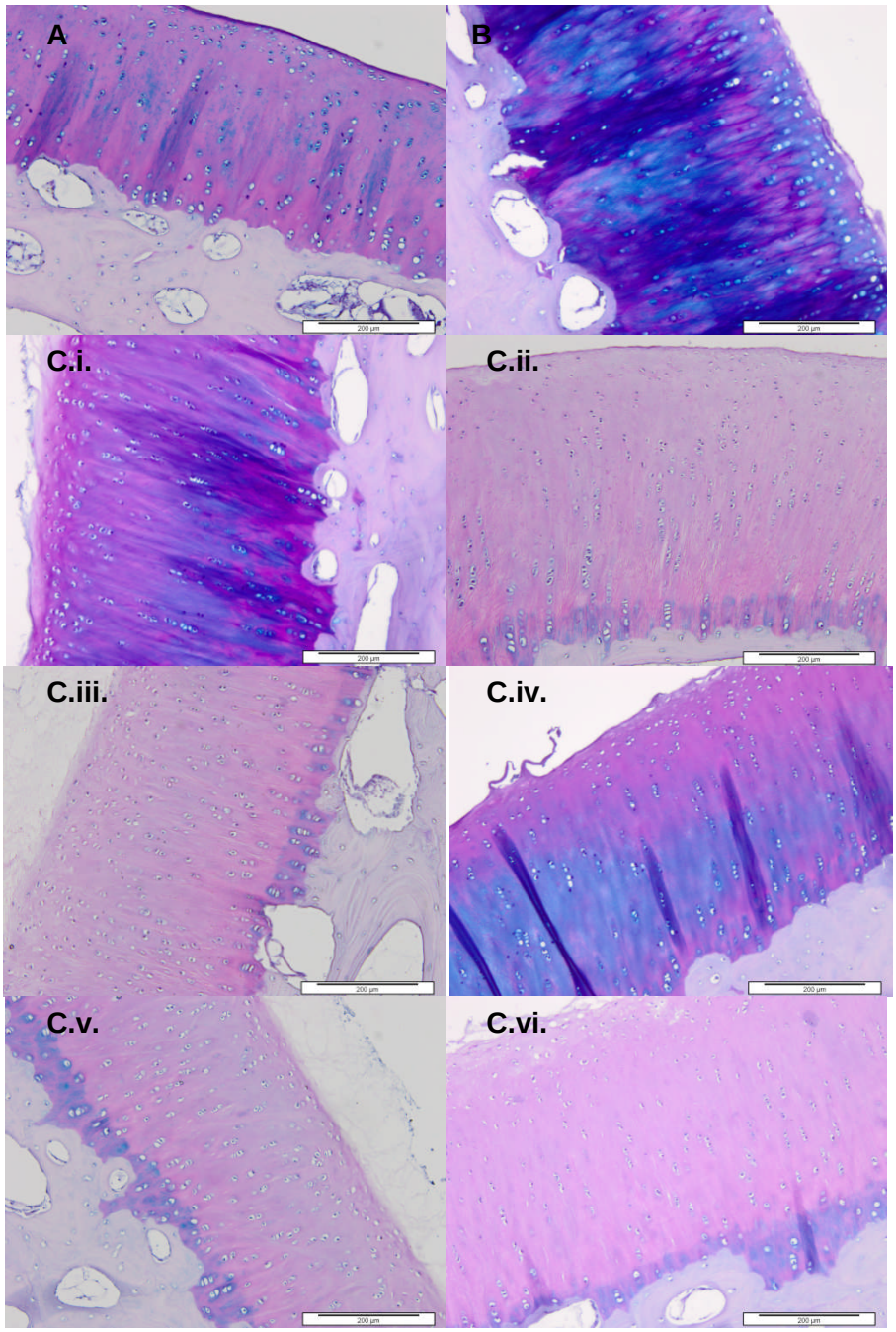


Figure 5.9: C4/C5 and C5/C6 facet sections stained with Alcian blue after chondroitinase ABC treatment including negative controls. A: C4/C5 right inferior facet, frozen negative control, B: C4/C5 right superior facet, buffer negative control, C.i: C4/C5 left inferior facet, C.ii: C4/C5 left superior facet, C.iii: C5/C6 right inferior, C.iv: C5/C6 right superior facet, C.v: C5/C6 left inferior facet, C.vi: C5/C6 left superior facet.

5.5.7. Characterisation of Chondroitinase ABC Treated Ovine Facet Cartilage Sections Stained with Sirius Red

Sections of the facet cartilage for each of the eight facets were obtained after treatment with chondroitinase ABC, fixation, decalcification, processing and wax embedding. The sections were stained with Sirius red and photographed.

Positive staining was present in the frozen negative control, C4/C5 right inferior facet, (Figure 5.10A) and was distributed randomly in the ECM. Only very small traces of stain could be observed in the superficial zone but large amounts were present in the middle, deep and calcified zones. Positive staining was also observed in the buffer negative control, C4/C5 right superior facet, (Figure 5.10B). This was largely distributed randomly in the ECM in the middle, deep and calcified zones. Similarly to the frozen negative control, only very faint staining was observed in the superficial zone. More staining was present in the frozen negative control than the buffer negative control.

The amount of positive Sirius red staining varied between all chondroitinase ABC facet cartilage samples (Figure 5.10C). Cartilage in left inferior facets of both C4/C5 and C5/C6 showed evenly distributed positive staining in the middle, deep and calcified zones. Some faint positive staining was observed in the C5/C6 left superior facet randomly distributed in the middle, deep and calcified zones. Very faint staining was observed in the C5/C6 right inferior facet around the lacunae of some of the cells and randomly distributed in the ECM in all four zones. No staining was present in the C4/C5 left superior and C5/C6 right superior facets. Images of all eight facets stained with Sirius red is shown in Figure 5.10.

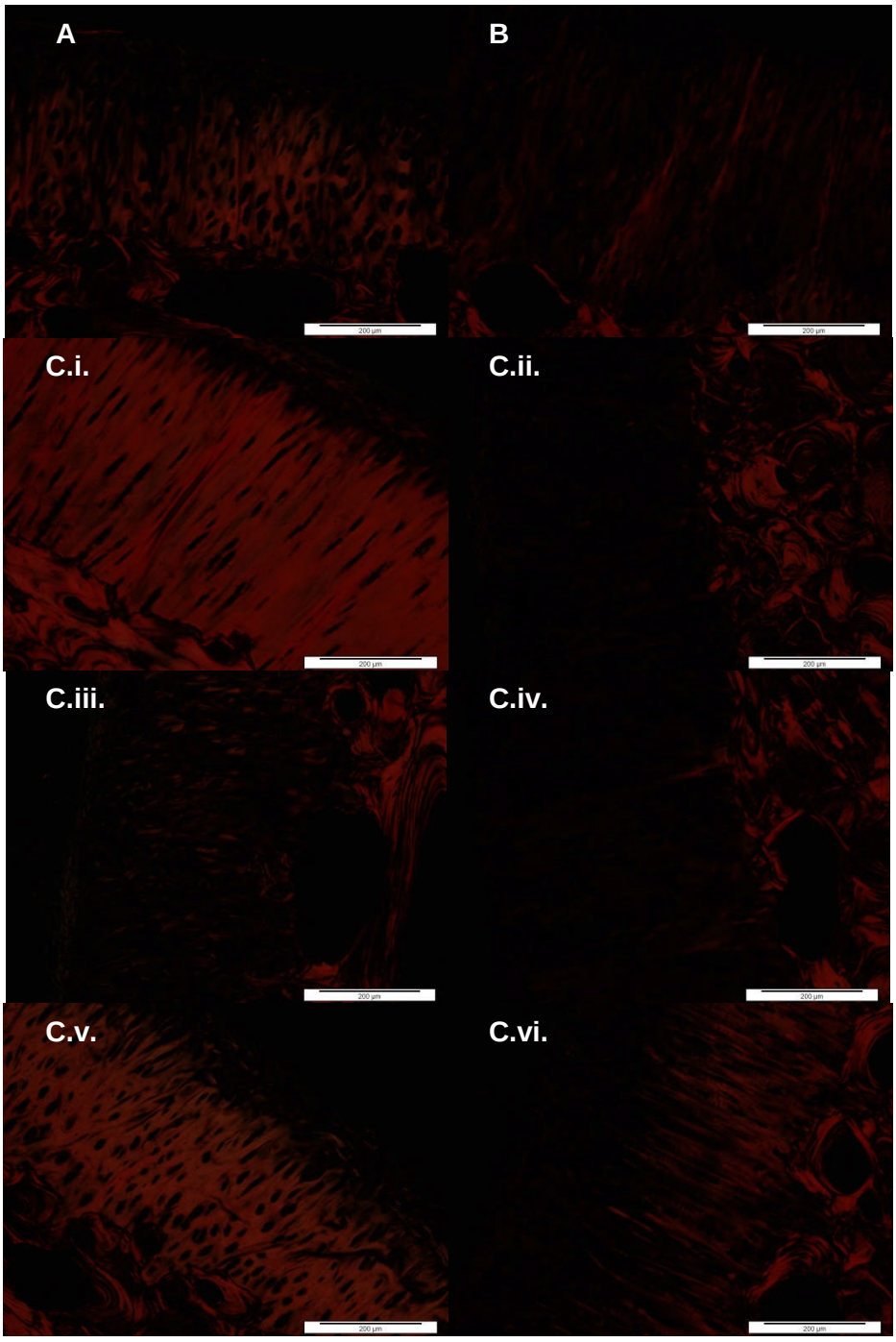


Figure 5.10: C4/C5 and C5/C6 facet sections stained with Sirius Red after chondroitinase ABC treatment including negative controls. A: C4/C5 right inferior facet, frozen negative control, B: C4/C5 right superior facet, buffer negative control, C.i: C4/C5 left inferior facet, C.ii: C4/C5 left superior facet, C.iii: C5/C6 right inferior, C.iv: C5/C6 right superior facet, C.v: C5/C6 left inferior facet, C.vi: C5/C6 left superior facet.

5.5.8. Characterisation of Chondroitinase ABC Treated Ovine Facet Cartilage Sections Stained with Miller`s Elastin

Sections of the facet cartilage for each of the eight facets were obtained after treatment with chondroitinase ABC, fixation, decalcification, processing and wax embedding. The sections were stained with Miller's elastin and photographed.

Some positive blue/black staining indicative of elastin was observed in the frozen negative control, C4/C5 right inferior facet, (Figure 5.11A) and the buffer negative control, C4/C5 right superior facet, (Figure 5.11B). In both controls, this was found in the lacunae within the deep zones of the cartilage.

Staining for elastin varied between facet samples treated with chondroitinase ABC (Figure 5.11C). Most facet cartilage samples were not positively stained. These included C4/C5 left inferior, C5/C6 left inferior, C5/C6 right inferior and C5/C6 left superior facet cartilage. The left superior C4/C5 facet cartilage samples showed positive staining around the lacunae of some of the chondrocytes in the deep zone. The cartilage in the C5/C6 right superior facet was positive for elastin around the lacunae of the cells in the deep zone and some traces of positive staining was found randomly distributed in the ECM in the middle and deep zones. Images of the eight facet cartilage samples stained with Miller's elastin are shown in Figure 5.11.

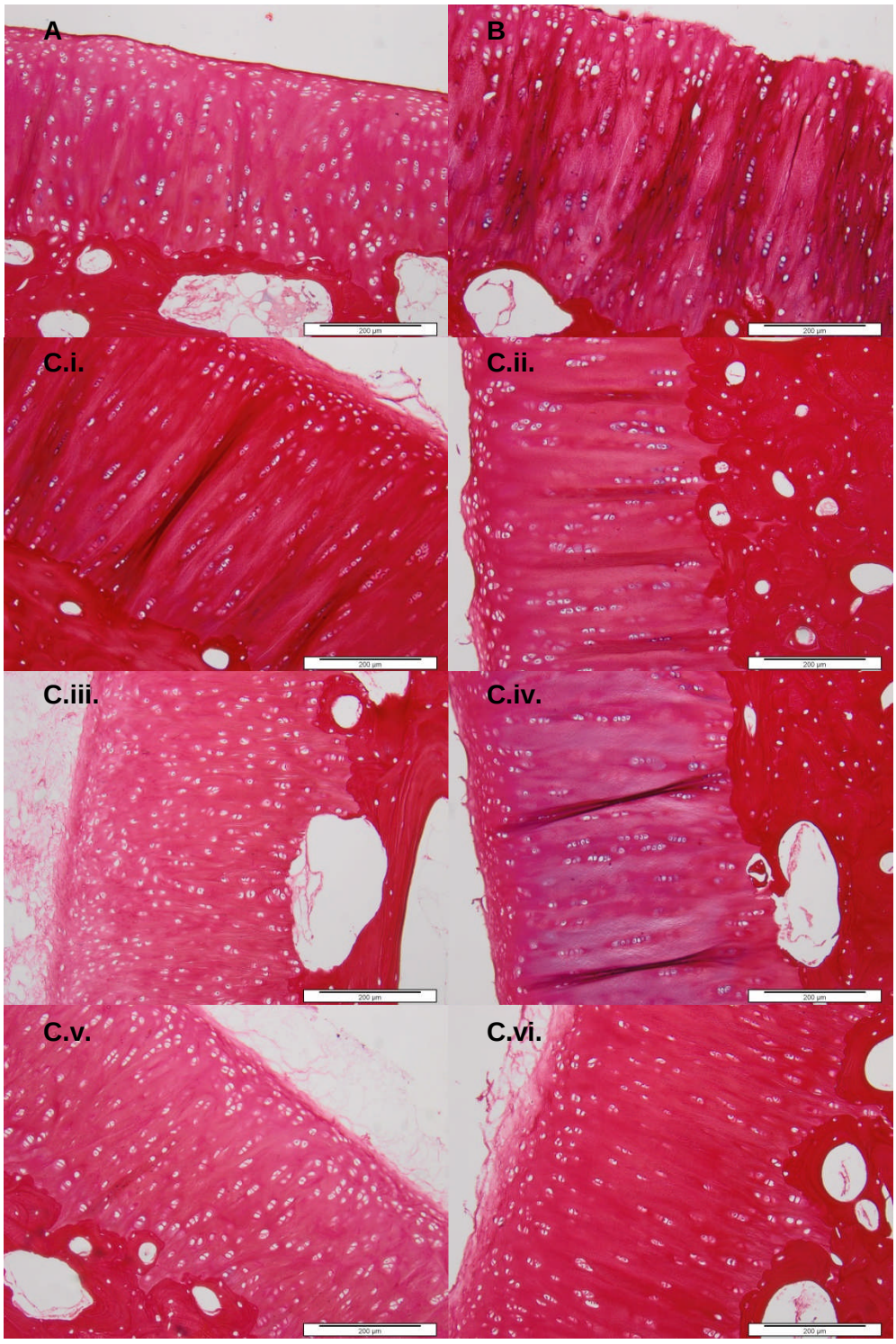


Figure 5.11: C4/C5 and C5/C6 facet sections stained with Miller's Elastin after chondroitinase ABC treatment including negative controls. A: C4/C5 right inferior facet, frozen negative control, B: C4/C5 right superior facet, buffer negative control, C.i: C4/C5 left inferior facet, C.ii: C4/C5 left superior facet, C.iii: C5/C6 right inferior, C.iv: C5/C6 right superior facet, C.v: C5/C6 left inferior facet, C.vi: C5/C6 left superior facet.

5.5.9. Localisation of Specific Markers in Sections of Chondroitinase Treated Ovine Facet Cartilage

In order to assess the presence and distribution of specific markers within the eight facet cartilage samples, immunohistochemistry was carried out using antibodies for chondroitin sulphate and collagen type II.

5.5.9.1. Chondroitin sulphate

Cartilage from frozen and buffer negative controls, facets C4/C5 right inferior (Figure 5.12A) and right superior (Figure 5.12B) respectively, showed the presence of intense brown staining in all zones of cartilage. More intense staining was present in the frozen negative control than the buffer negative control.

Chondroitin sulphate staining in chondroitinase ABC treated samples was considerably less than both negative controls. Staining in the left inferior facet (Figure 5.12C) was absent from the superficial and middle zones and was only present in the lower half of the deep zone and in the calcified zone. Staining in the left superior facet (Figure 5.12D) was absent in the superficial zone and present in the lower middle zone and both deep and calcified zones. Images of chondroitin sulphate staining in C4/C5 facet cartilage after chondroitinase ABC treatment and negative control facets are shown in Figure 5.12.

Cartilage from C5/C6 facets showed considerably less staining in comparison to the chondroitinase ABC treated C4/C5 facets and both negative controls. Staining was absent from the superficial, middle and deep zones. A band of staining was present in the lower calcified zone. Images of chondroitin sulphate staining in C5/C6 facet cartilage treated with chondroitinase ABC is shown in Figure 5.13.

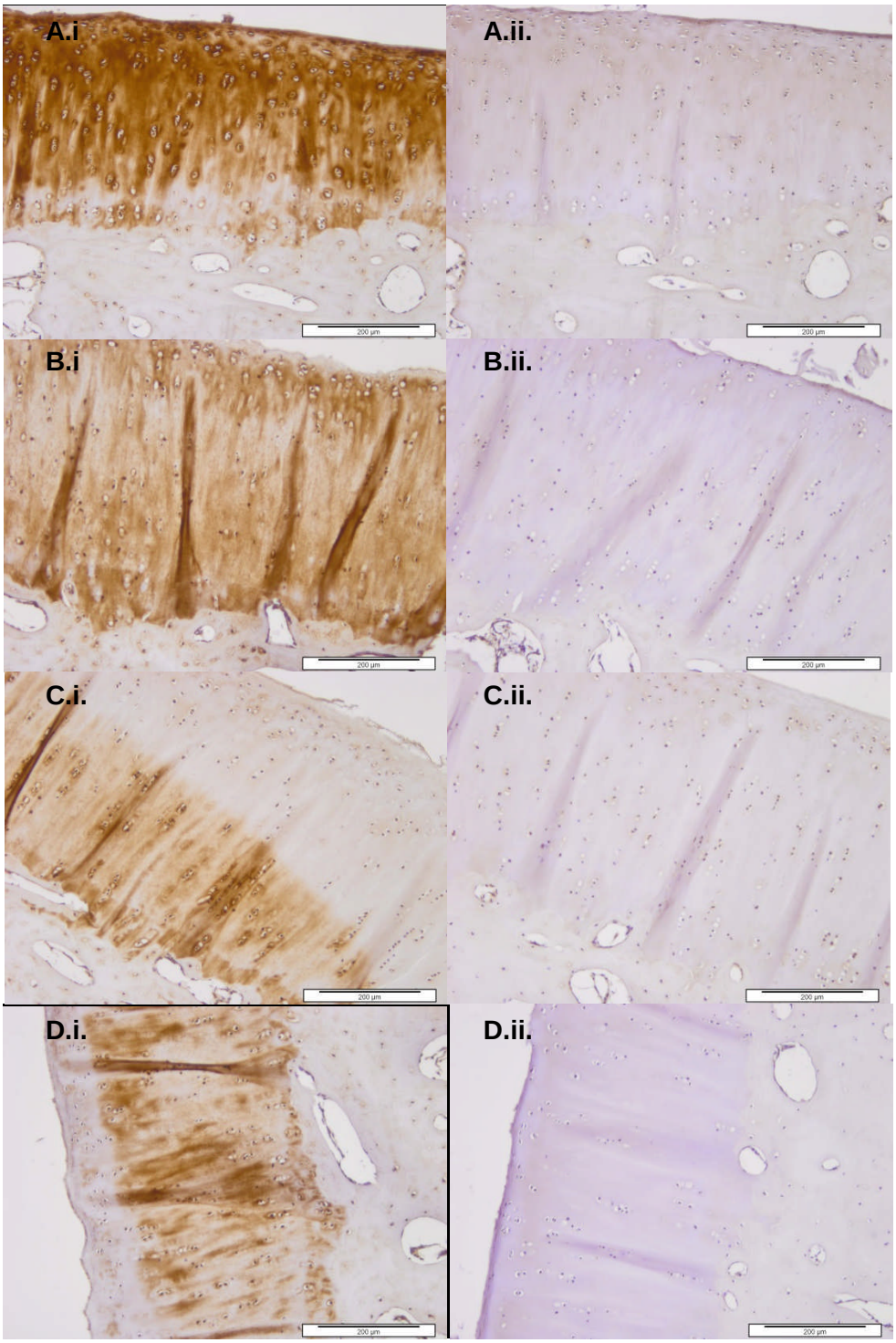


Figure 5.12: C4/C5 facet sections immunohistochemically stained with antibodies to chondroitin sulphate including negative controls. A: C4/C5 right inferior facet, the frozen negative control, B: C4/C5 right superior facet, the buffer negative control, C: C4/C5 left inferior facet, D: C4/C5 left superior facet stained with rabbit anti-sheep chondroitin sulphate polyclonal antibody (i) and rabbit IgG isotype control (ii).

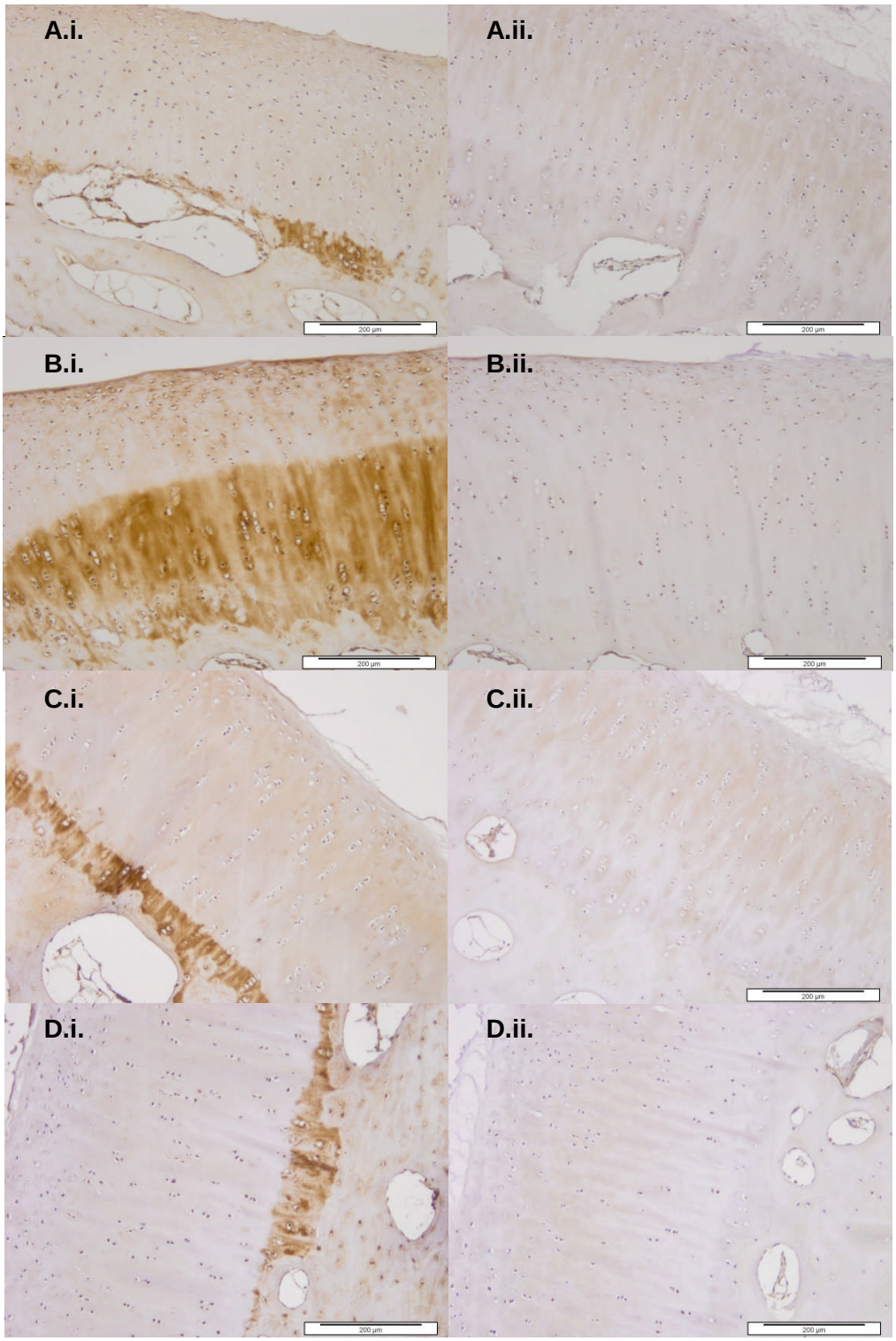


Figure 5.13: C5/C6 facet sections immunohistochemically stained with antibodies to chondroitin sulphate. A: C5/C6 right inferior facet, B: C5/C6 right superior facet, C: C5/C6 left inferior facet, D: C5/C6 left superior facet stained with rabbit anti-sheep chondroitin sulphate polyclonal antibody (i) and rabbit IgG isotype control (ii).

5.5.9.2. Collagen Type II

Positive staining for collagen type II was observed in the frozen negative control, C4/C5 right inferior facet, (Figure 5.14A). This was largely present in the superficial zone. Staining was also present in the middle, deep and calcified zones distributed randomly in the ECM. Similarly, positive staining was observed in the buffer negative control, C4/C5 right superior facet, (Figure 5.14B). This was largely present in the superficial and middle zones. Some staining was also observed in the deep and calcified zones randomly distributed in the ECM.

Cartilage from chondroitinase ABC treated C4/C5 facets (Figure 5.14C and 5.14D) showed positive staining for collagen type II in all four zones within their cartilage structure. Staining within the left inferior facet cartilage was less intense than that in the left superior facet. In the left inferior facet cartilage staining was largely observed in the superficial zones and sparsely distributed within the ECM. Staining was also present around the cells. In the inferior facet, staining was largely observed in the superficial and middle zones. Staining was sparsely distributed in the ECM randomly. No major differences were observed between the C4/C5 chondroitinase treated facet cartilage and the negative controls. Images of collagen type II staining within the cartilage of C4/C5 facets is shown in Figure 5.14.

Cartilage from the chondroitinase ABC treated C5/C6 facets showed positive staining for collagen type II in all four zones. Staining within the inferior facets was largely within the middle zones. Staining in the other three zones was distributed randomly within the ECM. In the left superior facet staining was largely present in the deep zone of the cartilage structure whilst in the right superior facet staining was largely found in the superficial zone. All remaining staining was found randomly distributed in the ECM. No major differences were observed between the C5/C6 chondroitinase treated facet cartilage and the negative controls. Images of C5/C6 facet cartilage stained with collagen type II is shown in Figure 5.15.

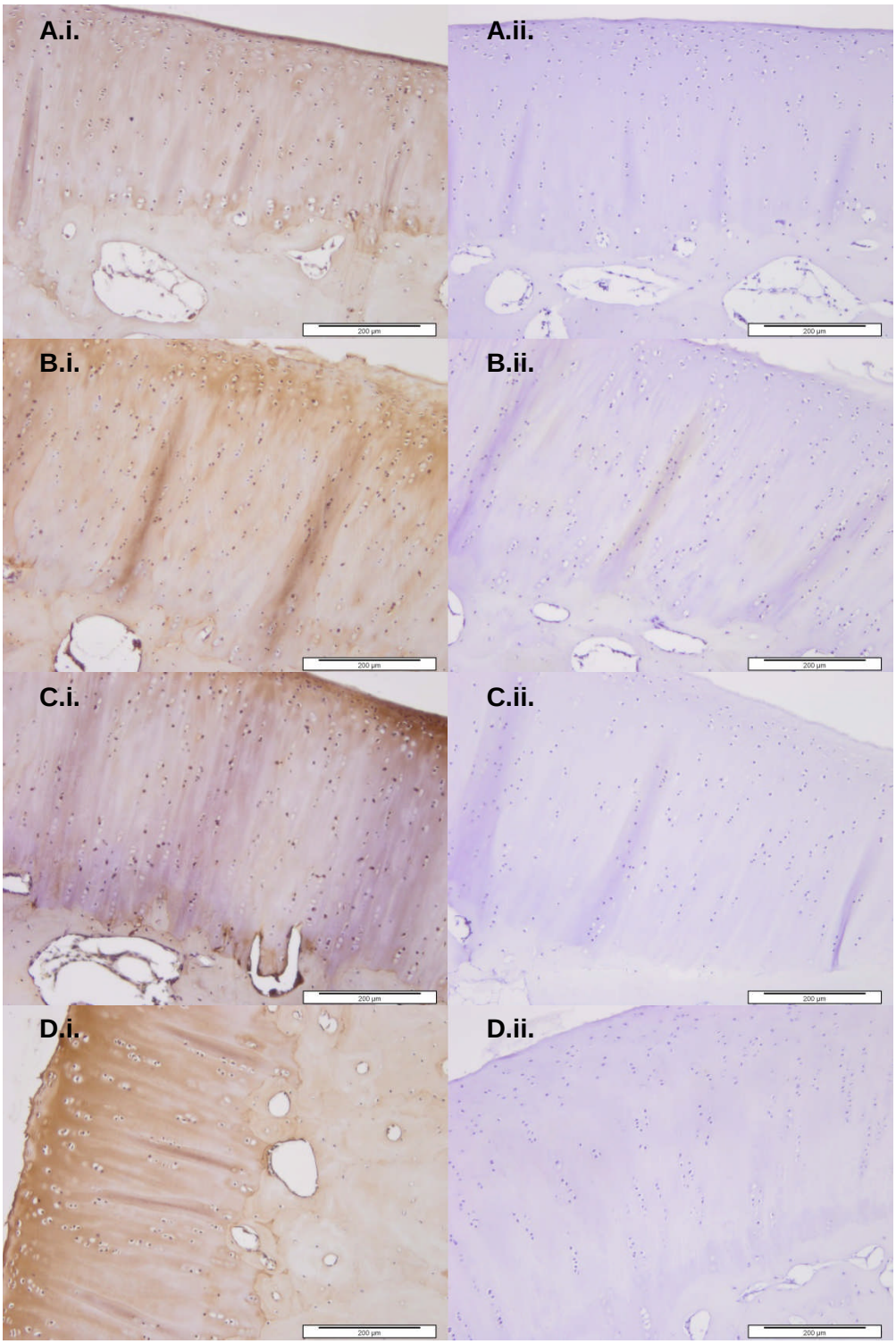


Figure 5.14: C4/C5 facet sections immunohistochemically stained with antibodies for collagen type II including negative controls. A: C4/C5 right inferior facet, the frozen negative control, B: C4/C5 right superior facet, the buffer negative control, C: C4/C5 left inferior facet, D: C4/C5 left superior facet stained with mouse anti-sheep collagen type II monoclonal antibody (i) and mouse IgG1 isotype control (ii).

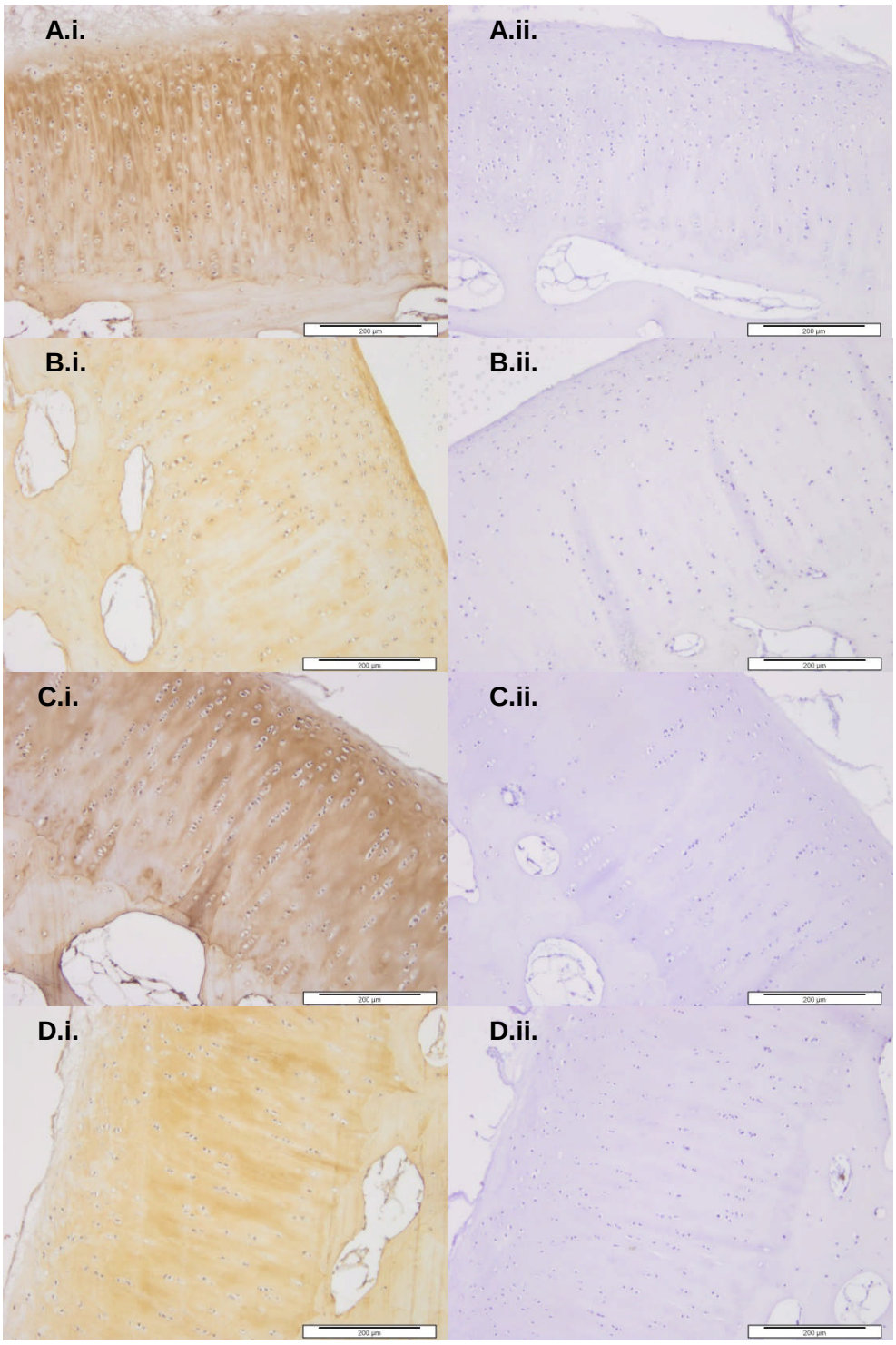


Figure 5.15: C5/C6 facet sections immunohistochemically stained with antibodies for collagen type II. A: C5/C6 right inferior facet, B: C5/C6 right superior facet, C: C5/C6 left inferior facet, D: C5/C6 left superior facet stained with mouse anti-sheep collagen type II monoclonal antibody (i) and mouse IgG1 isotype control (ii).

5.6. Discussion and Conclusions

The aim of this chapter was to develop a model of degenerated ovine facet cartilage which mimicked some properties of degenerated human facet cartilage. The work in this chapter used the enzyme chondroitinase ABC to remove GAGs from healthy ovine facet cartilage as this is one feature of degenerated human facet cartilage. Results from histology and immunohistochemistry showed that this was achieved whilst maintaining the general structure of the cells and collagen and some biomechanical properties.

The photographs of the treated and untreated facets showed that after undergoing enzyme buffer treatment with and without chondroitinase ABC, the tissue became white and paler in appearance. This would have been due to both the antibiotic and enzyme washes which removed any blood remaining after dissection. The enzyme treatment did not cause any visible damage to the surface of the cartilage after the washes at 4 and 37 °C. This finding was similar to that of a previous study which showed that chondroitinase ABC did not affect surface roughness (Katta *et al.*, 2008B).

The results from the GAG analysis of the tissues showed variation between samples. Again, the variation may have been due to the cartilage being sourced from facets at different positions which have been shown to have different cartilage thicknesses by needle indentation. The large difference between the high GAG content of the right inferior C4/C5 facet and low GAG content of the right superior C4/C5 facet may have been inherent in the tissues *in situ* or could have been due to the GAGs being washed out of the buffer treated control during incubation. The GAG content in chondroitinase ABC treated facets show that most samples had GAG reduction in comparison to the C4/C5 right inferior negative control, but not the buffer treated C4/C5 right superior facet control rendering the data equivocal. Previous studies have shown a reduction in GAG percentage in bovine articular cartilage after treatment with chondroitinase ABC (Basalo *et al.*, 2005; Basalo *et al.*, 2006; Katta *et al.*, 2008B).

Indentation testing of all eight facets suggested that depleting the GAGs from facet cartilage did not have a consistent effect on strain and deformation. Both negative controls had strain curves which reached equilibrium within the strain values of the treated facets. The C5/C6 right inferior facet had the lowest strain value and thickest cartilage in comparison to the other samples. However, facets with similar thicknesses had strain curves at the higher end of the scale. The differences between the strain curves were most likely due to differences in the properties of the cartilage from different facets within the FSUs, as indicated by the differences in thicknesses. These results were contradictory to the literature which suggests that chondroitinase ABC causes an increase in deformation and therefore strain (Katta *et al.*, 2008; Katta *et al.*, 2009). However, this is the first study carried out on chondroitinase ABC treated facet cartilage. The mechanical properties of ovine facet cartilage may differ to that from bovine knee cartilage. Despite this, the mean strain curve of the chondroitinase treated facets appeared to increase more rapidly in comparison to that of both negative controls (Figure 5.7). This suggested that although the overall deformation of the facet cartilage was not affected by chondroitinase ABC treatment, the rate at which the cartilage deformed was more rapid, which may have been due to the loss of GAGs. If this theory is correct, the biphasic properties of the treated cartilage may have been altered as the fluid phase reached equilibrium more rapidly due to increased permeability due to the GAG loss.

The H&E staining of both C4/C5 and C5/C6 facet cartilage showed that the general structure of the facet cartilage was maintained in comparison to the negative controls. The C4/C5 right inferior facet cartilage appeared to have a smoother surface in comparison to the surface of all other facet cartilage samples including that which underwent enzyme buffer only treatment. The tearing of the cartilage surface may have been due to incubating facet cartilage at 37 °C for 16 hours regardless of the content of the solution they were in. This was likely as the tissue had not been fixed and some initial breakdown of the tissue may have started occurring during the incubation stages. Therefore, it was unlikely that this was caused by the enzyme. Any small differences that occurred within the structure were likely to be a result of sample variation as no

two facets have the same structure and composition. The alcian blue staining showed great variation between the two control facet cartilage samples and those that had undergone chondroitinase ABC treatment. The C4/C5 right inferior facet, which was frozen after dissection and prior to analysis, showed much less staining than the C4/C5 right superior facet which had undergone enzyme buffer treatment. This was not expected, however, it is likely that sample variation may have contributed towards this observation. Alcian blue staining in all chondroitinase treated facet cartilage samples showed much less staining intensity. In most samples, the results showed that chondroitinase had stripped the GAGs through the cartilage zones as deep as the calcified zone. The band of blue staining appeared to show where the chondroitinase ABC enzyme had reached during the incubation time. Sirius red and Miller's elastin staining showed no differences between negative controls and chondroitinase ABC treated facet cartilage. This result was consistent with previous work which suggested that chondroitinase ABC did not alter the collagen type II framework within articular cartilage (Rieppo *et al.*, 2003; Basalo *et al.*, 2005). However, a previous study has suggested that chondroitinase ABC increased the number of exposed collagen fibrils (Jo *et al.*, 2006). Due to the limitations associated with Sirius red staining, it was not possible to deduce this from this study. Scanning electron microscopy would be suitable to determine this.

Similar findings were also seen in C4/C5 and C5/C6 facet cartilage sections immunohistochemically stained with antibodies to collagen type II and chondroitin sulphate. In facets treated with chondroitinase ABC, the enzyme had removed chondroitin sulphate from most zones within the cartilage. No observable differences were noted in collagen type II staining. Variations in collagen II and chondroitin sulphate staining within the facet cartilage samples was likely due to sample variation as each facet was located at different positions within the spine. The thickness measurements obtained using needle indentation showed that the thickness of the cartilage varied in each sample which may have also reflected the amount of chondroitin sulphate that chondroitinase ABC would have been able to remove.

A major limitation of this study was the number of replicates. Unlike cartilage from other joints, the facet has a small surface area and a curved shape. This makes removing flat pins from facets difficult and restricts the number that can be obtained from a spine. The only facets that are valid for pin taking are those from the cervical region as a result of this. Due to these restrictions in addition to a limited supply of ovine cervical spine tissue, only one of each type of negative control and only six facets were treated using chondroitinase ABC and analysed. If more time and a greater amount of tissue were available, the replicate number could be increased.

The results from this chapter suggest that chondroitinase ABC depletes GAGs from ovine cervical facet cartilage but that this does not have an effect on the deformation and strain. However, the data indicated that this was due to the variation between samples rather than the effect of the treatment. In retrospect, and given the knowledge on the variation between the facet samples it would have been prudent to conduct a paired experiment whereby analysis, using the methods described in this chapter, would be carried out both before and after treatment. Another method which could help to interpret the results in this chapter would be to carry out FE modelling in order to determine the permeability and elastic modulus of the treated and non-treated facet samples. This would allow evaluation of the biphasic properties of the negative controls in comparison to the chondroitinase ABC treated samples of ovine cervical facet cartilage. For example, the elastic modulus would give a more accurate measure of permeability and by how much cartilage deformed under a given load. If differences were found between articular cartilage in the facet in comparison to those found in other joints such as the hip or knee, this may help to explain the indentation properties deduced in this chapter.

Other treatment methods in addition to the incubation of cartilage with chondroitinase ABC have been previously used. Enzyme digestion is a common method for replicating cartilage damage. Trypsin is an enzyme which has been previously reported to remove proteoglycans in articular cartilage (DiSilvestro and Suh, 2002). However, the effect of trypsin on cartilage has been reported to be variable (Moody *et al.*, 2006). Other methods could also involve using

collagenases to remove collagen (Bank *et al.*, 2000). Removing collagen will make cartilage more permeable and less able to resist compressive loads by holding repelling proteoglycans together. This would ultimately lead to its degeneration. As well as enzymatic treatment, chemical treatment using a chemical such as SDS could also degrade the structure of cartilage as well as physical treatment. Physical treatment such as compression to induce degeneration may also be a potential method and has been previously reported to induce degeneration in the IVD *in vivo* (Lotz *et al.*, 1998). Another *in vivo* study involved injecting monosodium iodoacetate into the facet joints of mice (Kim *et al.*, 2011). The authors reported severely damaged facet joint cartilage, proteoglycan loss and changes in the structure of the subchondral bone.

As the characteristics of degenerate human facet cartilage have not yet been deduced in the study running parallel to the present work (Section 1.8), it was not possible to compare the features observed here. This will ultimately be the next step in this study.

Chapter 6:

General Discussion

Chapter 6: General Discussion

Back pain is currently a global problem affecting 84 % of people at some point in their lives. The condition not only causes a great deal of discomfort and affects quality of life, but leads to economic loss through work absence and health care costs. The causes of back pain are muscular or a result of the degeneration of FSU components including posterior ligaments, the IVD and facet joints (Maniadakis and Gray, 2000; Mosley *et al.*, 2012). Much attention has focused on the IVDs as a source of pain however, in recent years this attention has shifted towards the facet joints. Facet joint osteoarthritis is thought to affect up to 15 % of people suffering from back pain. Similarly to osteoarthritis in other joints in the body, including the knee and hip, the facet joint cartilage is thought to be the tissue primarily affected.

Current therapies for back pain include analgesics, physiotherapy, spinal fusion and TDRs (Section 1.5). Although some of these therapies have been reported to relieve patient symptoms and contribute to a better quality of life, they are not curative. Current therapies either treat the affected site leading only to short term relief or completely remove the source of pain and/or replace it with an artificial material which offers long term relief but may lead to additional problems including ASD (Section 1.5.3). An ideal treatment would involve replacing the tissue responsible for the source of pain with functioning tissue, developed using tissue engineering. Attempts have been made in the last decade to develop a tissue engineered functional IVD (Mizuno *et al.*, 2004; Mizuno *et al.*, 2006; Nesti *et al.*, 2008; Wan *et al.*, 2008). However, only one study has considered developing a cartilage substitution biomaterial for the facet joint cartilage (Elder *et al.*, 2010). A major limitation in the development of such a therapy for the facet joint cartilage is the current lack of knowledge of its biology.

Therapies for the IVD, developed using tissue engineering approaches have not currently reached the clinic. Before such therapies could be used in patients, they would require pre-clinical testing for safety and function. Limited literature

exists regarding any pre-clinical models that could be used. To ensure full testing of the replacement including mechanical and biological compatibility, it would be necessary to use an *in vivo* model. Whilst *in vivo* models can be used, it is both desirable and ethical that novel therapies are only tested in living animals following extensive pre-clinical evaluation *in vitro.* The use of a physiological, mechanically interactive natural FSU *in vitro* model for the pre-clinical testing of novel therapies in the spine would provide a means of testing a wide range of products for failure early in the product development cycle and hence minimise the use of living animals. The first steps towards the development of such a pre-clinical model were to determine a source of natural healthy FSU`s for use in the model, to fully characterise the tissues and develop degenerated FSU`s which exhibited biotribological characteristics similar to the degenerated human FSU.

The aim of this study was to characterise healthy ovine facet cartilage and IVD tissue including the AF, NP and CEP and develop a model for degeneration in the ovine FSU. The age of sheep that would provide healthy and degenerate tissue was investigated as well as determining whether major differences existed between sheep of different breeds. Biological characterisation was carried out to determine the structure of these tissues, the expression of collagen types, proteoglycans and other important proteins and the phenotype of the cells. Some biomechanical characterisation was carried out using indentation tests to determine the percentage deformation and strain of ovine facet cartilage. Chondroitinase ABC was used to deplete GAGs from ovine facet cartilage in an attempt to mimic the features of degenerated human facet cartilage.

The study was necessary because of the limited knowledge of the biology of facet cartilage. Ovine tissue was used since the sheep spine has been previously reported in the literature to exhibit similar biomechanical properties to the human spine (Wilke *et al*., 1997; Moore *et al.*, 1999; Wilke *et al.*, 1999; Kandziora *et al*., 2001). As a result, the sheep is the most suitable and accessible animal model to be used as a source of tissue for future *in vitro* models. However, the age at which sheep begin to show signs of spinal

degeneration was unknown at the start of this study and therefore it was necessary to undertake a detailed investigation of the relationship between the age of the animals and degeneration of the FSU. Chondroitinase ABC has been previously used to deplete GAGs from cartilage and was therefore used to achieve the same result in ovine facet cartilage. As the loss of GAGs is a well-known feature of cartilage degradation, this represented the first step towards developing an ovine FSU which mimicked the biotribology of degenerated human facet cartilage. In the future, this model could then be used in a simulator to pre-clinically test cartilage substitution biomaterials and other tissue engineering therapies.

This study was novel since, at the time of writing, only one study had investigated the biological features of facet cartilage (Elder *et al.*, 2009). This study was limited to canine lumbar facet cartilage tissue. In the present study, the biological features of ovine facet cartilage were studied from all cervical, thoracic and lumbar regions. In addition, the cell phenotype was also deduced. The anatomical study of ovine FSUs was also novel as there was no literature which had documented changes in IVDs and facet cartilage in sheep of different ages and breeds. Lastly, although chondroitinase ABC has been previously used to deplete GAGs from articular cartilage, the method had not been used on facet cartilage (Katta *et al.*, 2008B).

The aim of the anatomical study was therefore to determine the age at which ovine spines degenerate and whether significant differences were present between different breeds including the Charollais, Suffolk and Texel sheep. The different breeds of sheep used in this study were a major limitation. Due to difficulties in obtaining ovine tissue of different ages it was not possible to source spines of a given breed. As a result, some age groups consisted of more than one breed. This would have undoubtedly contributed to variation in the data generated. However, as statistical analysis only found one significant difference between Charollais, Suffolk and Texel breeds of the same age, it was assumed that the differences between these three breeds of sheep were acceptable. The 8-10 year age group, however, consisted of only the Hebridean sheep. This breed was not compared to sheep of different breeds in the 3-4

year old age group because it was not possible to obtain young Hebridean sheep. Therefore, it cannot be concluded that changes in the 8-10 year age group were independent of breed.

Another limitation of the anatomical study was the sample size. Due to cost and difficulties in obtaining ovine tissue, the sample size of each age group was limited to three (with the exception of the 3-4 year age group which also investigated differences in breed). The low sample size may have masked differences in the parameters analysed between age groups. Given more time to obtain sheep spines, a larger budget and more time, the sample size would ideally have been increased to 6-10 which may have highlighted more differences between age groups.

Grading systems were used to deduce the extent of degeneration present in the tissues of the IVD and facet cartilage. These grading systems or similar grading systems had been used in previous studies to track degenerative changes in the spine (Thompson *et al.*, 1990; Weishaupt *et al.*, 1999; Gries *et al.*, 2000; Sive *et al.*, 2002; Kettler and Wilke, 2006; Tischer *et al.*, 2006; Li *et al.*, 2011; Varlotta *et al.*, 2011A; Lee *et al.*, 2012). The limitation of using grading systems is that they are subjective and the grades assigned may vary considerably between graders, despite being trained in a similar manner, particularly when there is little distinction between each grade. This was evident in the results for the IVD grading of the transverse histological sections in which the kappa test found only a slight agreement between graders. This may have affected the correlation between grade and age and may explain why no significant differences were found between different age groups. Despite this, there was a fair agreement between graders for the grading of the sagittal histological sections of the IVDs and moderate agreements between graders for the grading of the facet photographs and histological sections. One way to ensure accuracy of grading data is to enrol a greater number of graders. In further studies of this nature, three or four trained graders should ideally be used. In addition, given more time, the grading would ideally have been repeated after six months and again after one year to check the repeatability of the results.

A limitation associated with the µCT data generated was the resolution of the scans. They were taken at a standard resolution of 74 µm. If a higher resolution had been used, this would have made it easier to distinguish between trabeculae and between bone and the IVD. However, this was a minor issue and one that did not have a great effect on the data. The use of µCT is a powerful tool for determining the properties of the FSU and is non-invasive.

The grading results confirmed that degeneration in the sheep spine increased with age particularly in the cervical samples where good correlations were found for grades of degeneration in the sagittal histological sections of the IVDs, the facet photography and the facet histology, with the exception of the transverse histological sections of the IVDs. There was also a significant difference between the 0-1 year and 5-6 year age group for the cervical sagittal histological sections of the IVDs. In general, an increase in grade in most samples was recorded at either 5-6 years or 8-10 years. The grading data therefore suggested that degeneration began at five years of age. The µCT results showed that IVD height generally decreased with age. Most of the significant differences present were between the 0-4 and 5-10 year age groups suggesting that degeneration began at 5-6 years of age. Generally, the greatest effects of age on degeneration in the sheep spine were found in the cervical FSU samples. This indicated that degeneration was present largely in the cervical region of the spines. This may have been due to the greater range of motion within the cervical spine of the sheep. As it was concluded that healthy tissue could be obtained from 0-4 year old tissue and that skeletally mature tissue was most likely to be present in the 3-4 year age group, 3-4 year old tissue was used in the characterisation study (Chapter 4).

The aim of the characterisation study was to determine the structure of 3-4 year old ovine Texel facet cartilage, AF, NP and CEP tissue including the distribution of common collagen types, proteoglycans and other proteins that have previously been reported to make up the extracellular matrix of these tissues in the sheep and in other species. The phenotype of the cells from each of the tissues (from a 3-4 year old Charollais sheep) was also determined as well as the quantity of GAGs (from a range of ages and breeds of sheep) and

percentage deformation within cervical facet cartilage from a 3-4 year old sheep.

Previous studies have reported on the biology of chondrocytes and IVD cells (Gruber and Hanley, 2000; Horner *et al.*, 2002; Gan *et al.*, 2003A; Risbud *et al.*, 2003; Brodkin *et al.*, 2004; Acosta *et al.*, 2006). This includes a study which isolated human AF cells and analysed them in monolayer cultures at passages one to four using antibodies to collagen types I and II, chondroitin sulphate and keratan sulphate (Gruber and Hanley, 2000). They found that cells in monolayer had a spindle-shaped morphology and chondroitin sulphate was present in abundance around the cells. Collagen types I and II expression within and around the cells, however, were sparse. Another study investigated the phenotype of rabbit NP cells which were found to express collagen types I and II and CD44 (Gan *et al.*, 2003A). The phenotype of chondrocytes from osteoarthritic sheep has also been investigated (Acosta *et al.*, 2006). In this study, gene expression and proliferation analysis of chondrocytes showed a decrease in collagen type II and aggrecan expression in aged, osteoarthritic and passaged cells. Facet cartilage cells have not been previously analysed.

A major limitation in the phenotyping of ovine FSU cells in the present study was the fact that this was carried out on cells that had been cultured in monolayer. Previous studies have reported a change in phenotype of chondrocytes and dedifferentiation to fibroblasts in monolayer culture particularly after passage 6 (von der Mark *et al.*, 1977; Archer *et al.*, 1990). In order to investigate this, FSU cells were analysed at passages four, six and eight to determine whether a change in phenotype occurred with increased passage. The expression of collagen types I and II was monitored to identify whether a change to the fibroblast phenotype occurred. The results showed no change in phenotype between the passages and maintenance of collagen type II expression indicating that the cells maintained their phenotype in culture and the validity of the data. Moreover, the aim of the cell characterisation study was to determine major difference in the phenotype of cells from the different tissues of the FSU rather than determine their exact phenotype. Monolayer cell culture can be used for comparative studies as the cells have undergone the same

treatment and are tested under the same conditions. In order to report a more accurate phenotype of the FSU cells, 3D culture could have been used. This would involve transferring cells after isolation to a 3D environment such as alginate beads or collagen gels (Horner *et al.*, 2002). The study showed that collagen types I and II were expressed by FSU cells with greater expression of type II than type I in contrast to the study by Gruber and Hanley (2000). Collagen types III and VI were also expressed along with small amounts of collagen type X in some cells. Collagen type V was not expressed by any cells. Other important markers including CD44, chondroitin-6-sulphate, fibronectin and SOX-9 were also highly expressed by the FSU cells as has been previously reported for chondrocytes and IVD cells (Hayashi *et al.*, 1996; Knudson and Loeser, 2002; Hattori *et al.*, 2010; Henrotin, 2010).

A limitation in the tissue characterisation study presented here was the sample size for the quantification of GAGs in facet cartilage. This was due to difficulties, as previously mentioned, in obtaining ovine tissue. Only one replicate was available in the 0-1 year and 5-6 year age groups and only two replicates in the 8-10 year age group. This in turn meant that no statistical analyses could be performed to determine whether significant variation existed between the age groups. However, as the main aim of the study was to determine the quantity of GAGs in the 3-4 year age group, this was achieved.

A major limitation in the study of facet cartilage was the small size of facets and small surface area of cartilage. This meant that only a small amount was available to analyse. In the case of histology and immunohistochemistry which only require thin sections of tissue, this was not an issue. However, for biochemical assays and mechanical tests this presented some problems. The GAG assay required dilution with papain buffer for optimal results and the hydroxyproline assay was not optimised due to time restrictions. For indentation testing, only cervical facets could be analysed as they were the only facets with a large enough flat surface area from which pins could be removed. Only one pin could be removed from each facet. As only one FSU was available for indentation (due to tissue restrictions), only four facets could be removed and four pins analysed. The percentage deformation of ovine (Texel) cervical facet

cartilage in general could have been more accurately determined, given more samples.

The tissues of the healthy IVD have been extensively investigated in previous studies (Beard *et al.*, 1980; Thompson *et al.*, 1990; Roberts *et al.*, 1991; Antoniou *et al.*, 1996; Bruehlmann *et al.*, 2002; MWale *et al.*, 2004; Wade *et al.*, 2011). These studies all report a tough collagenous AF, rich in collagen type I in the outer region and type II in the inner region, and a hydrophilic, gelatinous NP rich in collagen type II. Roberts *et al.* (1991) reported the presence of collagen type VI around AF and NP in the all regions of the human, cow, sheep and rat IVDs. Mwale *et al.* (2004) reported a GAG:hydroxyproline ratio of 27:1 in the human lumbar NP and a ratio of 2:1 in the human lumbar CEP. This study made an attempt to distinguish the ECM of the IVD and hyaline cartilage as their components are extremely similar. Only one study has reported on the biochemical structure of facet cartilage (Elder *et al.*, 2009). This, however, was from canines.

For the sheep FSU tissues analysed here, patterns of collagen and GAGs matched the distribution patterns previously reported in the literature (Antoniou *et al.*, 1996; Buckwalter and Mankin, 1997; Temenoff and Mikos, 2000). The average percentage of GAGs in dry weight facet cartilage was also in the similar range to that of articular cartilage. Similar staining patterns between collagens types III and VI and elastin appeared to exist within the facet cartilage and IVD tissues suggesting a relationship between them. A relationship between collagen types III and VI has previously been suggested in other studies (Koller *et al.*, 1989; Chu *et al.*, 1990; Roberts *et al.*, 1991A). Finally the deformation of 3-4 year old ovine cervical facet cartilage appeared to show a strain curve characteristic of articular cartilage. This suggests that facet cartilage exhibits similar biphasic properties.

The characterisation study provided essential knowledge on the biology of ovine facet cartilage and its nearby IVD tissue that has not previously been reported. As well as providing a clearer understanding of facet cartilage. This can now be compared to the biology of degenerated human facet cartilage to identify

similarities and differences which will be essential when modelling human FSU therapies in an ovine FSU model in a simulator. The next stage of the study was to begin to explore methods by which ovine facet cartilage could be manipulated to mimic the degenerate biotribology.

Studies have previously been carried out to try and mimic degenerated features seen in human osteoarthritis both *in vivo* and *in vitro* (Lotz *et al.*, 1998; Phillips *et al.*, 2002; Ariga *et al.*, 2003; Holm *et al.*, 2004; Jo *et al.*, 2006; Rousseau *et al.*, 2007; Katta *et al.*, 2008; Kim *et al.*, 2011). Models of experimentally induced degeneration can be the result of either mechanical or structural changes. Mechanical alterations involve a change in loading and therefore distribution of forces throughout the tissue whilst structural alterations affect tissue function by affecting the molecular components (Lotz, 2004). Some authors have reported disorganisation of tissue and an increase in the percentage of cells undergoing apoptosis when tissue such as the AF is exposed to external compression (Lotz *et al.*, 1998; Ariga *et al.*, 2003). Some studies have involved stab incision which has resulted in the loss of proteoglycans and cellularity in addition to structural changes (Holm *et al.*, 2004; Rousseau *et al.*, 2007). Chemical and biological treatments have also resulted in proteoglycan loss and alterations in the structures of neighbouring tissue including bone and cartilage (Jo *et al.*, 2006; Katta *et al.*, 2008; Kim *et al.*, 2011). Only one study has attempted to produce a degenerated facet joint (Kim *et al.*, 2011). This however was in an *in vivo* system. No previous studies have attempted to degenerate facet cartilage *in vitro*.

The initial approach that was taken to degenerate healthy ovine facet cartilage was to deplete the GAGs using chondroitinase ABC. The results showed that this successfully removed GAGs from facet cartilage. This had an effect on the intensity of alcian blue staining and in general did not affect the overall structure of the cartilage or the distribution of collagen and elastin. The major limitation of the study was the number of replicates. Two negative controls and six treated samples were analysed. The results from the GAG assay and indentation testing showed great variation between the samples despite the samples originating from neighbouring FSUs in the same spine. Testing of a greater

number of samples might have identified differences between controls and treated samples. In addition, if the study was repeated it would be useful to conduct a paired test by testing each sample before and after treatment. This was because in some cases, the differences in the biology between the treated and controls were greater than the effect of chondroitinase ABC. This made differences in GAG content and percentage deformation difficult to draw conclusions from.

This study has the potential to lead to future studies in order to further characterise ovine facet cartilage and its other surrounding tissues and develop an *in vitro* model of a degenerated ovine FSU for pre-clinical testing. Firstly, any future study should ideally have a high replicate number of at least n>10 to draw accurate conclusions. In addition, the source of ovine tissue for use in comparative and characterisation studies should be limited to only one breed. It may also be useful to conduct a wider study into the study of sheep of different breeds to highlight differences between them. This is important as currently many studies have used ovine tissue of different breeds (Reid *et al.*, 2002; Melrose *et al.*, 2009; Hasler *et al.*, 2010).

The anatomical study could be expanded to include more replicates. It would also be advantageous to include a greater number of graders and repeat grading over time. The study of breeds could also be expanded to include a greater range of sheep that have been used in research, such as the Merino and white Swiss Alp breeds (Melrose *et al.*, 2009; Hasler *et al.*, 2010).

Characterisation of the ovine facet cartilage and IVD cells and tissue could also be further expanded. Cells could be transferred to 3D culture immediately after isolation. This would allow for the cells to be in an environment closer to their natural one and therefore allow them to exhibit their true characteristics. Methods for 3D cell culture that have previously been used and have proved to be successful include culturing cells in alginate beads and hydrogels (Bonaventure *et al.*, 1994; Gruber and Hanley, 2000; Horner *et al.*, 2002). Another way in which FSU cells could be analysed is by organ culture as has been previously carried out (Risbud *et al.*, 2003). In this study, whole IVDs were

cultured with their end plates intact. NP tissue was then removed using a micro curette and the cells analysed under a confocal microscope using immunofluorescence. Another way of determining FSU phenotype more accurately would be to carry out gene expression studies. Similar studies have been previously carried out in IVD tissue (Sive *et al.*, 2002). In situ hybridisation was used to identify SOX-9 and collagen type II using ^{35}S cDNA probes which indicated strong mRNA signals in healthy tissue. The use of this type of method would provide information at the molecular level.

A limited range of chondrocyte and IVD markers were investigated in this study. Other potential markers which could be used in future cell and/or tissue studies include those for collagens types IV, V, X, keratan sulphate and COMP. In addition, the hydroxyproline and DNA content of both facet cartilage and IVD tissue could be quantified as has been previously carried out in canine facet cartilage (Elder *et al.*, 2009).

Different microscopy methods could be used to obtain more accurate and detailed information on the structure and organisation of cartilage at high magnification. For example, atomic force microscopy (AFM) and scanning electron microscopy (SEM) could be used to determine the surface roughness of facet cartilage in comparison to articular cartilage from other joints. Transmission electron microscopy (TEM) could also be used to examine very small sections of tissue from different areas of the facet cartilage and AF. Cupermuronic blue staining could be used to stain ultra-thin sections of the tissue prior to examination by TEM to view the arrangement of GAGs. As well as microscopy, another useful imaging technique that could be used is magnetic resonance imaging (MRI). This highlights differences in water content and therefore can be used to identify changes of hydration within the different zones of cartilage.

In order to improve the biomechanical characterisation of ovine facet cartilage in this study, FE modelling may be an option for determining the biphasic properties. FE modelling has been frequently used in the literature to obtain a clearer understanding of the biphasic properties of articular cartilage

(DiSilvestro and Suh, 2002; Latif *et al.*, 2012; Sakai *et al.*, 2012; Richard *et al.*, 2013). This would enable the permeability and Young's modulus of cartilage to be deduced. A previous study by Latif *et al.* (2012) has carried this out on 4-5 year old ovine facet cartilage rather than 3-4 year old samples.

In addition to chondroitinase ABC treatment, other methods could be used to initiate degeneration in facet cartilage. Chymopapain has been previously used in IVDs to initiate proteoglycan loss, decrease disc height and induce loss of biomechanical stability. The effects of chymopapain on facet cartilage have not been previously reported but may lead to similar changes. The limitations of using chymopapain are its toxicity at high doses and lack of matrix specificity (Lotz *et al.*, 1998). The use of monosodium iodoacetate in facet joints to stimulate osteoarthritis has been previously reported in the mouse (Kim *et al.*, 2011). This may have the potential to produce similar outcomes *in vitro* such as damage to the facet cartilage, loss of proteoglycans and changes in subchondral bone. Another biological treatment to degenerate facet cartilage is to use collagenase (Banks *et al.*, 2000). Mechanical treatment can also be used by compressing facet cartilage using excessive loading. It may also be useful to determine what happens after a stab incision has been created on the surface of facet cartilage after a certain period of time.

Once a set of methods have been optimised to produce similar features to that of degenerated human facet cartilage, other components of the FSU including the IVD, CEP and vertebral bodies could then be modified to mimic degeneration. Ideally, once a whole ovine FSU model, which mimics a degenerated human FSU, has been created, it will be essential to transfer this model into an *in vitro* organ culture system. This would allow a whole FSU to be alive and functioning as it would *in vivo*. As a result, cartilage substitution biomaterials and other therapies for the spine developed through tissue engineering could then be tested in the model to determine the response of viable degenerate tissue.

6.1. Conclusions

In summary, the main findings of this study are:

- Degeneration in the ovine spine begins at 3-4 years of age.
- Ovine FSU tissue is rich in collagen types I, III, VI, chondroitin sulphate, CD44, fibronectin and SOX-9.
- A structure/function relationship may exist between collagen types III and VI and elastin.
- Ovine cervical facet cartilage displays biphasic properties.
- Chondroitinase ABC depletes GAGs from ovine cervical facet cartilage but does not have a consistent effect on strain and deformation.

The work carried out in this study has contributed largely to increasing knowledge of facet cartilage. Research into this tissue was previously very limited and much of the work carried out was related to the biomechanics of the facet joint. Biological studies relating to the facet joint were previously limited to the joint capsule. In addition, an anatomical study of ovine FSUs of different ages and breeds showed that degeneration begins at 5-6 years of age. This has not previously been reported and is important information as the sheep model is currently widely used in research today particularly in the spine.

Chapter 7: References

Chapter 7: References

Abenhaim, L., Rossignol, M., Valat, J. P., Nordin, M., Avouac, B., Blotman, F., Charlot, J., Dreiser, R. L., Legrand, E., Rozenberg, S., Vautravers, P. (2000). The role of activity in the therapeutic management of back pain. Report of the international Paris Task Force on Back Pain. *Spine* **25**, 1S-33S.

Acosta, C. A., Izal, I., Ripalda, P., Douglas-Price, A. L., Forriol, F. (2006). Gene expression and proliferation analysis in young, aged, and osteoarthritic sheep chondrocytes Effect of growth treatment. *Journal of Orthopaedic Research* **24**(11), 2087-2094.

Adams, M. A., Hutton, W. C. (1980). The effect of posture on the role of the apophysial joints in resisting intervertebral compressive forces. *The Journal of Bone and Joint Surgery* **62**, 358-362.

Adams, M. A., Hutton, W. C. (1981). The relevance of torsion to the mechanical derangement of the lumbar spine. *Spine* **6**, 241-248.

Adams, M. A., Hutton, W. C. (1983). The mechanical function of the lumbar apophyseal joints. *Spine* **8**, 327-330.

Adams, M. A., Dolan, P. (2005). Spine biomechanics. *Journal of Biomechanics* **38**(10), 1972-1983.

Ahmed, N., Stanford, W. L., Kandel, R. A. (2007). Mesenchymal stem and progenitor cells for cartilage repair. *Skeletal Radiology* **36**(10), 909-912.

Aigner, T., Bertling, W., Stoss, H., Weseloh, G., von der Mark, K. (1993). Independent expression of fibril-forming collagens I, II and III in chondrocytes of human osteoarthritic cartilage. *Journal of Clinical Investigation* **91**, 829-837.

Aigner, T., Gresk-otter, K. R., Fairbank, J. C., von der Mark, K., Urban, J. P. G. (1998). Variation with age of type X collagen expression in normal and scoliotic human intervertebral discs. *Calcified Tissue International* **63**, 263-268.

Alini, M., Eisenstein, S. M., Ito, K., Little, C., Kettler, A. A., Masuda, K., Melrose, J., Ralphs, J., Stokes, I., Wilke, H. J. (2008). Are animal models useful for studying human disc disorders/degeneration? *European Spine Journal* **17**, 2-19.

An, H. S., Masuda, K., Inoue, N. (2006). Intervertebral disc degeneration: biological and biomechanical factors. *Journal of Orthopaedics Sciences* **11**, 541-552.

Antoniou, J., Steffen, T., Nelson, F., Winterbottom, N., Hollander, A. P., Poole, R. A., Aebi, M., Alini, M. (1996). The human lumbar intervertebral disc. Evidence for changes in the biosynthesis and denaturation of the extracellular matrix with growth, maturation, ageing and degeneration. *Journal of Clinical Investigation* **98**(4), 996-1003.

Archer, C. W., McDowell, J., Bayliss, M. T., Stephens, M. D., Bentley, G. (1990). Phenotypic modulation in subpopulations of human articular chondrocytes in vitro. *Journal of Cellular Science* **97**, 361-371.

Ariga, K., Yonenobu, K., Nakase, T., Hosono, N., Okuda, S., Meng, W., Tamura, Y., Yoshida, H. (2003). Mechanical stress-induced apoptosis of endplate chondrocytes in organ-cultured mouse intervertebral discs. *Spine* **28**(14), 1528-1533.

Bader, R. A., Rochefort, W. E. (2008). Rheological characterisation of photopolymerised poly(vinyl alcohol) hydrogels for potential use in nucleus pulposus replacement. *Journal of Biomedical Research A* **86**, 494-501.

Bai, X., Liu, G., Xu, C., Zhuang, Y., Zhang, J., Jia, Y., Liu, Y. (2012). Morphometry research of deer, sheep and human lumbar spine: Feasibility of using deer and sheep in spinal animal models. *International Journal of Morphology* **30**(2), 510-520.

Bali, J. P., Cousse, H., Neuzil, E. (2001). Biochemical basis of the pharmacologic action of chondroitin sulfates on the osteoarticular system. *Seminars in Arthritis and Rheumatism* **31**, 58-68.

Bank, R. A., Soudry, M., Maroudas, A., Mizrachi, J., TeKoppele, J. M. (2000). The increased swelling and instantaneous deformation of osteoarthritic cartilage

is highly correlated with collagen degradation. *Arthritis and Rheumatism* **43**, 2202-2210.

Barnsley, L., Lord, S. M., Wallis, B. J., Bogduk, N. (1994). Lack of effect of intra-articular corticosteroids for chronic pain in the cervical zygapophyseal joints. *New England Journal of Medicine* **330**, 1047-1050.

Basalo, I. M., Raj, D., Krishnan, R., Chen, F. H., Hung, C. T., Ateshian, G. A. (2005). Effects of enzymatic degradation on the frictional response of articular cartilage in stress relaxation. *Journal of Biomechanics* **38**(6), 1343-1349.

Basalo, I. M., Chen, F. H., Hung, C. T., Ateshian, G. A. (2006). Frictional response of bovine articular cartilage under creep loading following proteoglycan digestion with chondroitinase ABC. *Journal of Biomechanical Engineering* **128**(1), 131-134.

Bayliss, M. T., Johnstone, B., O'Brien, J. P. (1988). 1988 Volvo award in basic science. Proteoglycan synthesis in the human intervertebral disc. Variation with age, region and pathology. *Spine* **13**, 972-981.

Beard, H. K., Ryvar, R., Brown, R., Muir, H. (1980). Immunochemical localization of collagen types and proteoglycan in pig intervertebral discs. *Immunology* **41**, 491-501.

Becerra, J., Andrades, J. A., Guerado, E., Zamora-Navas, P., Lopez-Puertas, J. M., Reddi, A. H. (2010). Articular cartilage: structure and regeneration. *Tissue Engineering: Part B* **16**(6), 617-627.

Bernick, S., Caillet, R. (1982). Vertebral end-plate changes with aging of human vertebrae. *Spine* **7**, 97-102.

Bhattacharjee, M., Miot, S., Gorecka, A., Singha, K., Loparic, M., Dickenson, S., Das, A., Bhavesh, N. S., Ray, A. R., Martin, I., Ghosh, S. (2012). Orientated lamellar silk fibrous scaffolds to drive cartilage matrix orientation: towards annulus fibrosus tissue engineering. *Acta Biomaterialia* **8**, 3313-3325.

Bland, J. H., Boushey, D. R. (1990). Anatomy and physiology of the cervical spine. *Seminars in Arthritis and Rheumatism* Livingstone **20**(1), 1-20.

Bogduk, N., Engel, R. (1984). The menisci of the lumbar zygapophyseal joints. *Spine* **9**(5), 454-460.

Bogduk, N., Twomey, L. T. (1987). Clinical anatomy of the lumbar spine. Churchill Livingstone.

Bohlman, H. H., Freehafer, A., Dejak, J. (1985). The results of treatment of acute injuries of the upper thoracic spine with paralysis. *The Journal of Bone and Joint Surgery* **67**(3), 360-369.

Bonaventure, J., Kadhom, N., Cohen-Solal, L., Ng, K. H., Bourguignon, J., Lasselin, C., Freisinger, P .(1994). Reexpression of cartilage-specific genes by dedifferentiated human articular chondrocytes cultured in alginate beads. *Experimental Cell Research* **212**, 97-104.

Boos, N., Nerlich, A. G., Wiest, I., von der Mark, K., Aebi, M. (1997). Immunolocalisation of type X collagen in human lumbar intervertebral discs during aging and degeneration. *Histochemistry and Cell Biology* **108**, 471-480.

Boswell, M. V., Colson, J. D., Spillane, W. F. (2005). Therapeutic facet joint interventions in chronic spinal pain: a systematic review of effectiveness and complications. *Pain Physician* **8**, 101-114.

Boszczyk., B. M., Boszczyk, A. A., Putz, R., Buttner, A., Benjamin, M., Milz, S. (2001A). An immunohistochemical study of the dorsal capsule of the lumbar and thoracic facet joints. *Spine* **26**(15), E338-E343.

Boszczyk, B. M., Boszczyk, A. A., Putz, R. (2001B). Comparative and functional anatomy of the mammalian lumbar spine. *The Anatomical Record* **264**, 157-168.

Boszczyk, B. M., Boszczyk, A. A., Korge, A., Grillhosl, A., Boos, W. D., Putz, R., Milz, S., Benjamin, M. (2003). Immunohistochemical analysis of the extracellular matrix in the posterior capsule of the zygapophyseal joints in patients with degenerative L4-5 motion segment instability. *Journal of Neurosurgery: Spine* **99**, 27-33.

Boyd, L. M., Carter, A. J. (2006). Injectable biomaterials and vertebral endplate treatment for repair and regeneration of the intervertebral disc. *European Spine Journal* **15**(Suppl 3), 414-421.

Bray, B. A., Lieberman, R., Meyer, K. (1967). Structure of human skeletal keratosulfate. The linkage region. *The Journal of Biological Chemistry* **242**, 3373-3380.

Briggs, A. M., Greig, A. M., Wark, J. D., Fazzalari, N. L., Bennell, K. L. (2004). A review of anatomical and mechanical factors affecting vertebral body integrity. *International Journal of Medical Sciences* **1**(3), 170-180.

Brodkin, K. R., Garcia, A. J., Levenston, M. E. (2004). Chondrocyte phenotypes on different extracellular matrix monolayers. *Biomaterials* **25**, 5929-5938.

Broom, N. D. (1984). Further insights into the structural principles governing the function of articular cartilage. *Journal of Anatomy* **139**(part 2), 275-294.

Brown, R. A., Jones, K. L. (1990). The synthesis and accumulation of fibronectin by human articular cartilage. *The Journal of Rheumatology* **17**, 65-72.

Bruehlmann, S. B., Rattner, J. B., Matyas, J. R., Duncan, N. A. (2002). Regional variations in the cellular matrix of the annulus fibrosus of the intervertebral disc. *Journal of Anatomy* **201**, 159-171.

Buckwalter, J. A., Mankin, H. J. (1997). Articular cartilage. Part I: Tissue design and chondrocyte-matrix interactions. *The Journal of Bone and Joint Surgery* **79**, 600-611.

Bushell, G. R., Ghosh, P., Taylor, T. F. K., Akeson, W. H. (1977). Proteoglycan chemistry of the intervertebral disc. *Clinical Orthopaedic and Related Research* **129**, 115-123.

Carette, S., Marcoux, S., Truchon, R., Grondin, C., Gagnon, J., Allard, Y., Latulippe, M. (1991). A controlled trial of corticosteroid injections into facet joints for chronic low back pain. *New England Journal of Medicine* **325**, 1002-1007.

Cassinelli, E. H., Hall, R. A., Kang, J. D. (2001). Biochemistry of intervertebral disc degeneration and the potential for gene therapy applications. *The Spine Journal* **1**(3), 205-214.

Caterson, B., Flannery, C. R., Hughes, C. E., Little, C. B. (2000). Mechanisms involved in cartilage proteoglycan catabolism. *Matrix Biology* **19**, 333-344.

Cawston, T., Billington, C., Cleaver, C. (1999). The regulation of MMPs and TIMPs in cartilage turnover. *Annals of the New York Academy of Sciences* **878**, 120-129.

Chandran, P. L., Horkay, F. (2012). Aggrecan, an unusual polyelectrolyte: Review of solution behaviour and physiological implications. *Acta Biomaterialia* **8**, 3-12.

Chang, G., Kim, H. J., Kaplan, D., Vunjak-Novakovic, G., Kandel, R. A. (2007). Porous silk scaffolds can be used for tissue engineering annulus fibrosus. *European Spine Journal* **16**, 1848-1857.

Chang, G., Kim, H. J., Vunjak-Novakovic, G., Kaplan, D. L., Kandel, R. (2009). Enhancing annulus fibrosus tissue formation in porous silk scaffolds. *Journal of Biomedical Materials Research Part A* **92A**(1), 43-51.

Chelberg, M. K., Banks, G. M., Geiger, D. F., Oegema, T. R. (1995). Identification of heterogeneous cell populations in normal human intervertebral discs. *Journal of Anatomy* **186**, 43-53.

Chen, W. J., Lai, P. L., Niu, C. C. (2001). Surgical treatment of adjacent instability after lumbar spine fusion. *Spine* **26**, 519-524.

Chen, H., Shoumura, S., Emura, S., Bunai, Y. (2008). Regional variations of vertebral trabecular bone microstructure with age and gender. *Osteoporosis International* **19**, 1473-1483.

Chevalier, X. (1993). Fibronectin, cartilage and osteoarthritis. *Seminars in Arthritis and Rheumatism* **22**(5), 307-318.

Chou, R., Qaseem, A., Snow, V., Casey, D., Cross, T., Shekelle, P., Owens, D. K. (2007). Diagnosis and treatment of low back pain: A joint clinical practice

guideline from the American college of physicians and the American pain society. *Annals of Internal Medicine* **147**(7), 478-494

Chou, A. I., Nicoll, S. B. (2008). Characterisation of photocrosslinked alginate hydrogels for nucleus pulposus cell encapsulation. *Journal of Biomedical Materials Research Part A* **91A**(1), 187-194.

Chou, R. (2013). Commentary: Successful spinal fusion surgery: can we improve the odds? *The Spine Journal* **13**, 110-112.

Chu, M. L., Zhang, R. Z., Pan, T. C., Stokes, D., Conway, D., Kuo, H. J., Glanville, R., Mayer, U., Mann, K., Deutzmann, R. (1990). Mosaic structure of globular domains in the hman type VI collagen alpha 3 chain: similarity to von Willebrand factor, fibronectin, actin, salivary proteins and aprotinin type protease inhibitors. *The EMBO Journal* **9**(2), 385-393.

Crean, J. K. G., Roberts, S., Jaffray, D. C., et al. (1997). Matrix metalloproteinases in the human intervertebral disc. Role in disc degeneration and scoliosis. *Spine* **22**, 2877-2884.

Crock, H. V., Yoshizawa, H. (1977). The blood supply of the vertebral column and spinal cord in man. New York, Springer.

Crock, H. V., Goldwasser, M. (1984). Anatomic studies of the circulation in the region of the vertebral end-plate in adult Greyhound dogs. *Spine* **9**(7), 663-771.

Cs-Szabo, G., Ragasa-San Juan, D., Turumella, V., Masuka, K., Thonar, E. J., An, H. S. (2002). Changes in mRNA and protein levels of proteoglycans of the annulus fibrosus and nucleus pulposus during intervertebral disc degeneration. *Spine* **27**, 2212-2219.

Culav, E. M., Clark, C. H., Merrilees, M. J. (1999). Connective tissues: matrix composition and its relevance to physical therapy. *Physical Therapy* **79**, 308-319.

Cyron, B. M., Hutton, W. C. (1981). The tensile strength of the capsular ligaments of the apophyseal joints. *Journal of Anatomy* **132**, 145-150.

Deyo, R. A. (1983). Conservative therapy for low back pain: Distinguishing useful from useless therapy. *The Journal of the American Medical Association* **250**, 1057-1062.

Deyo, R. A. (1986). How many days of bed rest for acute low back pain? A randomized clinical trial. *The New England Journal of Medicine* **315**, 1064-1070.

Deyo, R. A., Ciol, M. A., Cherkin, D. C., Loeser, J. D., Bigos, S. J. (1993). Lumbar spinal fusion: A cohort study of complications, reoperations, and resource use in the medicare population. *Spine* **18**, 1463-1470.

DiSilvestro, M. R., Suh, J. K. F. (2002). Biphasic poroviscoelastic characteristics of proteoglycan-depleted articular cartilage: Simulation of degeneration. *Annals of Biomedical Engineering* **30**, 792-800.

Djurasovic, M., Glassman, S. D., Howard, J. M., Copay, A. G., Carreon, L. Y. (2011). Health-related quality of life improvements in patients undergoing lumbar spinal fusion as a revision surgery. *Spine* **36**(4), 269-276.

Dowson, D., Wright, V., Longfield, M. V. (1969). Human joint lubrication. *Biomedical Engineering* **4**(4), 160-165.

Drury, J. L., Mooney, D. J. (2003). Hydrogels for tissue engineering: scaffold design variables and applications. *Biomaterials* **24**(24), 4337-4351.

Ducy, P., Desbois, C., Boyce, B., Pinero, G., Story, B., Dunstan, C., Smith, E., Bonadio, J., Goldstein, S., Gundberg, C., Bradley, A., Karsenty, G. (1996). Increased bone formation in osteocalcin-deficient mice. *Nature* **382**, 448-452.

Dunlop, R. B., Adams, M. A., Hutton, W. C. (1984). Disc space narrowing and the lumbar facet joints. *The Journal of Bone and Joint Surgery* **66-B**(5), 706-710.

Eerola, I., Salminen, H., Lammi, P., Lammi, M., von der Mark, K., Vuorio, E., Saamanem, A. M. (1998). Type X collagen , a natural component of mouse articular cartilage: Association with growth, aging and osteoarthritis. *Arthritis and Rheumatism* **41**(7), 1287-1295.

Elder, B. D., Vigneswaran, K., Athanasiou, K. A., Kim, D. H. (2009). Biomechanical, biochemical and histological characterisation of canine lumbar facet joint cartilage. *Journal of Neurosurgery Spine* **10**, 623-628.

Elder, B. D., Kim, D. H., Athanasiou, K. A. (2010). Developing an articular cartilage decellulaisation process toward facet joint cartilage replacement. *Neurosurgery* **66**(4), 722-727.

Esses, S. I., Moro, J. K. (1993). The value of facet joint blocks in patient selection for lumbar fusion. *Spine* **18**, 185-190.

Ewing, C. L., King, A. I., Prasad, P. (1972). Structural consideration of the human vertebral column under +Gz impact acceleration. *Journal of Aircraft* **9**, 84-90.

Eyre, D. R., Muir, H. (1977). Quantitative analysis of types I and II collagens in human intervertebral discs at various ages. *Biochimica et Biophysica Acta – Protein Structure* **492**(1), 29-42.

Eyre, D. R. (1979). Biochemistry of the intervertebral disc. *International Review of Connective Tissue Research* **8**, 227-291.

Eyre, D. R., Wu, J. J., Apone, S. (1987). A growing family of collagens in articular cartilage: identification of 5 genetically distinct types. *Journal of Rheumatology* **14**, 25-27.

Eyre, D. R. (1988). Collagens of the intervertebral disc. Ghosh P. ed. Vol IBoca Raton, FL, CRC Press, 171-188.

Eyre, D. (2002). Collagen of articular cartilage. *Arthritis Research* **4**, 30-35.

Feinberg, J., Boachie-Adjei, O., Bullough, P. G., Boskey, A. L. (1990). The distribution of calcium deposits in intervertebral discs of the lumbosacral spine. *Clinical Orthopaedic Related Research* **254**, 303-310.

Fletcher, G., Haughton, V. M., Ho, K. C., Yu, S. W. (1989). Age related changes in the cervical facet joints: studies with cryomicrotomy, MR and CT. *American Journal of Roentgenology* **154**(4), 817-820.

Fogel, G. R., Cunningham, P. Y., Esses, S. I. (2004). Coccygodynia: Evaluation and management. *Journal of the American Academy of Orthopaedic Surgeons* **12**(1), 49-54.

Fraser, R. D., Ross, E. R., Lowery, G L., Freeman, B. J., Dolan, M. (2004). AcroFlex design and results. *The Spine Journal* **4**, 245S-251S.

Freemont, A. J., Watkins, A., Le Maitre, C., Jeziorska, M., Hoyland, J. A. (2002). Current understanding of cellular and molecular events in intervertebral disc degeneration: implications for therapy. *Journal of Pathology* **196**, 374-379.

French, S. D., Cameron, M., Walker, B. F., Reggars, J. W., Esterman, A. J. (2006). A Cochrane review of superficial heat or cold for low back pain. *Spine* **31**, 998-1006.

Fujiwara, A., Tamai, K., Yamato, M., An, H. S., Saotome, K., Kurihashi, A. (1999). The relationship between facet joint osteoarthritis and disc degeneration of the lumbar spine: an MRI study. *European Spine Journal* **8**, 396-401.

Furlan, A. D., Brosseau, L., Imamura, M., Irvin, E. (2002). Massage for low back pain: a systematic review within the framework of the Cochrane Collaboration Back Review Group. *Spine* **27**, 1896-1910.

Furlan, A. D., Sandoval, J. A., Mailis-Gagnon, A., Tunks, E. (2006). Opioids for chronic noncancer pain: a meta-analysis of effectiveness and side effects. *Canadian Medical Association Journal* **174**, 1589-1594.

Gagnier, J. J., van Tulder, M. W., Berman, B., Bombardier, C. (2007). Herbal medicine for low back pain: a Cochrane review. *Spine* **32**(1), 82-92.

Gan, J. C., Ducheyne, P., Vresilovic, E,. Shapiro, I. M. (2003A). Intervertebral disc tissue engineering I: Characterisation of the nucleus pulposus. *Clinical Orthopaedics* **411**, 305-314.

Gan, J. C., Ducheyne, P., Vresilovic, E. J., Shapiro, I. M. (2003B). Intervertebral disc tissue engineering II: cultures of nucleus pulposus cells. *Clinical Orthopaedics* **411**, 315-324.

Gannon, J. M., Walker, G., Fischer, M., Carpenter, R., Thompson, R. C., Oegema, T. R. (1991). Localisation of type X collagen in canine growth plate and adult canine articular cartilage. *Journal of Orthopaedic Research* **9**, 485-494.

Gay, S., Miller, E. J. (1978). Collagen in the physiology and pathology of connective tissue. *Stuttgart, New York: Gustav Fischer Verlag* **105**, 6-7.

Gellhorn, A. C., Katz, J. N., Suri, P. (2012). Osteoarthritis of the spine: the facet joints. *Nature Reviews Rheumatology* **9**(4), 216-124.

Gelse, K., Pöschl, E., Aigner, T. (2003). Collagens – Structure, function and biosynthesis. *Advanced Drug Delivery Review* **55**, 1531-1546.

Glant, T. T., Hadhazy, C. S., Mirkecz, K., Sipos, A. (1985). Appearance and persistence of fibronectin in cartilage. Specific interaction of fibronectin with collagen II. *Histochemistry* **82**, 149-158.

Gong, H., Zhang, M., Yeung, H. Y., Qin, L. (2005). Regional variations in microstructure properties of vertebral trabeculae with aging. *Journal of Bone Mineral Metabolism* **23**, 174-180.

Goupille, P., Jayson, M. I., Valat, J. P., Freemont, A. J. (1998). Matrix metalloproteinases: The clue to intervertebral disc degeneration? *Spine* **23**(14), 1612-1626.

Grenier, N., Kressel, H. Y., Schiebler, M. L., Grossman, R. I., Dalinka, M. K. (1987). Normal and degenerative posterior spinal structures: MR imaging. *Radiology* **165**, 517-525.

Gries, N. C., Berlemann, U., Moore, R. J., Vernon-Roberts, B. (2000). Early histologic changes in lower lumbar discs and facet joints and their correlation. *European Spine Journal* **9**, 23-29

Grieve, G. P. (1991). Mobilisation of the spine. Churchill Livingstone, fifth edition.

Gruber, H. E., Hanley, E. N. (1998). Analysis of aging and degeneration of the human intervertebral disc. *Spine* **23**(7), 751-757.

Gruber, H. E., Hanley, E. N. (2000). Human disc cells in monolayer vs 3D culture: cell shape, division and matrix formation. *BMC Musculoskeletal Disorders* **1**(1), 1-6.

Gruber, H. E., Hanley, E. N. (2003). Recent advances in disc cell biology. *Spine* **28**(2), 186-193.

Guerin, H. L., Elliot, D. M. (2006). Degeneration affects the fiber reorientation of human annulus fibrosus under tensile loading. *Journal of Biomechanics* **39**(8), 1410-1418.

Haher, T. R., O'Brien, M., Dryer, J. W., Nucci, R., Zipnick, R., Leone, D. J. (1994). The role of the lumbar facet joints in spinal stability. *Spine* **19**(23), 2667-2671.

Halloran, D. O., Grad, S., Stoddart, M., Dockery, P., Alini, M., Pandit, A. S. (2008). An injectable cross-linked scaffold for nucleus pulposus regeneration. *Biomaterials* **29**, 438-447.

Hardingham, T. E., Fosang, A. J. (1992). Proteoglycans: Many forms and many functions. *Federation of American Societies for Experimental Biology* **6**, 861-870.

Hasler, C., Sprecher, C. M., Milz, S. (2010). Comparison of the immature sheep spine and the growing human spine. *Spine* **35**(23), E1262-E1272.

Hattori, T., Muller, C., Gebhard, S., Bauer, E., Pausch, F., Schlund, B., Bosl, M. R., Hess, A., Surmann-Schmitt, C., von der Mark, H., de Crombrugghe, B., von der Mark, K. (2010). SOX9 is a major negative regulator of cartilage vascularisation, bone marrow formation and endochondral ossification. *Development* **137**, 901-911.

Hauschka, P. V., Reid, M. L. (1978). Vitamin D dependence of a calcium-binding protein containing gamma-carboxyglutamic acid in chicken bone. *Journal of Biological Chemistry* **253**, 9063-9068.

Hayashi, T., Abe, E., Jasin, H. E. (1996). Fibronectin synthesis in superficial and deep layers of normal articular cartilage. *Arthritis Rheumatism* **39**, 567-573.

Hedlund, H., Hedbom, E., Heinegard, D., Mengarelli-Widholm, S., Reinholt, F., Svensson, O. (1999). Association of the aggrecan keratan sulphate-rich region with collagen in bovine articular cartilage. *Journal of Biological Chemistry* **274**, 5777-5781.

Heinegard, D. (2009). Proteoglycans and more – from molecules to biology. *International Journal of Experimental Pathology* **90**, 575-586.

Helen, W., Gough, J. E. (2008). Cell viability, proliferation and extracellular matrix production of human annulus fibrosus cells cultured within PDLLA/Bioglass composite foam scaffolds in vitro. *Acta Biomaterialia* **4**, 230-243.

Henrotin, Y. (2010). Advances in the treatment of osteoarthritis and the role of chondroitin sulphate – a review. *European Musculoskeletal Review* **5**(2), 11-17.

Hernandez-Diaz, S., Rodriguez, L. A. (2000). Association between nonsteriodal anti-inflammatory drugs and upper gastrointestinal tract bleeding/perforation: an overview of epidemiologic studies published in the 1990s. *Archives of Internal Medicine* **160**, 2093-2099.

Hoffman, B. E., Newman-Tarr, T. M., Gibbard, A., Wang, S., Hanning, C., Pratta, M. A., Boyle, R. J., Kumar, S., Majumdar, M. K. (2010). Development and characterisation of a human articular cartilage-derived chondrocyte cell line that retains chondrocyte phenotype. *Journal of Cellular Physiology* **222**, 695-702.

Holm, S., Maroudas, A., Urban, J. P. (1981). Nutrition of the intervertebral disc: Solute transport and metabolism. *Connective Tissue Research* **8**, 101-119.

Holm, S., Holm, A. K., Ekstrom, L., Karladani, A., Hansson, T. (2004). Experimental disc degeneration due to endplate injury. *Journal of Spinal Disorders & Techniques* **17**(1), 64-71.

Homandberg, G. A., Wen, C. (1998). Exposure of cartilage to a fibronectin fragment amplifies catabolic processes while also enhancing anabolic processes to limit damage. *Journal of Orthopaedic Research* **16**, 237-246.

Horner, H. A., Roberts, S., Bielby, R. C., Menage, J., Evans, H., Urban, J. P. G. (2002). Cells from different region of the intervertebral disc. *Spine* **27**(10), 1018-1028.

Hsu, K. Y., Zucherman, J., White, A., Reynolds, J., Goldthwaite, N. (1988). Deterioration of motion segments adjacent to lumbar spine fusions. *Proceedings of the International Society for the study of the lumbar spine.* 10.

Hukins, D. W. L. (1988). The biology of the intervertebral disc CRC Press, Inc. Boca Raton, FL.

Hunter, C. J., Matyas, J. R., Duncan, N. A. (2003). The notochordal cell in the nucleus pulposus: a review in the context of tissue engineering. *Tissue Engineering* **9**, 667-677.

Hunter, C. J., Matyas, J. R., Duncan, N. A. (2004). Cytomorphology of notochordal and chondrocytic cells from the nucleus pulposus: a species comparison. *Journal of Anatomy* **205**, 357-362.

Igarashi, A., Kikuchi, S., Konno, S., Olmarker, K. (2004). Inflammatory cytokines released from the facet joint tissue in degenerative lumbar spinal disorders. *Spine* **29**(19), 2091-2095.

Inami, S., Kaneoka, K., Hayashi, K., Ochiai, N. (2000). Types of synovial fold in the cervical facet joint. *Journal of Orthopaedic Science* **5**, 475-480.

Inoue, H. (1981). Three-dimensional architecture of lumbar intervertebral discs. *Spine* **6**, 139-146.

Jay, G. D., Torres J. R., Warman, M. L., Laderer, M. C., Breuer, K. S. (2007). The role of lubricin in the mechanical behaviour of synovial fluid. *Proceedings of the National Academy of Sciences* **104**(15), 6194-6199.

Jin, L., Shimmer, A. L., Li, X. (2013). The challenge and advancement of annulus fibrosus tissue engineering. *European Spine Journal*, 1-11.

Jinkins, J. R. (2004). Acquired degenerative changes of the intervertebral segments at and suprajacent to the lumbosacral junction. A radioanatomic

analysis of the nondiscal structures of the spinal column and perispinal soft tissues. *European Journal of Radiology* **50**, 134-158.

Jo, C. H., Kim, E. M., Ahn, H. J., Kim, H. J., Seong, S. C., Lee, M. C. (2006). Degree of degeneration and chondroitinase ABC treatment of human articular cartilage affect adhesion of chondrocytes. *Tissue Engineering* **12**(1), 167-176.

Johnson, W. E. B., Eisenstein, S. M., Roberts, S. (2001). Cell cluster formation in degenerate lumbar intervertebral discs is associated with increased disc cell proliferation. *Connective Tissue Research* **42**(3), 197-207.

Kalichman, L., Hunter, D. J. (2007). Lumbar facet joint osteoarthritis: A review. *Seminars in Arthritis and Rheumatism* **37**, 69-80.

Kalichman, L., Li, L., Kim, D., Guermazi, A., Berkin, V., O'Donnell, C. J., Hoffmann, U., Cole, R., Hunter, D. J. (2008). Facet joint osteoarthritis and low back pain in the community-based population. *Spine (Phila Pa)* **33**(23), 2560-2565.

Kallakuri, S., Li, Y., Chen C., Cavanaugh, J. M. (2012). Innervation of cervical ventral facet joint capsule: Histological evidence. *World Journal of Orthopaedics* **3**(2), 10-14.

Kandel, R., Roberts, S., Urban, J. P. G. (2008). Tissue engineering and the intervertebral disc: the challenges. *European Spine Journal* **17** (suppl 4), S480-S491.

Kandziora, F., Pflugmacher, R., Scholz, M., Schnake, K., Lucke, M., Schroder, R., Mittlmeier, T. (2001). Comparison between sheep and human cervical spines: an anatomic, radiographic, bone mineral density, and biomechanical study. *Spine* **26**, 1028-1037.

Kang, J. D., Stefanovic-Racic, M., McIntyre, L. A., Georgescu, H. I., Evans, C. H. (1997). Toward a biochemical understanding of human intervertebral disc degeneration and herniation. Contributions of nitric oxide, interleukins, prostaglandin E2, and matrix metalloproteinases. *Spine* **22**, 1065-1073.

Katta, J., Pawaskar, S. S., Jin, Z. M., Ingham, E., Fisher J. (2007). Effect of load variation on the friction properties of articular cartilage. *Journal of Engineering Tribology* **221**(3), 175-181.

Katta, J., Jin, Z., Ingham, E., Fisher, J. (2008A). Biotribology of articular cartilage – A review of the recent advances. *Medical Engineering and Physics* **30**, 1349-1363.

Katta, J., Stapleton, T., Ingham, E., Jin, Z., Fisher, J. (2008B). The effect of glycosaminoglycan depletion on the friction and deformation of articular cartilage. *Journal of Engineering in Medicine* **222**, 1-11.

Katta, J., Jin, Z., Ingham, E., Fisher, J. (2009). Effect of nominal stress on the long term friction, deformation and wear of native and glycosaminoglycan deficient articular cartilage. *Osteoathritis and Cartilage* **17**. 662-668.

Kettler, A. A., Wilke, H. J. (2006). Review of existing grading systems for cervical and lumbar disc and facet joint degeneration. *European Spine Journal* **15**, 705-718.

Kettler, A., Werner, K., Wilke, H. J. (2007). Morphological changes of cervical facet joints in elderly individuals. *European Spine Journal* **16**, 987-992.

Keyes, D. C., Compere, E. L. (1932). The normal and pathological physiology of the nucleus pulposus of the intervertebral disc: An anatomical, clinical and experimental study. *The Journal of Bone and Joint Surgery Am* **14**, 897-938.

Kheir, E., Stapleton, T., Shaw, D., Jin, Z., Fisher, J., Ingham, E. (2011). Development and characterisation of an acellular porcine cartilage bone matrix for use in tissue engineering. *Journal of Biomedical Materials Research Part A* **99A**(2), 283-294.

Kim, J. S., Kroin, J. S., Buvanendran, A., Li, X., van Wijnen, A. J., Tuman, K. J., Im, H. J. (2011). Characterisation of a new animal model for evaluation and treatment of back pain due to lumbar facet joint osteoarthritis. *Arthritis and Rheumatism* **63**(10), 2966-2973.

Knudson, C. B., Knudson, W. (2001). Cartilage proteoglycans. *Cell and Developmental Biology* **12,** 69-78.

Knudson, W., Loeser, R. F. (2002). CD44 and integrin matrix receptors participate in cartilage homeostasis. *Cell and Molecular Life Sciences* **59**, 36-44.

Koepsell, L., Zhang, L., Neufeld, D., Fong, H., Deng, Y. (2011). Electrospun nanofibrous polycaprolactone scaffolds for tissue engineering of annulus fibrosus. *Macromolecular Bioscience* **11**, 391-399.

Koes, B. W., Scholten, R. J. P. M., Mens, J. M. A. (1997). Efficacy of nonsteroidal anti-inflammatory drugs for low back pain: A systematic review of randomised clinical trials. *Annals of the Rheumatic Diseases* **56**, 214-223.

Koller, E., Winterhalter, K. H., Trueb, B. (1989). The globular domains of type VI collagen are related to the collagen-binding domains of cartilage matrix protein and von Willebrand. *The EMBO Journal* **8**(4), 1073-1077.

Krus, J. V., Tanaka, K., Gilliland, T. M., Winkelstein, B. A. (2013). An anatomical and immunohistochemical characterisation of afferents innervating the C6-C7 facet joint after painful joint loading in the rat. *Spine* **38**(6), E325-E331.

Kurtz, S. M., Edidin, A. (2006). Spine technology handbook. Kindle Edition, Elsevier Inc.

Kyle, S., Aggeli, A., Ingham, E., McPherson, M. J. (2009). Production of self-assembling biomaterials for tissue engineering. *Trends in Biotechnology* **27**(7), 423-433.

Kyriakos, M., Totty, W. G., Riew, K. D. (2000). Synovial chondromatosis in a facet joint of a cervical vertebra. *Spine* **25**(5), 635-640.

Lamaire, J. P., Skalli, W., Lavaste, F. (1997). Intervertebral disc prosthesis. Results and prospects for the year 2000. *Clinical Orthopaedics and Related Research* **337**, 64-76.

Lamaire, J. P., Carrier, H., Eh SariAli. (2005). Clinical and radiological outcomes with the charite artificial disc: a 10-year minimum follow-up. *Journal of Spinal Disorders and Techniques* **18**, 353-359.

Lammi, P., Inkinen, R. I., von der Mark, K., Puustjarvi, K., Arokoski, J., Hyttinen, M. M., Lammi, M. J. (1998). Localisation of type X collagen in the intervertebral discs of mature beagle dogs. *Matrix Biology* **17**, 449-453.

Lark, M. W., Bayne, E. K., Flanagan, J., Harper, C. F., Hoerrner, L. A., Hutchinson, N. I., Singer, I. I., Donatelli, S. A., Weidner, J. I., Williams, H. R., Mumford, R. A., Lohmander, L. S. (1997). Aggrecan degradation in human cartilage. Evidence for both matrix metalloproteinase and aggrecanase activity in normal, osteoarthritic and rheumatoid joints. *The Journal of Clinical Investigation* **100**(1), 93-106.

Latif, M. J. A., Jin, Z., Wilcox, R. K. (2012). Biomechanical characterisation of ovine spinal facet joint cartilage. *Journal of Biomechanics* **45**, 1346-1352.

Lee, C. K., Langrana, N. A. (2004A). A review of spinal fusion for degenerative disc disease: need for alternative treatment approach of disc arthroplasty. *The Spine Journal* **4**(6), 173S-176S.

Lee, C., Straus, W. L., Balshaw, R., Barlas, S., Vogel, S., Schnitzer, T. J. (2004B). A comparison of the efficacy and safety of nonsteroidal antiinflammatory agents versus acetaminophen in the treatment of osteoarthritis: a mega-analysis. *Arthritis & Rheumatism* **51**, 746-754.

Lee, J. C., Cha, J. G., Yoo, J. H., Kim, H. K., Kim, H. J., Shin, B. J. (2012). Radiographic grading of facet degeneration, is it reliable ?- a comparison of MR or CT grading with histologic grading in lumbar fusion candidates. *The Spine Journal* **12**, 507-514.

Le Huec, J. C., Aunoble, S., Fiesem, T., Mathews, H., Zdeblick, T. (2004). Maverick total lumbar disk prosthesis: biomechanics and preliminary results. In: Gunzburg, R., Mayer, H. M., Szpalski, M., Aebi, M. (2004) eds. *Arthroplasty of the Spine* Berlin: Springer-Verlag, 36-43.

Le Maitre, C. L., Freemont, A. J., Hoyland, J. (2004). Localisation of degradative enzymes and their inhibitors in the degenerative human intervertebral disc. *Journal of Pathology* **204**(1), 47-54.

Le Maitre, C. L., Pockert, A., Buttle, D. J., Hoyland, J. A. (2007). Matrix synthesis and degradation in the human intervertebral disc degeneration. *Biochemical Society Transactions* **35**(4), 652-655.

Lewinnek, G. E., Warfield, C. A. (1986). Facet joint degeneration as a cause of lower back pain. *Clinical Orthopaedics and Related Research* **213**, 216-222.

Li, J., Muehleman, C., Abe, Y., Masuda, K. (2011). Prevalance of facet joint degeneration in association with intervertebral joint degeneration in a sample of organ donors. *Journal of Orthopaedic Research* **29**(8), 1267-1274.

Lilius, G., Laasonen, E. M., Myllynen, P., Harilainen, A., Gronlund, G. (1989). Lumbar facet joint syndrome. A randomised clinical trial. *Journal of Bone and Joint Surgery* **71**, 681-684.

Lindahl, U., Roden, L. (1966). The chondroitin-4-sulphate-protein linkage. *The Journal of Biological Chemistry* **241**(9), 2113-2119.

Lotz, J. C., Colliou, O. K., Chin, J. R., Duncan, N. A. (1998). Compression-induced degeneration of the intervertebral disc: An *in vivo* mouse model and finite-element study. *Spine* **23**(23), 2493-2506.

Lotz, J. (2004). Animal models of intervertebral disc degeneration. Lessons learned. *Spine* **29**(23), 2742-2750.

Lu, X. L., Mow, V. C. (2008). Biomechanics of articular cartilage and determination of material properties. *Medicine and Science in Sports and Exercise* **40**(2), 193-199.

Lust, G., Burton-Wurster, N., Leipold, H. (1987). Fibronectin as a marker for osteoarthritis. *Journal of Rheumatology* **14**, 28-29.

Mackie, E. J., Tatarczuch, L., Mirams, M. (2011). The skeleton: a multi-functional complex organ. The growth plate chondrocyte and endochondral ossification. *Journal of Endocrinology* **211**, 109-121.

Mahmoudifar, N., Doran, P. M. (2005). Tissue engineering of human cartilage in bioreactors using single and composite cell-seeded scaffolds. *Biotechnology and Bioengineering* **91**, 338-355.

Maniadakis, N., Gray, A. (2000). The economic burden of back pain. *Pain* **84**, 95-103.

Mankin, H. J., Mow, V. C., Buckwalter, J. A., Iannotti, J. P., Ratcliffe, A. (2000). Articular cartilage structure, composition and function in Buckwalter, J. S., Einhorn, T. A., Simon, S. R. (2000). Orthopaedic Basic Science: Biology and Biomechanics of the Musculoskeletal System, ed 2. Rosemont, IL: American Academy of Orthopaedic Surgeons, 449–450.

Maroon, J. C., Bost, J. W., LePere, D. B., Bost, S. M., Williams, L., Amos, A. S. (2013). Clinical evaluation of TruFUSE Lumbar facet fusion system. *Surgical Science* **4**, 166-175.

Maroudas, A., Stockwell, R. A., Nachemson, A., Urban, J. (1975). Factors involved in the nutrition of the human intervertebral disc: Cellularity and diffusion of glucose in vitro. *Journal of Anatomy* **120**, 113-130.

Martell, B. A., O'Connor, P. G., Kerns, R. D., Becker, W. C., Morales, K. H., Kosten, T. R. (2007). Systematic review: opioid treatment for chronic back pain: prevalence, efficacy, and association with addiction. *Annals of Internal Medicine* **146**(2), 116-127.

Martel-Pelletier, J., McCollum, R., Fujimoto, N., Obata, K., Cloutier, J. M., Pelletier, J. P. (1994). Excess of metalloproteinases over tissue inhibitor of metalloproteinase may contribute to cartilage degradation in osteoarthritis and rheumatoid arthritis. *Laboratory Investigation* **70**, 807-815.

Master, D. L., Toy, J. O., Eubanks, J. D., Ahn, N. U. (2012). Cervical endplate and facet arthrosis: An anatomic study of cadaveric specimens. *Journal of spinal disorders and techniques* **25**(7), 379-382.

Masuda, K., Oegema, T. R., An, H. S. (2004A). Growth factors and treatment of intervertebral disc degeneration. *Spine* **29**, 2757-2769.

Masuda, K., An, H. S. (2004B) Growth factors and the intervertebral disc. *Spine* **4**, 330S-340S.

Maurice, R. S. (1981). Spinal Degenerative Disease. John Wright and Sons Ltd.

Mayer, H. M. (2005). Total lumbar disc replacement. *The Journal of Bone and Joint Surgery* **87B**(8), 1029-1037.

Mayne, R. (1989). Carilage collagens. What is their function, and are they involved in articular disease? *Arthritis and Rheumatism* **32**(3), 241-246.

Melrose, J., Ghosh, P. (1988). The noncollagenous proteins of the intervertebral disc. *In* P. Ghosh (ed.), *The Biology of the Intervertebral Disc*, CRC Press, Boca Raton

Melrose, J., Ghosh, P., Taylor, T. K. F. (2001). A comparative analysis of the differential spatial and temporal distributions of the large (aggrecan, versican) and small (decorin, biglycan, fibromodulin) proteoglycans of the intervertebral disc. *Journal of Anatomy* **198**, 3-15.

Melrose, J., Burkhardt, D., Taylor, T. K. F., Dillon, C. T., Read, R., Cake, M., Little, C. B. (2009). Calcification in the ovine intervertebral disc: a model of hydroxyapatite deposition disease. *European Spine Journal* **18**, 479-489.

Mendler, M., Eich-Bender, S. G., Vaughan, L., Winterhalter, K. H., Bruckner, P. (1989). Cartilage contains mixed fibrils of collagen types II, IX, XI. *Journal of Cell Biology* **108**, 191-197.

Menzel, J., Borth, W. (1983). Influence of plasma fibronectin on collagen cleavage by collagenase. *Collagen Related Research* **3**, 217-230.

Mercier, N. R., Costantino, H. R., Tracy, M. A., Bonassar, L. J. (2004). A novel injectable approach for cartilage formation in vivo using PLG microspheres. *Annual Biomedical Engineering* **32**, 418-429.

Mikawa, Y., Hamagami, H., Shikata, J., Yamamuro, T. (1986). Elastin in the human interevertebral disc. A histological and biochemical study comparing it with elastin in the human yellow ligament. *Archives of Orthopaedic Trauma Surgery* **105**, 343-349.

Miller, J. A. A., Schmatz, C., Schultz, A. B. (1988). Lumbar disc degeneration: correlation with age, sex, and spine level in 600 autopsy specimens. *Spine* **13**(2), 173-178.

Mizuno, H., Roy, A. K., Vacanti, C. A., Kojima, K., Ueda, M., Bonassar, L. J. (2004). Tissue-engineered composites of annulus fibrosus and nucleus pulposus for intervertebral disc replacement. *Spine* **12**, 341-349.

Mizuno, H., Roy, A. K., Zaporojan, V., Vacanti, C. A., Ueda, M., Bonassar, L. J. (2006). Biomechanical and biochemical characterisation of composite tissue-engineered intervertebral discs. *Biomaterials* **27**, 362-370.

Modic, M. T., Pavlicek, W., Weinstein, M. A., Boumphrey, F., Ngo, F., Hardy, R. (1984). Magnetic resonance imaging of intervertebral disc disease. *Radiology* **152**, 103-111.

Moody, H. R., Brown, C. P., Bowden, J. C., Crawford, R. W., McElwain, D. L. S., Oloyede, A. O. (2006). In vitro degradation of articular cartilage: does trypsin treatment produce consistent results. *Journal of Anatomy* **209**, 259-267.

Moore R. J., Crotti, T. N., Osti, O. L., Fraser, R. D., Vernon-Roberts, B. (1999). Osteoarthrosis of the facet joints resulting from annular rim lesions in sheep lumbar discs. *Spine* **24**(6), 519-525.

Moore, R. J. (2000). The vertebral end plate: what do we know? *European Spine Journal* **9**, 92-96.

Moore, R. J. (2006). The vertebral endplate: disc degeneration, disc regeneration. *The European Spine Journal* **15**(3), S333-S337.

Morishita, Y., Hida, S., Miyazaki, M., Hong, S. W., Zou, J., Wei, F., Naito, M., Wang, J. C. (2008). The effects of the degenerative changes on the functional spinal unit on the kinematics of the cervical spine. *Spine* **33**(6), 178-182.

Mosley, D. E., Swain, R. A., Bergese, S. (2012). A basic approach to lumbar zygapophyseal joint disease: New technology for treatment, but does it improve outcome? *Pain and Relief* **1**(2), 1-2.

Mow, V. C., Lai, W. M. (1980). Recent developments in synovial joint biomechanics. *SIAM Review* **22**(3), 275-317.

Mow, V. C., Holmes, M. H., Lai, W. M. (1984). Fluid transport and mechanical properties of articular cartilage: a review. *Journal of Biomechanics* **17**(5), 377-394.

Mow, V. C., Hayes, W. C. (1997). Basic orthopaedic biomechanics. Lippincott-Raven 2nd edition.

Muir, H., Jacobs, S. (1967). Protein-polysaccharides of pig laryngeal cartilage. *Biochemical Journal* **103**, 367-374.

Mwale, F., Roughley, P., Antoniou, J. (2004). Distinction between the extracellular matrix of the nucleus pulposus and hyaline cartilage: a requisite for tissue engineering of intervertebral disc. *European Cells and Materials* **8**, 58-64.

Nadzir, M. M., Kino-oka, M., Maruyama, N., Sato, Y., Kim, M. H., Sugawara, K., Taya, M. (2011). Comprehension of terminal differentiation and dedifferentiation of chondrocytes during passage culture. *Journal of Bioscience and Bioengineering* **112**(4), 395-401.

Nelemans, P. J., de Bie, R. A., de Vet, H. C., Sturmans, F. (2001). Injection therapy for subacute and chronic benign low back pain. *Spine* **26**, 501-515.

Nemoto, H., Yamagishi, M., Kikuchi, T., Ozeki, Y., Shinmei, M. (1994). Effect of IL-1 and IL-6 on MMP-3 and TIMP-1 production in human degenerated disc tissue. *Rinsho Seikei Geka* **29**, 369-376.

Nerurkar, N. L., Elliot, D. M., Mauck, R. L. (2007). Mechanics of orientated electrospun nanofibrous scaffolds for annulus fibrosus tissue engineering. *Journal of Orthopaedic Research* **25**(8), 1018-1028.

Nesti, L. J., Li, W. J., Shanti, R. M., Jiang, Y. J., Jackson, W., Freedman, B. A., Kuklo, T. R., Giuliani, J. R., Tuan, R. S. (2008). Intervertebral disc tissue engineering using a novel hyaluronic acid-nanofibous scaffold (HANFS) amalgam. *Tissue Engineering: Part A* **14**(9), 1527-1537.

Ng, L. J., Wheatley, S., Muscat, G. E. O., Conway-Campbell, J., Bowles, J., Wright, E., Bell, D. M., Tam, P. P. L., Cheah, K. S. E., Koopman, P. (1997). SOX9 binds DNA, activates transcription and coexpresses with type II collagen during chondrogenesis in the mouse. *Developmental Biology* **183**, 108-121.

Nordin, M., Frankel, V. H. (2001). Basic Biomechanics of the musculoskeletal system. Third edition, New York, Lippincott Williams & Wilkins.

Northfield, D. W. C. (1973). The surgery of the central nervous system. Oxford, Blackwell.

Oda, J., Tanaka, H., Tsuzuki, N. (1988). Intervertebral disc changes with aging of human cervical vertebra from the neonate to the eighties. *Spine* **13**, 1205-1211.

Oegema, T. R., Johnson, S. L., Aguiar, D. J., Ogilvie, J. W. (2000). Fibronectin and its fragments increase with degeneration in the human intervertebral disc. *Spine* **25**(21), 2742-2747.

O'Halloran, D. M., Pandit, A. S. (2007). Tissue-engineering approach to regenerating the Intervertebral Disc. *Tissue Engineering* **13**(8), 1927-1932.

Osti, O. L., Vernon-Roberts, B., Moore, R., Fraser, R. D. (1992). Annular tears and disc degeneration in the lumbar spine. *The Journal of Bone and Joint Surgery* **74B**(5), 678-682.

Park, P., Garton, H. J., Gala, V. C., Hoff, J. T., McGillicuddy, J. E. (2004). Adjacent segment disease after lumbar or lumbosacral fusion: Review of the literature. *Spine* **29**(17), 1938-1944.

Park, S. H., Park, S. R., Chung, S. I., Pai, K. S., Min, B. H. (2005). Tissue-engineered cartilage using fibrin/hyaluronan composite gel and its *in vivo* implantation. *The International Journal of Artificial Organs* **29**, 838-845.

Park, S. H., Cho, H., Gil, E. S., Mandal, B. B., Min, B. H., Kaplan, D L. (2011). Silk-fibrin/hyaluronic acid composite gels for nucleus pulposus tissue regeneration. *Tissue Engineering Part A* **17**(23&24), 2999-3009.

Pathria, M., Sartoris, D. J., Resnick, D. (1987). Osteoarthritis of the facet joints: accuracy of oblique radiographic assessment. *Radiology* **164**, 227-230.

Phillips, F. M., Reuben, J., Wetzel, F. T. (2002). Intervertebral disc degeneration adjacent to a lumbar fusion. An experimental rabbit model. *Journal of Bone and Joint Surgery* **84**, 289-294.

Pickard, J., Ingham, E., Egan, J., Fisher, J. (1998). Investigation into the effect of proteoglycan molecules on the tribological properties of cartilage joint tissues. *Proceedings of the Institution of Mechanical Engineers, Part H: Journal of Engineering in Medicine* **212**(H3), 177-182.

Poole, C. A., Flint, M. H., Beaumont, B. W. (1987). Chondrons in cartilage: Ultrastructure analysis of the pericellular microenvironment in adult human articular cartilage. *Journal of Orthopaedic Research* **5**, 509-522.

Poole, C. A., Ayad, S., Schofield, J. R. (1988). Chondrons of articular cartilage: I. Immunolocalisation of type VI collagen in the pericellular capsule of isolated canine tibial chondrons. *Journal of Cell Science* **90**, 635-643.

Poole, C. A., Glant, T. T., Schofield, J. R. (1991). Chondrons from articular cartilage. (IV) Immunolocalisation of proteoglycan epitopes in isolated canine tibial chondrons. *Journal of Histochemistry and Cytochemistry* **39**, 1175-1187.

Poole, C. A. (1997). Articular cartilage chondrons: form, function and failure. *Journal of Anatomy* **191**, 1-13.

Porto Filho, M. R., Pastorello, M. T., Defino, H. L. A. (2005). Experimental study of the participation of the vertebral endplate in the integration of bone grafts. *European Spine Journal* **14**, 965-970.

Poser, J. W., Esch, F. S., Ling, N. C., Price, P. A. (1980). Isolation and sequence of the vitamin k-dependent protein from human bone. Undercarboxylation of the first glutamic acid residue. *Journal of Biological Chemistry* **255**, 8685-8691.

Prescher, A. (1998). Anatomy and pathology of the aging spine. *European Journal of Radiology* **27**, 181-195.

Pullig, O., Weseloh, G., Swoboda, B. (1999). Expression of type VI collagen in normal and osteoarthritic human cartilage. *Osteoarthritis and Cartilage* **7**, 191-202.

Pullig, O., Weseloh, G., Ronneberger, D. L., Kakonen, S. M., Swoboda, B. (2000). Chondrocyte differentiation in human osteoarthritis: Expression of

osteocalcin in normal and osteoarthritic cartilage and bone. *Calcified Tissue International* **67**, 230-240.

Putzier, M., Funk, J. F., Schneider, S. V., Gross, C., Tohtz, S. W., Khodadadyan-Klosterermann, C., Perka, C., Kandziora, F. (2006). Charite total disc replacement– clinical and radiographical results after an average follow-up of 17 years. *European Spine Journal* **15**, 183-195.

Radin, E. L., Paul, I. L. (1972). A consolidated concept of joint lubrication. *Journal of Bone and Joint Surgery* **54**, 607-616.

Reddi, A. H. (2000). Morphogenesis and tissue engineering of bone and cartilage: inductive signals, stem cells and biomimetic biomaterials. *Tissue Engineering* **6**(4), 351-359.

Reid, J. E., Meakin, J. R., Robins, S. P., Skakle, J. M. S., Hukins, D. W. L. (2002). Sheep lumbar intervertebral discs as models for human discs. *Clinical Biomechanics* **17**, 312-314.

Richard, F., Villars, M., Thibaud, S. (2013). Viscoeleastic modelling and quantitative experimental characterisation of normal and osteoarthritic human articular cartilage using indentation. *Journal of the Mechanical Behaviour of Biomedical Materials* **24**, 41-52.

Rieppo, J., Toyras, J., Nieminem, M. T., Kovanen, V., Hyttinen, M. M., Korhonen, R. K., Jurvelin, J. S., Helminen, H. J. (2003). Structure-function relationships in enzymatically modified articular cartilage. *Cells Tissues Organs* **175**(3), 121-132.

Risbud, M. V., Izzo, M. W., Adams, C. S., Arnold, W. W., Hillibrand, A. S., Vresilovic, E. J., Vaccaro, A. R., Albert, T. J., Shapiro, I. M. (2003). An organ culture system for the study of the nucleus pulposus: Description of the system and evaluation of the cells. *Spine* **28**(24), 2652-2659.

Roberts, S., Menage, J., Urban, J. P. G. (1989). Biochemical and structural properties of the cartilage end plate and its relation to the intervertebral disc. *Spine* **14**(2), 166-174.

Roberts, S., Menage, J., Duance, V., Wotton, S. (1991A). Type III collagen in the intervertebral disc. *Histochemistry Journal* **23**, 503-508.

Roberts, S., Menage, J., Duance, V., Wotton, S., Ayad, S. (1991B). Collagen types around the cells of the intervertebral disc and cartilage end plate: an immunolocalisation study. *Spine* **16**, 1030-1038.

Roberts, S., Caterson, B., Evans, H., Eisenstein, S. M. (1994). Proteoglycan components of the intervertebral disc and cartilage end plate: an immunolocalisation study of animal and human tissues. *The Histochemical Journal* **26**, 402-411.

Roberts, S., Caterson, B., Menage, J., Evans, E. H., Jaffray, D. C., Eisenstein, S. M. (2000). Matrix metalloproteinases and aggrecanase. *Spine* **25**(23), 3005-3013.

Roberts, S., Evans, H., Trivedi, J., Menage, J. (2006). Histology and pathology of the human intervertebral disc. *The Journal of Bone and Joint Surgery* **88**, 10-14.

Rong, Y., Sugumaran, G., Silbert, J. E., Spector, M. (2002). Proteoglycans synthesised by canine intervertebral disc cells grown in a type I collagen-glycosaminoglycan matrix. *Tissue Engineering* **8**, 1037-1047.

Rosenberg, L. C. (1992). Structure and function of dermatan sulphate proteoglycans in articular cartilage. In Articular cartilage and Osteoarthritis (ed. Kuettner KE, Schleyerbach R, Peyron JC, Hascall VC), pp. 45-63. New York: Raven Press.

Roughley, P. J. (2004). Biology of intervertebral disc aging and degeneration: involvement of the extracellular matrix. *Spine* **29**, 2691-2699.

Roughley, P., Hoemann, C., DesRosiers, E., Mwale, F., Antoniou, J., Alini, M. (2006). The potential of chitosan-based gels containing intervertebral disc cells for nucleus pulposus supplementation. *Biomaterials* **27**, 388-396.

Rousseau, M. A., Ulrich, J. A., Bass, E. C., Rodriguez, A. G., Liu, J. J., Lotz, J. C. (2007). Stab incision for inducing intervertebral disc degeneration in the rat. *Spine* **32**(1), 17-24.

Ruoslahti, E. (1988). Fibronectin and its receptors. *Annual Review of Biochemistry* **57**, 375-413.

Saad, L., Spector, M. (2004). Effects of collagen type on the behaviour of adult canine annulus fibrosus cells in collagen-glycosaminoglycan scaffolds. *Journal of Biomedical Material Research A* **71**, 233-241.

Sakai, L. Y., Keene, D. R., Glanville, R. W., Bachinger, H. P. (1991). Purification and partial characterisation of fibrillin, a cysteine-rich structural component of connective tissue microfibrils. *The Journal of Biological Chemistry* **266**, 14763-14770.

Sakai, N., Hagihara, Y., Furusawa, T., Hosoda, N., Sawae, Y., Murakami, T. (2012). Analysis of biphasic lubrication of articular cartilage loaded by cylindrical indenter. *Tribology International* **46**, 225-236.

Sandell, L. J., Aigner, T. (2001). Articular cartilage and changes in arthritis. An introduction: Cell biology of osteoarthritis. *Arthritis Research* **3**, 107-113.

Sarzi-Puttini, P., Fabiola, A., Fumagalli, M., Capsoni, F., Carrabba, M. (2005). Osteoarthritis of the spine. *Seminars in Arthritis and Rheumatism* **34**(6), 38-43.

Sasada, T., Abe, T., Morita, M., Mabuchi, K. (2005). Role of chondroitin sulphate in the low friction property of articular cartilages. In Proceedings of the Fifth Kobe International Forum on *Biotribology*, Kobe, Japan, 64-67.

Sato, M., Asazuma, T., Ishihara, M., Kikuchi, T., Masuoka, K., Ichimura, S. (2002). An atelocollagen honeycomb-shaped scaffold with a membrane seal (ACHMS-scaffold) for the culture of annulus fibrosus cells from an intervertebral disc. *J Biomedical Material Research* **64A**, 248-256.

Schendel, M. J., Wood, K. B., Buttermann, G. R., Lewis, J. L., Ogilvie, J. W. (1993). Experimental measurement of ligament force, facet force, and segment motion in the human lumbar spine. *Journal of Biomechanics* **26**, 427-438.

Schlegel, J. D., Smith, J. A., Schleusener, R. L. (1996). Lumbar motion segment pathology adjacent to thoracolumbar, lumbar and lumbosacral fusions. *Spine* **21**, 970-981.

Schmidt, M. B., Mow, V. C., Chun, L. E., Eyre, D. R. (1990). Effects of proteoglycan extraction on the tensile behaviour of articular cartilage. *Journal of Orthopaedic Research* **8**(3), 353-363.

Schmidt, T. A., Gastelum, N. S., Nguyen, Q. T., Schumacher, B. L., Sah, R. L. (2007a). Boundary lubrication of articular cartilage: role of synovial fluid constituents. *Arthritis and Rheumatism* **56**, 882-891.

Schmidt, T. A., Sah, R. L. (2007b). Effect of synovial fluid on boundary lubrication of articular cartilage. *Osteoarthritis Cartilage* **15**, 35-47.

Schollmeier, G., Lahr-Eigen, R., Lewandrowski, K. U. (2000). Observations on fiber-forming collagens in the annulus fibrosus. *Spine* **25**, 2736-2741.

Scott, J. E. (1993). Proteoglycan-fibrillar collagen interactions in tissues: dermatan sulphate proteoglycan as a tissue organiser. In *Dermatan sulphate proteoglycans: Chemistry, Biology, Chemical Pathology* (ed. Scott J E), pp. 165-192. London: Portland Press.

Shahin, K., Doran, P. M. (2011). Improved seeding of chondrocytes into polyglycolic acid scaffolds using semi-static and alginate loading methods. *Biotechnology Progress* **27**, 191-200.

Shao, X., Hunter, C. J. (2007). Developing an alginate/chitosan hybrid fiber scaffold for annulus fibrosus cells. *Journal of Biomedical Materials Research A* **82**, 701-710.

Sheng, S. R., Wang, X. Y., Xu, H. Z., Zhu, G. Q., Zhou, Y. F. (2010). Anatomy of large animal spines and its comparison to the human spine: a systematic review. *The European Spine Journal* **19**, 46-56.

Shultz, R. M., Bader, A. (2007). Cartilage tissue engineering and bioreactor systems for the cultivation and stimulation of chondrocytes. *European Biophysics Journal* **36**, 539-568.

Simon, P., Espinoza Orias, A. A., Andersson, G. B. J., An, H. S., Inoue, N. (2012). In vivo topographic analysis of lumbar facet joint space width distribution in healthy and symptomatic subjects. *Spine* **37**(12), 1058-1064.

Simpson, E. K., Parkinson, I. H., Manthey, B., Fazzalari, N. L. (2001). Intervertebral disc disorganisation is related to trabecular bone architecture in the lumbar spine. *Journal of Bone and Mineral Research* **16**(4), 681-687.

Sive, J. I., Baird, P., Jeziorsk, M., Watkins, A., Hoyland, J. A., Freemont, A. J. (2002). Expression of chondrocyte markers by cells of normal and degenerate intervertebral discs. *Molecular Pathology* **55**, 91-97.

Smith, T. J., Fernie, G. R. (1991). Functional biomechanics of the spine. *Spine* **16**(10), 1197-1203.

Staiger, T. O., Gaster, B., Sullivan, M. D., Deyo, R. A. (2003). Systematic review of anti-depressants in the treatment of chronic low back pain. *Spine* **28**, 2540-2545.

Stapleton, T. W., Ingram, J., Katta, J., Knight, R., Korossis, S., Fisher, J., Ingham, E. (2008). Development and characterisation of an acellular porcine medial meniscus for use in tissue engineering. *Tissue Engineering Part A* **14**(4), 505-518.

Stapleton, T. W., Ingram, J., Fisher, J., Ingham, E. (2010). Investigation of the regenerative capacity of an acellular porcine medial meniscus for tissue engineering applications. *Tissue Engineering Part A* **17**(1-2), 231-242.

Sun, Y., Hurtig, M., Pilliar, R. M., Grynpas, M., Kandel, R. A. (2001). Characterization of nucleus pulposus-like tissue formed in vitro. *Journal of Orthopaedic Research* **19**, 1078-1084.

Swanepoel, M. W., Adams, L. M., Smeathers, J. E. (1995). Human lumbar apophyseal joint damage and intervertebral disc degeneration. *Annals of the Rheumatic Diseases* **54**, 182-188.

Taylor, J. R., Twomey, L. T. (1986). Ages changes in lumbar zygapophyseal joints. Observations on structure and function. *Spine* **11**, 739-745.

Taylor, J. R., McCormick, C. C. (1991). Lumbar facet joint fat pads: their normal anatomy and their appearance when enlarged. *Neuroradiology* **33**, 38-42.

Temenoff, J. S., Mikos, A. G. (2000). Review: Tissue engineering for regeneration of articular cartilage. *Biomaterials* **21**, 431-440.

Thompson, J. P., Pearce, R. H., Schechter, M. T., Adams, M. E., Tsang, I. K. Y., Bishop, P. B. (1990). Preliminary evaluation of a scheme for grading the gross morphology of the human intervertebral disc. *Spine* **15**(5), 411-415.

Tischer, T., Aktas, T., Milz, S., Putz, R. V. (2006). Detailed pathological changes of human lumbar facet joints L1-L5 in elderly individuals. *European Spine Journal* **15**, 308-315.

Towheed, T. E., Judd, M. J., Hochberg, M. C., Wells, G. (2003). Acetaminophen for osteoarthritis. *Cochrane Database System Review* **25**(1).

Uhrenholt, L., Hauge, E., Vesterby Charles, A., Gregersen, M. (2008). Degenerative and traumatic changes in the lower cervical spine facet joints. *Scandinavian Journal of Rheumatology* **37**, 375-384.

Urban, J. P., Holm, S., Maroudas, A., Nachemson, A. (1977). Nutrition of the intervertebral disc. An in vivo study of solute transport. *Clinical Orthopaedics* **129**, 2700-2709.

Urban, J. P. G., Roberts, S., Ralphs, J. R. (2000). The nucleus of the intervertebral disc from development to degeneration. *American Zoology* **40**, 53-61.

Urban, J. P. G., Roberts, S. (2003). Degeneration of the intervertebral disc. *Arthritis Research and Therapy* **5**(3), 120-130.

van den Broek, P. R., Huyghe, J. M., Wilson, W., Ito, K. (2012). Design of next generation total disk replacements. *Journal of Biomechanics* **45**, 134-140.

van den Eerenbeemt, K. D., Ostelo, R. W., van Royen, B. J., Peul, W. C., van Tulder, M. W. (2010). Total disc replacement surgery for symptomatic degenerative lumbar disc disease: a systematic review of the literature. *European Spine Journal* **19**, 1262-1280.

van Middelkoop, M., Rubinstein, S. M., Kuijpers, T., Verhagen, A. P., Ostelo, R., Koes, B. W., van Tulder, M. W. (2011). A systematic review on the

effectiveness of physical and rehabilitation interventions for chronic non-specific low back pain. *European Spine Journal* **20**, 19-39.

Van Tulder, M. W., Scholten, R. J., Koes, B. W., Deyo, R. A. (2000). Nonsteriodal anti-inflammatory drugs for low back pain: a systematic review within the framework of the Cochrane Collaboration Back Review Group. *Spine* **25**, 2501-2513.

Van Tulder, M., Touray, T., Furlan, A., Solway, S., Bouter, L. (2003). Cockrane Back Review Group. Muscle relaxants for nonspecific low back pain: a systematic review within the framework of the Cochrane Collaboration. *Spine* **28**, 1978-1992.

Varlotta, G. P., Lefkowitz, T. R., Schweitzer, M., Errico, T. J., Spivak, J., Bendo, J. A., Rybak, L. (2011A). The lumbar facet joint: a review of current knowledge: part 1: anatomy, biomechanics, and grading. *Skeletal Radiology* **40**, 13-23.

Varlotta, G. P., Lefkowitz, T. R., Schweitzer, M., Errico, T. J., Spivak, J., Bendo, J. A., Rybak, L. (2011B). The lumbar facet joint: a review of current knowledge: part II: diagnosis and management. *Skeletal Radiology* **40**, 149-157.

Von der Mark, K., Gauss, V., von der Mark, H., Muller, P. (1977). Relationship between cell shape and type of collagen synthesised as chondrocytes lose their cartilage phenotype in culture. *Nature* **267**, 531-532.

Von der Mark, K. (1999). Structure, biosynthesis and gene regulation of collagens in cartilage and bone. Dynamics of Bone and Cartilage Metabolism, Academic Press, Orlando, 3-29.

Wade, K. R., Robertson, P. A., Broom, N. D. (2011). A fresh look at the nucleus-endplate region: new evidence for significant structural integration. *European Spine Journal* **20**(8), 1225-1232.

Wagenseil, J. E., Mecham, R. P. (2007). New insights into elastic fiber assembly. *Birth Defects Research (Part C)* **81**, 229-240.

Wan, Y., Wu, H., Cao, X., Dalai, S. (2008). Compressive mechanical properties and biodegradability of porous poly(caprolactone)/chitosan scaffolds. *Polymer Degradation and Stability* **93**, 1736-1741.

Wang, Z. L., Yu, S., Haughton, V. M. (1989). Age-related changes in the lumbar facet joints. *Clinical Anatomy* **2**, 55-62.

Wang, Y., Liu, G., Li, T., Xiao, Y., Han, Q., Xu, R., Li, Y. (2010). Morphometric comparison of the lumbar cancellous bone of sheep, deer and humans. *Comparative Medicine* **60**(5). 374-379.

Wegman, A., van der Windt, D., van Tulder, M., Stalman, W., de Vries, T. (2004). Nonsteriodal antiinflammatory drugs or acetaminophen for osteoarthritis of the hip or knee? A systematic review of evidence and guidelines. *Journal of Rheumatology* **31**, 344-354.

Weishaupt, D., Zanetti, M., Boos, N., Hodler, J. (1999). MR imaging and CT in osteoarthritis of the lumbar facet joints. *Skeletal Radiology* **28**, 215-219.

White, A. A., Panjabi, M. M. (1990). Clinical biomechanics of the spine. 2nd edn. JB Lippincott Company.

Wilke, H. J., Kettler, A., Wenger, K. H., Claes, L. E. (1997). Anatomy of the sheep spine and its comparison to the human spine. *The Anatomical Record* **247**, 542-555.

Wilke, H. J., Kettler, A., Gosh, P., Claes, L. (1999). Is the lumbar sheep spine an adequate model for the human lumbar spine? – a comparison of biomechanical properties, macroscopic and microscopic anatomy and bone mineral density. In: Proceedings of the 26th annual meeting, Hawaii, p 124.

Wilke, H. J., Zanker, D., Wolfram, U. (2012). Internal morphology of human facet joints: comparing cervical and lumbar spine with regard to age, gender and the vertebral core. *Journal of Anatomy* **220**(3), 233-241.

Wotton, S. F., Duance, V. C., Fryer, P. R. (1988). Type IX collagen: a possible function in articular cartilage. *FEBS Letters* **234**, 14-17.

Wotton, S. F., Duance, V. C. (1994). Type III collagen in normal human articular cartilage. *The Journal of Histochemistry and Cytochemistry* **26**, 412-416.

Wright, V., Dowson, D. (1976). Lubrication and cartilage. *Journal of Anatomy* **121**(1), 107-118.

Wu, J. J., Eyre, D. R., Slayter, H. S. (1987). Type VI collagen of the intervertebral disc. Biochemical and electromicroscopic characterisation of the native protein. *Biochemical Journal* **248**, 373-381.

Wu, J. J., Woods, P. E., Eyre, D. R. (1992). Identification of cross-linking sites in bovine cartilage type IX collagen reveals an antiparallel type II-type IX molecular relationship and type IX to type IX bonding. *Journal of Biological Chemistry* **267**, 23007-23014.

Wu, J. J., Murray, J., Eyre, D. R. (1996). Evidence for copolymeric cross-linking between types II and III collagens in human articular cartilage (abstract). *Transactions of the Orthopaedic Research Society* **21**, 42.

Xing, Z., Gauldie, J., Baumann, H. (1998). IL-6 is an anti-inflammatory cytokine required for controlling local or systematic acute inflammatory responses. *Journal of Clinical Investigation* **101**, 311-320.

Yamashita, T., Yasuhiko, M., Ozaktay, A. C., Cavanaugh, J. M., King, A. I. (1996). A morphological study of the fibrous capsule of the human lumbar facet joint. *Spine* **21**(5), 538-543.

Yang, K. H., King, A. I. (1984). Mechanism of facet load transmission as a hypothesis for low-back pain. *Spine* **9**, 557-565.

Yang, L., Kandel, R. A., Chang, G., Santerre, J. P. (2009). Polar surface chemistry of nanofibrous polyurethane scaffold affects annulus fibrosus cell attachment and early matrix accumulation. *Journal of Biomedical Material Research A* **91**, 1089-1099.

Yang, X., Li, X. (2009). Nucleus pulposus tissue engineering: a brief review. *European Spine Journal* **18**, 1564-1572.

Yoganandan, N., Knowles, S. A., Maiman, D. J., Pintar, F. A. (2003). Anatomic study of the morphology of human cervical facet joint. *Spine* **28**(20), 2317-2323.

Young, R. D., Lawrence, P. A., Duance, V. C., Aigner, T., Monaghan, P. (2000). Immunolocalisation of collagen types II and III in single fibrils of human articular cartilage. *The Journal of Histochemistry and Cytochemistry* **48**, 423-432.

Yu, J., Peter, C., Roberts, S., Urban, J. P. G. (2002). Elastic fibre orientation in the intervertebral discs of the bovine tail. *Journal of Anatomy* **201**, 465-475.

Yu, J., Fairbank, J. C. T., Roberts, S., Urban, J. P. G. (2005). The elastic fibre network of the annulus fibrosus of the normal and scoliotic human intervertebral disc. *Spine* **30**(16), 1815-1820.

Zaucke, F., Dinser, R., Maurer, P., Paulsson, M. (2001). Cartilage oligomeric matrix protein (COMP) and collagen IX are sensitive markers for the differentiation state of articular primary chondrocytes. *Biochemical Journal* **358**, 17-24.

Zdeblick, T. A. (1995). The treatment of degenerative lumbar disorders. A critical review of the literature. *Spine* **20**(24S), 126S-137S.

Zigler, J., Delamarter, R., Spivak, J. M., Linovitz, R. J., Danielson III, G. O., Haider, T. T., Cammisa, F., Zuchermann, J., Balderston, R., Kitchel, S., Foley, K., Watkins, R., Bradford, D., Yue, J., Yuan, H., Herkowitz, H., Geiger, D., Bendo, J., Peppers, T., Sachs, B., Girardi, F., Kropf, M., Goldstein, J. (2007). Results of the prospective, randomized, multicentre Food and Drug Administration investigational device exemption study of the ProDisc-L total disc replacement versus circumferential fusion for the treatment of 1-level degenerative disc disease. *Spine* **32**, 1155-1162.

Ziv, I., Maroudas, C., Robin, G., Maroudas, A. (1992). Human facet cartilage: Swelling and some physiochemical characteristics as a function of age. *Spine* **18**(1), 136-146.

Appendix I: Distributers of Materials and Chemicals

Chemical/Reagent	Distributer
Alcian Blue tissue stain.	Raymond A Lamb Ltd
Acetone	European Bios
Amphotericin B	Sigma-Aldrich Company Ltd.
Aprotonin	Mayfair house
Avidin/Biotin blocking kit	Vector Laboratories
Bovine serum albumin	Sigma-Aldrich Company Ltd
Cement powder	Cold Cure
Cement liquid	WHW Plastics
Chloramine T	Sigma-Aldrich Company Ltd
Chondroitin sulphate B	Sigma-Aldrich Company Ltd
Chondroitinase ABC	Sigma-Aldrich Company Ltd
Collagenase (Clostridium Histolyticum type IA)	Sigma-Aldrich Company Ltd
Citric acid	VWR International
DAB stain kit	Vector laboratories
DABCO	VWR International
1,9 dimethylene blue	Sigma Aldrich Company Ltd
Dimethyl Sulphoxide (DMSO).	Sigma-Aldrich Company Ltd
Disodium hydrogen orthophosphate	VWR International
DPX mounting medium	Thermo Fisher Scientific Ltd.
Dulbecco's modified Eagle's medium (DMEM)	Gibco Life Technologies Ltd
EDTA	Fisher scientific
Envision + dual link system – HRP (DAB+)	Dako Cytomation
Eosin tissue stain	Thermo Shandon
Ethanol	Thermo Fisher Scientific Ltd

Foetal calf serum (FCS)	Biosera
Formic acid	Sigma-Aldrich Company Ltd
Gentamycin sulphate	MP biomedical
Glacial acetic acid	VWR International
Glycerol	Sigma-Aldrich Company Ltd
Hoescht DNA stain 33258	Invitrogen
Hyaluronidase (type IV-S, bovine testes)	Sigma-Aldrich Company Ltd
Hydrochloric acid	VWR International
Hydrogen peroxide	Sigma-Aldrich Company Ltd
ImmEdge Hydrophobic barrier pen	Vector laboratories
Industrial methylated spirits	Genta Medical
Isopropanol	VWR International
L-Glutamine	Invitrogen Ltd
Methanol	Vickers Laboratories
Methylated Spirits	VWR International
Miller's stain	Raymond A Lamb
Neutral Buffered Formalin (NBF)	Sigma-Aldrich Company Ltd.
Nyastatin	Sigma-Aldrich Company Ltd.
Oxalic acid	VWR International
Paraffin wax pellets	Raymond A Lamb Ltd
Papain	VWR International
PBS tablets	Oxoid
p-dimethylaminobenzaldehyde	Sigma-Aldrich Company Ltd.
Penicillin	Invitrogen
Perchloric acid	Sigma-Aldrich Company Ltd.
Periodic acid	Sigma-Aldrich Company Ltd.
Picric acid	Sigma-Aldrich
Polymixin B	Sigma-Aldrich Company Ltd.
Potassium permanganate	Thermo Fisher Scientific Ltd.
Primaxin I. V.	Merck Sharp & Dohme Ltd.
Propan-1-ol	VWR International
Proteinase K	Dako Ltd

R.T.U Horseradish peroxidase streptavidin	Vector Laboratories
Safronin-O	Acros
Saponin	Sigma-Aldrich Company Ltd.
Schiffs reagent	Sigma-Aldrich Company Ltd.
Scott's tap water	European Bios
Silver nitrate	AnalaR
Sirius red	Raymond A Lamb Ltd
Sodium acetate	Thermo Fisher Scientific Ltd.
Sodium azide	VWR International
Sodium chloride	VWR International
Sodium di-hydrogen orthophosphate	VWR International
Sodium formate	VWR International
Sodium hydroxide	Thermo Fisher Scientific Ltd.
Sodium hydroxide (NaOH) pellets	BDH Laboratory Supplies
Sodium thiosulphate	AnalaR
Streptomycin	Invitrogen
Trans-4-hydroxyl-L-proline	Sigma-Aldrich Company Ltd.
TriGene disinfectant	Scientific Laboratory Supplies Ltd
Tris-HCl	Melford
Trizma base	Sigma-Aldrich Company Ltd.
Trypan blue Cell Stain	Sigma-Aldrich Company Ltd
Trypsin	Sigma-Aldrich Company Ltd
Tween 20	Sigma-Aldrich Company Ltd
Vancomycin	MP biomedical
Virkon disinfectant	Bios Europe
Weigerts haematoxylin	Raymond A Lamb
Xylene	Genta Medical

Appendix II: Distributers of Equipment, Consumables, Plastic and Glassware

Equipment/Consumables/Plastic and glassware	Supplier
Automatic pipettes	Gilson
Balances: GR200/GX2000	A & D
Bijous	Bibby Sterlin Ltd.
Bone saw	Exakt
Buffer tablets	VWR
Camera	Canon
Carbon dioxide incubator	SANYO, Biomedical Europe BV
Cell B Software	Olympus UK Ltd.
Cell culture flasks (T25 and T75)	Nange Nunc International Corperation.
Cell sieve (100µm)	Sigma-Aldrich Company Ltd.
Cell medium aspirator	Integra Biosciences
Centrifuge tubes	Nange Nunc International Corperation
Coplin jar	
Cryovials	Nange Nunc International Corperation
Culture slides tissue culture 4 wells	VWR International
Digital colour camera	Media Cybernetics
Disposable microtome blades	Raymond A Lamb Ltd.
Fine tip stainless steel forceps	Raymond A Lamb Ltd.
Flat bottomed 96 well plate	Scientific laboratory supplies
Freeze drier	Thermo Fisher Scientific Ltd.
Fume Hood	Whiteley, Hants, UK
Glass coverslips	Scientific laboratory supplies
Glifton water bath	Scientific laboratory supplies
Hacksaw	Thackray Instruments

Harrier 15/80 centrifuge	SANYO E&E Europe BV, Biomedical division.
Haemocytometer	Fisher Scientific
Heraeus Hera Safe class II safety cabinet	Thermo Electron Corporation, USA
Hotplate	Raymond A Lamb Ltd.
Image-Pro Plus	Media Cybernetics
Incubator (Heraeus)	Jencons PLC
Leica RM 2125 RTF microtome	Leica Microsystems (UK) Ltd.
Long hair brush No6	Raymond A Lamb Ltd.
Magnetic Stirrer	Stuart Scientific
Measuring cylinders	Fisher Scientific
Micro plate spectrophotometer	Thermo scientific
Microtome blades	Fisher Scientific
Nitrile powder free gloves	Starlab Ltd.
Multitest slides	MP Biomedicals.
Optical microscope (Olympus CK40-SLP)	Olympus optical Co Ltd.
Olympus C-4040 zoom digital camera	Olympus optical Co Ltd.
Paraffin section mounting bath	Barnstead Electrothermal (Thermo Fisher Scientific)
Pasteur pipettes	Alpha Laboratories Ltd.
Petri dishes	Bibby Sterlin Ltd.
pH meter: Jenway 3020	Jenway Ltd.
Pipette boy	Integra Biosciences
Pipettes	Gilson Inc.
Plastic histology casettes	Simport
Plastic syringes, 1ml, 2ml 10ml.	Terumo Medical Corporation.
Plate rocker	Bibby Sterlin Ltd.
Pots 60ml, 150ml, 250ml.	Bibby Sterlin Ltd.
Slide holder	Raymond A Lamb Ltd.
Stainless steel surgical blades (22) and scalpel (4)	Swan Morton

Strippette disposable serological pipettes	Corning Costar UK Ltd.
Surgical scissors	Thackray Instruments
Standard forceps	Thackray Instruments
Superfrost Plus slides	Scientific Laboratory Supplies
Syringe filters (0.2µm)	Sartorius Ltd.
Table shaker	IKA
TipOne pipette tips	Starlab UK Ltd.
Tissue processor	Leica Microsystems
Universals	Bibby Sterlin Ltd.
Water Bath	Grant
Windsor wax incubator E18/31	Sandrest
Vacuum pump	Edwards
µCT80	Scanco Medical, Switzerland
µCT100	Scanco Medical, Switzerland

Appendix III: Presentations and Publications

Publications:

- Gough, C. S., Wajayathunga, V. N., Tipper, J. L., Wilcox, R. K., Hall, R. M., Ingham, E. (2011). The biology of the ovine functional spinal unit. *European Cells and Materials* **22**(3), 67.

- Gough, C. S., Mitchell, E. A., Wijayathunga, V. N., Tipper, J. L., Wilcox, R. K., Hall, R. M., Ingham, E. (2012). The biology of the ovine functional spinal unit. *Journal of Tissue Engineering and Regenerative Medicine* **6**(S1), 396.

Presentations:

- Gough, C. S., Wajayathunga, V. N., Tipper, J. L., Wilcox, R. K., Hall, R. M., Ingham, E. (2011). The biology of the ovine functional spinal unit. Tissue and Cell Engineering Society Annual Meeting, Leeds, UK. (Poster presentation).

- Gough, C. S., Mitchell, E. A., Wijayathunga, V. N., Tipper, J. L., Wilcox, R. K., Hall, R. M., Ingham, E. (2012). The biology of the ovine functional spinal unit. 3rd Tissue Engineering and Regenerative Medicine International Society World Congress, Vienna, Austria. (Poster presentation).

- Gough, C. S., Mitchell, E. A., Wijayathunga, V. N., Tipper, J. L., Wilcox, R. K., Hall, R. M., Ingham, E. (2012). The biology of the ovine functional spinal unit. Regener8 Annual Meeting, Newcastle, UK. (Poster presentation).

- Gough, C. S., Mitchell, E. A., Wijayathunga, V. N., Tipper, J. L., Wilcox, R. K., Hall, R. M., Ingham, E. (2012). The biology of the ovine functional spinal unit. Biomaterials and Tissue Engineering Group, 14th Annual White Rose Work in Progress Meeting, York, UK. (Poster presentation).